Glutathione metabolism of *Plasmodium falciparum*

by

Dipl. Biol.

Eva-Maria Patzewitz

Thesis submitted for the degree of Doctor of Philosophy

April 2009

Division of Infection and Immunity,
Faculty of Biomedical and Life Sciences,
University of Glasgow

Abstract

Apicomplexan parasites of the genus *Plasmodium* are the causative agent of malaria, one of the most prevalent infectious diseases worldwide. Five different *Plasmodium* species can cause malaria in humans, leading to a total of approximately 500 million cases each year and of these, *P. falciparum* causes the most deadly form of the disease and is responsible for more than one million deaths annually. A major problem in the global fight against malaria is the widespread resistance of the parasites against the currently available drugs. It is of great importance to identify new drug targets as well as to understand the mechanisms that lead to drug resistance in the first instance in order to potentially reverse the resistant phenotypes and to avoid the development of resistance against currently effective drugs in the future.

The tripeptide glutathione (GSH) or γ-glutamyl-cysteinyl-glycine is the most abundant low molecular weight thiol in most eukaryotic organisms and serves a number of important functions as sulfhydryl-buffer, cofactor for enzymes and for the detoxification of xenobiotics and drugs. GSH is an important component of the antioxidant machinery and because malaria parasites live in an environment rich in iron and oxygen and thus increased oxidative stress, they depend on functional antioxidant systems. The biosynthesis pathway for GSH, consisting of γ-glutamylcysteine synthetase (γGCS) and glutathione synthetase (GS) is present in malaria parasites as well as in their host cells. Previous studies have shown that depletion of GSH has an antimalarial effect, but it remained unclear whether parasites were killed directly or died because their host cell could not survive the depletion of GSH. To address this question, the knockout of both genes encoding the enzymes of the GSH biosynthesis pathway in *P. falciparum* was attempted. While both gene loci were targeted by control constructs, the knockout of either *pfygcs* or *pfgs* was impossible, indicating both genes are essential for parasite survival in the erythrocytic stages. To analyse the localization of γGCS and GS, GFP-tagged recombinant fusion proteins were expressed in the parasites and showed that GSH biosynthesis is cytosolic.

Apart form its other functions GSH has previously been suggested to be involved in resistance to the antimalarial drug chloroquine (CQ). CQ was for a long time the first line antimalarial drug due to its high efficiency, low cost and low

toxicity, but is now widely inefficient in the treatment of the disease. CQ resistance is associated with mutations in the CQ resistance transporter (PfCRT), a membrane protein of the digestive vacuole that allows the efflux of the drug from its site of action. However, PfCRT mutations alone cannot explain the full array of phenotypes found in resistant parasites. Since GSH is able to degrade heme, the target of CQ *in vitro* it has been suggested that elevated GSH levels contribute to CQ resistance. However, analyses of isogenic parasite lines bearing different forms of PfCRT in this study revealed lower GSH levels and higher susceptibility to inhibition of GSH biosynthesis in the CQ resistant lines. These changes did not correlate with changes in the expression of enzymes involved in the *de novo* biosynthesis or consumption of GSH. In spite of this, the cellular accumulation ratio for CQ indicated a decrease of free heme in the resistant parasites. Mutant forms of PfCRT expressed in oocytes of *Xenopus laevis* were able to transport GSH, while the sensitive wild-type form did not transport the tripeptide. The findings of this study suggest that in parasites bearing mutant PfCRT, GSH is transported into the digestive vacuole where it is able to contribute to resistance by degrading heme, before the tripeptide itself is degraded by peptidases inside the vacuole, consistent with the overall reduction of GSH levels in CQ resistant parasites.

Author's Declaration

I, Eva-Maria Patzewitz hereby declare that I am the sole author of this thesis and performed all of the work presented, with the following exceptions:

Chapter 3:

- Some fluoresecence images were taken by Prof. Sylke Müller
- The constructs pHH1-Δ*ygcs* and pHH1-*ygcs*con were designed by S. Meierjohann
- Western analyses of PfγGCS-HA expression were performed by L. Sveen under my supervision.
- The L-BSO IC_{50} of PfγGCS-HA expressing parasites was determined by M. L. Laine under my supervision

Chapter 4:

- Some fluoresecence images were taken by Prof. Sylke Müller
- Constructs pHH1-Δ*gs* and pHH1-*gs*con were designed by S. Meierjohann
- The BugBuster test expression of $PfGS^{E206K/N208A}$ was performed by M. L. Laine
- Western analyses and IC_{50} assays for L-BSO of PfGS-HA expressing parasites were performed by M. L. Laine

Chapter 5:

- Data presented in section 5.7 were generated by Dr. E. Salcedo-Sora, Dr. P. Stocks, Dr. P. Bray and Prof S. Ward at the Liverpool School of Tropical Medicine

Acknowledgements

Here it is now, the result of the last three years and this is the place to thank everyone who contributed in one way or another…

First of all I am grateful to my supervisor Prof Sylke Müller for giving me the opportunity to do a PhD in her laboratory and for her support and advice over the last years. The Müller group was a brilliant place to be and I want to thank all the past and present members for their help and support whenever it was needed and the fun time inside and outside the lab. Special thanks to Andy, Anne, Lynsey, Janet, Fiona, Svenja and Sylke for looking after my parasites whenever I was away and to Lene and Larissa, who contributed to some of the data presented here.

Thank you to everyone on level 5 and 6 of the GBRC and especially to Mhairi and Janet for proofreading parts of this thesis.

Thank you goes to Pat Bray and everyone at the Liverpool School of Tropical Medicine, for teaching me a lot of methods within three very short weeks.

I am thankful to my assessor Graham Coombs for his sound advice and his valuable suggestions.

A huge thank you to my family, my sister Katja and her family Andreas, Sophie and Jan and my parents Uwe and Christel, who didn't really get to see me a lot recently. Without their support and help I would not have been able to get this far.

And last but definitely not least, thank you to Jason, for your love and understanding and for bearing with the mad scientist. I am sorry about the lack of monkeys.

für meine eltern

Table of Contents

List of Figures

List of Tables

Abbreviations / Definitions

γGC	Gamma-glutamylcysteine
γGCS	Gamma-glutamylcysteine synthetase
µ	Micro
µF	Microfarrad
µg	Microgram
µl	Microliter
µm	Micrometer
µM	Micromolar
µmol	Micromoles
3' UTR	Three prime untranslated region
5-FC	5-Fluorocytosine
5' UTR	Five prime untranslated region
A	Adenine
A	Ampere
ABC	ATP binding cassette
ACT	Artemisinin based combination therapies
ADP	Adenosine diphosphate
AMP	Adenosine monophosphate
AmpR	Ampicillin resistance cassette
At	*Arabidopsis thaliana*
ATP	Adenosine triposphate
att	Recombination site in MuliSite Gateway® vectors
Bla	Blasticidine-S-HCl
bp	Base pairs
BSA	Bovine serum albumin
BSD	Blasticidine-S-deaminase
C	Cytosine
°C	Degrees Celsius
CAR	Cellular accumulation ratio
cd	Cytosine deaminase
CDC	Centre of disease control
CDNB	1-Chloro-2,4-dinitrobenzene
CQ	Chloroquine
C-terminal	Carboxy terminal
cDNA	Complementary DNA
CoA	Coenzyme A
Da	Dalton
ddH_2O	double distilled water
DEPC	Diethyl pyrocarbonate
DHFR	Dihydrofolate reductase
DHFR/TS	Dihydrofolate reductase / thymilidate synthase
DHPS	Dihydropteroate synthase
DMSO	Dimethyl sulphoxide
DNA	Deoxyribonucleic acid
dNTP	Deoxynucleotide triphosphate
dsDNA	Double stranded deoxyribonucleic acid
DTNB	5,5-Dithiobis-(2-nitrobenzoate)
DTT	Dithiothreitol
DV	Digestive vacuole
EBSS	Earle's balanced salt solution

ECL	Enhanced chemiluminescence
EDTA	Ethylene diamine tetraacetic acid
EGTA	Ethylene glycol tetraacetic acid
ER	Endoplasmatic reticulum
Ero1	Endoplasmatic reticulum oxidase 1
f	femto
FAD	Flavin adenine dinucleotide
FKBP12	12 kDa FK506- and rapamycin-binding protein
FK506	Fujimycin / Tacrolimus, immunosuppressive drug
FPIX	Ferriprotoporphyrin IX
fwd	Forward
G	Guanine
g	Gram
gDNA	Genomic deoxyribonucleic acid
GFP	Green fluorescent protein
Glx	Glutaredoxin-like protein
GR	Glutathione reductase
Grx	Glutaredoxin
GS	Glutathione synthetase
GSH	Glutathione (reduced form)
GSSG	Glutathione disulphide (oxidized form)
GST	Glutathione-S-transferase
HA	Hemagglutinin
hDHFR	Human dihydrofolate reductase
HEPES	4-(2-Hydroxyethyl)-piperazineethanesulphonic acid
HRP	Horseradish peroxidase
Hs	*Homo sapiens*
IC_{50}	Concentration at which 50 % growth inhibition occurs
IgG	Immunoglobulin G
IPTG	Isopropyl-ß-D-thiogalactopyranoside
J	Joule
KAHRP	Knob-associated histidine rich protein
KanR	Kanamycin resistance cassette
k	Kilo
kb	Kilobases
kDa	Kilodaltons
KO	Knockout
KOcon	Knockout control
kpsi	Kilo pound-force per square inch
l	liter
LB	Luria Bertani
L-BSO	L-buthionine-sulfoximin
m	Meter
m	Mili
M	Molar
MACS	Magnet activated cell sorting
mbar	Milibar
mg	Miligram
min	Minute
ml	Mililiter
mM	Milimolar
n	Nano
N	Normal
NAC	N-acetylcysteine

NAD^+	Nicotinamide adenine dinucleotide (oxidized)
NADH	Nicotinamide adenine dinucleotide (reduced)
$NADP^+$	Nicotinamide adenine dinucleotide phosphate (oxidized)
NADPH	Nicotinamide adenine dinucleotide phosphate (reduced)
ng	Nanogram
Ni^{2+}-NTA	Nickel-nitriloacetic acid
nm	Nanometer
nM	Nanomolar
N-terminal	Amino terminal
OD	Optical density
ORF	Open reading frame
p	Pico
PAGE	Polyacrylamide gel electrophoresis
Pb	*Plasmodium berghei*
PbDT	*Plamsodium berghei* dihydrofolate reductase terminator
PbECP1	*Plasmodium berghei* egress cysteine protease 1
PBS	Phosphate buffered saline
PCR	Polymerase chain reaction
PDH	Pyruvate dehydrogenase
Pf	*Plasmodium falciparum*
PfAOP	*Plasmodium falciparum* antioxidant protein
PfCAM	*Plasmodium falciparum* calmodulin
PfCK2α	*Plasmodium falciparum* cysteine kinase 2 α-subunit
PfCRT	*Plasmodium falciparum* chloroquine resistance transporter
PfEMP-1	*Plasmodium falciparum* erythrocyte membrane protein 1
PfγGCS	*Plasmodium falciparum* gamma-glutamylcysteine synthetase
PfGS	*Plasmodium falciparum* glutathione synthetase
PfHRPII	*Plasmodium falciparum* histidine rich protein 2
PfHsp86	*Plasmodium falciparum* heat shock protein 86
PfKAHRP	*Plasmodium falciparum* knob-associated histidine rich protein
Pfmdr1	*Plasmodium falciparum* multidrug resistance gene 1
PfMRP	*Plasmodium falciparum* multidrug resistance associated protein
PfPgh1	*Plasmodium falciparum* P-glycoprotein homologue 1
P_i	Inorganic phosphate
PMSF	Phenylmethyl sulphonyl fluoride
pmol	Picomoles
Px	Peroxiredoxin
qPCR	Quantitative polymerase chain reaction
RBC	Red blood cell
rev	Reverse
rif	Repetitive interspersed family
RNA	Ribonucleic acid
ROS	Reactive oxygen species
RT-PCR	Reverse transcriptase polymerase chain reaction
rpm	Revolutions per minute
S.D.	Standard Deviation
SDS	Sodium dodecyl sulphate
sec	Seconds
S.E.M.	Standard error of the mean
SERA	Serine repeat antigen
SERCA	Sarcoplasmatic reticulum calcium ATPase
Shld1	Shield 1

SOC	Super optimal broth with catabolite repression
SOD	Superoxide dismutase
SSC	Saline sodium citrate
STEVOR	Subtelomeric variable open reading frames family
strs	Seryl-tRNA synthetase
T	Thymine
TAE	Tris-acetate containing EDTA
Tb	*Trypanosoma brucei*
TBE	Tris-borate containing EDTA
TCA	Tricarbolic acid
TE	Tris containing EDTA
TEMED	N,N,N',N'-tetramethylethylenediamine
TfB I	Transformation buffer 1
TfB II	Transformation buffer 2
TNB^-	5-Thio-2-nitrobenzoate anion
Tris	Tris [hydroxymethyl] aminomethane
Trx	Thioredoxin
TrxR	Thioredoxin reductase
TVN	Tubulovesicular network
UV	Ultraviolet
V	Volt
var	Variant antigen
v/v	Volume per volume
w/v	Weight per volume
WHO	World health organisation
WT	Wild-type

1 Introduction

1.1 Malaria

Malaria is one of the most important infectious diseases with approximately 40 % of the world's population at risk of infection, particularly in tropical and subtropical regions (Figure 1-1A). Worldwide an estimated 500 million clinical cases occur each year leading to the death of approximately 1 million people. The disease is particularly serious in Africa, where malaria causes about 20 % of all childhood deaths under the age of five. Another high risk group are pregnant women, where complications of the disease can lead to severe malaria or severe anaemia in the mother or to reduced birth weight, premature delivery, spontaneous abortion or stillbirth of the child (World Health Organisation, WHO, http://www.who.int/topics/malaria/en/).

The disease is caused by protozoan parasites of the genus *Plasmodium*. Five different *Plasmodium* species cause malaria in humans, *P. falciparum*, *P. vivax*, *P. malariae*, *P. knowlesi* and *P. ovale*. The parasites are transmitted by female *Anopheles* mosquitoes and the disease is prevalent in those areas supporting the development of the vector. Of the approximately 430 different *Anopheles* species only 30-40 are vectors for the parasites (Center for Disease Control and Prevention, CDC, http://www.cdc.gov/Malaria/biology/mosquito). Environmental factors such as rainfall levels influence mosquito numbers and thus the transmission rate of malaria and epidemics frequently occur when the parasites are introduced to areas where the local population has little immunity to the disease, e.g. in times of flooding, or when non-immune people move into areas where malaria is endemic such as refugees in times of conflict. Vector control offers the best preventative measure against malaria in endemic areas so far (World Health Organisation, WHO, http://www.who.int/topics/malaria/en/).

Clinical symptoms of malaria include high fever, myalgia, vomiting and headaches in recurring bouts every 48-72 hours and usually appear 10-15 days after the bite by an infected mosquito. The most severe forms of the disease are caused by *P. falciparum* infections, which exceed more than 75% of all malaria cases in most African countries (Figure 1-1B) (WHO, http://www.who.int/topics/malaria/en/).

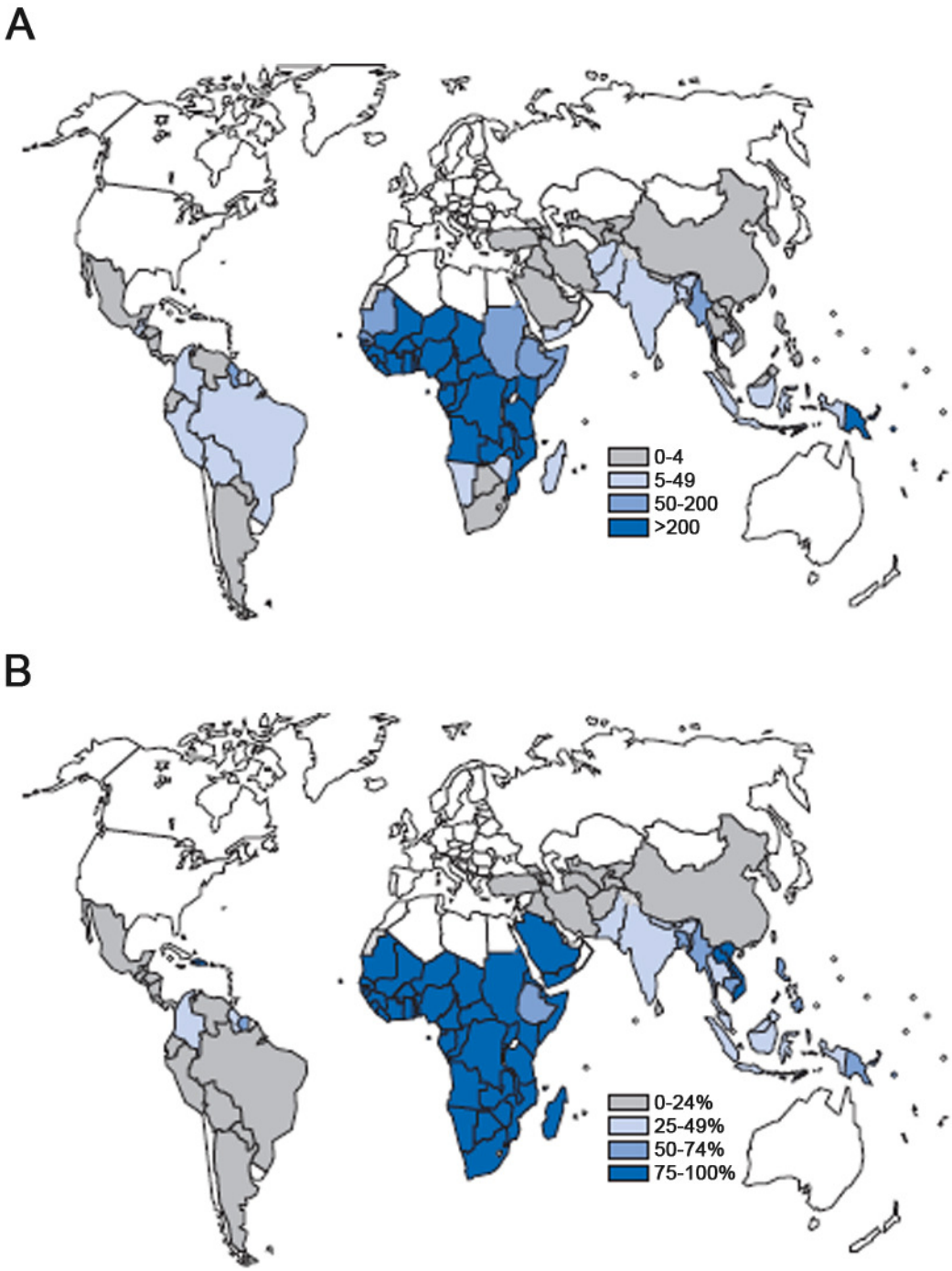

Figure 1-1: Distribution of malaria in 2006
Panel A: Estimated incidence of malaria in 2006 per 1000 population. The vast majority of cases occurred in the African region (89 %) followed by Southeast-Asia (9 %). In white regions no malaria transmission occurs. Grey areas have limited risk of transmission and in the dark blue areas transmission is high. Worldwide most cases of malaria are caused by *P. vivax*, followed by *P. falciparum*, which causes the most severe form of the disease. **Panel B:** Estimated percentage of malarial cases due to *P. falciparum* in 2006. The percentage of malaria cases caused by *P. falciparum* exceeds more than 75 % in most African counties but is lower in most other countries where malaria occurs. This figure was constructed from figures taken from the World Malaria Report 2008, World Health Organisation (http://www.who.int/malaria/wmr2008).

In cases of severe malaria, patients suffer from severe anaemia, acute renal failure, pulmonary oedema and cerebral malaria. Adhesion of parasite infected red blood cells (RBC) to non-infected RBCs and capillary walls leads to

disruptions of the blood supply in small capillaries and subsequent organ failure (Miller et al., 2002). Even after recovery from the acute disease children can be impaired in their intellectual and physical development.

Malaria has an enormous economic impact on endemic countries. Up to 40 % of all public health expenditure is consumed by malaria and 30-50 % of all hospital admissions are due to the disease in heavy burdened endemic countries. Not only medical costs, but also days lost for labour take a huge toll, leading to an average loss of 1.3 % of annual economic growth (WHO, http://www.who.int/topics/malaria/en/).

1.2 The lifecycle of *Plasmodium*

Plasmodium species undergo a complex life cycle, switching between two hosts and between sexual and asexual development (Figure 1-2). Once a female mosquito takes a blood meal from an infected patient, female macrogametocytes and male microgametocytes are taken up. In the mosquito midgut, the male gametocyte develops into 4-8 flagellated microgametes while the female develops into a spherical macrogamete (Sinden et al., 1978). Fertilisation of a macrogamete by a single microgamete leads to a zygote, which develops into a motile ookinete. The ookinete migrates through the midgut epithelium and encysts on the basal lamina (Matuschewski, 2006). Inside this oocyst, sporozoites form through several rounds of asexual multiplication until they are released into the body cavity of the mosquito in an active process which in *P. berghei* involves the proteolytic activity of the egress cysteine protease ECP1, a homologue to the *P. falciparum* SERA8 (Aly and Matuschewski, 2005). The sporozoites migrate to the salivary gland of the mosquito where they invade gland cells (Matuschewski, 2006). Once the mosquito takes another blood meal, now highly infective sporozoites are released into the human host. They migrate through the bloodstream and the lymphatic system to the liver where they invade hepatocytes. Inside hepatocytes, sporozoites develop to schizonts and asexually multiply to produce between 10,000-30,000 merozoites (exo-erythrocytic schizogony) (Prudencio et al., 2006; Sherman, 2005). *P. vivax* and *P. ovale* can prevail as dormant hypnozoites in the liver and can cause relapses of the disease years after the initial infection (Cogswell, 1992). Merozoite filled vesicles, so-called merosomes, bud from the host hepatocyte and merozoites are

released into the bloodstream where they infect erythrocytes and continue their asexual reproduction in the intra-erythrocytic schizogony (Prudencio et al., 2006; Silvie et al., 2008). The intra-erythrocytic development of *P. falciparum* takes approximately 48 hours before parasites egress from the infected RBC and merozoites are released which invade fresh erythrocytes. The rupture of the infected blood cells causes the pathogenesis of the disease and the typical bouts of fever.

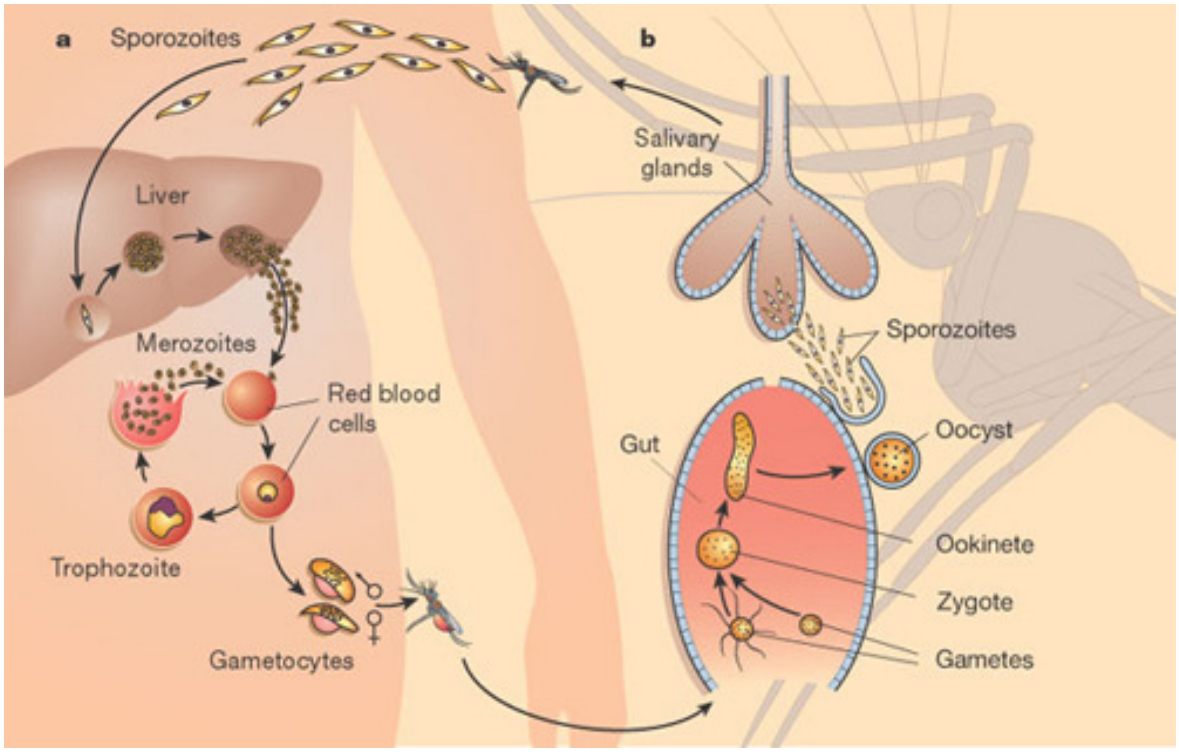

Figure 1-2: The life cycle of *Plasmodium*.
During its life cycle *Plasmodium* changes between human (a) and female *Anopheles* mosquito hosts (b) and between asexual and sexual development. Once an infected mosquito takes a blood meal, sporozoites are released into the blood stream and migrate to the liver of the human host. Inside hepatocytes the parasites asexually multiply until up to 30,000 merozoites are released again into the blood stream. The merozoites invade red blood cells and develop from ring stages to trophozoites and schizonts. The schizonts divide asexually into merozoites which are released once the host erythrocyte ruptures. This lysis of the blood cells causes the typical symptoms of malaria. The released merozoites infect new erythrocytes and the next intra-erythrocytic cycle continues. In some cases merozites enter red blood cells and develop into male and female gametocytes, the sexual stages of *Plasmodium*. If these stages are ingested by another mosquito, male gametocytes develop into motile male microgametes and the female gametocytes develop into macrogametes. Once a macrogamete is fertilized by a microgamete, the resulting zygote develops into a motile ookinte, which moves to the outside of the midgut epithelium and forms an oocyst. Inside the oocyst, sporozites are asexually produced and finally released into the mosquito's body cavity. The sporozoites migrate into the salivary glands from where they can be finally transmitted to the next human host. This Figure was taken from Wirth (2002), with permission from Nature Publishing Group.

1.3 Blood stages of *P. falciparum*

During the intra-erythrocytic stages, *P. falciparum* asexually develops in a 48 hour cycle. After the release from hepatocytes, merozoites immediately invade

erythrocytes in a process involving multiple receptor-ligand interactions. During invasion of the *P. falciparum* merozoite, the RBC membrane invaginates and parts of it finally separate to form a parasitophorous vacuole which completely encases the parasite and separates it from the erythrocyte cytosol (Cowman and Crabb, 2006; Silvie et al., 2008). In Figure 1-3 a 3D-reconstruction of the ultra-structure of a merozoite is displayed. Merozoites are ellipsoidal with a group of secretory vesicles called the apical organelles located at one pole and the large hemispherical nucleus at the other pole. The apical organelles consist of the rhoptries, micronemes and dense granules, all surrounded by a single membrane. They are essential for the invasion of the parasite into the RBC and release their contents during this process. A single elongated mitochondrion is closely associated with a plastid-like organelle, the apicoplast.

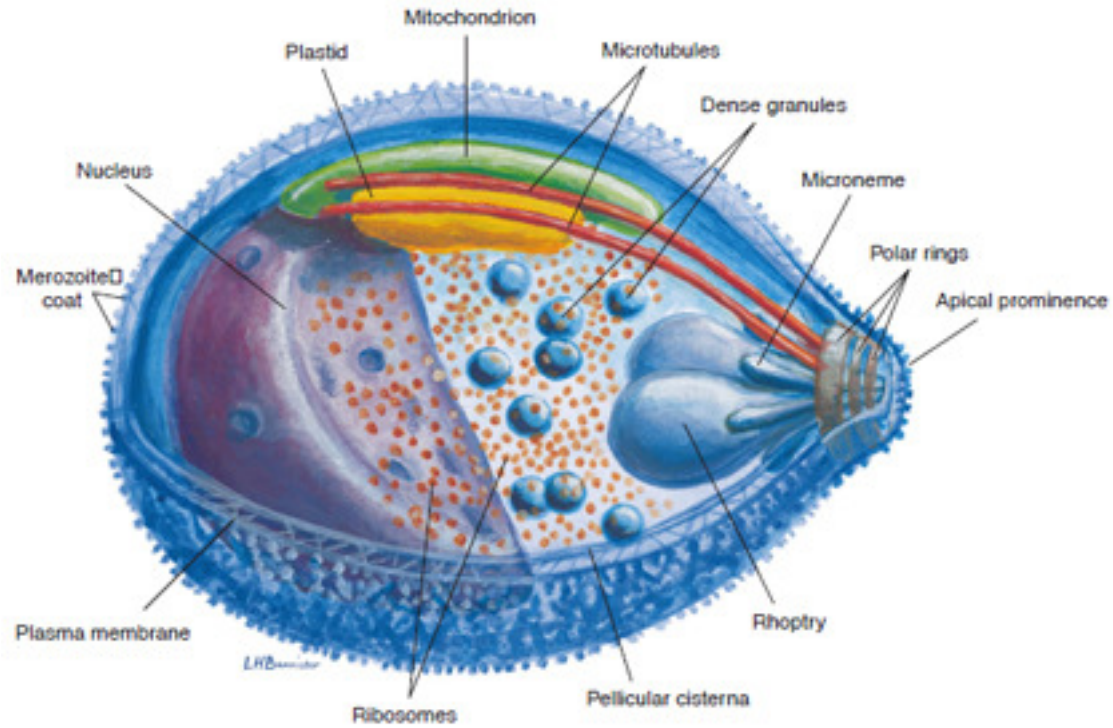

Figure 1-3: 3D-organisation of a *P. falciparum* merozoite.
This reconstituted image is based on serial electron microscope slices. This image was taken from Bannister et al. (2000) with permission from Elsevier Publishing Group.

The apicoplast arose through secondary endosymbiosis of a plastid carrying eukaryote, likely to be a red algae (Sherman, 2005; Waller and McFadden, 2005). It is enclosed by four membranes and has its own 35 kb genome encoding for 30 proteins, most of which are involved in their own synthesis. Most of the genes encoded for in the originally engulfed organism were transferred to the nuclear genome of *P. falciparum* and the encoded proteins have to be imported into the apicoplast after their biosynthesis. The major functions of the apicoplast appear

to be type II fatty acid biosynthesis, assembly of [Fe:S] clusters, synthesis of isopentenyl diphosphate, the precursor for isoprenoid biosynthesis and in conjunction with the mitochondrion, heme biosynthesis (Sherman, 2005; Waller and McFadden, 2005).

The mitochondrion arose through the endosymbiosis of an α-proteobacterium. It is surrounded by a double membrane and contains a very small mitochondrial genome of only 6 kb which only encodes for three protein genes and 20 mitochondrial rRNAs (Feagin et al., 1997; Feagin et al., 1992; Sherman, 2005; van Dooren et al., 2006). Most of the mitochondrial genes were transferred to the nuclear genome. In other organisms the mitochondrion is the major organelle responsible for the generation of ATP. However, for erythrocytic stages of *Plasmodium*, the major energy source is glycolysis in the cytosol and the pyruvate generated is converted to lactate rather than acetyl-CoA to feed into the tricarbolic acid (TCA) cycle (Sherman, 2005). Despite the presence of all TCA cycle enzymes in the *P. falciparum* genome, a mitochondrial pyruvate dehydrogenase (PDH) to produce acetyl-CoA is lacking and the single PDH present in the parasites is localized in the apicoplast. It has therefore been suggested that the TCA cycle instead serves to provide substrates for biosynthesis pathways such as succinyl-CoA for heme biosynthesis (Bozdech et al., 2003; Foth et al., 2005; Gardner et al., 2002). Potentially the TCA cycle serves a more important function during insect stage development. The other important function of the mitochondrion in mammals is the electron transport chain and ATP synthesis by the F_0F_1ATP synthase. No homologues to the mammalian complex I dehydrogenase of the electron transport chain are present, but several other dehydrogenases present can provide electrons instead and compensate for its absence (Gardner et al., 2002; Painter et al., 2007). Homologues to complex II, III and IV are present in the *P. falciparum* genome and can generate a membrane potential across the inner mitochondrion membrane (Gardner et al., 2002). However, two subunits of the F_0F_1ATP synthase are missing, suggesting that this enzyme cannot synthesize ATP (Gardner et al., 2002). Recently it was thus suggested that a major function of the electron transport chain is to act as electron acceptor for dihydroorotate, an essential step in the synthesis of pyrimidine (Baldwin et al., 2002; Krungkrai et al., 1990; Krungkrai et al., 1991; Painter et al., 2007; Sherman, 2005). The pyrimidine biosynthesis pathway is essential for *P. falciparum* parasites, which

cannot scavenge pyrimidines. Other functions of the mitochondrion are the synthesis of [Fe:S] clusters and heme biosynthesis together with the apicoplast. Both apicoplast and mitochondrion remain associated on at least one or two contact points throughout the intra-erythrocytic cycle, suggesting that potentially metabolites are exchanged between the two organelles (Bannister et al., 2000; Hopkins et al., 1999; Kobayashi et al., 2007; van Dooren et al., 2005).

After invasion, the parasite enters the ring stage of the intra-erythrocytic cycle, lasting from 1-18 hours after invasion. Parasites are small at this stage and often resemble a miniature of the RBC in shape. Several food vacuoles are present which contain material of the host cell's cytosol endocytosed through the cytostome. These vacuoles initially possess two membranes, the outer being derived from the parasite plasma membrane and the inner derived from the parasitophorous membrane (Francis et al., 1997; Sherman, 2005). The inner membrane is broken down during the processing of the vacuoles' contents and malaria pigment, or hemozoin begins to form. Globin, the protein component of hemoglobin, is degraded by peptidases, thus providing amino acids for the parasite (Francis et al., 1997). Degradation of globin is a process involving several proteases and peptidases such as plasmepsin aspartic proteases I, II, III and IV, the falcipain cysteine proteases falcipain-2, falcipain-2' and falcipain-3, the metalloprotease falcilysin and aminopeptidases (Banerjee et al., 2002; Dahl and Rosenthal, 2005; Francis et al., 1997; Murata and Goldberg, 2003a; Murata and Goldberg, 2003b; Sherman, 2005). Digestion of large amounts of hemoglobin leaves the parasite with large quantities of free heme containing Fe^{2+}, which once released are oxidized to ferriprotoporphyrin IX (FPIX), containing Fe^{3+}. FPIX causes damage to membranes and proteins and the parasites therefore depend on its efficient detoxification (Orjih et al., 1981). FPIX is initially dimerized to ß-hematin which is then converted to hemozoin. It has been argued that lipids are the primary mediator of non-enzymatic hemozoin formation (Egan et al., 2006; Egan et al., 2002; Pisciotta et al., 2007), but a recent study identified a heme detoxification protein which when recombinantly expressed and purified was able to bind to heme and to convert it into hemozoin (Jani et al., 2008). The parasitophorous membrane begins to undergo changes in this stage as the parasite starts remodelling its host cell.

In the trophozoite stage 18-28 hours post invasion the parasites have rounded up and a single large hemozoin containing vacuole, the digestive vacuole (DV), is present. Smaller vacuoles are formed at the two or three cytostomes containing erythrocyte cytosol which move towards and merge with the DV. Large quantities of host cell hemoglobin are being broken down in the DV. The mitochondrion and apicoplast increase further in size (Sherman, 2005).

The surface of the parasite begins to form deep invaginations and the parasitophorous vacuolar membrane equally begins to form several extensions, forming an interconnected network of tubular and vesicular membranes. These structures mediate both export and import pathways across the intraerythrocytic space and can be divided into several different structures, such as Maurer's clefts, circular cisternae and small vesicles. Some authors use the term tubulovesicular network (TVN) for all these structures, while others refer to only circular cisternae as TVN. The overall functions of these membrane enclosed structures are the uptake of nutrients by providing access to the RBC surface and transport of parasite proteins to the RBC surface (Sherman, 2005).

Proteins exported from the parasite include variant surface antigens such as members of the subtelomeric variable open reading frames family (STEVOR) (Niang et al., 2009) and A-Type RIFINS of the repetitive interspersed family (rif) (Khattab and Klinkert, 2006; Petter et al., 2007). Of particular importance for the development of severe malaria is the *P. falciparum* erythrocyte membrane protein 1 (PfEMP1) encoded by the variant antigene (var) gene family (Pasternak and Dzikowski, 2008). On the erythrocyte membrane PfEMP1 is associated with other parasite secreted proteins which together form "knobs" on the host cell surface. The major structural component of the macromolecular complexes forming these knobs is the knob-associated histidine-rich protein (KAHRP), which itself interacts with PfEMP1 and the erythrocyte cytoskeleton (Crabb et al., 1997; Rug et al., 2006). PfEMP1 interacts with several proteins found on the membrane of endothelial cells or with proteins found on the surface of uninfected RBC. This interaction leads to the sequestration of infected RBC in several tissues and to the rosetting of uninfected and infected RBC. Both can cause occlusions in the vascular system and lead to organ and tissue damage. Sequestration helps the parasite to evade the host's immune system by avoiding clearance of infected RBC by the spleen (Miller et al., 2002).

RNA and protein synthesis are at high levels in the trophozoite stage and the replication of DNA begins. These processes continue in the schizont stage 28-48 hours after erythrocyte invasion. In this stage nuclear divisions take place, leading to 16-32 nuclei while the digestion of host cell hemoglobin and the export of proteins to the RBC surface continue. In preparation for the division into daughter cells, several centres of merozoite formation are created and the assembly of the apical organelles begins with formation of the rhoptries (Bannister et al., 2000). Micronemes and dense granules are formed later in parasite development. The apicoplast begins to elongate and branches before dividing. The mitochondrion begins branching during the trophozoite stage and exists as a branched structure until late in the schizont stage, when it finally divides. Both apicoplast and mitochondrion segregate as a pair into the daughter merozoites (van Dooren et al., 2005).

At the end of schizogony, the DV remains in the residual body, while the daughter merozoites separate. The merozoites remain in the parasitophorous vacuole, until the vacuolar membrane and the erythrocyte plasma membrane break open to release them (Bannister et al., 2000). There is some controversy about the detailed mode of egress and the order in which vacuolar membrane and plasma membrane are broken down. However, despite some controversial data of different studies it is generally suggested that an important role in the egress process is held by parasite proteolytic enzymes (Blackman, 2008).

1.4 Chemotherapies

1.4.1 Antifolates

Antifolates such as pyrimethamine and proguanil target the parasites dihydrofolate reductase (DHFR) (Hyde, 2005; Le Bras and Durand, 2003). Proguanil is a prodrug, which is converted to the active form cycloguanil by the parasite. Antifolates are often used in combination with sulpha drugs such as sulphonamides and sulphones, which inhibit dihydropteroate synthase (DHPS). Both enzymes are involved in the biosynthesis pathway of folate, a cofactor essential for DNA synthesis and other metabolic pathways. Combinations of DHFR and DHPS inhibitors such as sulfadoxine and pyrimethamine (Fansidar) or chloroproguanil-dapson (LapDap) are used as antimalarials. Proguanil is not only

effective on the erythrocytic stages but also on the liver stages of the parasite. However, resistance to antifolates and their combinations with sulpha drugs soon emerged after their introduction due to point mutations in both DHFR and DHPS (Hyde, 2005; Le Bras and Durand, 2003).

1.4.2 Artemisinin

Artemisinin is the active component extracted from the Chinese herb *Artemisis annua*, which has been used in traditional Chinese medicine for centuries to treat fevers and malaria. Analogues such as the water soluble artesunate and the oil soluble artemether are now commonly used in combination therapies with other anti-malarials like mefloquine. The artemisinin based combination therapies (ACT) are recommended by the WHO as the best current treatment of *falciparum* malaria. Several modes of action have been suggested for artemisinins, such as inhibition of heme detoxification (Meshnick, 1998; Pandey et al., 1999). Studies in a yeast model suggested that artemisinin affects the membrane potential in the mitochondria of *P. falciparum* in a mechanism different to atovaquone and leads to the generation of reactive oxygen species (Li et al., 2005). Another target of artimisinin is the SERCA-type ATPase PfATP6 in the parasites endoplasmatic reticulum (Eckstein-Ludwig et al., 2003; Uhlemann et al., 2005).

The artetmisinins were considered to be the only family of drug components fully effective against all strains of *P. falciparum*, but recently a decrease in the efficacy of ACT on the Thai-Cambodian border has been reported (Lim et al., 2005; Vijaykadga et al., 2006).

1.4.3 Atovaquone

Atovaquone is a hydroxynaphthoquinone and an analogue of ubiquinone which targets the electron transfer chain in the parasite mitochondrion by inhibition of the cytochrome bc_1 complex. (Srivastava et al., 1997). However, resistance to this drug emerged fast when the drug was tested as a single therapy due to mutations of cytochrome *b* (Srivastava et al., 1999). Atovaquone is therefore only used in combination therapy with the synergistic partner proguanil trademarked as Malarone (Sherman, 2005). The conversion of the prodrug

proguanil to the active DHFS inhibitor cycloguanil is not required for this synergy (Srivastava and Vaidya, 1999). It has been shown *in vitro* that despite inhibition of the cytochrome bc_1 complex, atovaquone does not eliminate the mitochondrial membrane potential, whereas in combination with proguanil the membrane potential collapses (Painter et al., 2007). It was therefore suggested that proguanil is an efficient inhibitor of an alternative pathway for the generation of this potential and the authors hypothesized that this pathway most likely involves the F_1 subunit of the mitochondrial ATP synthase and the ATP/ADP transporter in the mitochondrial membrane (Painter et al., 2007).

The high cost makes Malarone essentially unaffordable for the population in endemic countries and the drug is usually used by travellers as Malaria prophylaxis.

1.4.4 Quinolines

Quinoline antimalarials are derived from quinine, the active component extracted from the bark of cinchona trees (*Quinona officinalis*). The ground tree bark has been used since the beginning of the 17th century to treat malaria. Derived from quinine, several other quinolines were developed such as chloroquine (CQ), amodiaquine, mefloquine and primaquine. The quinolines can be divided into subclasses, CQ and amodiaquine are 4-aminoquinolines, primaquine is an 8-aminoquinoline and quinine and mefloquine belong to the quinoline-4-methanol drugs.

Of the quinolines, CQ was for a long time the preferred drug for the treatment of malaria due to its low cost, effectiveness and low toxicity. CQ targets the heme detoxification mechanisms in the parasite. It accumulates in the digestive vacuole of the parasite where it binds to FPIX and prevents its detoxification, thus leading to the accumulation of this toxic compound. However, resistance to the drug is now widespread and chloroquine is largely ineffective. Reasons for this drug resistance will be discussed in section 1.6. Amodiaquine like CQ binds to heme and prevents its detoxification.

The modes of action for quinine, mefloquine and primaquine are less well understood. Quinine and mefloquine both interact with heme, but bind with lower affinity to FPIX than CQ (Chou and Fitch, 1993; Slater and Cerami, 1992).

Both partially prevent and reverse some of the abnormalities observed when parasites are treated with CQ. Mefloquine binds with high affinity to phospholipids and even though quinine accumulation in infected RBC has been less well studied, there is evidence that it also binds to phospholipids, suggesting inhibition of the endolysosomal system as their mode of action (Fitch, 2004). Resistance to both mefloquine and quinine has been reported, but while mefloquine resistance arose rapidly, quinine remains widely effective and is often used in combination with antibiotics like tetracycline and clindamycin for the treatment of CQ resistant malaria (Sherman, 2005).

The exact mechanism of primaquine action is equally unknown, but it has been suggested that the drug acts on the parasite's mitochondrion (Foley and Tilley, 1998). Primaquine is effective against liver stages of *Plasmodium* and is therefore used for the treatment of the hypnozoite forming species *P. vivax* and *P. ovale* in combination with quinine or chloroquine.

1.5 Redox and antioxidant systems of *P. falciparum*

1.5.1 Generation of reactive oxygen species

The generation of reactive oxygen species (ROS) such as hydrogen peroxide (H_2O_2), hydroxyl radicals (OH·) and superoxide anions (O_2^-·) are a challenge faced by all organisms living in an oxygenated environment, as ROS directly or indirectly damage macromolecules such as DNA, proteins and lipids inside cells in various ways (Imlay, 2003; Imlay et al., 1988; Storz and Imlay, 1999). *P. falciparum* erythrocytic stages live in an environment of increased oxidative stress, rich in iron and oxygen, the key components for the generation of ROS via the Fenton reaction (Reaction 1). In the parasite's DV, where large quantities of hemoglobin are digested at acidic pH, the conversion of oxidized oxy-hemoglobin containing ferroprotoporphyrin IX (Fe^{2+}) to met-hemoglobin containing ferriprotoporphyrin IX (Fe^{3+}) and O_2^-· is increased compared to uninfected RBC, where only 3% of total hemoglobin is converted in this way (Atamna and Ginsburg, 1993; Becker et al., 2004; Hunt and Stocker, 1990; Misra and Fridovich, 1972).

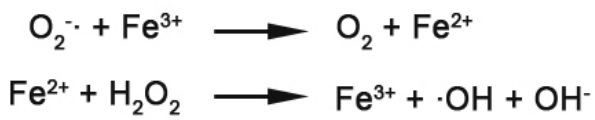

Reaction 1: The Fenton reaction.
ROS are generated in the Fenton reaction in the presence of iron and oxygen.

In infected RBC, not only the parasite but also the host cell itself is subject to increased oxidative stress and oxidative damage. Several blood cell disorders such as α- and ß-thalassaemia and sickle cell anaemia as well as glucose 6-phosphate dehydrogenase deficiency cause a naturally higher level of oxidative stress in the RBC and confer a certain protection against infection with *Plasmodium* (Aslan and Freeman, 2007; Fibach and Rachmilewitz, 2008; Ho et al., 2007; Kwiatkowski, 2005; Rachmilewitz et al., 2005; Williams, 2006). This may either be caused by impaired infection and growth of the parasites in these host cells due to increased oxidative stress or by earlier damage induced alterations to the red blood cell membranes during the development of the parasite and earlier recognition of the infected cells by the immune system (Cappadoro et al., 1998; Eaton et al., 1976; Friedman, 1978; Giribaldi et al., 2001; Pasvol et al., 1978; Williams et al., 2002).

1.5.2 Superoxide dismutases

Superoxide dismutases (SOD) are metalloproteins responsible for the detoxification of superoxide anions. They can be copper/zinc, iron or manganese dependent. *P. falciparum* possesses two distinct Fe-dependent SODs, one localized in the cytosol and one in the mitochondrion (Gratepanche et al., 2002; Sienkiewicz et al., 2004). Both enzymes are responsible for the conversion of superoxide anions generated by the electron transport chain and other metabolic processes to molecular oxygen and hydrogen peroxide. It has previously been suggested that large amounts of the host cell Cu/Zn-SOD taken up into the DV can contribute to the detoxification of superoxide anions generated in this organelle before the enzyme is digested (Fairfield et al., 1983). However, the dismutation of superoxide anions can occur spontaneously in this organelle and might be efficiently accelerated by the low pH and not in need of enzymatic catalysis (Ginsburg and Atamna, 1994). No gene for a catalase has been identified in *P. falciparum*.

1.5.3 Glutathione

In most aerobic organisms low molecular mass thiols function as the principal redox buffer of the cells. The most abundant low molecular weight thiol is the tripeptide glutathione (GSH) or γ-glutamyl-cysteinyl-glycine, which is found in eukaryotes and gram-negative bacteria, whereas gram-positive bacteria synthesize mycothiol (Fahey et al., 1978; Newton and Fahey, 2002; Sies, 1999). An interesting exception are trypanosomatids like the causative agents of African sleeping sickness (*Trypanosoma brucei gambiense*, *Trypanosoma brucei rhodesiense*) and leishmaniasis (for instance *Leishamnia major*, *Leishmania donovani*), where two GSH molecules are conjugated to spermidine to form trypanothione (Fairlamb and Cerami, 1992; Steenkamp, 2002).

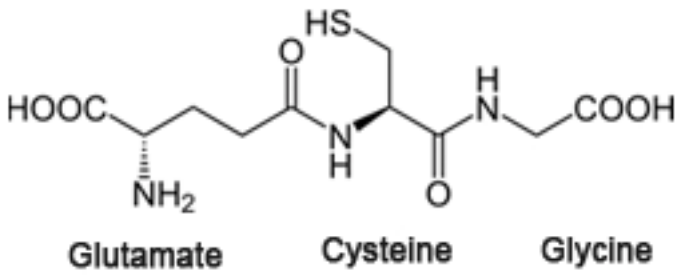

Figure 1-4: Structure of GSH.
The tripeptide GSH consists of the amino acids glutamate, cysteine and glycine. Glutamate and cysteine are ligated through a γ-glutamyl amide linkage.

GSH serves various different functions in cells apart from being a redox buffer. It is a cofactor for detoxifying enzymes and proteins such as glutathione-S-transferases (GSTs), glutatredoxins and glyoxalases and is involved in non-enzymatic reactions such as the termination of radical chain reactions.

1.5.3.1 Glutathione metabolism of *P. falciparum*

Figure 1-5 displays an overview of the GSH metabolism in *P. falciparum* parasites. GSH is synthesized in two consecutive steps by the enzymes γ-glutamylcysteine synthetase (γGCS) and glutathione synthetase (GS) (Figure 1-5). Both enzymes have been identified in the malaria parasite *P. falciparum* (Lüersen et al., 1999; Meierjohann et al., 2002a) and because their roles and importance for the survival of the intra-erythrocytic stages of *P. falciparum* is analysed in this study, both are described in more detail in section 1.5.3.2.

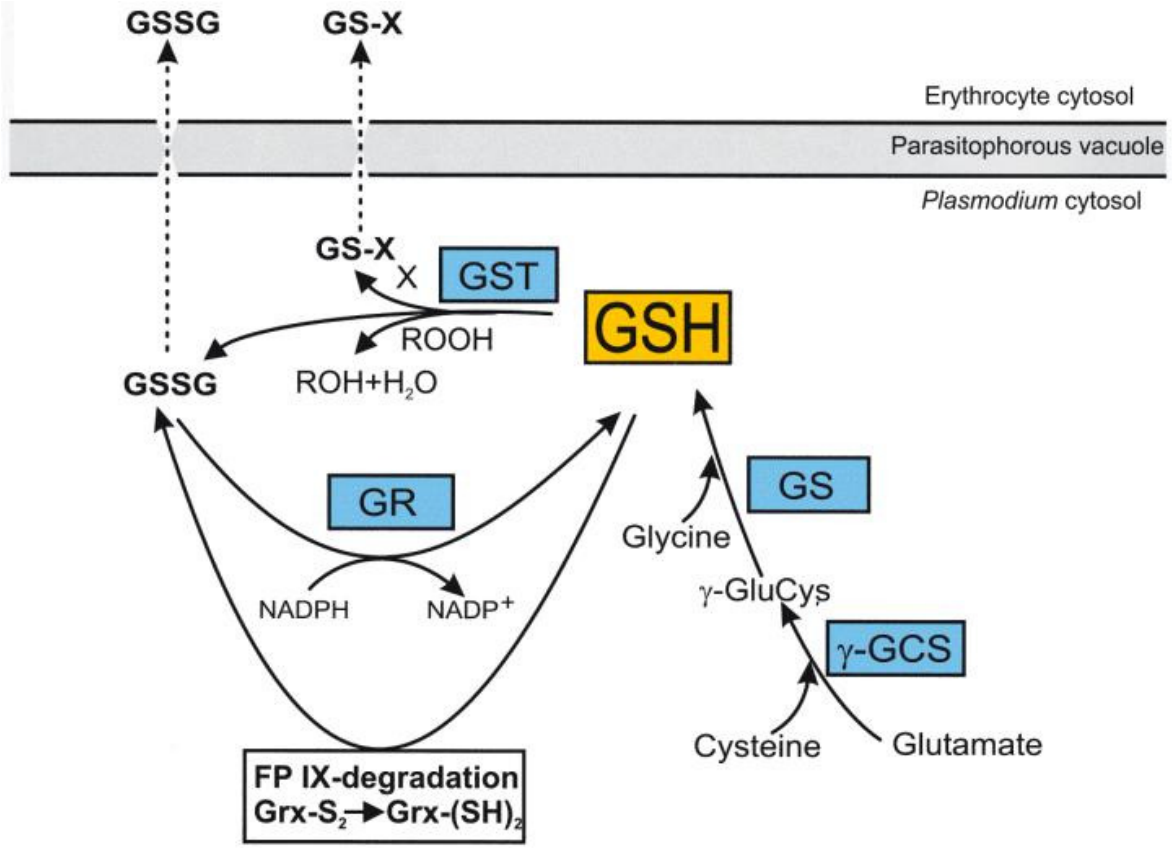

Figure 1-5: GSH metabolism of *P. falciparum*.
GSH is synthesized in two consecutive steps by the enzymes γ-glutamylcysteine synthetase (γGCS) and glutathione synthetase (GS). GSH is used by the single glutathione-S-transferase found in *P. falciparum* to label xenobiotics (X) for export (GS-X). GS-X adducts are excreted from cells via pumps such as multidrug resistance proteins. GST can also use GSH to detoxify peroxides which leads to the formation of oxidized glutathione disulphate (GSSG). GSSG is also produced by the reduction of glutaredoxins (Grx-S_2 to Grx$(SH)_2$) and the degradation of ferriprotoporphyrin IX (FPXI). GSSG is either excreted from the parasite or reduced to GSH by glutathione reductase (GR). This figure was taken from Müller (2004) with permission from Blackwell publishing group.

Oxidation of GSH leads to the formation of glutathione disulphide (GSSG), which is reduced back to GSH by the flavoenzyme glutathione reductase (GR) in a NADPH dependent mechanism in order to maintain a high GSH:GSSG ratio (Figure 1-5) (Meister and Anderson, 1983). The NADPH needed for the reduction of GSH is mainly provided by the hexose monophosphate shunt, which shows an approximately 78 times higher activity in infected RBC than in uninfected RBC (Atamna et al., 1994; Meister and Anderson, 1983). PfGR has been biochemically characterized and received a lot of interest as a potential drug target (Farber et al., 1996; Gilberger et al., 2000; Krauth-Siegel et al., 1996). The antimalarial dye methylene blue is a selective inhibitor of PfGR and chemosensitizes parasites by the depletion of reduced GSH (Becker et al., 2003b; Farber et al., 1998).

In order to maintain a high GSH:GSSG ratio, parasites not only reduce GSSG, but also excrete large amounts of the disulphide (Figure 1-5). Ginsburg and colleagues previously suggested that this might be a way in which the parasites supply their host cell with GSH, as erythrocytes contain high levels of HsGR (Atamna and Ginsburg, 1997). However, later studies found that the disulphide is lost entirely from the infected RBC and is released into the culture medium (Lüersen et al., 2000; Meierjohann et al., 2002b). This efflux of GSSG is possibly the reason why infected RBC contain lower GSH concentrations than non-infected RBC (Ayi et al., 1998; Lüersen et al., 2000; Meierjohann et al., 2002b).

Earlier studies detected glutathione peroxidase activity in *P. falciparum* (Fritsch et al., 1987), but no glutathione peroxidase protein was identified and a potential candidate turned out to be thioredoxin-dependent rather than GSH-dependent (Sztajer et al., 2001). Potentially the detected activity was due to peroxidase activity of the single glutathione-S-transferase (GST) found in *P. falciparum*, which serves as an alkyl hydroperoxide peroxidase *in vitro* (Figure 1-5) (Harwaldt et al., 2002; Liebau et al., 2002). This GSH-dependent enzyme is present in high concentrations in the parasites. GSTs conjugate GSH to a variety of substrates such as mutagens and drugs and thus label them for export. Another interesting function that has been suggested for PfGST is the sequestration of FPIX, which binds uncompetitively to this protein (Harwaldt et al., 2002; Liebau et al., 2002).

P. falciparum possesses one classical glutaredoxin (Grx1) in addition to three glutaredoxin-like proteins (GLPs) (Becker et al., 2003b; Rahlfs et al., 2001). Glutatredoxins are small heat-stable dithiol-dilsufide oxidoreductases, which protect cells from oxidative damage and can interact with sulphydryl groups of other proteins in order to either reduce or oxidize them (Becker et al., 2003b; Müller, 2004). One function suggested for Grx1 in *P. falciparum* is to reduce ribonucleotide reductase, which is involved in the first step of DNA synthesis. Glutaredoxins are reduced by GSH, which leads to the formation of GSSG (Figure 1-5). In rice Grx was also found to have glutathione peroxidase activity (Lee et al., 2002).

GSH is also used as a cofactor for the detoxification of toxic 2-oxoaldehydes such as glyoxal and methylglyoxal by the glyoxalases GlxI and GlxII in *P. falciparum*.

In the first reaction step, GlxI forms a thiol ester bond between GSH and the aldehyde, thus producing an S-2-hydroxyacylglutathione conjugate. This ester is hydrolysed by GlxII, thus releasing GSH and a non-toxic 2-hydroxycarbolic acid (Akoachere et al., 2005).

1.5.3.2 Glutathione biosynthesis

The PfγGCS is encoded by a single exon gene on chromosome 9 (PFI0925w, http://plasmodb.org) and is related to the γGCS of other non-plant eukaryotes. The predicted PfγGCS amino acid sequence of the 3D7 strain has a molecular mass of 124 kDa and is thus almost twice the size of the human catalytic subunit. The *P. falciparum* enzyme has not been biochemically characterized. Alignment of the deduced amino acid sequence with the human and *T. brucei* homologues reveals an overall sequence identity of only 19.7 and 18.6 %, respectively, but in four more conserved regions the homologies are much higher and share 31.3 -43.9 % identities (Figure 1-6) (Lüersen et al., 1999). Within these regions of homology, several amino acid residues involved in substrate binding in other species are conserved (Chang, 1996; Lueder and Phillips, 1996; Lüersen et al., 1999). The PfγGCS further possesses a conserved cysteine residue in or near the proposed active site. Three large insertions divide the regions of homology and the function of these insertions is unclear. Several other plasmodial proteins contain such insertions and their function in those is also unknown. The first insertion (from residue 151-389) contains a repetitive sequence motif (Y/C)QS(N/D)LQQ(Q/R). This octamer is only present once in 3D7 PfγGCS, but other strains investigated by Lüersen *et al.* contained eight (FCBR, FCH5, K1, 7G8), nine (HB3) or ten (Dd2) repeats, leading to an increase in the predicted size for PfγGCS in those strains (Lüersen et al., 1999). The function of such repetitive elements is unknown, but they have also been found in other *Plasmodium* proteins (Cowman et al., 1984; Eisen et al., 1998). No correlation between the repeats and the geographic origin of the parasite strains investigated was found for PfγGCS (Lüersen et al., 1999). Northern analysis showed a stage specific transcription pattern of PfγGCS, with a baseline level of transcription throughout the intra-erythrocytic life cycle and a peak in the mature trophozoite stage (Lüersen et al., 1999). Microarray data published on PlasmoDB (http://plasmodb.org) shows a continuous expression with a peak in the schizont stage.

```
P.f.   MGFLKIGT-P LSW--DDVQD VKSLIRLYGI LQFVHVYKLN KDRYDENIMF GDEIEYIIIR   57
T.b.   MGLLTTGGQP LQWGTEENNR AKEYVSAHGI QQFLWVYNKQ KELPDFPFLW GDEIEHQLVR   60
H.s.   MGLLSQGS-P LSW--EETKR HADHVRRHGI LQFLHIYHAV KDRHKDVLKW GDEVEYMLVS   57

P.f.   ND-ESLKESS ALLCASDLID EMMNLESVID CQYGSHWTPE YSSFTIEGTP SVPFKLDINS  116
T.b.   L--ESRKVKL SLNAADVIKR LSQSSGESTA -----EWRPE YGSFMVESLP GKPYSSNVDS  113
H.s.   FDHENKKVRL VLSGEK-VLE TLQEKGERTN PNHPTLWRPE YGSYMIEGTP GQPYGGTMSE  116

P.f.   SCFVEDCMRI RRSKLNNVLS AVQGARAITL PCFPNVLLNN SVLMARRITG HESTKKKFDS  176
T.b.   LCSVEVNMRR RYHMLD--AA AGDNTFAVTL VTFP------ ---------- ----------  145
H.s.   FNTVEANMRK RRKEAT--SI LEENQALCTI TSFP------ ---------- ----------  148

P.f.   KGKVEFIENA KIKEKVHNSN NNIHKIINNK NNESKIVNNA FDQNKISSIE MVSYEMDENK  236
T.b.   ---------- ---------- ---------- ---------- ---------- ----------
H.s.   ---------- ---------- ---------- ---------- ---------- ----------

P.f.   STNFVNSDTV FAKNDEEGEV EEEDENENEQ QQQQQQYQSN LQQQYQSNLQ QQYQSNLQQQ  296
T.b.   ---------- ---------- ---------- ---------- ---------- ----------
H.s.   ---------- ---------- ---------- ---------- ---------- ----------

P.f.   YQSDLQQQYQ SDLQQQYQSD LQQQYQSDLQ QQYQSDLQQQ NVQPKQRQQM IQYVYDDEIE  356
T.b.   ---------- ---------- ---------- ---------- ---------- ----------
H.s.   ---------- ---------- ---------- ---------- ---------- ----------

P.f.   NKNKEKDNTP RSCNDYNNVN DSSNTQDIFI SSLKKTDSLF E-CEVFKPEQ TNKYSKSALI  415
T.b.   ---------- ---------- ---------- ---LMGVGGF T----TSTET ESPCSQSLFV  168
H.s.   ---------- ---------- ---------- ---RLGCPGF TLPEVKPNPV EGGASKSLFF  175

P.f.   TDMTISP-HA RYVTLTQNIR HRHGTKIVSF NPIYKDINTE KMDHWKMSLD CNDKRLFKKV  474
T.b.   PDACINDSHP RFKALTNNIR IRHGRKVCIQ VPMFIDRYTM ERTVDPRVNI DLHPRNVEIV  228
H.s.   PDEAINK-HP RFSTLTRNIR HRHGEKVVIN VPIFKDKNTP SPFIETFTED DEASRASK--  221

P.f.   KKKLTLDEHL IWNKSMTNKK IIDRKNNNPR DEVLNTSNFT LAMTNKEENN NENSLMDRVL  534
T.b.   CTFSGEKTSS KGKKFSCDTI TPKRVPLENE AITNMTHLYT PVTHYYYAQY FQNLQAERVK  288
H.s.   ---------- -------- ---------- ---------- ---------- ----------  232

P.f.   KNSLFANMDD EGDYIYVYNR EFIQEYSEKC KNPIKNYVYL DAMFFGMSMC CQQLTMSFPT  594
T.b.   QRYQACPCPV PSVN------ ---------- ----HPCIYM DCMAFGMGCN CLQLTMQLPN  328
H.s.   ---------- ---------- ---------- ----PDHIYM DAMGFGMGNC CLQVTFQACS  258

P.f.   VDDAKYVYDQ LAVIAPLFLA LTACTPYLGG FLTETDTRWR VISNSVDCRT EEE-------  647
T.b.   EAQARHIYDQ LGILCPLFLA LSSATPFQKG ILCESDVRWL TITASVDIRK YEE-------  381
H.s.   ISEARYLYDQ LATICPIVMA LSAASPFYRG YVSDIDCRWG VISASVDIRT REERGLEPLK  318

P.f.   --LSYICKPR YSGISLYISS ELPLKRNYYF YNDVDVILDK NVYDKLKKEN VDEYLARHIA  705
T.b.   --VPHIIKSR YDSISVFVSS LTPNLEE--- FNDEVLRIND SYYNLLTREG VDSRLATHIA  436
H.s.   NNNYRISKSR YDSIDSYLSK CGEK------ YNDIDLTIDK EIYEQLLQEG IDHLLAQHVA  372

P.f.   SLFVRDPIVV FEGSYSERDI ATIQKKIMEL SNDEDKIKGM VEGSSSNSLS SKVLLDNEDR  765
T.b.   HLFIRDPLVI Y--------- ---------- ---------- ---------- ----------  447
H.s.   HLFIRDPLTL F--------- ---------- ---------- ---------- ----------  383

P.f.   NKNDSSIKEM NKSNDNNHNN NCHIEYNNKK DINMNKIYLS DNFEFIEDYE EKVLSSHQHF  825
T.b.   ---------- ---------- ---------- ---------- -----DQMID IDDHTHVDHF  462
H.s.   ---------- ---------- ---------- ---------- -----EEKIH LDDANESDHF  398

P.f.   ENFQSTNWNS VRFKPPPILD NHFKGPSSIG WRVEERTPDI QITDFENSCV VTLVMLLSKF  885
T.b.   ENIQSTNWQT VRLKLP-VLD ------STLG WRVERRMDV MPTPFENAAY SVFVVLLTRA  515
H.s.   ENIQSTNWQT MRFKPPPPN- ------SDIG WRVERRMEV QLTDFENSAY VVFVVLLTRV  451

P.f.   ILKERLNLYI PMTLLEENLF RASKREALTK EKFYFRKDLS YDTLNNEFEE KSI-------  938
T.b.   IMRFGAVFYT KLSIVDENMG RAHNINPC-Q QHYIMRRDIF ASKVTTDPSE NC--------  566
H.s.   ILSYKLDFLI PLSKVDENMK VAQKRDAVLQ GMFYFRKDIC KGGNAVVDGC GKAQNSTELA  511

P.f.   --------YD IFFNETNGLF FLCYKYVDEL FKEGLLNQSA KNKIDEYIEF VKQRCSGKIC  990
T.b.   -----ELTVG EVINGKPGEY YGLIPLVRRY LEEENIQSDV ---VEGYLNF ISKRACGEIP  618
H.s.   AEEYTLMSID TIINGKEGVF PGLIPILNSY LENMEVDVDT RCSILNYLKL IKKRASGELM  571

P.f.   TGAMYIRNFI LNHPAYEKNS YINSKINYDI CKLIADIGKG LIIPQELLGV FVDPYKERIK 1050
T.b.   TAAQYIRNFV KKHPDYREDS RLTEQIAHDV VNHVHQLACG GNASESMIGA YTLGSKRQRE  678
H.s.   TVARWMREFI ANHPDYKQDS VITDEMNYSL ILKCNQIANE LCECPELLGS AFRKVKYSGS  631

P.f.   SDIRQINESQ YLKSLAYKYI SGEDYTQYLL LNEVLKDDQD YCTCTRRTIY EESMDNTVEF 1110
T.b.   G                                                                 679
H.s.   KTDSSN                                                            637

P.f.   AKKMYELSA                                                        1119
```

Figure 1-6: Alignment of PfγGCS with human γGCS catalytic subunit and *T. brucei* γGCS. Insertions in PfγGCS are in italics while invariant amino acid residues are bold. Lys and Arg residues potentially involved in substrate binding and the putative active site Cys are boxed.

Shaded areas and arrows indicate primers used in the previous study by Lüersen *et al.* This figure was taken from Lüersen *et al.* with permission from Elsevier Publishing Group (Lüersen et al., 1999).

An inhibitor for γGCS, L-buthionine sulfoximine (L-BSO) (Griffith, 1982) has previously been shown to inhibit *P. falciparum* growth *in vitro* (Lüersen et al., 2000). Inhibition of γGCS activity takes place in both the host cell and the parasite compartment and leads to a decrease in cellular GSH in both. Within 2 hours, half of the cellular GSH is lost from infected RBC after inhibition of the biosynthesis of the tripeptide. Therefore the effect of L-BSO was related to an increased physiological need for GSH in infected RBC instead of specific inhibition of PfγGCS (Lüersen et al., 2000). Administration of extracellular GSH relieves the effect. It remained unclear whether the animalarial effect of L-BSO observed was due to a direct killing of the parasite through inhibition of PfγGCS, or if the effect was a consequence of the death of the host cell due to inhibition of the human enzyme, or indeed a combination of both.

In various species, γGCS catalyses the rate limiting step of GSH biosynthesis. Studies of recombinant *T. brucei* γGCS showed that TbγGCS is active as a monomer and feedback inhibited by GSH (Lueder and Phillips, 1996). Further studies of γGCS in this organism showed that a gene knock-down using RNAi is lethal for *T. brucei*. This phenotype was rescued by extracellular GSH, suggesting that *T. brucei* has the ability to take up the tripeptide (Huynh et al., 2003). Human γGCS is active as a heterodimer consisting of a catalytic and a regulatory subunit (Tu and Anders, 1998). Activities of both the catalytic subunit and the holoenzyme are regulated by intracellular GSH levels by feedback inhibition. Other mechanisms regulating the activity and abundance of human γGCS were suggested to be subunit interactions and control of gene expression (Tu and Anders, 1998). Disruption of the catalytic γGCS subunit in mice is lethal during embryonic development (Shi et al., 2000). Interestingly, cell lines isolated from blastocysts in the same study were viable in the presence of N-acetylcysteine or GSH, but failed to grow in their absence. Similar results were found for the fungi *Saccharomyces cervisiae* and *Candida albicans*. A mutation in γGCS abolishing enzyme activity leads to GSH auxotrophy in *S. cervisiae* (Grant et al., 1996) as does the knockout of γGCS in *C. albicans* (Baek et al., 2004). In contrast to the *S. cervisiae* mutants which can survive the loss of γGCS activity in the presence of other thiols such as dithiothreitol, cysteine and ß-

mercaptoethanol, *C. albicans* γGCS knockout cells required exogenous GSH, GSSG or γGC for survival.

Recently a knockout of the *ygcs* gene was reported in *P. berghei* (Vega-Rodriguez et al., 2009). The knockout line displayed only a mild growth defect in the intra-erythrocytic stages, while the development in the mosquito was severely affected and the genetically modified parasites were unable to produce sporozoites. Interestingly, the knockout parasites still contained low levels of GSH in the erythrocytic stages, albeit 7 to 26 times less than the wildtype. The authors suggested that the remaining GSH may be attributable to uptake from the host cell and is sufficient for intra-erythrocytic development (Vega-Rodriguez et al., 2009).

γ-GCS sequences can be divided into three different groups: those of γ-protobacteria, those of non-plant eukaryotes and those of α-protobacteria and plants (Copley and Dhillon, 2002). Their origin is not clear, one hypothesis is that the gene arose amongst the bacteria and was transferred by lateral gene transfer from a mitochondrial progenitor. Another hypothesis is that the gene arose in the last common ancestor and was subsequently lost from archea, many bacteria and those eukaryotes lacking mitochondria (e.g. *Giardia*, *Trichomonas*). Even though the massive disappearance of the gene from anaerobe living organisms is plausible, it would mean that the *ygcs* gene originated before the emergence of an aerobic atmosphere (Copley and Dhillon, 2002).

A single exon gene on chromosome 5 encodes for the second enzyme for GSH biosynthesis, PfGS (PFE0605c, http://plasmodb.org) and the enzyme has previously been characterized (Meierjohann et al., 2002a). The recombinant enzyme is active as a homodimer with a subunit mass of 77 kDa. PfGS only displays a moderate degree of amino acid identity compared with its homologues in humans, *Arabidopsis thaliana* and *S. cervisiae* (18.2, 19.8 and 18.5 %, respectively), but several residues involved in binding of substrates and cofactors are conserved (Figure 1-7) (Meierjohann et al., 2002a). A highly conserved region is a glycine rich loop between Lys-517 and Lys-525, which in the *E. coli* homologue is involved in binding of ATP and stabilisation of the γ-glutamyl-cysteinyl-phosphate intermediate. Due to several insertions, the *P. falciparum* enzyme is 150 to 200 amino acids longer than its homologues

(Meierjohann et al., 2002a). These insertions are spread over the entire sequence, the largest being between residues 351-392 (Figure 1-7).

Knockout studies revealed that GS is not essential for the survival of *S. cervisiae* (Grant et al., 1997), where mutants are viable, albeit showing reduced growth and presumably depend on the precursor of GSH, γ-GC. In mammals a decreased activity of GS can cause mild to debilitating diseases including 5-oxoprolinuria, haemolytic anaemia and neurological dysfunction (Dahl et al., 1997; Shi et al., 1996). No complete loss of GS activity in humans has been reported, indicating an essential role for the enzyme in humans.

GS sequences fall into two distinct groups, bacterial GS and eukaryotic GS. GS most likely was recruited from the ATP-grasp superfamily of proteins after a γGCS gene was acquired and evolved independently in bacteria and eukaryotes (Copley and Dhillon, 2002).

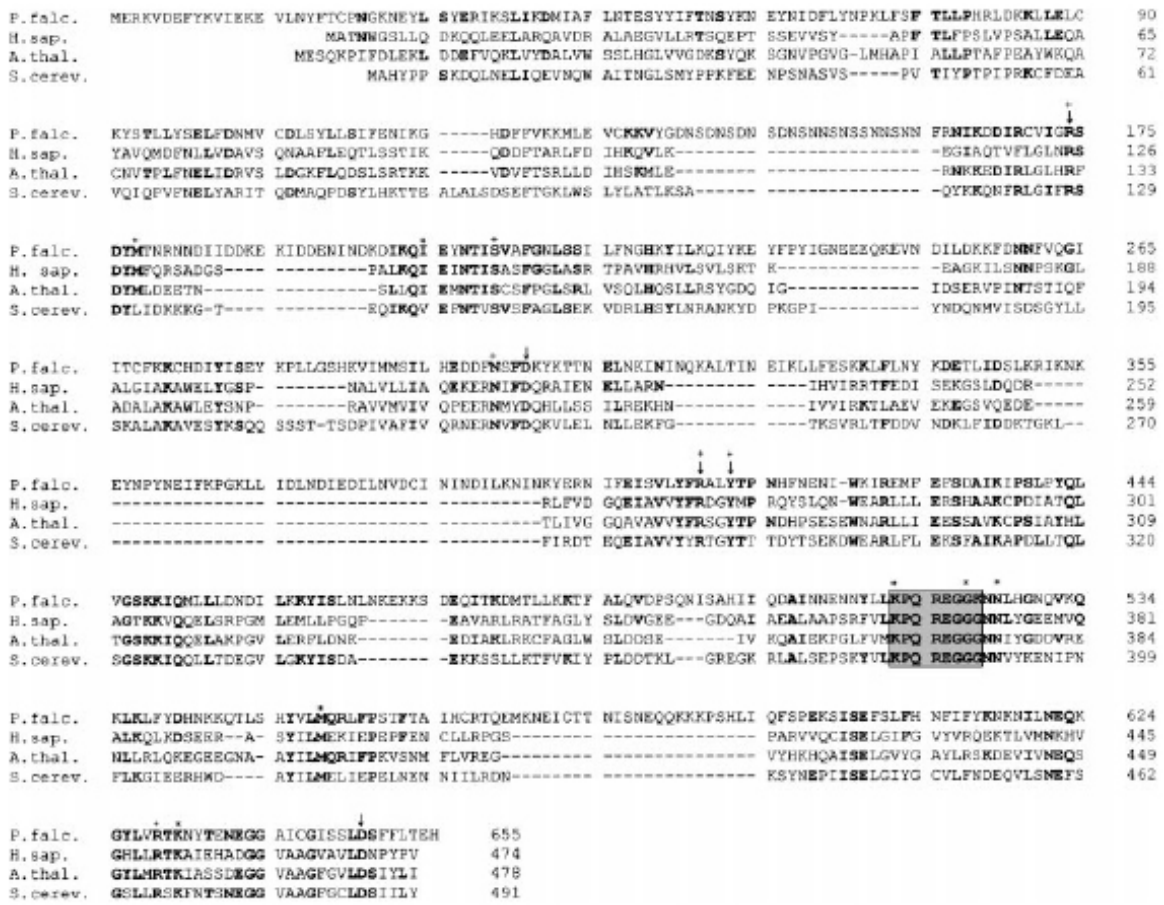

Figure 1-7: Alignment of the PfGS amino acid sequence with the *Homo sapiens*, *A. thaliana* and *S. cervisiae* sequences.
Asterisks, arrows and crosses indicate conserved residues for ATP, γGC and GSH binding, respectively. A highly conserved glycine rich loop is marked by the shaded box. This figure was taken from Meierjohann et al. (2002a), with permission from the Biochemical society.

1.5.4 Thioredoxin

Another important thiol antioxidant system is the thioredoxin (Trx) system. Similar to GSH, the small 12 kDa Trx proteins detoxify ROS and nitrogen metabolites, are involved in protein folding and provide reducing equivalents for enzymes such as ribonucleotide reductase. Trx and the glutaredoxins belong to the thioredoxin superfamily characterized by the active site CXXC motif (Rahlfs et al., 2003). Often more than one Trx can be found in a single organism. *P. falciparum* possess a classical Trx, PfTrx1 which localizes to the cytosol (Kanzok et al., 2000; Krnajski et al., 2001a; Rahlfs et al., 2002) as well as a second mitochondrial Trx, PfTrx2 (Boucher et al., 2006). In addition, two thioredoxin-like proteins have been identified as well as the Trx related protein plasmoredoxin (Becker et al., 2003a; Sherman, 2005). Plasmoredoxin appears to be a unique antioxidant of *Plasmodium* species, but it is not essential for the survival of the rodent species *P. berghei* (Buchholz et al., 2008).

To maintain Trx in a reduced state, *P. falciparum* possesses a high molecular weight Trx reductase (TrxR), similar to the TrxR found in mammals and insects (Müller et al., 1996). Similar to GR, TrxR is a flavoenzyme and uses NADPH as reducing cofactor. The function of TrxR is essential for parasite survival (Krnajski et al., 2002).

1.5.5 Peroxiredoxins

P. falciparum possesses five peroxiredoxins, antioxidant enzymes which act as peroxidases and thus contribute to the detoxification of hydrogen peroxide and other peroxides. Two of the peroxiredoxins are Trx-dependent, belong to the family of typical 2-Cys peroxiredoxins and are localized in the cytosol (PfTrx-Px1) (Krnajski et al., 2001b; Rahlfs and Becker, 2001) and mitochondrion (PfTrx-Px2) (Boucher et al., 2006). A third is a typical 1-Cys peroxiredoxin which has only slight activity with Trx and the electron donor is still controversial (Kawazu et al., 2000; Kawazu et al., 2007; Krnajski et al., 2001b). The two groups of peroxiredoxins differ in the number of conserved cysteine residues within the active site. The *P. falciparum* antioxidant protein (PfAOP) is another 1-Cys peroxiredoxin which displays some homologies to atypical 2-Cys peroxiredoxins (Sarma et al., 2005). The fifth peroxiredoxin is the glutathione-peroxidase like

protein, which despite its homology to glutathione peroxidases prefers Trx as a reducing agent (Sztajer et al., 2001). Even though disruption of the single Trx reductase is lethal for the parasites and thus suggests an important role of the Trx system for the parasites survival (Krnajski et al., 2002), there is some redundancy between the peroxiredoxins. PfTrx-Px1 appears to be the major cytosolic peroxidase, but a knockout of this gene is not lethal in erythrocytic stages (Komaki-Yasuda et al., 2003; Sherman, 2005).

1.6 Chloroquine resistance

CQ is a lipophilic, weak base which crosses membranes by passive diffusion and accumulates in the DV of *Plasmodium* species due to protonation in this acidic environment and binding to free heme (Bray et al., 1999; Saliba et al., 1998). Several mechanisms have been suggested to be involved in the establishment of CQ resistance: (1) Reduced access of CQ to hematin (2) increased efflux of CQ (3) decreased influx of CQ, potentially caused by changes of vacuolar pH (4) increased detoxification of CQ, heme and CQ-heme complexes.

CQ resistant strains of *P. falciparum* have been shown to accumulate significantly less CQ in their DV than CQ sensitive strains, thus keeping the concentration of the drug below the toxic level. The phenotype of reduced CQ accumulation in these studies is reversible with verapamil, a Ca^{2+} channel blocker and inhibitor of ABC transporters (Bray et al., 1998; Fidock et al., 2000; Fitch, 2004; Sanchez et al., 2003). Recent studies showed that reduced CQ accumulation did not correlate with changes in the vacuolar pH as sensitive and resistant parasites have comparable steady-state pH values (Hayward et al., 2006; Kuhn et al., 2007). Without changes in the vacuolar pH and hemoglobin digestion, CQ accumulation should be comparable between sensitive and resistant strains; this suggests the presence of a permeation pathway in resistant parasites.

1.6.1 *P. falciparum* Chloroquine Resistance Transporter

Analyses of a genetic cross between the CQ sensitive HB3 and the CQ resistant Dd2 strain of *P. falciparum* led to the identification of a gene locus and finally to the identification of one particular gene within this locus whose inheritance

matched with the inheritance of CQ resistance (Fidock et al., 2000; Su et al., 1997; Wellems et al., 1991). The hypothetical protein encoded by this gene was named chloroquine-resistance transporter (PfCRT) because of the predicted 10 transmembrane domains (Figure 1-8). PfCRT has since been shown to be expressed in erythrocytic stages and to localize to the membrane of the parasite's DV (Cooper et al., 2002; Fidock et al., 2000). Bioinformatic studies placed PfCRT within the drug/metabolite transporter (DMT) superfamily. The bioinformatic analyses suggested that PfCRT might be active as a dimer with its N- and C-terminus and the even numbered loops facing the cytosol (Martin and Kirk, 2004; Tran and Saier, 2004).

Several mutations in PfCRT have been found in various CQ resistant and sensitive parasite lines, but the single mutation found in almost all resistant lines and absent in the sensitive lines is the mutation of a lysine residue to a threonine in amino acid position 76 (Figure 1-8). This mutation is in *P. falciparum* always accompanied by several other mutations, suggesting that the K76T substitution interferes with the natural function of PfCRT and compensatory mutations need to be established concomitantly to allow this exchange. The additional mutations vary in relation to the geographic origin of the isolates. However, most CQ resistant field isolates carry an A220S mutation in addition to K76T while the other mutations vary, indicating a special importance of this mutation for the maintenance of PfCRT function (Cooper et al., 2005). The exceptions are strains isolated from the Philippines, where instead of the A220S mutation two mutations, A144T and L160Y, are found in combination with K76T (Chen et al., 2003). Allelic exchange studies showed that replacement of the wild-type *pfcrt* allele in a CQ sensitive strain with the *pfcrt* alleles of resistant strains is sufficient to establish CQ resistance (Sidhu et al., 2002). Further studies showed that the reversal of the single K76T mutation to T76K abolishes CQ resistance (Lakshmanan et al., 2005). In laboratory strains it was also possible to generate CQ resistance by replacing the lysine residue at position 76 with a neutral residue other than threonine such as asparagine or isoleucine (Fidock et al., 2000; Lakshmanan et al., 2005).

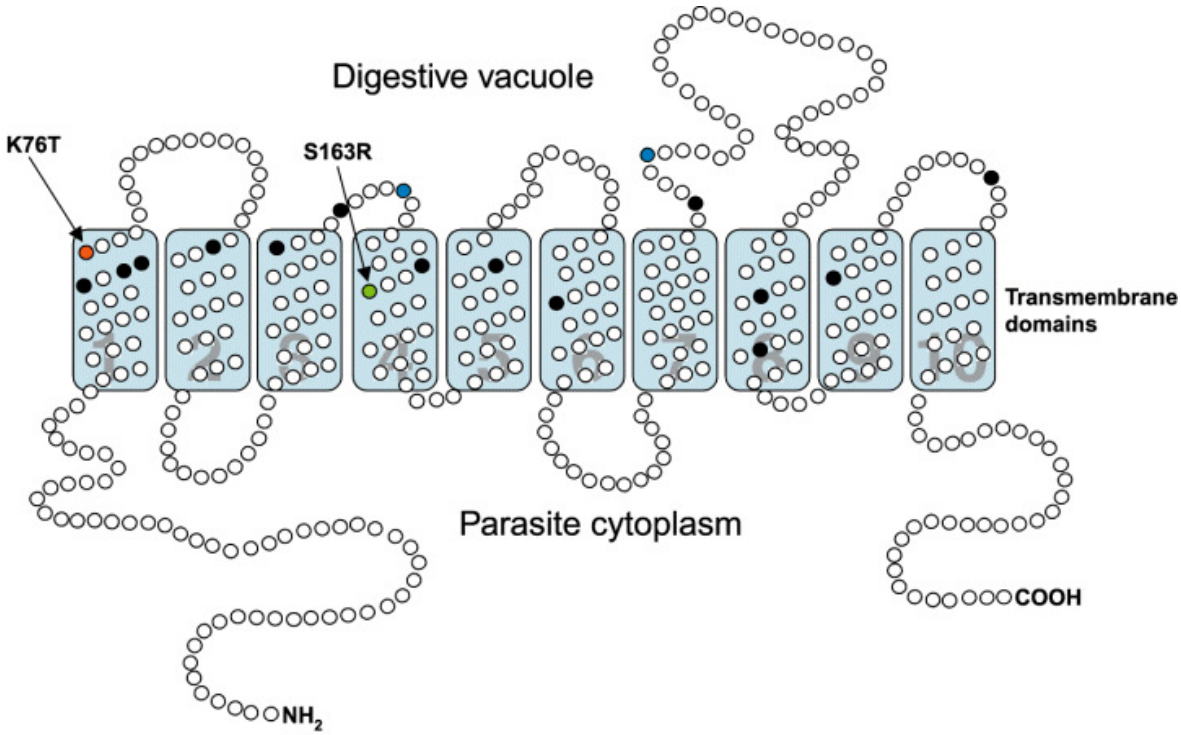

Figure 1-8: Predicted structure of PfCRT.
The PfCRT protein is predicted to possess 10 transmembrane domains with the N- and C-terminus extending into the parasite cytosol. The red circle indicates the critical K76T mutation found in CQ resistant parasites. Black circles indicate additional mutations found in CQ resistant field isolates. Green and blue circles indicate mutations selected for in amantadine resistant parasites, where the S163R mutation (green) re-establishes CQ sensitivity. This Figure was taken from Bray et al. (2005) with permission from Wiley-Blackwell publishing group.

Two models currently exist for the functions of PfCRT in CQ resistance, that of a channel allowing protonated CQ to exit the DV along the electrochemical and concentration gradient and that of an active transporter (Sanchez et al., 2007b).

Data arguing for PfCRT being an active transporter were presented by Sanchez *et al.*, who observed the phenomenon of *trans*-stimulation in CQ resistant parasites. Trans-stimulation describes the apparent stimulation of the transport of one substrate from the *cis* to the *trans*-site of a membrane (e.g. from cytosol to the DV) by the presence of the substrate on the *trans* site. Indeed the amount of radioactive CQ taken up by resistant parasites was higher, when parasites were preloaded with low concentrations of unlabelled CQ before the uptake of radio-labelled CQ was measured. This was not observed in sensitive strains or if the parasites were energy starved (Sanchez et al., 2005; Sanchez et al., 2003). Investigation of efflux under reverse trans-stimulation conditions however revealed a trans-stimulation effect in sensitive as well as resistant parasites (Sanchez et al., 2007a). The interpretation by Sanchez *et al.* is that wild-type PfCRT may be a predominantly exchange-only carrier which is converted to a

net-transporting carrier by the K76T mutation and co-transports CQ with protons (Sanchez et al., 2007b).

Data in favour of the channel model show that efflux of CQ is energy independent and also independent of the vacuolar pH gradient. (Bray et al., 2006). Moreover, CQ efflux occurs in starved sensitive parasites and resistant lines (Bray et al., 2006). The authors of this study argued that their data were more in favour of PfCRT acting as a gated aqueous pore, a model originally proposed by Warhurst *et al.*, who noted that PfCRT shows some sequence resemblance to the *E. coli* ClC channel (Warhurst et al., 2002). In analogy to the bacterial channel, PfCRT is suggested to be in an open conformation while the interior of the food vacuole is positively charged (Bray et al., 2006). The K76T mutation leads to the loss of a positive charge in the interior of the pore, thus allowing charged protonated CQ to move through. The importance for this loss of a positive charge is supported by the fact that introducing a positive charge in a different position on transmembrane domain 4 (S163R mutation) after selection for amantadine resistant parasites restores the sensitivity to CQ despite the presence of the K76T mutation (Figure 1-8) (Johnson et al., 2004). Verapamil and amantadine presumably block the pore and thus reverse CQ resistance (Johnson et al., 2004). The trans-stimulation of CQ accumulation observed if parasites are preloaded with CQ is alternatively explained in the gated channel model with the depolarization of the DV by the escape of protonated CQ and closure of the gated channel (Bray et al., 2006).

1.6.2 Other transporters involved in chloroquine resistance

Several other transporters have been associated with CQ resistance, such as members of the ABC transporter superfamily like the multidrug resistance transporter 1 (*pfmdr*-1) (Cowman et al., 1991; Reed et al., 2000) and the multidrug resistance associated protein 1 (*pfmrp-1*) (Klokouzas et al., 2004; Raj et al., 2008).

Although *pfcrt* is the main determinant for CQ resistance, polymorphisms in the *pfmdr1* gene frequently correlate with CQ resistance and though this does not confer resistance by itself, it does modulate the level of resistance. The *pfmdr1* gene encodes the P-glycoprotein homologue-1 (Cowman et al., 1991), a

homologue of the human multidrug resistance transporters, which are frequently associated with drug resistance in cancer cells. Pgh-1 is a 162 kDa protein with 12 predicted transmembrane domains and sequence similarities to primary active ATP-binding cassette (ABC) transporters.

Some point mutations in *pfmdr1* have been found to alter CQ sensitivity and changing a certain mutated *pfmdr1* allele back to the wild-type form can half the level of CQ resistance, while other mutations in the transporter do not affect the susceptibility of parasites to CQ (Reed et al., 2000; Sidhu et al., 2005). Amplification of *pfmdr1* has also been implicated in drug resistance. Interestingly, parasites with multiple copies of *pfmdr1* appear to be rather more sensitive to CQ, while the amplification leads to a decrease in susceptibility to mefloquine, quinine, halofantrine, artesunate and dihydroartemisinin (Cowman et al., 1994; Price et al., 2004).

Similar to Pgh-1, the PfMRP1 transporter can modify CQ resistance. An association between mutations in *pfmrp1* and quinoline resistance has been reported from field isolates (Ursing et al., 2006) and a recent study showed that the knockout of the *pfmrp1* gene in a CQ resistant parasite line increased the susceptibility of these parasites to the drug, albeit without complete reversal of the resistance (Raj et al., 2008).

1.6.3 Glutathione mediated heme detoxification

Previous studies have suggested a role for GSH in the establishment of CQ resistance. Several studies on cancer cells found a correlation between drug resistance and elevated GSH levels, often due to increased γGCS activity. The elevated GSH levels are often associated with over-expression of GSTs and efflux pumps for GSH-labelled xenobiotics such as homologues of MRP and MDR transporters (Balendiran et al., 2004; Fojo and Bates, 2003; Yang et al., 2006).

Studies on the rodent malaria parasite *P. berghei* found increased GSH levels in CQ resistant strains in correlation with a three times higher GST activity compared to sensitive parasites (Dubois et al., 1995). Treatment with L-BSO led to a much more spectacular depletion of GSH in the resistant strains, indicating a higher turnover of the tripeptide in these parasites and partly reversed CQ resistance. Atamna and Ginsburg demonstrated *in vitro* that GSH is able to non-

enzymatically degrade the cellular target of CQ, FPIX, in a radical mediated mechanism, which is however independent of the presence of GST (Atamna and Ginsburg, 1995). Further studies on CQ resistant *P. berghei* by Platel *et al.* found that the resistant parasites displayed a lower hemozoin content, which could be increased when infected mice were treated with L-BSO to deplete GSH (Platel et al., 1999). In an *in vitro* assay in the same study GSH was shown to partly inhibit hemin polymerization, which was not influenced by the absence or presence of GST. The role for GST in CQ resistant *P. berghei* remains unclear, if GSH alone is able to mediate decreased drug susceptibility by removing the target FPIX. No correlation was found between CQ resistance and GST in *P. falciparum* and no CQ conjugates or metabolites have been found in the resistant parasites (Berger et al., 1995).

Because GSH is usually synthesized in the cytosol, Platel *et al.* suggested that the increased GSH levels they detected in CQ resistant *P. berghei* parasites are of erythrocyte origin, as they observed a preference of the resistant parasites for reticulocytes which contain higher GSH levels than mature erythrocytes (Sailaja et al., 2003). They hypothesized that the parasites take up erythrocytic GSH during the digestion of the host cell cytosol (Platel et al., 1999). Support for the uptake of GSH from the host cell comes from the observation that blood stages of genetically modified *P. berghei* parasites lacking the *pbygcs* gene still contain appreciable levels of GSH, despite no longer having a functional biosynthesis pathway (Vega-Rodriguez et al., 2009). Studies in *P. falciparum* led to the suggestion that FPIX exits the DV in large amounts and is degraded by GSH of parasite origin in the cytosol (Ginsburg et al., 1998; Ginsburg and Golenser, 2003). These studies found that GSH degrades FPIX at a much higher rate at neutral pH than at the acidic pH of the DV.

Consistent with the hypothesis that GSH affects CQ resistance, increased levels of mRNA for PbγGCS were found in CQ resistant *P. berghei* (Perez-Rosado et al., 2002) and several drugs able to decrease or increase cellular GSH levels were found to decrease or increase CQ susceptibility of murine malaria species, respectively (Deharo et al., 2003). Increased PfγGCS activity and higher GSH levels were also found in the multi-drug resistant *P. falciparum* isolate Dd2 in comparison to the sensitive strain 3D7 (Meierjohann et al., 2002b).

However, analysis of the distribution of FPIX by Mössbauer spectroscopy showed that more than 90 % of FPIX are retained in the DV, which argues against the degradation of FPIX by GSH in the cytosol (Egan et al., 2002). Analysis of the hemozoin content of several resistant and sensitive strains found no correlation between CQ susceptibility and the level of hemozoin accumulation, suggesting that higher GSH levels in resistant parasites are not resulting in increased FPIX degradation (Zhang et al., 1999). In another rodent parasite, *P. chabaudi*, no alteration of the GSH metabolism was found in correlation to CQ resistance and CQ resistance is most likely independent of GSH (Ferreira et al., 2004).

1.7 Aims of this study

- Establish that the GSH biosynthesis pathway is present in the *P. falciparum* cytosol.

- Determination of the role and importance of GSH biosynthesis for *P. falciparum* survival and possible validation of γGCS and GS as drug targets in erythrocytic stages by reverse genetics.

- Investigation into the role of GSH in the degradation of FPIX in CQ sensitive and resistant parasites and the influence of mutations in PfCRT on GSH metabolism.

The results of this study are presented in three chapters. In Chapters 3 and 4 the GSH biosynthesis enzymes PfγGCS and PfGS are investigated, respectively. The influence of GSH on CQ resistance and the influence of PfCRT mediated CQ resistance on GSH metabolism are described in Chapter 5. The results and their implications are discussed in Chapter 7.

2 Material and Methods

2.1 Consumables, biological and chemical reagents

Abcam	Mouse monoclonal anti-FKBP12 antibody
ABgene	2x PCR Reddy Mix
BD biosciences	Mouse monoclonal anti-His-antibody
BDH	Saponin
Bio-Rad	Bradford protein assay reagent, Gene pulser electroporation cuvette (0.2 cm), Precision plus dual color protein standard
Blood transfusion service	Human full blood
BOC	Malaria culture gas (5% CO_2, 1% O_2, 94% N_2)
Clontech	Shld1
Eurogentec	Oligonucleotides
Fisher Scientific	10 x Phosphate buffered saline (PBS)
Fluka	1-Choro-2,4-dinitrobenzene
GE Healthcare	Gene images AlkPhos direct labeling and detection system, Gene images CDP-Star detection module, Hypercassettes (18 x 24 cm), Hyperfilm ECL
Invitrogen	Accuprime *Pfx* SuperMix, Albumax II, chemically competent *E. coli* TOP10 and *ccdB* Survival T1 cells, gentamycin, PCR SuperMix, TOPO TA cloning kit, Trizol, RPMI 1640 (with 25mM HEPES, L- glutamine, without $NaHCO_3$), SYBR Safe
Jacobus pharmaceuticals	WR99210
Machery & Nagel	NucleoBond Xtra Maxi Plus Kit
Melford	Ampicillin, Carbenicillin, Isopropyl-ß-D-thiogalacopyranoside (IPTG), dithiothreitol

	(DTT), ß-nicotinamide adenine dinucleotide reduced (NADH), ß-nicotinamide adenine dinucleotide phosphate reduced (NADPH), proteinase K
Millipore	Immobilon Western Blot detection kit
Nalgene	1.0 ml cryotubes
New Engand Biolabs	1 kb DNA ladder, PCR marker, all restriction endonucleases and associated buffers,
Novagen	BugBuster protein extraction solution, benzonase, Chemically competent E. coli BLR (DE3)
Promega	Anti-mouse IgG (HRP conjugated), anti-rabbit IgG (HRP conjugated)
Qiagen	Qiaprep spin DNA miniprep Kit, Qiaquick gel extraction kit, Qiaamp DNA mini kit, Qiaquick PCR purification kit
Roche	Bovine Serum Albumin (BSA), Expand High Fidelity PCR system, Mouse monoclonal anti-GFP antibody, Rapid DNA ligation kit
Schleicher & Schuell	Protran Nitrocellulose
Sigma	All chemicals unless otherwise stated
Stratagene	Chemically competent E. coli XL10-Gold, Chemically competent Strataclone Solo Pack cells, Strataclone Blunt PCR cloning kit
VWR	Giemsa stain
Zeiss	Imersol

2.2 Equipment

Beckman	Avanti J-26 XP centrifuge with JA20 rotor and JSP F10 rotor
Billups Rothenberg	Modular incubation chamber

Biorad	Gel tanks, Gene pulser Xcell electroporator, Power Pac 300, Power Pac Basic, Transblot semi-dry transfer cell
Constant Systems	One shot cell disrupter
Eppendorf	Microcentrifuge 5415D with F45-24-11 rotor
Fisher	Gel tanks, Microcentrifuge Accuspin MicroR with 24 place rotor, Waterbath
GE Healthcare	Vacu Gene Pump, Vacu Gene XL
G Storm	PCR machine
Grant	Heat block QBT2
Haereaus	Incubator
Heidolph	Shaker Titramax 100
IKA	Minishaker MS2
Kuehner	Shaking incubator ISF-1-W
Sciquip	Sigma 6K 15 centrifuge with 11150 rotor and 12500 rotor
Shimadzu	UV-2401 and UV-2501 spectrophotometer
Thermo electron	Jouan CR3i centrifuge with T40 rotor
UVP	Hybridization oven HB-1000, UV cross linker
Zeiss	Axioplan 2 microscope

2.3 Buffers, Solutions and Media

2.3.1 General Buffers

1 x PBS	140 mM NaCl, 3 mM KCl, 10 mM Na_2HPO_4, 1.8 mM KH_2PO_4, pH 7.4

2.3.2 DNA analysis

6x DNA loading buffer	0.25 % (w/v) bromophenol blue, 0.25 % (w/v) xylene cyanol FF, 0.25 % (w/v) orange-G, 40 % (w/v) sucrose
20 x SSC	300 mM Trisodium citrate, 3 M NaCl, pH 7-8
Southern depurination	0.25 N HCl
Southern denaturing	1.5 M NaCl, 0.5 M NaOH
Southern hybridization	Gene images AlkPhos hybridization buffer, 0.5 M NaCl, 4 % (w/v) blocking reagent
Southern first wash buffer	2 M Urea, 0.1 % (w/v) SDS, 50 mM sodium phosphate pH 7.0, 150 mM NaCl, 1 mM $MgCl_2$, 0.2 % (w/v) blocking reagent
Southern second wash buffer	50 mM Tris base, 100 mM NaCl, 2 mM $MgCl_2$
TE	10 mM Tris-HCl, 1 mM EDTA, pH 8.0
1 x TAE	40 mM Tris-acetate, 1 mM EDTA, pH 8.0

2.3.3 Protein analysis

Coomassie stain	40 % (v/v) Methanol, 10 % (v/v) acetic acid, 0.1 % (w/v) Coomassie brilliant blue R-250
Destaining solution	20 % (v/v) Methanol, 10 % (v/v) acetic acid
GS activity assay buffer	100 mM Bicine / Bis-Tris propane / Mes pH 7.5, 10 mM $MgCl_2$, 75 mM KCl
6 x SDS loading buffer	62.5 mM Tris / HCl pH 6.8, 2 % (w/v) SDS, 10 % (v/v) glycerol, 0.001 % (w/v) bromophenol blue, 5 % (v/v) 2- mercaptoethanol
2D Lysis buffer	100 mM HEPES pH 7.4, 5 mM $MgCl_2$, 10 mM EDTA, 0.5 % Triton X-100, 5 µg/ml RNase A, 1 mM PMSF, 1 mM benzamidine, 2 µg/ml leupeptin, 10 µM E-64, 2 mM 1,10-phenanthroline, 4 µM pepstatin A (protease inhibitors added fresh prior to use)

Running gel mix	375 mM Tris-base pH 8.9, 0.1 % SDS (w/v), 5-15 % (v/v) acrylamide
1x SDS PAGE running buffer	25 mM Tris, 192 mM glycine, 0.1 % (w/v) SDS
Stacking gel mix	122 mM Tris-HCl pH 6.7, 0.1 SDS (w/v), 5 % acrylamide
Towbin buffer	25 mM Tris, 192 mM glycine, 20 % (v/v) methanol
Protein purification buffer A	50 mM NaH_2PO_4, pH 8.0, 300 mM NaCl, 10 mM imidazole, 1mM DTT
Protein purification buffer B	50 mM NaH_2PO_4, pH 8.0, 300 mM NaCl, 20 mM imidazole, 1mM DTT
Protein elution buffer C	50 mM NaH_2PO_4, pH 8.0, 300 mM NaCl, 300 mM imidazole, 1mM DTT

2.3.4 Bacteria culture

Ampicillin	100 mg/ml in ddH_2O
Carbenicillin	100 mg/ml in ddH_2O
Chloramphenicol	34 mg/ml in ethanol
Kanamycin	50 mg/ml in ddH_2O
Luria Bertani (LB) medium	10 g/l Tryptone, 5 g/l yeast extract, 5 g/l NaCl
LB agar	1.5 % (w/v) agar in LB medium
Terrific Broth medium	12 g/l Tryptone, 24 g/l yeast extract, 0.4 % (v/v) glycerol, 9.4 g/l K_2HPO_4, 2.2 g/l KH_2PO_4 pH 7.2
Tetracycline	5 mg/ml in ethanol
TfB I	100 mM RbCl, 50 mM $MnCl_2$ x 4 H_2O, 30 mM potassium acetate, 10 mM $CaCl_2$ x 2 H_20, 15 % (v/v) glycerol
TfB II	10 mM MOPS, 10 mM RbCl, 75 mM $CaCl_2$ x 2 H_20, 15 % (v/v) glycerol

2.3.5 *P. falciparum* culture

Ancotil	1 mM in blood wash medium
Blasticidin-S-HCl	10 mg/ml in blood-wash medium
Blood-wash medium	15.9 g/l RPMI 1640 (with 25 mM HEPES and L-glutamine), 0.1 % (w/v) sodium bicarbonate, 10 mM glucose, 200 µM hypoxanthine, 20 µg/ml gentamycin, pH 7.4
Complete RPMI 1640 medium	Blood wash medium supplemented with 0.5 % (w/v) Albumax II
Earle's balanced salt solution (EBSS)	6.8 g/l NaCl, 0.4 g/l KCl, 0.2 g/l $MgSO_4$ x $7H_2O$, 0.158 g/l NaH_2PO_4 x 2 H_2O, 0.264 g/l $CaCl_2$ x $2H_2O$, 2.2 g/l $NaHCO_3$, 1 g/l D-glucose
IC_{50} Medium	Complete RPMI 1640 medium without hypoxanthine
Cytomix	120 mM KCl, 0.15 mM $CaCl_2$, 2 mM EGTA, 5 mM $MgCl_2$, 10 mM K_2HPO_4 / KH_2PO_4 pH 7.6, 25 mM HEPES pH 7.6
Freezing solution	30 % (v/v) glycerol in PBS
WR99210	Stock solution: 20 mM in dimethylsulphoxide
	Working solution: 20 µM in blood- wash medium

2.3.6 Bacteria strains

BLR (DE3) (Novagen):

F^- *ompT hsdS*$_B$(r_B- m_B-) *gal dcm* (DE3) Δ(srl-recA)306::Tn*10* (Tet^R)

One Shot® *ccdB* Survival T1 (Invitrogen):

F^- *mcrA* Δ(*mrr-hsd*RMS-*mcr*BC) Φ80*lac*ZΔM15 Δ*lac*X74 *recA1 ara*Δ139 Δ(*ara-leu*)7697 *gal*U *gal*K *rps*L (Str^R) *end*A1 *nup*G *tonA*::P_{trc}-*ccd*A

One Shot® Top10 (Invitrogen):

F^- *mcrA* Δ(*mrr-hsd*RMS-*mcr*BC) Φ80*lac*ZΔM15 Δ*lac*X74 *recA1 ara*Δ139 Δ(*ara-leu*)7697 *gal*U *gal*K *rps*L (Str^R) *end*A1 *nup*G

XL10-Gold (Stratagene):

Tet^r Δ(mcrA)183 Δ(marc-hsdSMR-mrr)173 end A1 supE44 thi-1 recA1 gyrA96 relA1 lac The [F' proAB $lacI^q$ ZΔM15 Tn10 (Tet^r) Amy Cam^r]^a

2.3.7 *P. falciparum* strains

3D7	The Netherlands
D10	Papua New Guinea
GC03	Progeny of Dd2 X HB3 cross (Wellems et al., 1990)
$C2^{GC03}$	kind gift of D. Fidock (Sidhu et al., 2002)
$C3^{Dd2}$	kind gift of D. Fidock (Sidhu et al., 2002)
$C6^{7G8}$	kind gift of D. Fidock (Sidhu et al., 2002)

2.3.8 Oligonucleotide Primers

Oligonucleotide primers were designed to amplify genes or gene fragments for knockout and localization studies, to introduce mutations or for quantitative real time PCR. To allow cloning into destination vectors, primers for knockout studies contained a 5'-extension containing the appropriate restriction sites. The primers used in this study are listed below according to application. Restriction sites are highlighted in bold print. Sites changed to introduce mutations are underlined.

2.3.8.1 Mutagenesis

GS muta fwd	GAT ATA AAA CAA ATA AAG TAC GCT ACA ATA TCT GTT GCC
GS muta rev	GGC AAC AGA TAT TGT AGC GTA CTT TAT TTG TTT TAT ATC

2.3.8.2 Knockout studies in *P. falciparum*– cloning and analysis

γGCS pHH1 KO fwd	GCGC **AGATCT** CGT TAT GAT GAA AAT ATA ATG TTT GG (*Bgl*II)
γGCS pHH1 KO rev	GCGC **CTCGAG** ATC TTG TGT ATT TGA ACT ATC ATT AAC (XhoI)
γGCS pHH1 KOcon fwd	GCGC **AGATCT** GAT GTA ATA CTT GAC AAA AAT G (*Bgl*II)
γGCS pHH1 KOcon rev	GCGC **CTCGAG** TTA TGC ACT CAG TTC GTA C (XhoI)
GS pHH1 KO fwd	GCGC **AGATCT** GAT ATG ATT GCT TTT TTG AAT AC (BglII)
GS pHH1 KO rev	GCGC **CTCGAG** GTC GTT CAA ATC GAT AAG AAG (XhoI)
GS pHH1 KOcon fwd	GCGC **AGATCT** CAT GAA GAT GAT TTT AAT AGT TTT G (BglII)
GS pHH1 KOcon rev	GCGC **CTCGAG** CTC AAT GTT CAG TTA AAA AAA AAG (XhoI)
γGCS pCC 5’ fwd	GCGC **CCGCGG** CGG AAC GCC ATT AAG CTG GGA TG (SacII)
γGCS pCC 5’ rev	GCGC **CTTAAG** CAT GGC CAG TAA TTC TTC TAG CC (AflII)
γGCS pCC 3’ fwd	GCGC **CCATGG** GAG CAT CCA AAA GAG AAG CTT TAA C (*Nco*I)
γGCS pCC 3’ rev	GCGC **GGCGCC** GCA AGT ATT GCG TAT AAT CCT CTC C (*Nar*I)
GS pCC 5’ fwd	GCGC **CCGCGG** GTC CCA ATG GAA AGA ATG AAT ATC (SacII)
GS pCC 5’ rev	GCGC **CTTAAG** CGA TTA GTC ATA TAA TCA GAT CTT CC (*Afl*II)
GS pCC 3’ fwd	GCGC **CCATGG** GCC TTA CAA GTA GAC CCA TCT C (*Nco*I)
GS pCC 3’ rev	GCGC **GGCGCC** CCA AGC TTG ATA TAC CAC AAA TGG (*Nar*I)

pCC 5' sequencing fwd	CTT TAA ATT CAT GCA AAA ATT TAC
pCC 5' sequencing rev	CCA ATA GAT AAA ATT TGT AGA G
pCC 3' sequencing fwd	CAT ATG TTA AAT ATT TAT TTC TC
pCC 3' sequencing rev	CGG CAT CAG AGC AGA TTG TAC

2.3.8.3 Expression constructs for *P. falciparum*– cloning and analysis

γGCS gateway fwd	CACC ATG GGT TTT CTA AAA ATC GGA ACG
γGCS gateway rev	TGC ACT CAG TTC GTA CAT TTT TTT TGC
GS gateway fwd	CACC ATG GAA AGA AAG GTA GAT GAG TT
GS gateway rev	ATG TTC AGT TAA AAA AAA AGA ATC C
γGCS sequencing 1	CGA ATT TAC AAC AAC AAA ATG
γGCS sequencing 2	GCT ATG ACA AAT AAA GAA G
GS sequencing	CTG TTG CCT TTG GTA ATC TTT C

2.3.8.4 Quantitative real time PCR

γGCS-RT-fwd	TCC TTG CTC TTA CTG CAT GTA CT
γGCS-RT-rev	TTC CGT TCT ACA ATC AAC ACT GT
GS-RT-fwd	CTT TAG AGC ATT ATA TAC ACC TAA CCA
GS-RT-rev	CGA ACC AAC AAG TTG ATA AGG TA
CRT-RT-fwd	GGA AAT ATC CAA TCA TTT GTT CTT
CRT-RT-rev	CAA CAA TAA TAA CTG CTC CGA GAT
stRNAS-fwd	AAG TAG CAG GTC ATC GTG GTT
stRNAS-rev	TTC GGC ACA TTC TTC CAT AA

2.3.9 Constructs

Constructs generated and used for this study are listed in Table 2-1. The constructs were either used for recombinant expression of proteins or knockout studies in *P. falciparum* or for recombinant expression of proteins in *E. coli*.

Name	Insert	Oligonucleotides	Selectable Marker for *P.falciparum*	Purpose
pCC4-ΔγGCS	nucleotides 18-502 (5'flank) and 2549-3070 (3' flank) of *ygcs* ORF	γGCS pCC 5' fwd and rev γGCS pCC 3' fwd and rev	*bsd, cd*	knockout of *pfygcs* by gene replacement
pCC4-ΔGS	nucleotides 65-542 (5'flank) and 1468-1942 (3' flank) of *gs* ORF	GS pCC 5' fwd and rev GS pCC 3' fwd and rev	*bsd, cd*	knockout of *pfgs* by gene replacement
pCHD-Hsp86-γGCS-GFP	full length *ygcs* ORF	γGCS gateway fwd γGCS gateway rev	*hdhfr*	recombinant expression of PfγGCS-GFP in *P. falciparum*
pCHD-Hsp86-γGCS-HA	full length *ygcs* ORF	γGCS gateway fwd γGCS gateway rev	*hdhfr*	recombinant expression of PfγGCS-HA in *P. falciparum*
pCHD-Hsp86-GS-GFP	full length *gs* ORF	GS gateway fwd GS gateway rev	*hdhfr*	recombinant expression of PfGS-GFP in *P. falciparum*
pCHD-Hsp86-GS-HA	full length *gs* ORF	GS gateway fwd GS gateway rev	*hdhfr*	recombinant expression of PfGS-HA in *P. falciparum*
pCHD-HSP86-$GS^{E206K/N208A}$-FKBP12	full length *gs* ORF	GS gateway fwd GS gateway rev	*hdhfr*	recombinant expression of $PfGS^{E206K/N208A}$-FKBP12 in *P. falciparum*
pHH1-ΔγGCS	nucleotides 181-981 of *ygcs* ORF	γGCS pHH1 KO fwd γGCS pHH1 KO rev	*hdhfr*	knockout of *pfygcs* by gene disruption
pHH1-γGCScon	nucleotides 1870-3150 of *ygcs* ORF	γGCS pHH1 KOcon fwd γGCS pHH1 KOcon rev	*hdhfr*	knock-in control for targeting of *pfygcs* locus in *P. falciparum*
pHH1-ΔGS	nucleotides 121-1125 of *gs* ORF	GS pHH1 KO fwd GS pHH1 KO rev	*hdhfr*	knockout of *pfgs* by gene disruption
pHH1-GScon	nucleotides 886-1965 of *gs* ORF	GS pHH1 KOcon fwd GS pHH1 KOcon rev	*hdhfr*	knock-in control for targeting of *pfgs* locus in *P. falciparum*
pJC40-PfGS	full length wild type *gs* ORF	n.a.	-	recombinant expression of PfGS in *E. coli*
pJC40-$PfGS^{E206K/N208A}$	full length *gs* ORF with E206K/N208A mutation	GS muta fwd GS muta rev	-	recombinant expression of $PfGS^{E206K/N208A}$ in *E. coli*

Table 2-1: Constructs generated and used in this study.
Listed above are the constructs I generated in this study with the exception of pJC40-*Pf*GS which was generated by S. Meierjohann (Meierjohann et al., 2002a). The oligonucleotides used for their generation are given. All of the constructs contain an ampicillin resistance cassette for selection in *E. coli*.

2.3.10 Antibodies

Antibodies were used in this study for western blot analyses of recombinant proteins or parasite extracts.

	Raised in	Dilution for western blot	Source
anti-$(His)_{10}$	mouse	1:10000	BD Biosciences
anti-FKBP12	mouse	1:2000	Abcam
anti-GFP	mouse	1:1000	Roche
anti-HA	mouse	1:1000	Eurogentec
anti-PfCK2α	rabbit	1:200	kind gift of Prof. C. Doerig
anti-PfCRT	rabbit	1:2000	kind gift of Dr. P. Bray
anti-PfGST	rabbit	1:5000	kind gift of Prof. E. Liebau
anti-PfGR	rabbit	1:15000	Eurogentec

Table 2-2: Primary antibodies and their dilutions.

	Dilution in western blot	Source
anti-mouse IgG (H+L) HRP conjugate	1:10000	Promega
anti-rabbit IgG (H+L) HRP conjugate	1:10000	Promega

Table 2-3: Secondary antibodies and their dilutions.

2.4 Molecular Biology

2.4.1 Agarose gel electrophoresis

For electophoresis, agarose was dissolved at the required concentration (between 0.8 and 2 % w/v) in 1 x TAE buffer (see 2.3.2) containing 0.5 µg / ml Sybr safe. For subsequent gel extraction low melting point agarose was used. DNA samples were mixed with 6 x DNA loading dye and electrophoresis was performed in 1x TAE at 5-10 V/cm gel. To determine the size of DNA bands 1 kb ladder (New England Biolabs) was run alongside samples. The DNA was visualized on a transilluminator.

2.4.2 Determination of nucleic acid concentrations

Concentrations of DNA and RNA solutions were determined by measuring the absorbance at 260 nm. Typically 1:50 or 1:100 dilutions in ddH_2O were used for

standard preparations of DNA or RNA to keep the detected absorbance in the linear range between 0.1 and 1. Concentrations were calculated using the following equation:

Concentration [µg /ml] = $absorbance_{260}$ x DF x MF

DF= dilution factor, e.g. 100 for a 1:100 dilution

MF= multiplication factor: 50 for dsDNA, 40 for RNA

DNA concentrations were alternatively determined by running small aliquots of samples alongside a standardized 1 kb DNA ladder of known concentration (NEB) on agarose gels. The concentration was determined by comparing the intensity of marker bands of the same size to the intensity of the sample on a transilluminator. The intensity of a DNA band is directly proportional to the amount of DNA.

2.4.3 Ethanol precipitation of DNA

Precipitation of DNA was performed to concentrate plasmid DNA or to exchange buffers before transfection of plasmids into *P. falciparum*. For each transfection 100 µg plasmid DNA was precipitated. DNA solutions were mixed with 1/10 volume of 3 M sodium acetate pH 5.2 and 3 volumes of 100 % ethanol. To facilitate precipitation 1 µl glycogen (Invitrogen; 20 µg/µl) was added. The DNA was kept at -20°C for at least one hour before being centrifuged for 20 min at 15,000 g at 4°C. The supernatant was removed and the DNA pellet was washed with 70 % ethanol and centrifuged for 10 min at 15,000 g at 4°C. The following steps were carried out under a sterile category 2 tissue culture hood. The supernatant was removed and the pellet air dried. DNA for transfections was resuspended in 30 µl sterile TE buffer.

2.4.4 Restriction endonuclease digests

All restriction endonucleases used were purchased from New England Biolabs and used with the appropriate NEB buffer and BSA according to manufacturer's instructions. All digests in this study were preformed in a heat block at 37°C. To analyse plasmids typically 2-3 µl of standard small scale purifications were

digested for 1.5 hours. For Southern blots 1 µg of genomic DNA was digested for approximately 24 hours.

2.4.5 Polymerase Chain Reaction

2.4.5.1 From *P. falciparum* genomic DNA or plasmid DNA templates

For amplification of *P. falciparum* 3D7 genomic DNA for cloning, 100 ng of template DNA was mixed with each forward and reverse primers and either AccuPrime *Pfx* supermix (Invitrogen) or the components of the Expand High Fidelity PCR supermix (Roche) according to manufacturer's instructions. Both kits contain a 3'-5' exonuclease with proofreading activity. For the generation of probes for Southern blots appropriate plasmids containing the desired sequence were used as template (typically 1:20 dilution of a standard miniprep) with PCR Supermix (Invitrogen) and forward and reverse primers. Primer concentrations were 0.4 µM for *Pfx* supermix and PCR supermix and 0.2 µM for the Expand High Fidelity PCR supermix. The programmes used were:

Pfx supermix / PCR supermix:

Step 1: 95°C, 5 min
Step 2: 95°C, 30 sec
Step 3: annealing temperature between 40 – 60°C, 30 sec
Step 4: 68°C, 1.5 min per 1000 base pairs to be amplified
Repeat steps 2-4 for 30 cycles
Step 5: 68°C, 10 min
Step 6: Store at 10°C

Expand High Fidelity Supermix

Step 1: 95°C, 5 min
Step 2: 95°C, 30 sec
Step 3: annealing temperature between 40 – 60°C, 30 sec
Step 4: 68°C, 1 min per 1000 base pairs to be amplified
Repeat step 2-4 for 10 cycles
Step 5: 95°C, 30 sec
Step 6: annealing temperature between 40 – 60°C, 30 sec

Step 7: 68°C, 1 min per 1000 base pairs to amplified, elongate for 10 sec with every additional cycle

Repeat steps 5-7 for 20 cycles

Step 8: 68°C for 10 min

Step 9: Store at 10°C

The resulting PCR products were analysed by agarose gel electrophoreses before being used for cloning or the generation of probes for Southern blot analyses.

2.4.5.2 Colony PCR

Colony PCR was performed on bacteria clones to facilitate identification of correct clones following transformation of ligation reactions between destination vectors and inserts. Bacteria colonies were used as templates for the PCR and the primers used were specific for the insert. Before the PCR reaction was set up, an LB-plate containing the appropriate antibiotic was labelled with a numbered grid. PCR reactions were set up as 10 µl reactions per colony using Reddymix (ABgene) with each primer at 4 µM concentration according to manufacturer's instructions. Single colonies were picked from transformation plates and used to inoculate the prepared gridded plate at a defined position, thus giving each colony screened a number before the remainder of the colony was transferred into a PCR tube containing the reaction mix. The gridded plate was incubated at 37°C overnight. The PCR conditions were:

Step 1: 94°C, 10 min

Step 2: 94°C, 60 sec

Step 3: annealing temperature between 40 – 60°C, 60 sec

Step 4: 68°C, 2 min per 1000 base pairs to be amplified

Repeat steps 2-4 for 30 cycles

Step 5: 68°C, 10 min

Step 6: Store at 10°C

PCR products were analysed by agarose gel electrophoreses. Potentially correct clones were identified by the presence of a PCR product of the correct size. These clones were subsequently analysed by plasmid isolation, restriction analyses and sequencing.

2.4.5.3 Site directed mutagenesis

Site directed mutagenesis was carried out as previously described (Braman et al., 1996). Using this method, complete plasmids containing the required mutation were generated. The template used for mutagenesis was the pJC40-PfGS wild-type construct previously described (Meierjohann et al., 2002a). Both forward and reverse primers contained the desired mutation. The PCR was set up using Accuprime *Pfx* supermix (Invitrogen) as a set of 25 µl reactions, each reaction containing 10 ng of plasmid DNA template and forward and reverse primers at 0.2 µM. The PCR was performed as a gradient PCR with separate reactions incubating at different annealing temperatures between 40 and 65°C. The PCR programme was as follows:

Step 1: 95°C, 5 min
Step 2: 95°C, 30 sec
Step 3: 40- 65°C gradient, 15 sec
Step 4: 68°C, 5 min
Repeat steps 2- 4 for 15 cycles
Step 5: 68°C, 10 min
Step 6: store at 10°C

To remove template DNA, PCR products were subsequently treated with 20 units *Dpn*I at 37°C for 5 to 16 hours. This method removes the methylated plasmid template DNA while leaving the non-methylated PCR products containing the desired mutation, because *Dpn*I is a restriction endonuclease specific for the sequence GATC in methylated and hemi-methylated DNA. The *Dpn*I treated PCR products were subsequently transformed into *E. coli* Top10 cells (Invitrogen) (see 2.4.7.2).

2.4.5.4 Quantitative real time PCR

The transcription levels of *pfygcs*, *pfgs* and *pfcrt* were analysed using the 7500 Real Time PCR system by Applied Biosystems. Real time PCR reactions were performed in 25 µl reactions using QuantiTect SYBR green master mix (Qiagen) and primers at a final concentration of 0.3 µM according to Salanti et al. (Salanti et al., 2003). As template 5 µl of a 1:10 dilution of cDNA generated with the Ambion RETROscript® kit (see 2.4.9) was used. *Seryl-tRNA-synthetase* (*strs*) was

used as the mRNA control of a housekeeping gene as it has been described by Salanti *et al.* to have a uniform transcription pattern throughout the parasite life cycle and initial tests showed that the abundance of *strs* mRNA was similar to the mRNA of the genes analysed. PCR cycling conditions were 50°C for 2 min, 95°C for 15 min, followed by 40 cycles of 95°C for 15 sec, 54°C for 30 sec and 68°C for 35 sec. The length of the fragments amplified was 100 bp for *pfygcs*, 117 bp for *pfgs*, 117 bp for *pfcrt* and 157 bp for *pfstrs*. Relative expression levels were calculated using the ΔΔCT method (User Bulletin 2, Applied Biosystems).

2.4.6 Cloning techniques

2.4.6.1 TOPO Cloning of PCR products

PCR products were initially cloned into TOPO vectors (Invitrogen) before cloning into the destination vectors pHH1 or pCC4 (Maier et al., 2006; Reed et al., 2000). This step was introduced because it can facilitate cloning of AT-rich fragments if the yield of the PCR reaction is poor and it allows sequencing of the fragments prior to introducing them into the destination vectors. Depending on the polymerase used for amplification two different types of vectors were used for subcloning. PCR products generated using *Taq* based polymerases, such as in the Expand High fidelity PCR supermix (Roche) contained adenine overhangs at the 3'-ends. These were cloned into the pCR2.1-TOPO vector (Figure 2-1) using the TOPO TA® PCR cloning kit (Invitrogen). PCR products generated using *Pfx*/*Pfu* based polymerases such as the Accuprime *Pfx* supermix had blunt ends and were cloned into the pCR-Blunt II-TOPO vector (Figure 2-2) using the Zero Blunt TOPO® PCR cloning kit (Invitrogen).

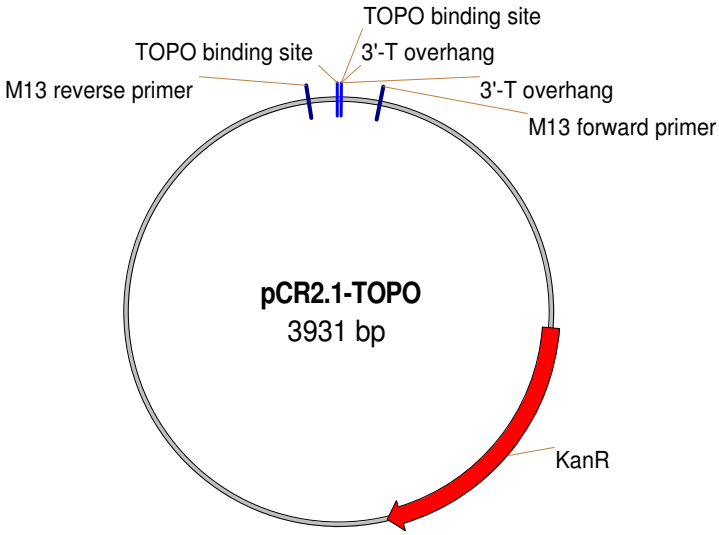

Figure 2-1: Vector map of pCR2.1-TOPO.
This figure displays the important features of the pCR2.1-TOPO plasmid. This plasmid was used to clone PCR fragments amplified with *Taq* based polymerase. The plasmid contains a kanamycin resistance cassette (KanR, 795 bp) for selection in *E.coli*. Topoisomerase I is covalently bound at the TOPO binding sites. The binding sites also contain a 3' T-overhang to allow cloning of PCR products with 3' A-overhangs. After cloning PCR products could be sequenced using the M13 forward and M13 reverse primers.

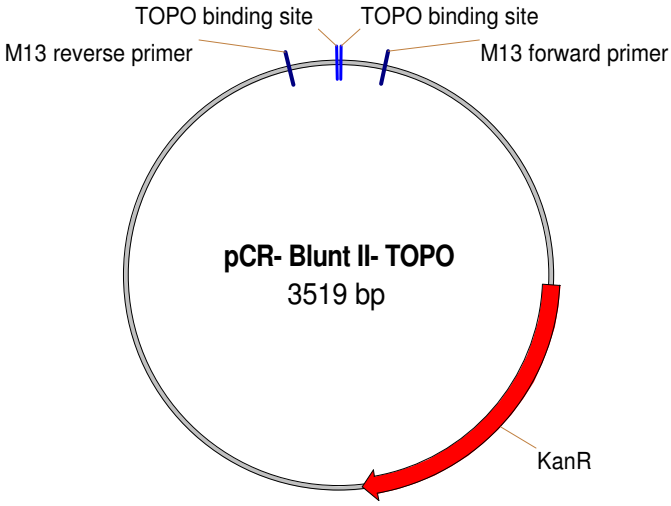

Figure 2-2: Vector map of pCR-Blunt II- TOPO.
This figure displays the important features of the pCR-Blunt II- TOPO plasmid. This plasmid was used to clone PCR fragments amplified with *Pfx*/*Pfu* based polymerase and contains a kanamycin resistance cassette (KanR, 795 bp) for selection of constructs in *E. coli*. Topoisomerase I is covalently bound at the TOPO binding sites to allow cloning of blunt PCR products and PCR fragments could be sequenced following cloning using M13 forward and M13 reverse primers.

A special type of TOPO- cloning was performed to generate entry clones for MultiSite Gateway® cloning. In this case the forward primer used for the amplification of the gene of interest contained four additional bases at the 5' end, creating a CACC overhang homologous to a GTGG overhang in the cloning vector. This allowed directional cloning of the gene into the vector pENTR/D-TOPO (Figure 2-3).

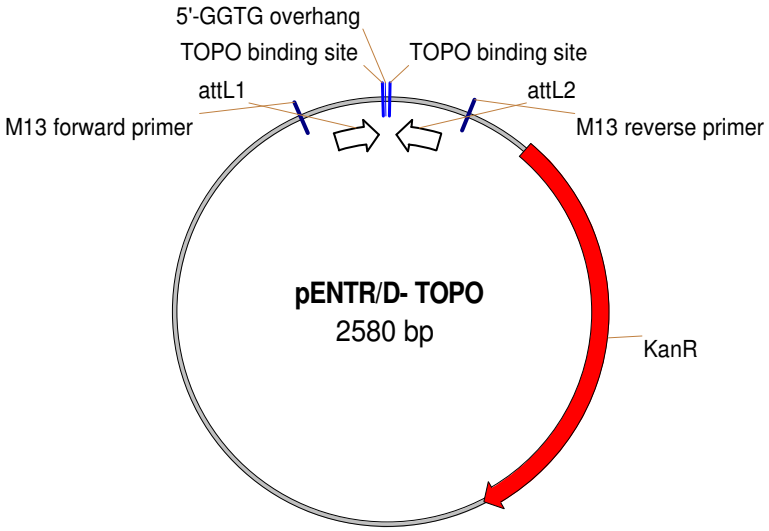

Figure 2-3: Vector map of pENTR/D-TOPO.
This figure displays the important features of the pENTR/D-TOPO plasmid. This plasmid was used to generate entry clones for the MultiSite Gateway® system (Invitrogen). The plasmid possesses a kanamycin resistance cassette (KanR, 795 bp) for selection in *E. coli*. Topoisomerase I is covalently bound at the TOPO binding sites and to allow directional cloning of PCR fragments the plasmid contains a 5' GGTG- overhang which stabilizes PCR products with a 3' CACC extension on the forward primer in the right orientation. Cloned PCR products can be sequenced using M13 forward and M13 reverse primers. The vector contains attL1 and attL2 sites compatible with the MultiSite Gateway® system.

All kits were used following manufacturer's instructions. Ligations were transformed into *E.coli* TOP10 chemically competent cells (Invitrogen) and selected with kanamycin (see 2.4.7.2). From the transformation plates a number of colonies were picked for analyses. Plasmid DNA was isolated and analysed by restriction digests (see 2.4.8.1 and 2.4.4, respectively). Plasmids containing inserts of the right size were sent for sequencing (The Sequencing Service, University of Dundee) using M13 forward, M13 reverse or internal primers.

2.4.6.2 Subcloning into destination vectors

TOPO-clones containing the desired inserts were used for subcloning into the destination vectors. 3 µg of the respective TOPO vector containing the desired inserts and 3 µg of destination plasmid were digested overnight with the relevant restriction enzymes (see 2.4.4). The digested DNA was separated on agarose gels (see 2.4.1) followed by gel extraction using the Qiaquick gel purification kit (Qiagen) according to manufacturer's instructions. Samples were eluted in 30 µl of water and 3 µl per sample were subsequently analysed by agarose gel electrophoresis to asses the purity of the samples and to quantify DNA concentrations.

Ligation reactions of inserts and vectors were performed using 20 units T4 DNA ligase (NEB) with the provided buffer in a final reaction volume of 20 µl. Vector and insert DNA were mixed at ratios ranging from 1:3 to 1:10. Ligation reactions were incubated at 14°C overnight and were subsequently transformed into chemically competent TOP10 cells (Invitrogen). Transformed bacteria were analysed by colony PCR (see 2.4.5.2) and clones containing the desired inserts were analysed by plasmid extraction followed by diagnostic restriction digests. Clones with the correct restriction patterns for insert and vector were verified by DNA sequencing.

2.4.6.3 Gateway cloning

MultiSite Gateway® technology (Invitrogen) is based on the site specific recombination system of the bacteriophage lambda (Landy, 1989) and allows the simultaneous cloning of multiple DNA fragments in a defined order and orientation. The Gateway® technology allows cloning of PCR products into MultiSite Gateway® Donor vectors with the BP reaction, which resembles integration of the lambda phage into the *E. coli* chromosome in the lysogenic cycle. Thus generated, entry clones can then be combined and cloned into destination vectors in an LR reaction, resembling the excision of lambda at the start of the lytic cycle.

In this study, only LR reactions were performed using LR Clonase II Plus enzyme mix (Invitrogen) according to manufacturer's instructions. Gateway cloning was preformed to generate expression constructs for C-terminally tagged PfγGCS and PfGS. The tags introduced were either green fluorescent protein (GFP), hemagglutinin (HA) or a mutant form of the human 12 kDa FK506 binding protein (FKBP12) (Armstrong and Goldberg, 2007; van Dooren et al., 2005). The FKBP12-tag contained two mutations: F36V which allows the binding of the ligand Shld1 and L106P which destabilizes the tagged protein in absence of Shld1 (Banaszynski et al., 2006). The destination plasmid used was pCHDR-3/4 (Figure 2-4) previously described by van Dooren (van Dooren et al., 2005).

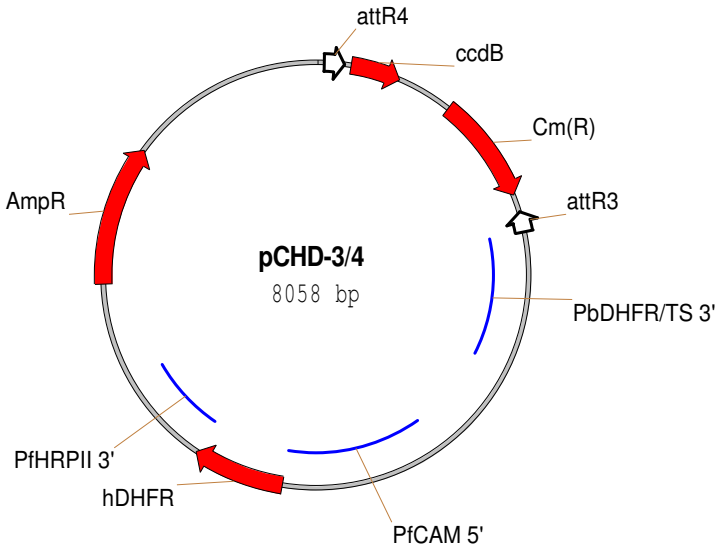

Figure 2-4: Vector map of pCHD-3/4.
This figure displays the important features of the pCHD-3/4 MultiSite Gateway® destination vector. The plasmid contains an ampicillin resistance cassette (AmpR, 861 bp) for selection in bacteria. Further, the plasmid contains a negative selection cassette containing the *ccdB* death gene (306 bp) flanked by two recombination sites attR4 and attR3 which allow recombination with entry clones in a multisite gateway® LR reaction. After recombination the death gene is replaced by the expression cassette flanked by the *P. berghei* dihydrofolate reductase / thymidilate synthase 3' UTR (PbDHFR/TS 3', 853 bp). The plasmid contains the human *dihydrofolate reductase* gene (hDHFR, 564 bp) for selection in *P. falciparum*. The *hDHFR* is under control of the *P. falciparum* calmodulin promoter (PfCAM 5', 631 bp) and flanked by the *P. falciparum* histidine- rich protein2 3' UTR (PfHRPII 3').

The genes of interest were amplified by PCR and directionally cloned into the pENTR/D-TOPO (Invitrogen) vector (see 2.4.6.1). To introduce a promoter to the expression cassette, the PfHsp86 5'-pDONR4/1 entry clone was used (van Dooren et al., 2005). This construct contains the *P. falciparum* Hsp86 5' UTR (Figure 2-5).

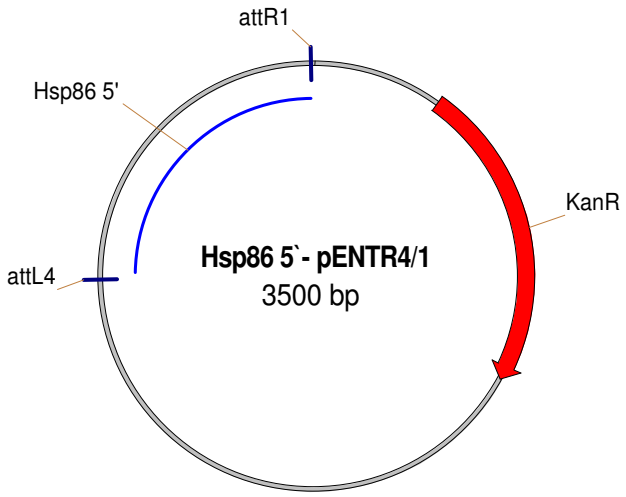

Figure 2-5: Vector map of Hsp86 5'- pENTR4/1.
This figure displays the important features of the promoter entry clone Hsp86 5'-pENTR4/1. The plasmid contains a kanamycin resistance cassette (KanR, 810bp) for selection in *E. coli*. The Hsp86 5' element is flanked by the recombination sites attL4 and attL1 which allow recombination in a multisite gateway® LR reaction.

To introduce the tags, the construct GFPmut2-pENTR2/3 was used for the GFP-tag, the construct 3x HAc-pENTR2/3 for the HA-tag (van Dooren et al., 2005) and the construct FKBP12-pENTR2/3 for the FKBP12-tag (Armstrong and Goldberg, 2007) (Figure 2-6).

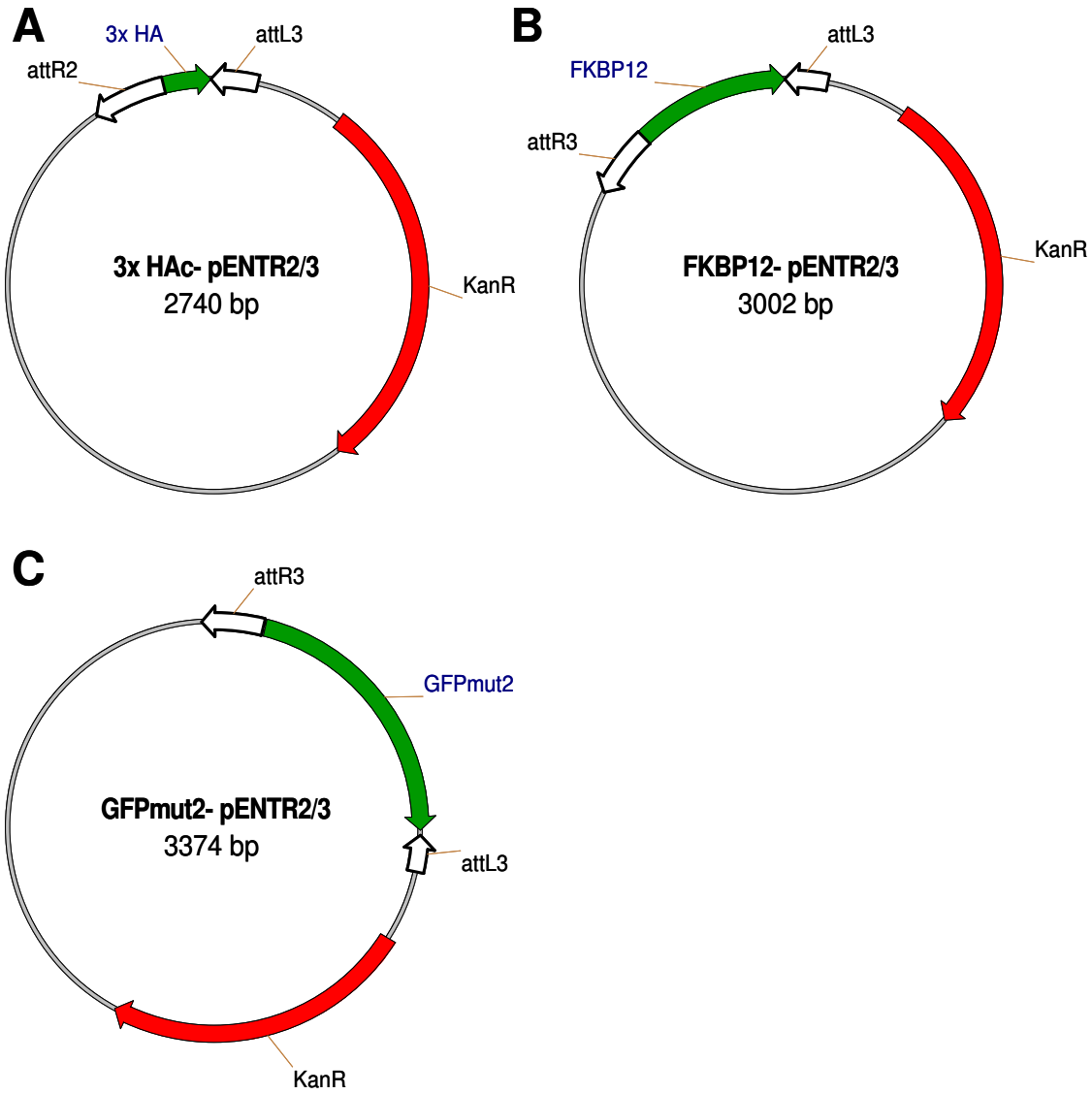

Figure 2-6: Vector maps of 3x HAc- pENTR2/3, FKBP12- pENTR2/3 and GFPmut2- pENTR2/3. This figure displays the important features of the tag-entry vectors 3x HAc-pENTR2/3 (Panel A), FKBP12-pENTR2/3 (Panel B) and GFPmut2-pENTR2/3 (Panel C). All three contain a kanamycin resistance cassette (KanR, 810 bp) for selection of the plasmids in bacteria. The tags 3x HAc, FKBP12 and GFPmut2 to be introduced into the destination vector are flanked by the recombination sites attR3 and attL3 which will fuse the tags to the C-terminus of the gene of interest in the MultiSite Gateway® LR reaction.

2.4.7 Transformation of *E. coli*

2.4.7.1 Preparation of chemically competent cells

A 5 ml pre-culture was grown overnight in LB-medium (see 2.3.4) and used to inoculate 500 ml fresh medium the next morning. Cells were grown at 37°C in a

shaking incubator until the OD_{600} of the culture reached 0.5. The bacteria culture was subsequently cooled on ice for 15 min before being transferred into sterile centrifuge tubes. Cells were spun down at 6,000 g for 10 min at 4°C. The supernatant was discarded and the cells were resuspended in 30 ml Tfb I (see 2.3.4). The cells were incubated on ice for 15 min before centrifugation at 6,000 g for 5 min. The supernatant was again discarded and the cells were resuspended in 6 ml TfB II (see 2.3.4). The cells were aliquoted into 1.5 ml Eppendorf tubes and shock frozen on dry ice. Chemically competent cells were stored at -80°C.

2.4.7.2 Transformation of chemically competent cells

Chemically competent cells were thawed on ice and gently mixed with plasmid DNA, either of existing plasmids or ligation reactions. The cells were incubated on ice for 30 min before being heat shocked in a heat block at 42°C for 30 to 45 sec. The cells were immediately transferred back on ice. After 2 min, 5-10 volumes of SOC- or LB-medium (see 2.3.4) were added. Cells were incubated at 37°C with constant shaking at 200 rpm for 45 to 60 min before being plated on LB-agar plates containing the appropriate antibiotic for selection of the plasmids.

For general cloning either chemically competent OneShot® Top10 cells (Invitrogen) or chemically competent Strataclone SoloPack® cells (Stratagene) were used. For gateway cloning reactions OneShot® Top10 cells were used whereas for amplification of existing plasmids self made chemically competent Top10 cells were used. For protein expression self made chemically competent BLR (DE3) cells were used.

2.4.8 Isolation of plasmid DNA from *E.coli*

Plasmid DNA was isolated from *E.coli* by two methods depending on the desired amount of plasmid. Both methods involved alkaline lysis of bacteria followed by precipitation of most bacterial proteins and genomic DNA with SDS and final purification using silica columns.

2.4.8.1 Small scale plasmid purification (Miniprep)

Small scale purifications were performed using the Qiaprep Spin Miniprep Kit (Qiagen). Single bacteria colonies were picked from agar plates to inoculate 3 ml of LB-medium containing the appropriate antibiotic for selection of the respective plasmids (see 2.3.4). Cultures were grown at 37°C overnight with constant shaking at 200 rpm. Plasmid DNA was isolated following manufacturer's instructions and eluted with 50 µl sterile water. The typical yield was between 10 -30 µg of plasmid DNA.

2.4.8.2 Large scale plasmid purification (Maxiprep)

Large scale purifications were performed using the Nucleo Bond Xtra Maxi Plus Kit from Machery and Nagel. Single bacterial colonies were picked from fresh agar plates to inoculate 5 ml pre-cultures of terrific broth medium (see 2.3.4) containing antibiotics for selection of the respective plasmids. Pre-cultures were incubated for 8 hours at 37°C before being diluted 1:100 into 500 ml of fresh terrific broth medium with the appropriate antibiotic. These main cultures were incubated at 37°C overnight with constant shaking at 200 rpm. The plasmid DNA was extracted following manufacturer's instructions. The typical yield was between 0.5 and 2 mg of plasmid DNA.

2.4.9 Reverse transcription

Reverse transcription of RNA was performed using the RETROscript® reverse transcription for real time PCR kit from Ambion according to manufacturer's instructions. Prior to reverse transcription, parasite RNA was treated with Turbo DNA-free (Ambion) according to manufacturer's instructions to remove any traces of contaminating DNA (see 2.7.8 for RNA preparation). 10 µg of extracted RNA were used in a 50 µl reaction for this treatment. Of the DNase treated RNA, 10 µl corresponding to 1-2 µg of RNA was used for the generation of cDNA. Reverse transcription was preformed following the two step RT-PCR protocol with heat denaturation step according to manufacturer's instructions. The cDNA was stored at -20°C.

2.4.10 Southern blot analyses

To analyse genotypes of transfected *P. falciparum* lines, 1 µg samples of isolated genomic DNA were analysed by Southern blotting (see 2.7.7 for gDNA preparation). The DNA was digested with appropriate restriction endonucleases for 24 hours (see 2.4.4). The digested DNA was separated on a 0.8 % agarose gel at 20 V overnight. For the transfer, a VacuGene XL apparatus (Amersham) was used. The porous filter membrane of the blotter was wetted with ddH_20 and a Hybond N^+ nitrocellulose membrane was placed on top. The plastic mask was placed around the membrane and the membrane covered with 0.25 N HCl before the gel was placed on top, taking care to achieve a tight seal between membrane, mask and gel. The gel was covered with 0.25 N HCl and the vacuum pump turned on, keeping the pressure between 50 and 60 mbar. The DNA was depurinated with 0.25 N HCl until the colour of bromophenolblue used in the DNA loading dye changed from blue to yellow. After the change in colour, the HCl was removed and the gel covered with denaturing solution until the colour changed back to blue (see 2.3.2 for all buffers and solutions). The denaturing solution was removed and the gel covered with 20 x SSC. The transfer continued for further 60 min. Afterwards all remaining 20 x SSC was removed and the sample wells marked on the membrane with a blunt pencil. The blotting apparatus was dismantled and the DNA cross linked with the membrane in a UV cross linker at 700 x 100 $\mu J/cm^2$. Membranes were pre-hybridized in hybridization buffer without probe for at least 15 min at 55°C.

For the labelling of probes the Gene images AlkPhos direct labelling and detection system (GE Healthcare) was used according to manufacturer's instructions. Probes were either gene-specific or specific for the selectable marker of the transfection plasmids. DNA for probes was amplified by PCR (see 2.4.5.1) and the resulting PCR product was purified using the Qiaquik PCR purification kit (Qiagen) according to manufacturer's instructions. The probes were added to the hybridization solution and incubated with the membrane overnight at 55°C. Membranes were washed twice for 10 min with primary wash buffer at 55°C followed by two 5 min wash steps at room temperature with secondary wash buffer. CDP Star detection solution (GE Healthcare) was added to the membrane for 5 min. After excess detection reagent was removed, membranes were heat sealed in plastic bags and the light produced by the

decomposition of the detection reagent was detected by exposure to autoradiography films (Amersham).

2.5 Biochemistry

2.5.1 Sodium dodecyl sulphate polyacrylamide gel electrophoreses (SDS PAGE)

Separation of proteins was performed by SDS-PAGE according to Laemmli (Laemmli, 1970). Gels consisted of a running gel and a stacking gel and were run using the NuPAGE electrophoresis system by Invitrogen. The percentage of running gels ranged from 7.5-15 %, depending on the size of the protein of interest. For all buffers and solutions see 2.3.3. The gels were poured into empty 1 mm plastic cassettes (Invitrogen) and per gel, 6 ml running gel mix was polymerized by addition of 25 µl ammonium persulfate (20 %, w/v) and 5 µl N,N,N',N'- tetramethylethylenediamine (TEMED). Once the running gel was set, 2 ml stacking gel mix was poured on top after addition of 10 µl ammonium persulfate and 2 µl TEMED and an appropriate comb was inserted. 5-20 µg of parasite protein extract was mixed with 6 x protein loading dye and denatured at 100°C for 5 min. Samples were loaded and the gels ran in 1 x SDS PAGE running buffer at 40 mA and a maximum of 200 V. Following electrophoreses, gels were either stained with Coomassie or were used for western blots.

2.5.2 Coomassie blue staining of polyacrylamide gels

Following electrophoresis, polyacrylamide gels were removed from cassettes and stained with Coomassie staining solution for one hour at room temperature with gentle agitation. Afterwards, gels were destained with destaining solution for several hours at room temperature with gentle agitation.

2.5.3 Bradford Assay

Concentrations of parasite protein extracts were determined according to Bradford (Bradford, 1976) using 5x Bio-Rad assay reagent. 4 parts protein solution were mixed with 1 part Bradford reagent and the absorbance at 595 nm determined. BSA solutions of known concentration were used to generate a

standard curve as a reference to calculate the concentration of unknown samples.

2.5.4 Western blot analyses

Proteins were transferred onto Protran nitrocellulose membranes (Schleicher & Schuell) following separation by SDS-PAGE. A Transblot semi-dry transfer system from Biorad was used according to manufacturer's instructions. Blots were set up as a sandwich of six pieces of Whatman paper cut to size and soaked in Towbin buffer (see 2.3.3 for all buffers and solutions), nitrocellulose, gel and another six pieces of soaked Whatman paper from bottom to top. Transfer was in a downward direction at a fixed voltage of 20 V for 40 min. Following transfer membranes were stained with Ponceau S solution (Sigma) and lanes were marked on the membrane with a blunt pencil. The Ponceau stain was removed by washing the membrane with PBS containing 0.1 % Tween 20 (v/v). Blots were blocked in 5 % (w/v) skimmed milk in PBS (see 2.3.1) on a shaker, either for 60 min at room temperature or overnight at 4°C in the cold room. Following blocking membranes were washed 3 x 10 min with PBS/ 0.1 % Tween20 (v/v) and subsequently incubated with primary antibodies for at least 60 min at room temperature with constant shaking. The antibodies were diluted to the required concentration (see Table 2-2) in 2 % (w/v) skimmed milk in PBS/ 0.1 % Tween (v/v). Blots were washed three times in PBS/ 0.1 % Tween20 (v/v) for 10 minutes with shaking. Secondary antibodies were diluted to the required concentration (see Table 2-3) in 2 % (w/v) skimmed milk in PBS / 0.1 % (w/v) Tween20 and incubated with membranes for 60 min. The membranes were washed again three times in PBS / Tween20 as before. Horseradish peroxidase (HRP) conjugated secondary antibodies were detected with the immobilon western blot detection kit (Milipore) and visualized by exposing blots to X-ray films.

2.5.5 BugBuster protein extraction

The Novagen BugBuster protein extraction solution was used to confirm the optimal expression conditions for recombinantly expressed PfGS. A 5 ml overnight culture of *E. coli* BLR (DE3) transformed with the expression construct was used to inoculate four 50 ml flasks of fresh LB-medium (1:50 dilution, see 2.3.4) containing the appropriate antibiotic. Bacteria cultures were incubated at

37°C until they reached an OD_{600} of 0.6 and subsequently induced with 1 mM isopropyl-ß-D-thiogalactopyranoside (IPTG). Each flask was incubated at a different temperature (37°C, 30°C, 25°C, and 18°C) and 1 ml samples were taken from each culture at the time of induction and at every following hour. The final samples were taken after overnight expression. The samples were centrifuged at 15,000 g for 1 min and the supernatant discarded. Bacterial pellets were resuspended in 100 µl BugBuster reagent and 0.5 µl benzonase were added to digest bacterial DNA. Samples were incubated at room temperature for 15 min with constant shaking followed by 15 min centrifugation at 15,000 g at 4°C. The supernatants were transferred into clean 1.5 ml tubes and the pellets resuspended in 100 µl PBS. 5 µl of the pellet fractions and 15 µl of the supernatant fractions were separated by SDS-PAGE (see 2.5.1) and analysed by western blotting (see 2.5.4).

2.5.6 Expression of *P. falciparum* glutathione synthetase

Expression of PfGS and $PfGS^{E206K/N208A}$ was performed as previously described (Meierjohann et al., 2002a). The expression constructs for pJC40-GS and pJC40-$GS^{E206K/N208A}$ were transformed into chemically competent *E. coli* BLR (DE3) cells. The properties of the expression vector pJC40 are displayed in Figure 2-7.

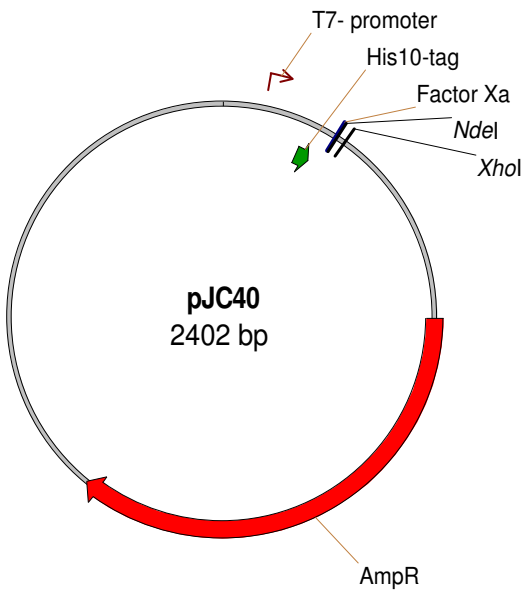

Figure 2-7: Vector map of pJC40
This figure displays the important features of the pJC40 recombinant protein expression plasmid. The plasmid contains an ampicillin resistance cassette (AmpR, 861 bp) for selection in *E.coli*. Restriction sites *Nde*I and *Xho*I were used for cloning the PfGS ORF. Expression is under the control of the T7 promoter and a $His_{(10)}$- tag is attached to the N- terminus of the protein and can be cleaved off with factor Xa.

Single colonies were picked to inoculate 5 ml LB-ampicillin-medium and incubated at 37°C for 8 hours. This starter culture was diluted into 50 ml fresh LB-ampicillin medium and incubated overnight. Again the culture was diluted 1:50 with fresh LB-ampicillin medium and the bacteria were incubated at 37°C until the OD_{600} reached 0.5. The temperature was reduced to 25°C and the PfGS expression was induced by addition of IPTG (1 mM final concentration). Expression took place overnight and the following day cells were centrifuged for 15 min at 4°C at 6,000 g in 500 ml aliquots. Each bacteria pellet corresponding to 500 ml culture was resuspended in 10 ml buffer A (see 2.3.3) and stored at -20°C. To purify PfGS, bacteria pellets were thawed and 50 µg/ml lysozyme added. The pellets were incubated for 30 min on ice and protease inhibitors phenylmethylsulfonylfluoride (PMSF, 1 mM), leupeptin (2 µg/ml) and pepstatin-A (1.5 µM) were added. Bacteria were disrupted using a one shot cell disrupter (Constant Systems) at 15 kpsi. Subsequently the disrupted bacteria were centrifuged at 48,000 g for 60 min at 4°C.

2.5.7 Purification of PfGS and PfGS$^{E206K/N208A}$

Following centrifugation, bacterial lysate (see 2.5.6) was filtered through a 0.8 µm syringe filter. Nickel-nitrilotriacetic acid (Ni^{2+}-NTA) agarose was washed with ddH_2O and equilibrated with buffer A (for all buffers see 2.3.3). The filtered lysate was added to the Ni^{2+}-NTA agarose and incubated for 60 min on a rotating wheel to allow binding of the His-tagged recombinant protein. All steps were carried out at 4°C. Approximately 5-10 mg of protein was bound to 1 ml of agarose. The agarose was pelleted by centrifugation at 150 g for 5 min. The supernatant was carefully removed and the agarose washed with buffer A for 30 min with rotation. Agarose beads were pelleted as before and washed twice for 20 min with buffer B. After the last wash the resin was poured into an Econo-Pac column (Bio-Rad) and allowed to set. The protein was eluted with elution buffer C. For a 500 ml bacterial pellet 1 ml of elution buffer was used.

2.5.8 Determination of PfGS and PfGS$^{E206K/N208A}$ activity

The enzyme activity of PfGS and PfGS$^{E206K/N208A}$ was determined as previously described (Meierjohann et al., 2002a). The assay was performed in a 1 ml volume of reaction buffer (see 2.3.3) at 30°C. NADH was added to a final

concentration of 0.2 mM and ATP, sodium phosphoenolpyruvate and glycine were added to final concentrations of 5 mM, 5 mM and 40 mM, respectively. 2 mM γ-L-glutamyl-L-α-aminobutyrate was used as substrate instead of γ-L-glutamyl-L-cysteine to avoid thiol oxidation. 5 units / ml of pyruvate kinase (type III rabbit muscle) and 10 units / ml lactate dehydrogenase (type II rabbit muscle) were added and the reaction was started by addition of the purified PfGS or $PfGS^{E206K/N208A}$. The enzyme activity was measured by following the change in absorbance at 340 nm. Active GS consumes ATP during the formation of GSH and thus leads to the accumulation of ADP. Pyruvte kinase uses phosphoenolpyruvate to convert ADP back to ATP, thereby generating pyruvate. The pyruvate is in turn converted to lactate by the lactate dehydrogenase in a reaction that leads to the oxidation of NADH to NAD^+. This oxidation process leads to a decrease in absorption at 340 nm detected in a Shimadzu UVPC 2501 spectrophotometer.

2.6 Bioinformatics

2.6.1 Statistical analysis

Statistical analyses were performed using Prism 3.0 software. In order to analyse if two groups of samples were significantly different an unpaired Student t-test was performed. More than two groups of samples were analysed by one-way analysis of variance (ANOVA) followed by Newman-Keuls post hoc analyses if differences were significant.

2.6.2 Sequence alignment

Alignments of multiple protein sequences were performed using either ClustalW (http://www.ebi.ac.uk/Tools/clustalw2/index.html) or TCoffee (http://www.ebi.ac.uk/Tools/t-coffee/index.html) software.

2.7 *P. falciparum* cell culture

2.7.1 Culturing of *P. falciparum*

Erythrocytic stages of *P. falciparum* were cultured according to Trager and Jensen (Trager and Jensen, 1976). All culture work was performed in a category

2 tissue culture hood and all solutions used were filter sterilized prior to use. Parasites were kept in sterile cell culture flasks at 37°C in an atmosphere of 5 % CO_2, 1 % O_2 and 94 % N_2. Erythrocytes were washed in blood wash medium (see 2.3.5) by centrifuging at 700 g at 4°C for 10 min and subsequently replacing the supernatant with fresh blood wash medium. This was repeated 3 to 4 times until the supernatant appeared clear. Washed erythrocytes were stored at 4°C and used for up to four weeks. Erythrocytes were added to cultures at 5 % hematocrit. Every 24 hours the medium was carefully aspirated without disturbing the cell layer at the bottom of the flasks and fresh RPMI 1640 complete medium (see 2.3.5) was added. Cultures were regularly diluted with fresh erythrocytes and medium so that the parasitemia was kept below 10 %. A parasitemia of 2-4 % was considered optimal.

2.7.2 Giemsa staining of blood smears

To determine the parasitemia, Giemsa stained thin smears of infected red blood cells were examined using a light microscope with 100 x objective. For the smears small amounts of sedimented erythrocytes were taken from the cultures and spread on a glass slide. After drying, cells were fixed in 100 % methanol and stained for 10 min in Giemsa solution (1:25 dilution). Excess staining solution was washed off with water and the slides were air dried. Afterwards slides were examined with a 100 x oil immersion objective under the light microscope. To determine the parasitemia the ratio of erythrocytes to parasites was determined. Erythrocytes infected with multiple parasites were counted as single infections.

2.7.3 Parasite stabilates

For stabilates, a 10 ml culture with 5-7 % parasitemia containing mostly ring stages was used. The infected red blood cells were sedimented by centrifugation at 400 g at 4°C for 5 min. The medium was removed and the cell pellet resuspended in one pellet volume of cold RPMI 1640 complete medium. Two pellet volumes of cold freezing solution (30 % (v/v) glycerol in PBS) were added and carefully mixed. 600 µl aliquots of the cell suspension were transferred into cryotubes and incubated on ice for 15 min before storage in liquid nitrogen.

2.7.4 Thawing of *P. falciparum* stabilates

Cells were thawed in a 37°C water bath and immediately placed on ice. The stabilates were transferred into a 15 ml tube and 2 volumes of ice cold 27 % sorbitol (w/v in 10 mM potassium phosphate pH 7.2) were drop-wise added with constant shaking. The cells were incubated on ice for 13 min before twice the original pellet volume of ice cold 5 % sorbitol was added. After incubation on ice for 10 min the cells were centrifuged at 400 g at 4°C for 5 min. The supernatant was removed and the cell pellet carefully resuspended in 5 % sorbitol (w/v in 10 mM potassium phosphate pH 7.2). After incubation for 8 min the cells were pelleted again as before. The supernatant was removed and the cells were washed twice with cold RPMI 1640 complete medium. After the final wash, cells were resuspended in RPMI 1640 complete medium and erythrocytes were added to a hematocrit of 2.5 %. Once parasites had grown to a density of approximately 2 % the hematocrit was raised to 5 %. If required, the adequate drug was added as soon as parasites reached a sufficiently high parasitemia (1-2 %).

2.7.5 Synchronising of *P. falciparum* cultures with sorbitol

Parasites were synchronized in ring stages as previously described (Lambros and Vanderberg, 1979). Cultures were centrifuged at 400 g at room temperature for 5 min and the supernatant was discarded. The cell pellet was resuspended in 5 pellet volumes of 5 % sorbitol (w/v in 10 mM potassium phosphate pH 7.2) and incubated at 37°C for 5 min. After incubation, the cells were centrifuged as before and the supernatant removed. The cells were resuspended in complete RPMI 1640 medium and cultured as described above (see 2.7.1).

2.7.6 Saponin lysis of *P. falciparum* infected red blood cells

For the subsequent isolation of genomic DNA, RNA or protein, the cells were resuspended in the culture medium and 1/10 of the culture volume of 2 % saponin in PBS was added. The cells were incubated for 10 minutes on ice to allow complete lysis of the red blood cells and the freed parasites were precipitated by spinning at 2,700 g for 10 min at 4°C. The supernatant was discarded and the parasites were resuspended in 1 ml PBS and transferred into a 1 ml tube. The parasites were precipitated by spinning in a micro-centrifuge at

2,500 g for 3 min at 4°C before the supernatant was removed and the parasites were washed again in 1 ml PBS. The parasites were again pelleted by spinning as before. The wash step was repeated until the supernatant was clear of traces of hemoglobin. The supernatant was removed and the parasite cells were used for the preparation of DNA, RNA or protein.

2.7.7 Extraction of genomic DNA from *P. falciparum*

Genomic DNA (gDNA) was extracted using the Qiagen QiaAmp DNA mini kit following the blood or body fluid spin protocol according to manufacturer's instructions. For standard preparations, trophozoite stage parasites of a 25 ml culture at a parasitemia of 4-5 % were isolated from erythrocytes by saponin lysis (see 2.7.6) prior to gDNA extraction. The gDNA was eluted with ddH_2O and stored at 4°C.

2.7.8 Extraction of RNA from *P. falciparum*

RNA was extracted as previously described (Smith et al., 1998). Following saponin extraction of parasites (see 2.7.6) parasite pellets were resuspended in 10 x their volume of TRIZOL® reagent (Invitrogen) and stored at –80°C until further use. After defrosting, RNA was extracted by addition of 0.2 volumes of chloroform. Samples were mixed by shaking for 15 sec followed by 2 min incubation at room temperature and subsequent centrifugation at 13,000 g at 4°C for 15 min. The aqueous phase was transferred to a clean 1.5 ml tube and 0.7 volumes of isopropanol added. The RNA was precipitated at 4°C overnight. On the following day samples were centrifuged at 13,000 g at 4°C for 30 min. The supernatant was removed and the RNA pellet washed with 70 % ethanol. The samples were again centrifuged at 13,000 g at 4°C for 15 min and the supernatant removed. The RNA pellet was air dried before being resuspended in an appropriate volume of DEPC- treated RNase free water (20-40 µl) by heating to 60°C for 10 min. RNA was stored at -80°C.

2.7.9 Extraction of protein from *P. falciparum*

Following saponin lysis (see 2.7.6) parasite pellets were resuspended in 2D-lysis buffer and stored at -80°C until further processing. To extract protein, pellets

were thawed at 37°C followed by immediate freezing on dry ice. This was repeated three times. The samples were sonicated in a sonicating waterbath for 5 min and centrifuged at 15,000 g at 4°C for 5 min. The supernatant was transferred into a clean 1.5 ml tube and the protein concentration determined by Bradford assay (see 2.5.3).

2.7.10 Transfection of *P. falciparum*

For transfections synchronized cultures (see 2.7.5) of ring stage infected erythrocytes at a parasitemia of 4-7 % were used (Crabb and Cowman, 1996; Crabb et al., 2004). The medium of the culture was aspirated and the cells resuspended in cytomix (see 2.3.5). Cells were centrifuged at 400 g for 5 min at 4°C and the supernatant removed. 100 µg of precipitated plasmid DNA (see 2.4.3) was resuspended in 30 µl of sterile TE buffer and mixed with 370 µl of cytomix. 200 µl of infected erythrocytes were added and carefully mixed. The cell suspension was transferred into a 0.2 mm electroporation cuvette (Bio-Rad) and the cells electroporated at 310 V and 950 µF using a Gene Pulser Xcell electroporator (Bio-Rad). The time constant values were between 10- 15 ms. The transfected cells were immediately transferred into a culture flask containing 300 µl of uninfected erythrocytes and 9 ml of pre-warmed complete medium. After 6 hours the medium was changed and the appropriate drugs were added to the cultures.

2.7.11 Gene knockout in *P. falciparum*

Two strategies were used for gene knockout studies in *P. falciparum*. The first method was based on gene disruption following a single crossover event between the gene of interest and a construct based on the pHH1 vector ((Reed et al., 2000) (Figure 2-8). The plasmid contains the *human dehydrofolate reductase* gene (*hDHFR*) for positive selection of transfected parasites with the drug WR99210. Further, the plasmid contains an ampicillin resistance cassette for selection of the constructs in *E. coli*. Using the restriction sites *Bgl*II and *Xho*I, fragments homologous to the target gene were cloned into the plasmid. For knockout constructs these fragments were truncated at the N-terminus and thus missing the start codon ATG as well as being truncated at the C-terminus and containing an artificial stop codon. A single crossover recombination event

between such constructs and their target gene leads to disruption of the target gene and the formation of two truncated, non-functional copies. Similarly, pHH1 based constructs were used as knock-in controls. In this case the fragment cloned into the vector was only truncated at the N-terminus but contained the full C-terminus. Single crossover events between knock-in control constructs and the target gene lead to the formation of one full length copy and one truncated copy of the gene.

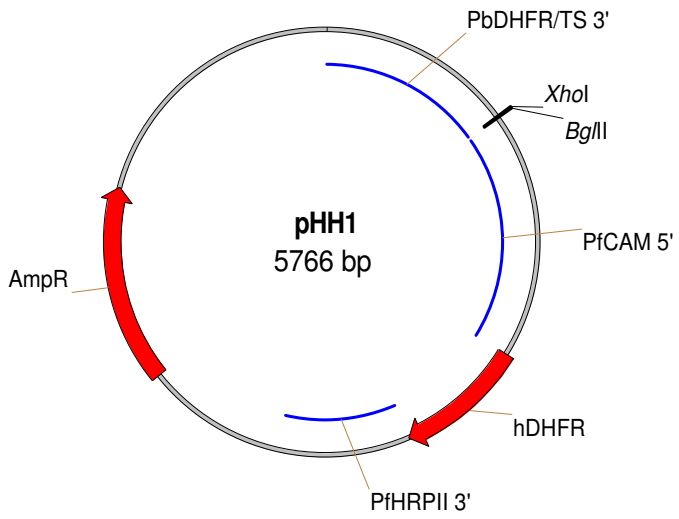

Figure 2-8: Vector map of pHH1.
This figure displays the features of the pHH1 vector used for single crossover knockout studies in *P. falciparum*. The plasmid contains an ampicillin resistance cassette (AmpR, 861 bp) for selection and propagation of the plasmid in *E. coli*. For selection in *P. falciparum* the vector contains the *human dehydrofolate reductase* gene (hDHFR, 569 bp) under control of the *P. falciparum* calmodulin promotor (PfCAM 5', 631 bp) and flanked by the *P. falciparum* histidine rich protein II 3' UTR (PfHRPII 3', 574 bp). Fragments homologous to target genes were cloned using the *Bgl*II / *Xho*I restriction sites. The cloning site was flanked by the *P. berghei* dihydrofolate reductase / thymilidate synthase 3' UTR (PbDHFR/TS 3', 855 bp).

The second strategy was based on gene replacement following a double cross-over event and used the pCC-4 plasmid (Maier et al., 2006) (Figure 2-9). Two fragments homologous to the start and end of the target genes were cloned into this plasmid. A fragment homologous to the 5'-end of the gene was cloned into the plasmid using the *Sac*II / *Afl*II restriction sites and a fragment homologous to the 3'-end was cloned using the *Nco*I / *Nar*I sites. The plasmid contained the *blasticidin-S-deaminase* gene which confers resistance to the drug blasticidin-S-HCl and allows for positive selection of transfected parasites. Furthermore the plasmid contains the *E. coli cytosine deaminase* (*cd*) gene which converts 5-fluorocytosine, the active component in Ancotil®, into 5-fluorouracil, an inhibitor for RNA synthesis and *thymidylate synthase*. The *cd* gene is lost in the case of double crossover recombination between the plasmid and the target gene, thus allowing for negative selection against parasites maintaining episomal

copies of the constructs and enrichment of those parasites that have integrated the plasmid.

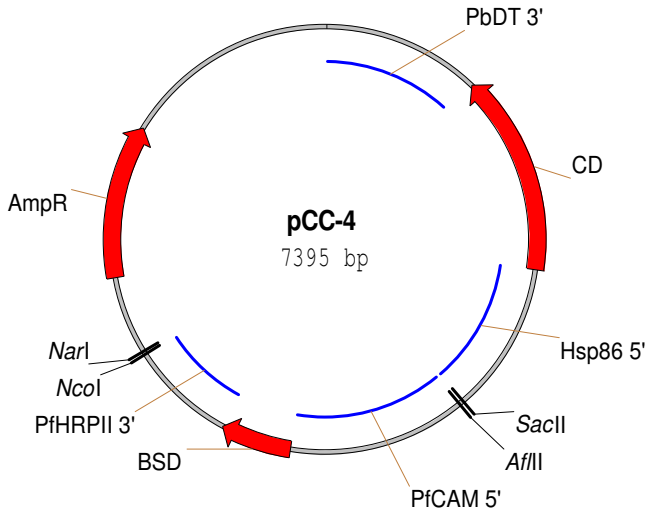

Figure 2-9: Vector map of pCC-4
This figure displays the important features of the pCC-4 vector for double crossover knockout studies in *P. falciparum*. The plasmid contains an ampicillin resistance cassette (AmpR, 861 bp) for selection of the plasmid in *E. coli*. For positive selection in *P. falciparum* the plasmid contains the balsticidin-S deaminase gene (BSD, 399 bp) under control of the *P. falciparum* calmodulin promoter (PfCAM 5', 631 bp) and flanked by the *P. falciparum* histidine rich protein II 3' UTR (PfHRPII 3', 574 bp). For negative selection the plasmid contains the *E. coli cytosine deaminase* (CD, 1122 bp) flanked by the *P. falciparum* heat shock protein 86 promoter (Hsp86 5', 841 bp) and the *P. berghei dhfr* terminator (PbDT, 845 bp). Restriction sites *Sac*II and *Afl*II were used for cloning of the 5' fragment and restriction sites *Nco*I and *Nar*I were used for cloning of the 3' fragment homologous to the target gene.

2.7.12 Determination of IC_{50} values

IC_{50} values were determined by measuring [^{3}H]-hypoxanthine incorporation in the presence of increasing drug concentrations according to Desjardins *et al.* (Desjardins et al., 1979). Cultures were diluted to 0.5 % parasitemia and 2 % hematocrit in IC_{50} medium (see 2.3.5). A serial dilution of twice the drug concentration to be tested was prepared on a 96 well plate in IC_{50} medium. To 100 µl of drug in each well 100 µl of cells were added, creating a 1 x final concentration of the drug. Incorporation of [^{3}H]-hypoxanthine in empty red blood cells and parasites incubated without drug was measured as control. Plates were placed in an incubation chamber, gassed with malaria gas and incubated for 48 hours at 37°C. After 48 hours 100 µl of medium was removed from each well and 100 µl of fresh medium containing 5 µCi [^{3}H]-hypoxanthine / ml were added. Plates were incubated for further 24 hours before being frozen at -20°C. Plates were thoroughly defrosted before being harvested using a Tomtec Mach III harvester and Wallac Printed Filter Mat A filter mats. The filter mats were dried at room temperature before being sealed in a sample bag with

4 ml scintillation liquid. Decay was measured in a Wallac Trilux MicroBeta counter for 1 min per well. IC_{50} values were calculated using GraFit 5 software.

2.7.13 Magnet activated cell sorting columns

Trophozoite infected red blood cells were purified using magnet activated cell sorting (MACS) columns to obtain highly synchronized cultures with ~90 % parasitemia. CS-MACS columns were used with the VarioMACS separator (Miltenyi Biotech) and 21 G x 11'' blunt needles. Columns were assembled according to manufacturer's instructions and equilibrated with 60 ml buffer (0.5 % (w/v) BSA, 2 mM EDTA pH 8.0 in PBS for subsequent determination of GSH levels, Earle's balanced salt solution (EBSS, see 2.3.5) for subsequent uptake studies). The first 10 ml of buffer were applied to the column from the bottom using the provided syringe, thereby removing all air bubbles from the resin. The remaining buffer was added to the top of the column and entered the resin by gravity flow. The medium of 100 ml culture was removed and the cells were resuspended in ice cold buffer. Cells were centrifuged at 700 g and the supernatant removed. The cells were resuspended in 20 ml buffer and loaded onto the equilibrated column. The cells were allowed to slowly drip through the column (~1.5 ml/min). In the magnetic field of the MACS separator late stage parasites are retained due to the paramagnetic properties of hemozoin in the food vacuoles of these stages. Once the cells had completely entered the column it was washed with 50 ml buffer to remove any unbound cells. To elute the bound cells, the column was removed from the magnetic field and turned upside down. Cells were then carefully eluted by gently pressing 30 ml of buffer through the column with a syringe. The purified infected cells were centrifuged at 400 g and used for further experiments.

2.7.14 Determination of total glutathione levels in *P. falciparum*

The intracellular levels of total glutathione in *P. falciparum* were determined according to Meierjohann (Meierjohann et al., 2002b) with modifications. Initial experiments were performed using MACS purified trophozoite infected red blood cells. However, in a second set of experiments 100 ml of tightly synchronized culture containing young trophozoites were used instead of MACS or Percoll

enriched cultures as it was noted that enriching of parasites had a negative effect on GSH levels. All steps were performed at 4°C. The medium was removed and the cells washed in cold EBSS. Cells were centrifuged at 400 g for 5 min and the supernatant removed. The infected red blood cells were carefully resuspended in 5 volumes of 0.15 % saponin in EBSS. The cells were incubated on ice for 5 min and subsequently pelleted by centrifugation at 2,000 g for 5 min. A small sample was taken to control the quality of the parasite preparation under a light microscope. The remaining parasite cells were washed twice with 13 ml EBSS and centrifuged again for 5 min at 2,000 g. After the second wash parasites were resuspended in 5 ml EBSS and a 10µl sample was taken to determine the number of cells using a hemacytometer. The remaining cells were centrifuged at 2,000g for 5 min. After the supernatant was completely removed, parasites were resuspended in 250 µl 0.1 M HCl and transferred into a 1.5 ml microfuge tube and vortexed for 30 sec to break the cells. Protein was precipitated by centrifugation at 15,000 g for 5 min at 4°C. The supernatant was used to determine GSH levels according to Tietze (Tietze, 1969). 25 µl and 50 µl aliquots of parasite extract were mixed with 700 µl of 143 mM sodium phosphate (pH 7.5) containing 6.3 mM EDTA. 10 µl of 34 mM NADPH and 100 µl of 6 mM 5,5-Dithiobis-(2-nitrobenzoate) (DTNB, Ellman reagent) were added and the volume was adjusted to 950 µl with water. The mixture was incubated at room temperature for 20 min to allow full reaction of thiols with the DTNB and the reaction was started by addition of 50 µl of *S. cervisiae* GR (Sigma, 15 units ml^{-1}). GSH reacts with DTNB non-enzymatically to GSSG and 2 molecules of chromophoric TNB^-. In the presence of GR, GSSG is reduced to GSH which can react again with DTNB. The TNB^- generated is directly proportional to the GSH concentration of the sample or standard. The extinction coefficient of TNB^- at 412 nm is 13,600 M^{-1} cm^{-1}. The change in absorbance at 412 nm was determined using a Shimadzu UV-2501 PC spectrophotometer. GSH levels were calculated relative to known standard concentrations of GSH. Standard curves ranged from 0.5 µM to 3 µM.

2.7.15 Determination of glutathione uptake

GSH uptake was measured using MACS column purified trophozoite infected RBC and uninfected RBC. Cells were diluted to 2 x 10^8 cells/ ml in EBSS and kept on ice. At time point t= 0 an equal volume of uptake solution containing 100 nCi

[^{3}H]-GSH (= 24 pmol) / 100 µl was added and the cells were placed in a 37°C water bath. At the time points of interest, 200 µl aliquots were removed and layered onto 300 µl of dibutylphthalate and immediately centrifuged at 10,000 g to terminate the uptake. The cells were sedimented below the oil while the uptake solution remained on top. The uptake solution was removed and the tube walls above the oil were carefully rinsed with ddH_2O. The water was removed and the tube walls wiped with a cotton bud to remove any traces of label. The oil was removed and the cells lysed by addition of 100 µl ddH_2O. The lysate was transferred into a scintillation vial and 50µl H_2O_2 and 50 µl acetic acid were added in order to bleach the hemoglobin in the samples and to ensure complete lysis. 3 ml of scintillation liquid were added and samples were counted on the following day in a Wallac Trilux MicroBeta counter.

3 γ-Glutamylcysteine Synthetase

3.1 Introduction

The first step of the biosynthesis of GSH, the ligation of L-glutamate (L-Glu) and L-cysteine (L-Cys) to form γ-glutamylcysteine (γGC) is catalysed by the enzyme γ-glutamylcysteine synthetase (γGCS) (Reaction 2).

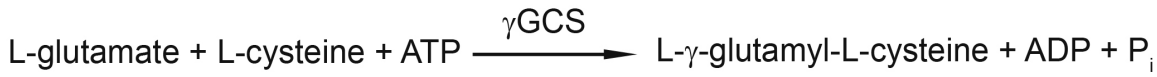

Reaction 2: First step of GSH biosynthesis.
The ATP dependent ligation of L-Glu and L-Cys to form γGC is catalysed by γGCS.

In this chapter the localization of PfγGCS was determined by episomal expression of PfγGCS-GFP in parasites. In order to determine if the gene is essential a knockout of the *pfygcs* gene was attempted using two different strategies. The first strategy is based on a single crossover recombination and leads to gene disruption if the gene is non-essential. The second strategy is based on a double crossover recombination that leads to a replacement of non-essential genes. Further, it was determined if targeting of the *pfygcs* gene locus with a knock-in control construct is possible and whether the knockout in the presence of an additional episomal copy of the gene can be achieved. In addition, the effects of over-expressing PfγGCS-HA were also investigated.

3.2 Sequence considerations

The predicted PfγGCS protein sequence is almost twice the size of its homologues in yeast, humans or *T. brucei* (Lüersen et al., 1999). The overall amino acid sequence identity between PfγGCS and the human and *T. brucei* γGCS is low at 19.7 and 18.6 %, respectively. However, several residues involved in binding of substrates and cofactors are conserved in homologous regions (Lüersen et al., 1999). An interesting feature of PfγGCS is the presence of a repetitive motif whose abundance varies in different strains characterized (Lüersen et al., 1999). Due to this variation in repeats of (Y/C)QS(N/D)LQQ(Q/R), the predicted molecular mass for PfγGCS also varies between different *P. falciparum* strains and ranges from 124.4 kDa in the 3D7 strain to 133.2 kDa in the K1 strain. In order to determine the number of repeats

for the repetitive element in *P. falciparum* D10, a part of the *pfygcs* coding sequence containing the repetitive sequence was amplified by PCR (Figure 3-1), cloned into the plasmid pCR-BluntII-TOPO and sequenced. The primers used for PCR were those designed for cloning of the pHH1-Δ*ygcs* plasmid (see Table 2-1) as the sequence of the insert of this plasmid includes the repetitive element.

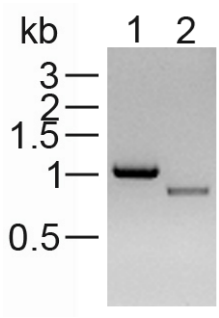

Figure 3-1: PCR analysis of the *pfygcs* variable repetitive motif in *P. falciparum* strains D10 and 3D7.
A fragment of the *pfygcs* gene containing a variable repetitive motif was amplified by PCR from D10 (lane 1) and 3D7 gDNA (lane 2). The fragment sizes differ between the strains due to different numbers of a variable repetitive motif.

Sequencing results showed that the D10 PfγGCS contains a total of nine repeats of the repetitive motif, while the sequencing strain *P. falciparum* 3D7 only contains this motif once (Figure 3-2). The predicted molecular mass of the D10 PfγGCS protein is 130.8 kDa.

```
3D7    263 ENEQQQQQQQ YQSNLQQQ -------- -------- --------
D10    263 ENEQQQQQQQ YQSNLQQQ YQSNLQQQ YQSNLQQQ YQSDLQQQ

3D7    -------- -------- -------- -------- -------- NVQPK 285
D10    YQSDLQQQ YQSDLQQQ YQSDLQQQ YQSDLQQQ CQSDLQQQ NVQPK 349
```

Figure 3-2: Alignment of the repetitive sequence motif of *P. falciparum* 3D7 and D10.
The D10 PfγGCS enzyme contains a total of nine repeats of a variable repetitive motif as opposed to only one repeat found in 3D7, thus increasing the predicted molecular size of the enzyme from 124.4 kDa to 130.8 kDa.

3.3 Localization

To determine the subcellular localization of PfγGCS, recombinant C-terminally GFP-tagged PfγGCS was episomally expressed in *P. falciparum*. Using MultiSite Gateway® technology (van Dooren et al., 2005), the full length *ygcs* ORF of *P. falciparum* 3D7 containing the repetitive motif only once was cloned in frame with the sequence for a C-terminal GFP-tag. Expression was under the control of the Hsp86 promotor. The construct pCHD-Hsp86-γGCS-GFP was transfected twice independently into D10 wild-type parasites and transfected parasites were

observed in thin smears five to six weeks post transfection. The transfected parasite lines D10$^{\gamma GCS\text{-}GFP}$-1 and D10$^{\gamma GCS\text{-}GFP}$-2 were analysed by fluorescence microscopy.

Both parasite lines showed fluorescence in the cytosol, albeit the fluorescent signal was stronger in the D10$^{\gamma GCS\text{-}GFP}$-2 parasites, indicating higher expression levels of the PfγGCS-GFP recombinant protein in these parasites. Therefore only images taken of D10$^{\gamma GCS\text{-}GFP}$-2 are displayed here (Figure 3-3A). To confirm that the fluorescence observed was due to the full-length recombinant protein tagged with GFP and not due to degradation products or cleaved off GFP alone, protein was extracted from the parasites and analysed by western blotting using an anti-GFP antibody (Figure 3-3B). A band of the expected size for PfγGCS-GFP was detected at 153.0 kDa. Some bands indicating degradation were also observed at smaller molecular sizes and a band at approximately 27 kDa likely to be GFP alone is also visible. Despite the presence of some degradation products these results indicate that full-length PfγGCS-GFP is cytoplasmic.

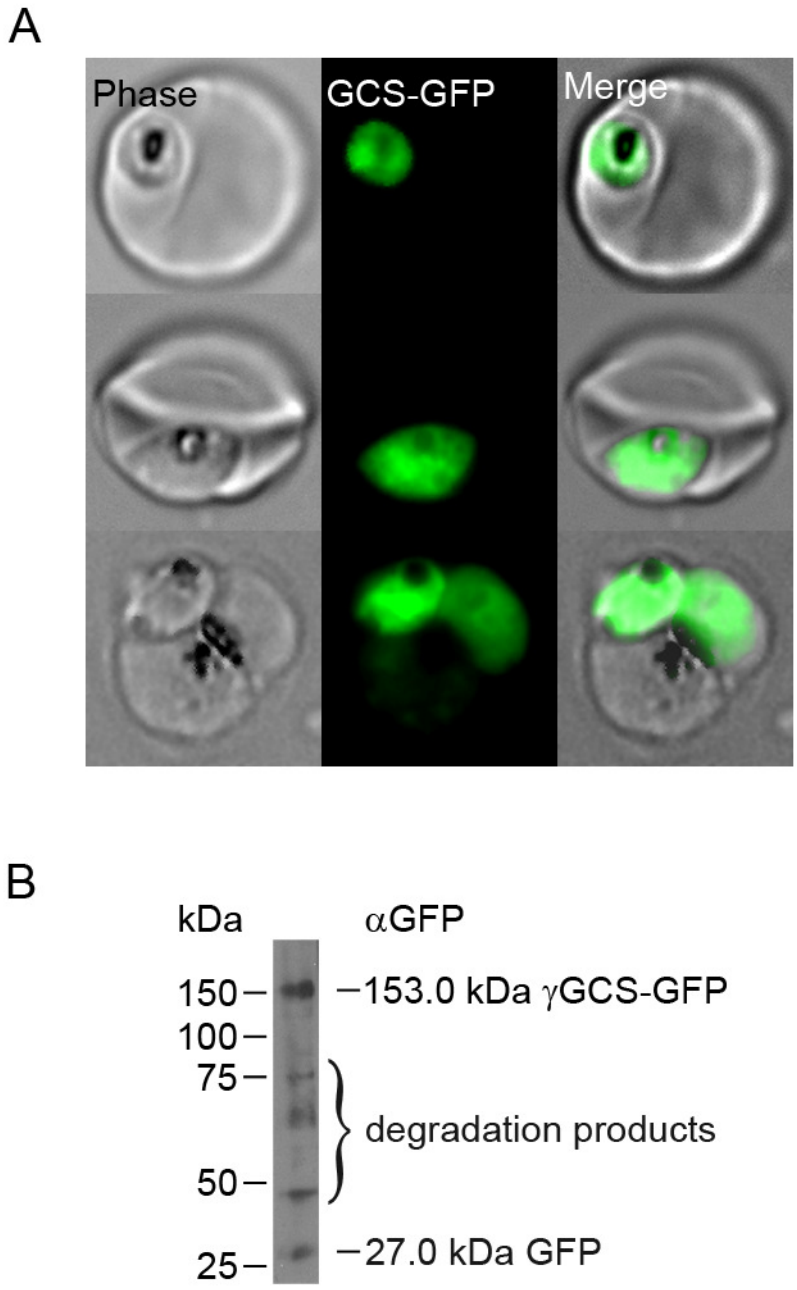

Figure 3-3: Subcellular localization of PfγGCS-GFP.
Panel A: To determine the subcellular localization of PfγGCS, a recombinant C-terminally tagged PfγGCS-GFP fusion protein was expressed in *P. falciparum* D10. Expression was under control of the Hsp86 promotor. Images were taken from parasite line $D10^{\gamma GCS\text{-}GFP}$-2. The fusion protein localized to the parasite cytosol. **Panel B**: Western analysis of protein extract of $D10^{\gamma GCS\text{-}GFP}$-2 with anti-GFP antibody showed the full length PfγGCS-GFP fusion protein at 153 kDa and some smaller degradation products.

3.4 Knockout by gene disruption

In order to assess whether the *pfygcs* gene is essential for the survival of intra-erythrocytic stages of *P. falciparum in vitro*, a knockout by gene disruption was attempted. For this an 864 bp fragment of *P. falciparum* 3D7 *pfygcs* truncated at the 5'- and 3'-end was cloned into the plasmid pHH1 (Reed et al., 2000), thus generating the construct pHH1-Δ*ygcs* (see Table 2-1). The insert lacks the start

ATG and contains an artificial stop codon. Because the insert includes the area that encompasses the repetitive motif, pHH1-Δ*ygcs* is homologous to the 3D7 strain of *P. falciparum*. A single crossover recombination event between the homologous insert of this construct and the *pfygcs* target gene leads to disruption of the gene into two truncated copies to form a pseudo-diploid gene locus. It is expected that integration of this plasmid results in one copy of *pfygcs* truncated at the 3'-end by the artificial stop codon and one copy truncated at the 5'-end and lacking a start codon, should the gene be non-essential (Figure 3-4A). pHH1 contains a *human dihydrofolate reductase* (*hdhfr*) cassette which allows for positive selection of transfected parasites with the drug WR99210. The construct was transfected into the 3D7 wild-type strain and WR99210 resistant parasites were visible in Giemsa stained thin smears after 4-5 weeks. Genomic DNA (gDNA) was isolated from the parasites and used for Southern blot analysis of the genotype of the transfected parasites.

In the meantime transfected parasites were taken through drug selection cycles. This means that the drug pressure was removed from the cultures for three weeks at a time. During this time, many parasites lose the episomal plasmid and thus the *hdhfr* gene and become sensitive to the drug again. However, if the plasmid has already integrated into the target gene locus it cannot be lost from the parasites and these parasites remain resistant. After three weeks the drug is added back to the cultures and as a consequence parasites that have lost the plasmid die, while parasites which retained the episomal plasmid or integrated the plasmid into their genome survive. It is thought that this procedure enriches for parasites that have integrated the plasmid into their genome and allows for faster isolation of knockout parasite lines.

The transfected line $3D7^{pHH1\text{-}\Delta ygcs}$ was taken through two drug selection cycles and after each cycle, when parasites were growing under drug pressure again, gDNA was isolated and analysed by Southern blotting. The schematic diagram in Figure 3-4A displays the expected banding pattern of the Southern blot after diagnostic digest with the enzymes *Nde*I and *Xho*I. The fragments expected to be visible with a gene specific probe are indicated by red arrows, while fragments expected with a probe specific for the *hdhfr* selectable marker are indicated by blue arrows. For the endogenous *pfygcs* locus of 3D7 (Figure 3-4A, I) a single band at 3.69 kb is expected when a gene specific probe is used. This fragment

cannot be detected with the *hdhfr* probe. For the episomal plasmid pHH1-Δ*ygcs* (Figure 3-4A, II) a single band at 2.59 kb is expected for both a *pfygcs* gene-specific probe and an *hdhfr*-specific probe. In the case of a recombination event and integration of the plasmid into the *pfygcs* locus (Figure 3-4A, III), two bands at 1.19 kb and 5.08 kb are expected to appear with the *pfygcs*-specific probe whereas only the 5.08 kb band is expected to be visible when a *hdhfr* probe is used. For the generation of the *pfygcs* gene-specific probe used in this Southern blot, the insert of pHH1-Δ*ygcs* was amplified by PCR and labelled as described in Chapter 2. For the *hdhfr*-specific probe the full length *hdhfr* ORF was amplified.

Figure 3-4B shows a Southern Blot using the gene-specific probe for *pfygcs*. Lane 1 contains gDNA of untransfected 3D7 wild-type parasites and only one band at 3.69 kb corresponding to the endogenous gene locus can be detected. Lanes 2 and 3 contain gDNA isolated from $3D7^{pHH1\text{-}\Delta ygcs}$ in drug selection cycles 0 and 2, respectively. In both lanes the wild-type band at 3.69 kb and the pHH1-Δ*ygcs* plasmid band at 2.59 kb are detected. However, an additional band of approximately 3.4 kb is visible on the blot (Figure 3-4B, lanes 2 and 3) and this additional band does not correspond to either of the expected integration bands at 1.19 kb and 5.08 kb.

To analyse this further, a second Southern Blot was performed using an *hdhfr*-specific probe (Figure 3-4C). As expected, no signal is detected for non-transfected wild-type parasites (Figure 3-4C, lane 1). For selection cycle 0 and cycle 2 of the transfected $3D7^{pHH1\text{-}\Delta ygcs}$ parasites (Figure 3-4C, lanes 2 and 3, respectively) a 2.59 kb band corresponding to the episomal plasmid is visible, as well as the same additional band of approximately 3.4 kb that can be detected when a gene-specific probe is used. This additional band potentially indicates a random integration event of the pHH1-Δ*ygcs* plasmid into the *P. falciparum* genome. No disruption of the target gene was observed. These results suggest that the *pfygcs* gene is either essential or that the gene locus is refractory to integration.

A second transfection of pHH1-*Δygcs* into 3D7 wild-type parasites was performed, but no parasites could be detected in the cultures up to three months after transfection. Further attempts to generate a second $3D7^{pHH1\text{-}\Delta ygcs}$

parasite line were abandoned and I focused on the gene replacement strategy instead (see 3.5).

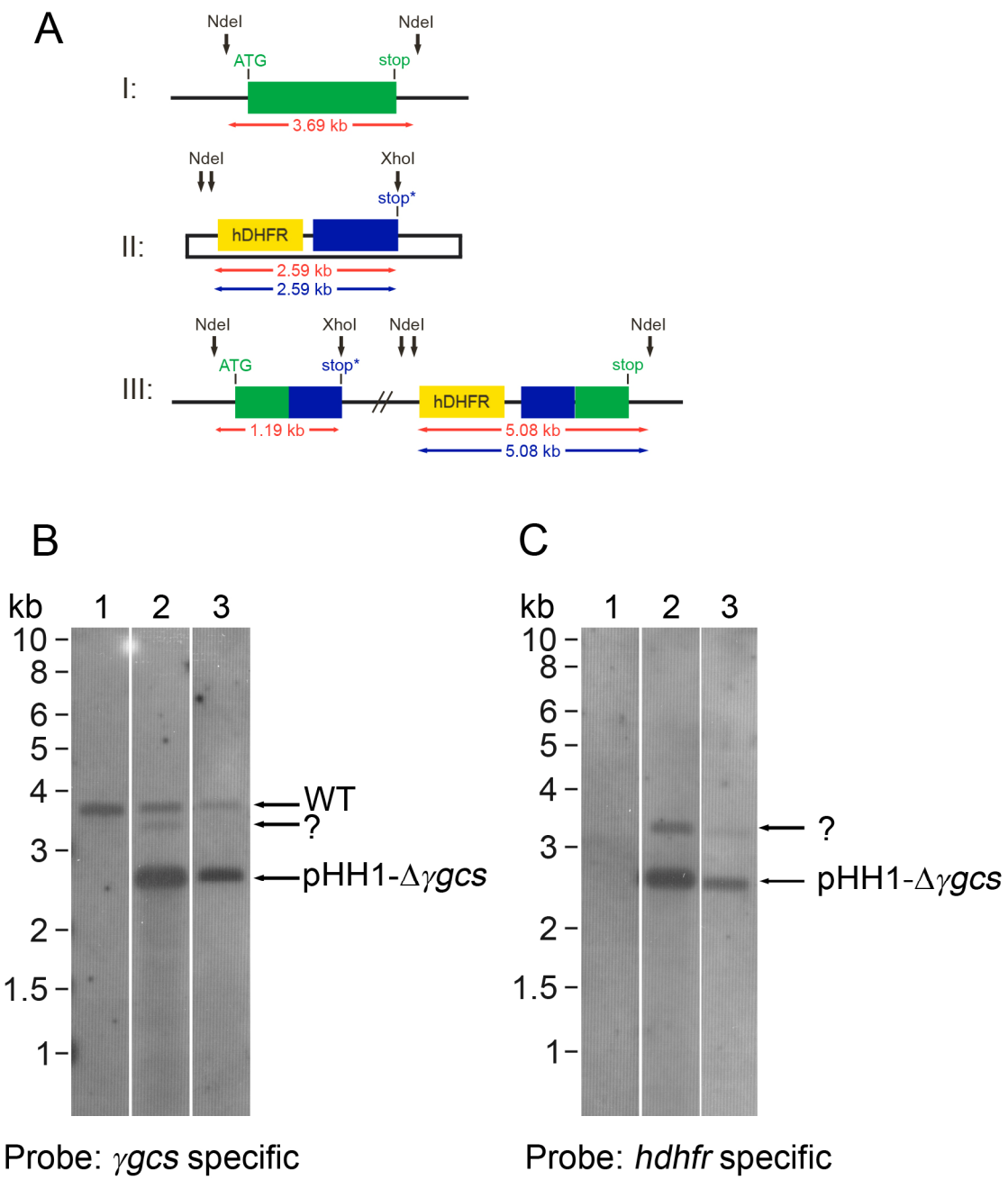

Figure 3-4: Knockout studies of *P. falciparum γgcs* by gene disruption.
For knockout studies by single crossover the plasmid pHH1 was used. **Panel A** displays a schematic diagram (not to scale) of the wild-type 3D7 *pfγgcs* locus (I), the pHH1-Δ*γgcs* plasmid (II) and the gene locus following a single crossover recombination event (III). The plasmid (II) contains an 864 bp insert (II, blue box) homologous to a part of the *pfγgcs* ORF (I, green box). This insert lacks part of the 5'-end including the ATG start codon and contains an artificial stop codon (stop*) whilst lacking the 3'-end. The plasmid contains an hDHFR selectable marker cassette (yellow box) for positive selection of transfected parasites. Knockout is achieved by gene disruption following a single crossover event. This leads to a pseudo-diploid locus (III) with two truncated copies of the gene, one being truncated at the 3'-end by the artificial stop codon (III, stop*, green-blue box) and one being truncated at the 5'-end and lacking the ATG start codon (III, blue-green box). Restriction sites for *Nde*I and *Xho*I are indicated by black arrows and the expected fragments detected with a gene-specific probe are indicated by red arrows. Blue arrows indicate the expected fragments detected with a probe specific for the *hdhfr* gene in the hDHFR cassette. **Panel B** shows a Southern blot after digestion of gDNA with *Nde*I and *Xho*I probed with a *pfγgcs* specific probe. The red arrows in Panel A indicate the expected sizes. Lane 1 contains gDNA of untransfected 3D7

wild-type parasites. Lanes 2 and 3 contain gDNA isolated from 3D7$^{pHH1-\Delta ygcs}$ after drug selection cycle 0 and 2, respectively. In all three lanes a band corresponding to the endogenous *pfygcs* locus (WT) at 3.69 kb can be detected. The transfected parasites (lanes 2 and 3) contain the plasmid and the corresponding band at 2.59 kb is visible. An additional band of unexpected size is also detected in these parasites. **Panel C** displays a Southern blot after diagnostic digest of gDNA with *Nde*I and *Xho*I probed with an *hdhfr* specific probe. Blue arrows in Panel A indicate the expected pattern and sizes. Lane 1 contains gDNA of untransfected 3D7 wild-type parasites. No bands can be detected in these parasites. Lanes 2 and 3 contain gDNA isolated from 3D7$^{pHH1-\Delta ygcs}$ after selection cycle 0 and 2, respectively. A band corresponding to pHH1-Δ*ygcs* can be detected at 2.59 kb in these lanes. In addition a second band is detected which does not correspond to the expected pattern.

3.5 Knockout by gene replacement

During this study several plasmids were generated by Maier *et al*. which permit the knockout of genes in *P. falciparum* by gene replacement and we obtained the plasmids pCC4 and pCC1 (Maier et al., 2006). The pCC4 plasmid contains a *blasticidin-S-deaminase* (*bsd*) selectable marker for positive selection of transfected parasites with Blasticidin-S-HCl (Bla) while pCC1 contains the selectable marker *hdhfr* for selection with WR99210. Only the pCC4 plasmid was used to create a construct for knockout studies on *pfygcs* because I planned to use the construct for co-transfections with an expression construct containing an *hdhfr* selectable marker at a later stage (see section 3.8). In addition to the *bsd* marker for positive selection of transfected parasites the pCC4 plasmid contains a *cytosine deaminase* (*cd*) cassette to allow for negative selection with Ancotil®. The active component of Ancotil® is 5-fluorocytosine (5-FC) which is converted by CD into 5-fluorouracil. 5-Fluorouracil is toxic for cells due to its inhibition of RNA synthesis and of the thymidylate synthase (Maier et al., 2006). In case of recombination between a pCC4 construct and its target gene by double crossover the target gene is replaced by the *bsd* gene and the *cd* gene is lost. Whilst parasites can be Bla resistant by retaining the plasmid episomally, they can only be resistant to Ancotil® and Bla if the target gene has been replaced with the *bsd* marker in a double crossover event and the *cd* death gene has been lost. The double crossover is extremely rare in *P. falciparum* erythrocytic stages. The negative selectable marker is thought to select for parasites in which this rare event has occurred, as opposed to the much more frequent single crossover event which has been the basis of previous knockout studies.

Two inserts were cloned into the pCC4 plasmid, a 485 bp insert homologous to part of the 5'-end of the *pfygcs* ORF and a 522 bp insert homologous to part of the 3'-end (see Table 2-1). The inserts did not contain any part of the repetitive element and are thus homologous to both D10 and 3D7 parasites. The plasmid

was designed to contain regions homologous to the *pfygcs* ORF rather than the 5'- and 3'-UTRs because the flanking regions of *pfygcs* are very AT rich and thus cloning is difficult. Because of the size of *pfygcs,* it was possible to use part of the coding region for the generation of the pCC4 construct. The construct was named pCC4-Δ*ygcs* and it was transfected once into D10 wild-type parasites and on two independent occasions into 3D7 wild-type parasites. Bla resistant parasites were detected in Giemsa stained thin smears four weeks after transfection for D10 and five to six weeks after transfection for 3D7. In case the parasites could compensate for the loss of PfγGCS by taking up extracellular GSH, cultures were supplemented with 2 mM GSH.

The transfected parasite lines were named D10$^{pCC4\text{-}\Delta ygcs}$, 3D7$^{pCC4\text{-}\Delta ygcs}$-1 and 3D7$^{pCC4\text{-}\Delta ygcs}$-2. Similar as described for the 3D7$^{pHH1\text{-}\Delta ygcs}$ line in section 3.4, parasites were subjected to drug selection cycles by removing Bla from the cultures for three weeks before adding the drug again. Parasites took typically between 3 to 5 days before growing normally again after addition of the drug. Once their growth was normal, the cultures were divided into two independent cultures. One of the cultures was treated with Ancotil® at a concentration equivalent to 1 µM 5-FC, whilst the other was cultured without. The cultures that remained untreated were used for the isolation of gDNA and taken through the next Bla selection cycle. Parasites in the Ancotil® treated cultures typically died within the next 2 to 4 days and no living parasites were observed anymore after one week of treatment. For all three transfected lines Ancotil® resistant parasites were obtained after Bla selection cycle 3. 3D7$^{pCC4\text{-}\Delta ygcs}$-1 was taken through one additional selection cycle to cycle 4 and again resistant parasites were obtained after selection with Ancotil®. It took approximately 4 weeks from the first day of Ancotil® treatment until Ancotil® and Bla resistant parasites were observed in Giemsa stained thin smears of the cultures.

In order to analyse the genotype of the transfected parasites, gDNA was isolated, digested with *Nde*I and analysed by Southern blotting. In the diagram in Figure 3-5A the expected banding pattern for the Southern blot is shown. Gene specific probes were generated by amplification of both inserts of pCC4-Δ*ygcs* by PCR and labelling as described in chapter 2. Due to the variations of the repetitive motif between 3D7 and D10 parasites, either a 3.69 kb or a 3.88 kb band is expected for the *pfygcs* wild-type locus, respectively. For the plasmid

two bands are expected at 7.27 kb and at 0.65 kb with the same probes. The larger of the two fragments contains the *cd* death gene. In the case of double crossover recombination and replacement of the *pfygcs* gene two bands at 2.18 kb and 1.01 kb are expected for both 3D7 and D10 parasite lines. Red arrows in the diagram in Figure 3-5A indicate the respective fragments.

Figure 3-5B shows a Southern blot analysis of D10$^{pCC4\text{-}\Delta ygcs}$ in Bla selection cycle 0 (lane 2) and in cycle 3 (lane 3). Lane 4 contains gDNA of Ancotil® resistant parasites obtained after selection cycle 3. In lane 1 gDNA of untransfected D10 wild-type parasites was loaded for comparison. In all four lanes of Figure 3-5B the 3.88 kb band corresponding to the endogenous D10 *pfygcs* locus is present. The plasmid can be detected in D10$^{pCC4\text{-}\Delta ygcs}$ in selection cycle 0 and cycle 3 and is still present after Ancotil® treatment (Figure 3-5B, lanes 2-4). No integration into the *pfygcs* gene locus had occurred; none of the diagnostic bands indicating recombination are visible. It is surprising that the plasmid is still present in the Ancotil® resistant line (Figure 3-5, lane 4) as the presence of the *cd* gene should make these parasites susceptible to the drug.

In Figure 3-6 Southern blots of 3D7$^{pCC4\text{-}\Delta ygcs}$-1 (Figure 3-6A) and 3D7$^{pCC4\text{-}\Delta ygcs}$-2 (Figure 3-6B) are displayed. The gDNA was again digested with *Nde*I prior to Southern blotting. In comparison to the transfected parasite lines 3D7 wild-type gDNA was analysed. On both blots, the wild-type gDNA was loaded in lane 1 and only a 3.69 kb band corresponding to the 3D7 wild-type *pfygcs* locus is visible. In lane 2 of Figure 3-6A and B, gDNA of 3D7$^{pCC4\text{-}\Delta ygcs}$-1 and 3D7$^{pCC4\text{-}\Delta ygcs}$-2 in selection cycle 0 was loaded, respectively. Both parasite lines contained the plasmid in this selection cycle with the two diagnostic bands at 7.27 kb and 0.65 kb visible and they still contained the plasmid in cycle 3 (lane 3, Figure 3-6A and B, respectively). Ancotil® resistant parasites were obtained from both lines after selection cycle 3. Similar to D10$^{pCC4\text{-}\Delta ygcs}$, Ancotil® resistant parasites obtained from 3D7$^{pCC4\text{-}\Delta ygcs}$-1 and from 3D7$^{pCC4\text{-}\Delta ygcs}$-2 after selection cycle 3 still contained the plasmid; both diagnostic bands at 7.27 kb and 0.65 kb were visible on the Southern blot (Figure 3-6A and B, lane 5). The 3D7$^{pCC4\text{-}\Delta ygcs}$-1 line was taken through one additional drug cycle and Southern analysis of gDNA obtained after selection cycle 4 showed again the wild-type gene and the plasmid, albeit there appeared to be less plasmid present (Figure 3-6A, lane 4). No integration specific bands were visible at 2.18 kb and 1.01 kb. Like in the previous selection

cycle, Ancotil® resistant parasites were isolated again for 3D7$^{pCC4\text{-}\Delta ygcs}$-1 in cycle 4, but no bands diagnostic for integration were visible on the Southern blot and a band corresponding to the *pfygcs* endogenous locus at 3.69 kb was still present (Figure 3-6A, lane 6). Interestingly, the smaller band at 0.65 kb corresponding to the plasmid was still detected while the larger 7.27 kb band was no longer visible. This potentially means that the plasmid has undergone some kind of recombination, albeit not with the target gene. As the *cd* death gene is located on the larger fragment of the plasmid it might be lost from these parasites, but this will need to be confirmed by reprobing the blot with a *cd* specific probe in the future.

These results indicate again that the *pfygcs* locus is either refractory to integration, or that the gene is essential for survival of intra-erythrocytic stages of *P. falciparum*.

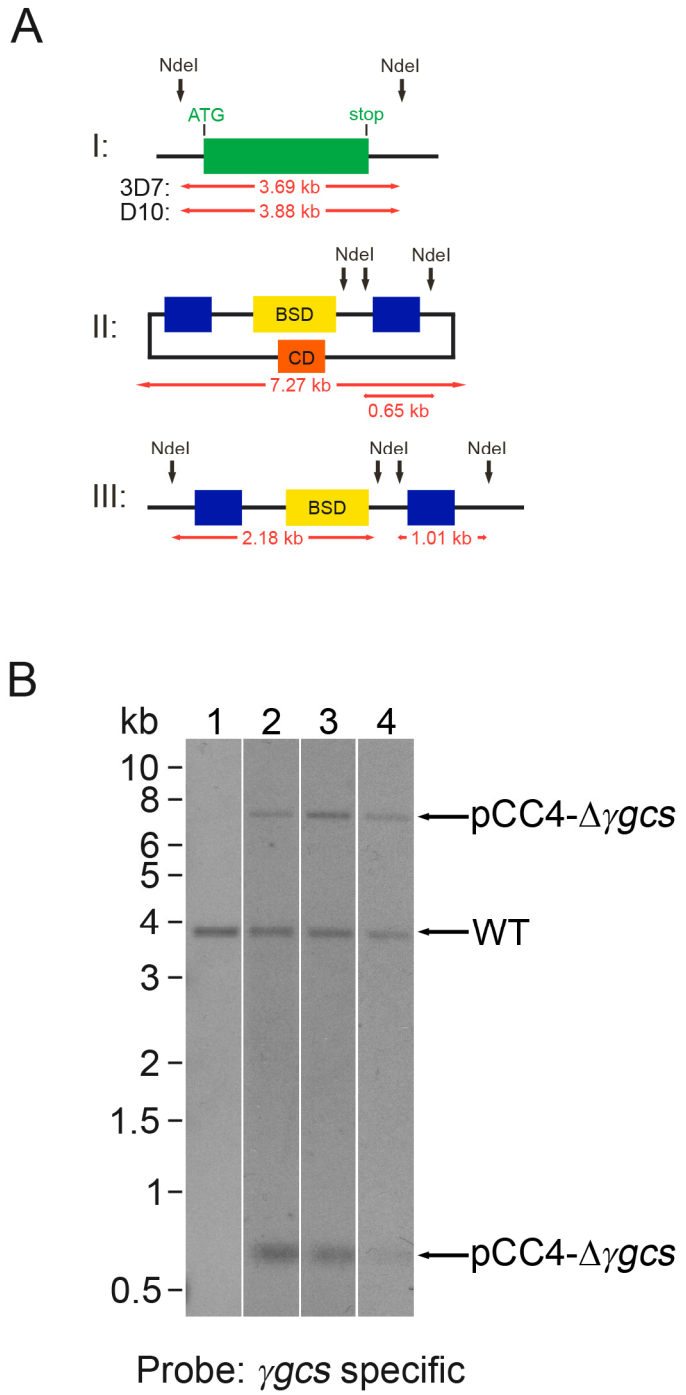

Figure 3-5: Knockout studies by gene replacement of *P. falciparum γgcs*.
For gene knockout by gene replacement the plasmid pCC4 was used. **Panel A** displays a diagram (not to scale) of the *pfγgcs* wild-type locus (I), the pCC4-Δ*γgcs* plasmid (II) and the *pfγgcs* gene locus following a double crossover recombination event (III). The length of the *pfγgcs* ORF (green box) varies between the 3D7 and D10 strain due to a different number of repeats of a variable repetitive motif. The pCC4-Δ*γgcs* plasmid contains two 485 bp and 522 bp inserts (blue boxes) homologous to regions of the 5'-and 3'-end of *pfγgcs* in both 3D7 and D10. For positive selection of transfected parasites the plasmid contains a BSD selectable marker cassette (yellow box). For negative selection against parasites maintaining the plasmid as episome the plasmid contains a CD cassette (orange box). Following a double crossover event the target gene is replaced with the BSD cassette and the CD cassette is lost. Diagnostic digests to analyse the genotype of transfected parasites were performed with *Nde*I. Restriction sites are indicated by black arrows. The lengths of the expected fragments detectable with *pfγgcs* specific probes homologous to the inserts of the plasmid are indicated by red arrows. **Panel B**: Southern blot of transfected parasite line D10$^{pCC4\text{-}\Delta\gamma gcs}$ with a gene specific probe after diagnostic *Nde*I digest. Lane 1 contains gDNA of untransfected D10 wild-type. Lanes 2 and 3 contain gDNA of D10$^{pCC4\text{-}\Delta\gamma gcs}$ in Bla selection cycle 0 and 3, respectively. Lane 4 contains gDNA of Ancotil resistant parasites obtained form D10$^{pCC4\text{-}\Delta\gamma gcs}$ after cycle 3. The 3.88 kb band corresponding to the *pfγgcs* wild-type gene (WT) is visible in all four lanes. In the transfected D10$^{pCC4\text{-}\Delta\gamma gcs}$ parasite line the two bands corresponding to the plasmid at

7.27 kb and 0.65 kb are visible in cycle 0, cycle 3 and after Ancotil treatment in cycle 3 (lanes 2-4, respectively). No integration was observed, the diagnostic bands are absent.

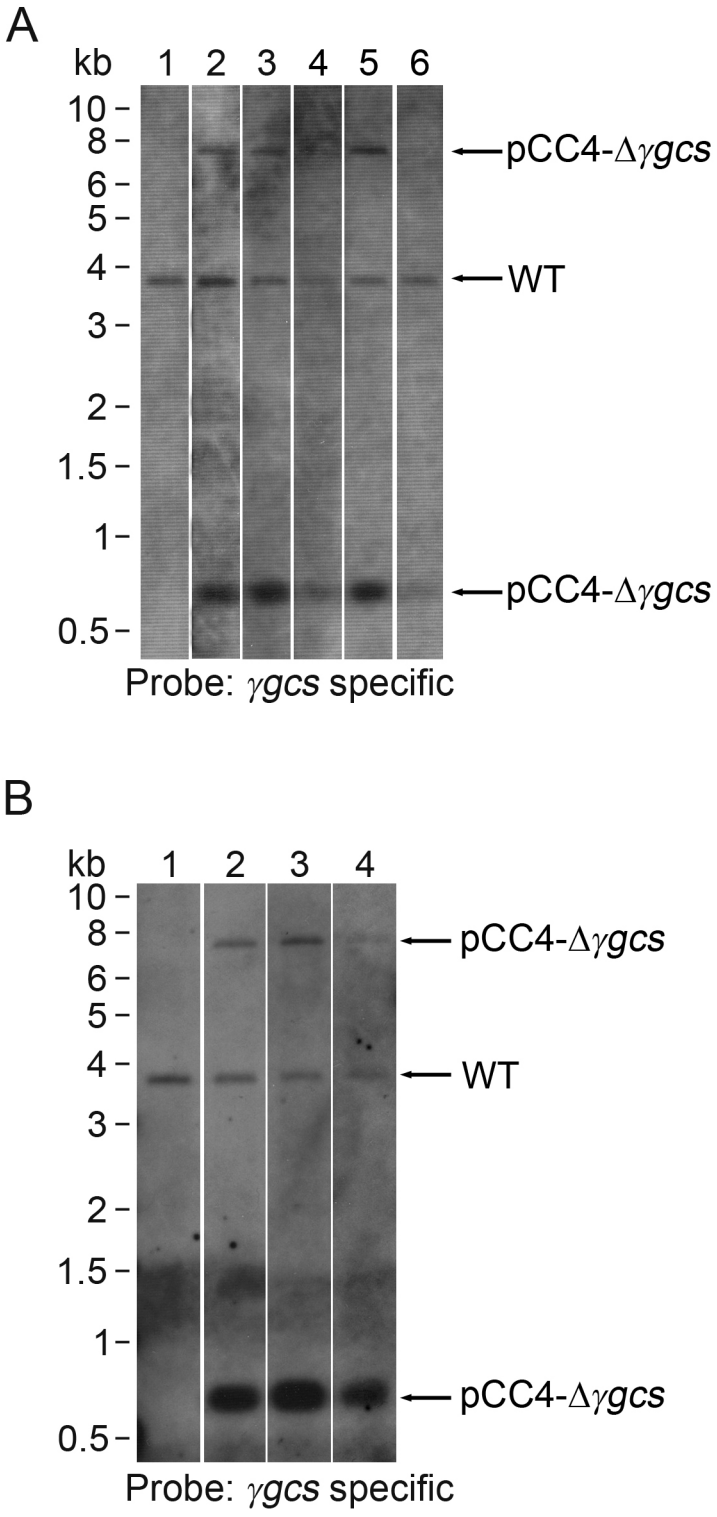

Figure 3-6: Knockout studies by gene replacement of *γgcs* in *P. falciparum* 3D7.
Panel A shows a Southern blot of parasite line 3D7$^{pCC4\text{-}\Delta\gamma gcs}$-1 (lanes 2-6) in comparison to non-transfected 3D7 wild-type parasites (lane 1). Expected fragments after a diagnostic *Nde*I digest are 3.69 kb for the endogenous *pfγgcs* gene, 7.27 kb and 0.65 kb for the plasmid and 2.18 kb and 1.01 kb for integration (see diagram in Figure 3-5A). The band corresponding to the wild-type (WT) can be observed in all samples. Lane 2 contains gDNA of 3D7$^{pCC4\text{-}\Delta\gamma gcs}$-1 in Bla selection cycle 0 with the endogenous gene fragment and the two plasmid bands visible. The plasmid is still present in selection cycles 3 and 4 in lanes 3 and 4, respectively. Lanes 5 and 6 contain gDNA of Ancotil resistant parasites obtained after Bla cycles 3 and 4, respectively. In lane 5 both bands corresponding to the plasmid are still detected while in lane 6 the higher 7.27 kb band is not visible. No bands indicating integration can be observed in any sample of 3D7$^{pCC4\text{-}\Delta\gamma gcs}$-1. **Panel B** displays a Southern blot of parasite line 3D7$^{pCC4\text{-}\Delta\gamma gcs}$-2 (lanes 2-4) in comparison to wild-type 3D7 parasites

(lane 1). As for 3D7$^{pCC4\text{-}\Delta ygcs}$-1, expected fragments after diagnostic *Nde*I digest are 3.69 kb for the endogenous *pfygcs* gene, 7.27 kb and 0.65 kb for the plasmid and 2.18 kb and 1.01 kb for integration (see diagram in Figure 3-5A). In the untransfected 3D7 parasites in lane 1 only the 3.69 kb band corresponding to the wild-type *pfygcs* gene (WT) is visible. The same band can be detected in 3D7$^{pCC4\text{-}\Delta ygcs}$-2 in Bla selection cycle 0 (lane 2), cycle 3 (lane 3) and in Ancotil resistant parasites obtained after cycle 3 (lane 4). Both plasmid bands at 7.27 kb and 0.65 kb are visible in all samples of 3D7$^{pCC4\text{-}\Delta ygcs}$-2 (lane 2-4). No integration specific fragments were detected.

3.6 Knock-in control

In order to analyse whether the *pfygcs* gene locus can be targeted, a knock-in control construct based on the pHH1 plasmid (Reed et al., 2000) was generated. The pHH1-*ygcs*con plasmid contains a 1323 bp insert homologous to the 3'-end of the *pfygcs* gene which includes the endogenous stop codon (Table 2-1). The 5'-end of the gene is not part of the insert. Integration of this construct into the gene locus should lead to a pseudo-diploid locus with two copies of *pfygcs*, one full length copy and one truncated copy lacking the 5'-end and ATG start codon. The plasmid was transfected into 3D7 wild-type parasites generating the parasite line 3D7$^{pHH1\text{-}ygcscon}$. Live parasites were observed five weeks after transfection. To analyse the genotype of the transfected cell lines, gDNA was isolated and analysed by Southern blot after diagnostic digest with *Nde*I.

The schematic diagram in Figure 3-7A describes the expected banding pattern of the Southern blot for the endogenous gene locus (I), the transfected plasmid (II) and the gene locus after a single crossover recombination event (III). Red arrows indicate the sizes of the expected fragments that can be detected with a *pfygcs* specific probe. The probe was generated by amplifying the *pfygcs* insert of pHH1-*ygcs*con by PCR and labelling as described in Chapter 2. For the wild-type *pfygcs* locus of 3D7 a 3.69 kb band is expected and a 6.35 kb band is expected for the plasmid. Following integration, the recombined gene locus should appear as two bands at 6.70 kb and 3.34 kb.

The 3D7$^{pHH1\text{-}ygcscon}$ parasite line was taken through one drug selection cycle as described in section 3.4. Once the selection cycle was completed, gDNA was prepared and analysed by Southern blotting. After one selection cycle integration specific bands were detectable in the Southern Blot and the 3D7$^{pHH1\text{-}ygcscon}$ parasite line was subsequently cloned by limiting dilution. Figure 3-7B displays a Southern blot of one of the clones obtained (lane 2) in comparison to non-transfected 3D7 wild-type parasites (lane 1). The 3.69 kb band for the

endogenous *pfygcs* gene is clearly visible in the wild-type in lane 1 but absent in the clone in lane 2. Instead two diagnostic bands at 6.70 kb and 3.34 kb corresponding to integration of pHH1-*ygcs*con into the *pfygcs* gene locus are visible in this clone. Potentially this clone still contains some episomal plasmid. The expected plasmid band would be visible at 6.35 kb and thus relatively close to the 6.70 kb integration band. Indeed the signal in Figure 3-7 lane 2 at this position is very strong compared to the other bands and it is not possible to tell if there is a single or double band at this position. Due to the strong intensity in comparison to the other bands it seems likely that there are indeed two bands at this position. This can be tested by diagnostic PCR in the future. Episomal plasmids are sometimes still present following recombination events even though they are no longer essential to provide the *hdhfr* resistance marker for parasite survival, as there is already an integrated copy in the recombined target gene locus. Potentially the plasmids are maintained because multiple copies of the *hdhfr* gene provide a higher expression of hDHFR protein and thus an advantage for parasite survival. This clearly shows that the *pfygcs* locus can be targeted and suggests that failure to generate a gene disruption or gene deletion is due to the *pfygcs* gene being essential for the survival of intra-erythrocytic stages of *P. falciparum in vitro*.

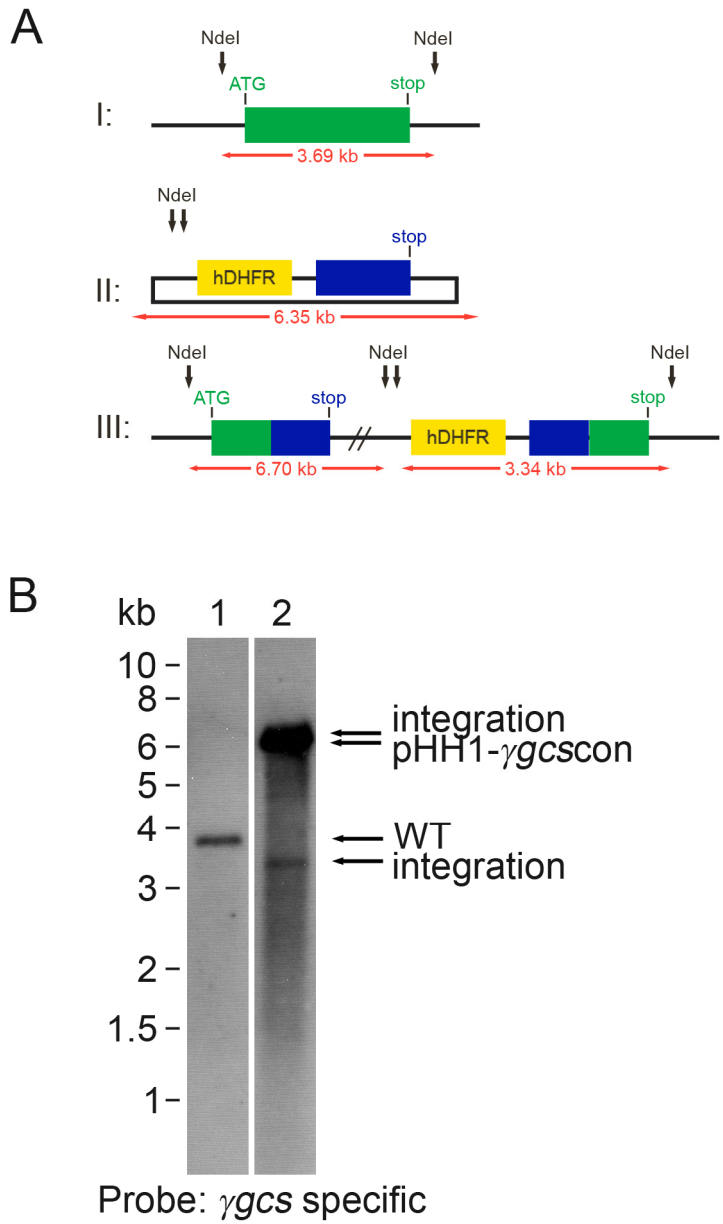

Figure 3-7: Knock-in control studies on *P. falciparum γgcs*.
Panel A shows a schematic diagram (not to scale) of the *pfγgcs* locus (I), the pHH1-*γgcs*con plasmid (II) and the gene locus following integration of the plasmid by single crossover recombination (III). The plasmid contains a 1323 bp insert (II, blue box) homologous to the 3'-end of the *pfγgcs* coding region (I, green box) including the endogenous stop codon (stop) and an hDHFR selectable marker cassette for selection of transfected parasites (II, III, yellow box). Following recombination between plasmid and endogenous gene, the locus is disrupted leading to one full length copy of *pfgs* (III, green-blue box) and one copy truncated at the 3'-end (III, blue-green box). DNA was digested with *Nde*I prior to Southern blotting. Restriction sites are indicated by black arrows and the resulting fragments that can be detected with a *pfγgcs* specific probe are indicated by red arrows. **Panel B** displays a Southern blot of *Nde*I digested parasite gDNA probed with a gene specific probe (For expected sizes see red arrows in Panel A). Lane 1 contains gDNA of untransfected 3D7 wild-type parasites and a 3.69 kb band corresponding to the wild-type *pfγgcs* locus (WT) can be detected. In lane 2 an exemplary clone of the 3D7$^{\text{pHH1-}\gamma gcscon}$ line is shown. In this clone the wild-type diagnostic band is absent and two integration specific bands at 6.70 kb and 3.34 kb can be detected instead. It cannot be determined if there is a second band just below the 6.70 kb integration band corresponding to the 6.35 kb plasmid band due to the intensity of the signal and overexposure of the film in this area.

3.7 Expression of PfγGCS-HA in *P. falciparum*

3.7.1 Genotypic analysis

The expression construct for C-terminally HA-tagged PfγGCS, pCHD-Hsp86-γGCS-HA (see Table 2-1), was generated using MultiSite Gateway technology (van Dooren et al., 2005). The construct contained the full-length *pfygcs* ORF of the 3D7 strain cloned in frame with the sequence for an HA-tag under the control of the Hsp86 promoter. The Hsp86 promotor is a strong promotor and allows for high levels of expression of the fusion protein throughout the intra-erythrocytic parasite life cycle. This plasmid was used to express PfγGCS-HA in *P. falciparum* for phenotypical studies and at a later stage for co-transfection studies with a knock-out construct. The plasmid was first transfected into wild-type D10 parasites on two independent occasions creating the parasite lines $D10^{\gamma GCS\text{-}HA}$-1 and $D10^{\gamma GCS\text{-}HA}$-2. Transfected parasites were selected with WR99210 and were first observed four to five weeks after transfection.

To determine whether the episomal plasmid was present, diagnostic Southern blot analyses were performed on the two parasite lines once parasites were observed in cultures after transfection. The diagram in Figure 3-8A displays the expected banding pattern of the Southern blot with a *pfygcs* gene specific probe after a diagnostic digest with the enzyme *Nde*I. The probe used was identical to the probe used for the knock-in control studies (Section 3.6) and homologous to the *pfygcs* insert of pHH1-*ygcs*con. For the endogenous D10 *pfygcs* locus a 3.88 kb band is expected and the size of the expected band diagnostic for the episomal plasmid is 9.89 kb. Even though the plasmid was not intended for recombination with the endogenous locus, such an event is possible due to the homologous *pfygcs* sequence in the plasmid. Recombination between wild-type gene and plasmid would result in a pseudo-diploid locus with two functional copies of the gene. One copy would be under control of the endogenous promoter and be fused in frame with the HA-tag while the other copy would be under control of the Hsp86 promotor and untagged. Because the repetitive sequence motif of *pfygcs* is present 9 times in the endogenous D10 locus and only once in the 3D7 *pfygcs* sequence cloned into the expression plasmid, two variations are possible for the recombined locus. This depends on whether the D10 sequence motif is present in the first or the second copy following a single-

cross over recombination. If a recombination event occurrs downstream of the motif, the 5'-copy of *pfygcs* resembles the 3D7 sequence and the 3'-copy resembles the D10 sequence (Variation A). Should the recombination occur upstream of the repetitive motif, the 5'-copy will resemble the D10 *pfygcs* and the 3'-copy the 3D7 form (Variation B). The sizes of the diagnostic bands for this recombination event are 6.66 kb and 7.08 kb for variation A and 6.85 kb and 6.89 kb for variation B.

To test whether the plasmid undergoes recombination with the endogenous gene locus, D10$^{\gamma GCS\text{-}HA}$-1 was taken through one drug selection cycle. Indeed, integration was observed in selection cycle 1 and the parasites were subsequently cloned by limiting dilution. Figure 3-8B shows two of the clones isolated after limiting dilution that were later used for phenotypical analyses. Clone 4 of D10$^{\gamma GCS\text{-}HA}$-1 still contains some episomal plasmid, indicated by the 9.89 kb band as well as possessing a recombined *pfygcs* locus (Figure 3-8B, lane 2). Clone 5 only possesses the recombined locus indicated by a double band (Figure 3-8B, lane 3) whereas the diagnostic plasmid band cannot be detected in this clone, indicating the absence of episomal plasmid. Because of the size of the double band for the recombined locus and because the double band has not clearly separated, it can be assumed that the recombined locus resembles variation B in both clones. In case of variation B the two fragments are only 40 bp different in size and thus unlikely to be properly segregated on this gel, whereas the two bands for variation A at 6.66 kb and 7.08 kb would be clearly separated. Therefore the sequence of the HA-tagged protein is expected to be a mixture of the 3D7 and D10 form of PfγGCS in Clone 4 possessing the plasmid and a recombined locus while only D10 PfγGCS-HA is expected in Clone 5 possessing only the recombined locus. The recombination between the expression plasmid pCHD-Hsp86-γGCS-HA and the endogenous *pfygcs* locus shows again that the gene locus can be targeted.

The Southern blot in Figure 3-8C shows the genotype of the parasite line D10$^{\gamma GCS\text{-}HA}$-2. This line possesses the endogenous *pfygcs* locus and the episomal expression plasmid, indicated by the diagnostic bands at 3.88 kb and 9.89 kb, respectively. No integration specific bands are visible, showing that no single crossover recombination has occurred in this parasite line.

Thus three different PfγGCS over-expressing lines were generated: (1) Clone 5 contains a *pfygcs* gene under control of the endogenous promotor with an HA-tag and a second copy of the gene under control of the Hsp86 promotor and untagged; this should lead to a higher *pfygcs* expression than observed in wild-type parasites; (2) Clone 4 has the integrated gene locus as described for (1) plus the additional episomal HA-tagged version of the gene; presumably gene expression is higher than in the wild-type and in Clone 5; (3) $D10^{\gamma GCS\text{-}HA}$-2 only carries the episome in addition to the endogenous *pfygcs* locus.

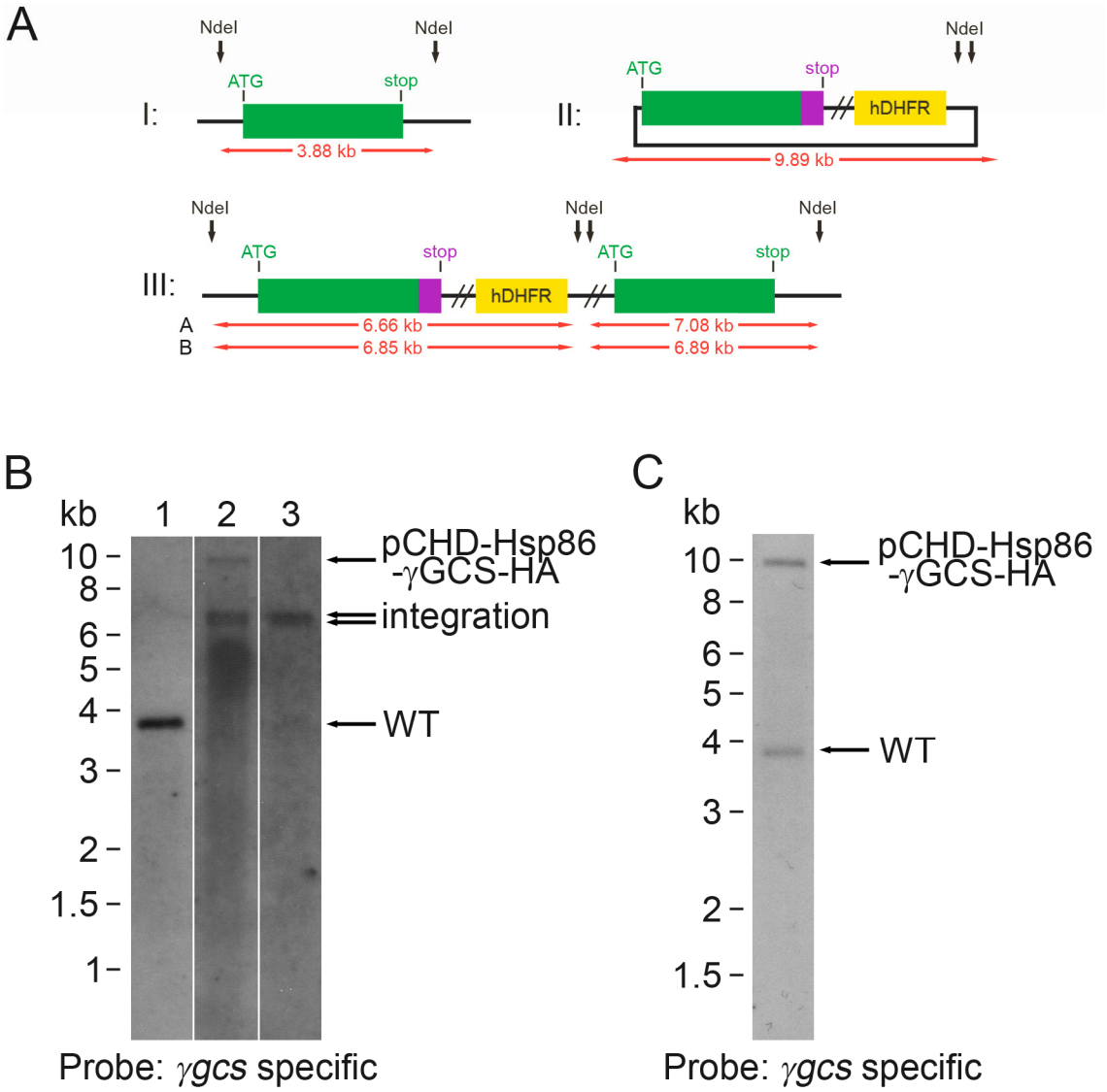

Figure 3-8: Genotypic analyses of D10$^{\gamma GCS\text{-}HA}$-1 and D10$^{\gamma GCS\text{-}HA}$-2.
For expression of PfγGCS-HA in *P. falciparum*, parasites were transfected with the construct pCHD-Hsp86-γGCS-HA. **Panel A** shows a schematic diagram (not to scale) of the expected banding pattern for the endogenous D10 *pfγgcs* locus (I), the expression plasmid pCHD-Hsp86-γGCS-HA (II) and the gene locus following recombination with the plasmid (III) after diagnostic digest of parasite gDNA with *Nde*I. To analyse transfected parasites, a *pfγgcs*- specific probe homologous to the 3'-end of the gene was used. This probe was also used for the analysis of parasites transfected with pHH1-*γgcs*con (see 3.6). The expected bands are indicated by red arrows. A 3.88 kb fragment is expected for the endogenous D10 *pfγgcs* locus (I) and for the expression plasmid a 9.89 kb fragment is expected. The plasmid contains the full length 3D7 *pfγgcs* ORF (II, green box) in frame with an HA-tag (II, purple box) and an hDHFR cassette (II, yellow box) for selection of transfected parasites. Single crossover recombination between the plasmid and the endogenous locus results in a pseudo-diploid locus with two functional full length copies of the gene (III, green boxes). In case of a recombination event, the first copy of the gene is under control of the endogenous promotor and contains the HA-tag, whereas the second copy is untagged and under control of the Hsp86 promotor. Due to the differences in the repetitive motif present in the endogenous locus and the expression construct, two different variations are possible for an integration event. In variation A, the first copy of *pfγgcs* contains the motif as it is present in the 3D7 strain and the second copy contains the D10 motif. This would lead to two bands of 6.66 kb and 7.08 kb. In variation B, the D10 motif is present in the first copy, while the second copy contains the 3D7 motif, leading to two bands of 6.85 kb and 6.89 kb, respectively. **Panel B** shows a Southern blot of two clones of the parasite line D10$^{\gamma GCS\text{-}HA}$-1 in comparison to wildtype D10 parasites (lane 1). Prior to blotting, gDNA was digested by *Nde*I. The expected fragments are indicated in Panel A by red arrows. Only in lane 1 containing wild type gDNA the endogenous *pfγgcs* locus (WT) is present. Clone 4 (lane 2) possesses a recombined *pfγgcs* locus and the episomal expression plasmid. Clone 5 (lane 3) possesses the recombined gene locus and has lost

the plasmid. **Panel C** displays a Southern blot of the parasite line D10$^{\gamma GCS\text{-}HA}$-2. The expected banding pattern following diagnostic *Nde*I digest is indicated by red arrows in Panel A. D10$^{\gamma GCS\text{-}HA}$-2 possesses the endogenous *pfygcs* locus (WT) and the expression plasmid pCHD-Hsp86-γGCS-HA. No recombination has occurred between the plasmid and the wild-type gene locus in this parasite line.

3.7.2 Phenotypic analyses

In order to determine whether PfγGCS-HA is expressed, protein was extracted from parasites and analysed by western blotting using an anti-HA antibody. The western blot displayed in Figure 3-9 was performed by L. Sveen under my supervision and shows protein extract of Clones 4 and 5 of D10$^{\gamma GCS\text{-}HA}$-1 (lanes 1 and 2, respectively) and the non-clonal D10$^{\gamma GCS\text{-}HA}$-2 parasites (lane 3). The presence of protein in all lanes was confirmed by Ponceau-S staining of the membrane prior to blocking and incubation with antibodies. A band of the expected size for PfγGCS-HA between 129.9 kDa for the 3D7 and 130.8 kDa for the D10 variation was detected in all three transfected parasite lines (lanes 1-3). The two forms of the protein are too similar in size to be separated on this gel. In comparison, no signal was detected in protein extract of wild-type D10 parasites (lane 4). For all lines 20 µg of total protein according to Bradford assay were loaded, but the signal strength varies between the three transfected lines, indicating different amounts of the HA-tagged fusion protein are present in the parasites. The signal is weakest in lane 2 (Figure 3-9), containing the protein extract of Clone 5 of D10$^{\gamma GCS\text{-}HA}$-1. For this line no episomal plasmid was detected on the Southern blot (Figure 3-8B), only the recombined *pfygcs* locus was present. Clone 4 of D10$^{\gamma GCS\text{-}HA}$-1, which still contained episomal plasmid according to the Southern blot in Figure 3-8B appears to contain more of the PfγGCS-HA fusion protein, as indicated by the stronger signal detected in lane 1. This suggests that the amount of the HA-tagged protein present is dependent on the presence or absence of the episomal plasmid, as one would expect. Clone 4 with the episomal plasmid possesses more than one copy of the tagged gene encoding for PfγGCS-HA. Thus this line contains more of the recombinant protein than Clone 5, which only possesses one copy of the tagged gene under control of the endogenous promotor in the recombined locus. The strongest signal is detected on the protein extract from the non-clonal D10$^{\gamma GCS\text{-}HA}$-2 parasites. D10$^{\gamma GCS\text{-}HA}$-2 does not have a recombined *pfygcs* locus, only the episomal expression plasmid is present in this parasite line. Some smaller fragments than the expected size of 129.9 kDa indicate that some degradation of the fusion

protein occurs in this parasite line. Because more than one copy of the expression plasmid can be present per parasite cell, these parasites potentially contain several copies of the gene encoding for γGCS-HA which are under control of the strong Hsp86 promotor. This indicates that high level of PfγGCS-HA expression from an episomal plasmid is possible.

Ideally this blot should be stripped and probed again with a "loading control" antibody recognising a protein not affected by the over-expression of PfγGCS, to confirm that equal amounts of protein were loaded. Because on this blot only the HA-tagged form of PfγGCS is detected, it does not allow any conclusions about the total amount of PfγGCS present in these parasite lines. Unfortunately no PfγGCS specific antibody is available to analyse the amount of total PfγGCS.

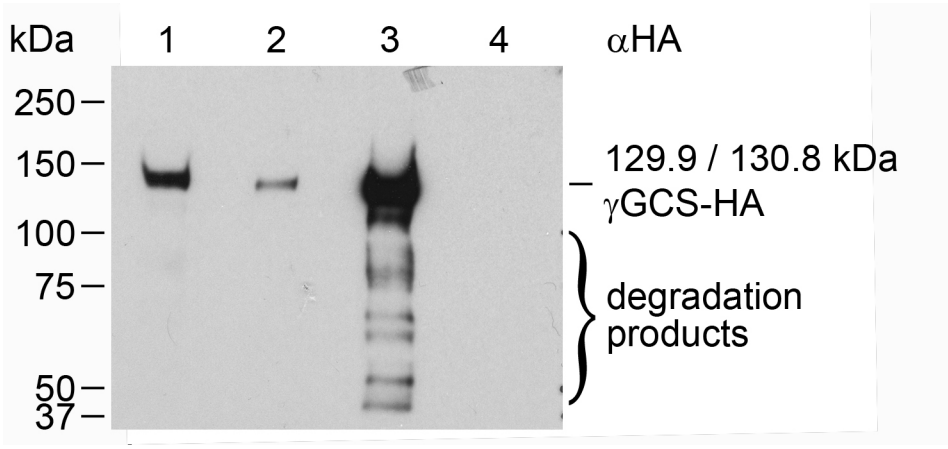

Figure 3-9: Expression of PfγGCS-HA.
Western blot analysis of protein extract from parasite lines transfected with pCHD-Hsp86-γGCS-HA was performed with an anti-HA antibody. Because of variations of a repetitive sequence element, two sizes are expected for recombinant PfγGCS-HA. The plasmid encodes for the 3D7 variation at a size of 129.9 kDa, whereas the recombined locus resembles the D10 variation and is larger at a size of 130.8 kDa. The two different sizes were not separated on this gel. For all samples 20 µg of total protein were loaded. Lane 1 contains protein extract of $D10^{\gamma GCS\text{-}HA}$-1 Clone 4. In lane 2 protein extract of $D10^{\gamma GCS\text{-}HA}$-1 Clone 5 was loaded. Both clones possess a recombined *pfγgcs* locus. In addition, Clone 4 still contains the episomal expression construct pCHD-Hsp86-γGCS-HA, which is absent in Clone 5. In lane 3 protein extract of the non-clonal $D10^{\gamma GCS\text{-}HA}$-2 line was loaded. This parasite line possesses the endogenous wild-type locus and the episomal expression construct. Protein extract of non-transfected wild-type D10 parasites was loaded in lane 4. This Western Blot was carried out by L. Sveen, IASTE student at the University of Glasgow, under my supervision.

The susceptibility of $D10^{\gamma GCS\text{-}HA}$-2 to the specific inhibitor of γGCS, L-BSO, was tested and the concentration at which 50 % of growth inhibition of the parasites occurs (IC_{50} value) was determined (Meister, 1983). The IC_{50} assays were also performed in the presence of 5 mM N-acetylcysteine (NAC), because availability of L-cysteine might be a limiting factor for GSH biosynthesis and over-expression of PfγGCS may not be sufficient to increase the GSH levels in the cytosol of $D10^{\gamma GCS\text{-}HA}$-2, if there is a lack of available substrates.

The IC_{50} growth assay for the effect of L-BSO on D10$^{\gamma GCS\text{-}HA}$-2 in comparison to D10 wild-type was performed once in duplicate by L. M. Laine under my supervision (Figure 3-10A). At 165 ±21 µM the IC_{50} determined for D10$^{\gamma GCS\text{-}HA}$-2 was approximately 2.5 times higher than the wild-type IC_{50} at 64 ±5 µM (Figure 3-10). This suggests that there is indeed more target protein in this mutant line compared to the D10 wild-type. IC_{50} values determined in the presence of 5 mM NAC were 178 ±39 µM and 72 ±7 µM for D10$^{\gamma GCS\text{-}HA}$-2 and D10, respectively and thus only slightly higher, indicating that NAC does only marginally influence the susceptibility of the parasites to L-BSO.

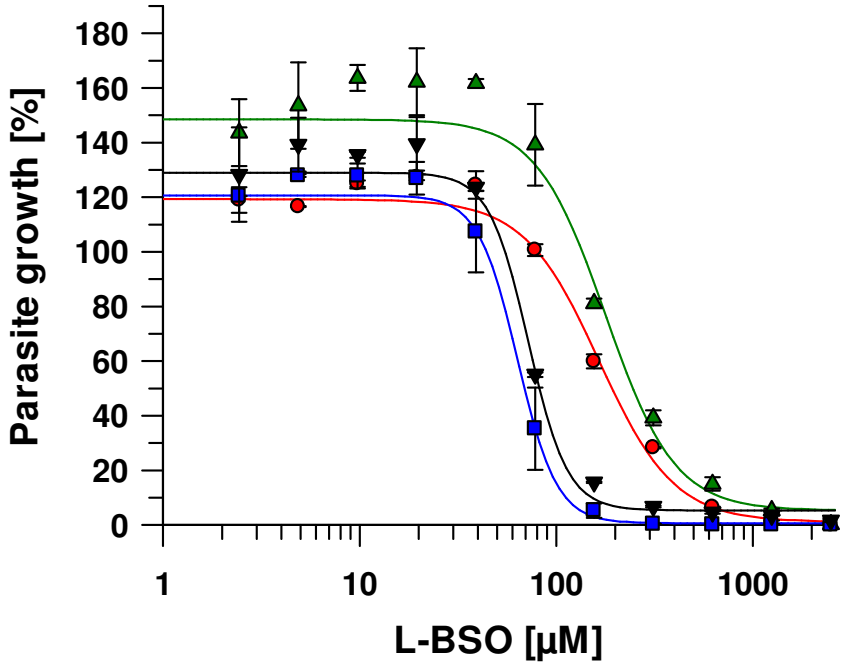

Figure 3-10: Determination of IC_{50} values for L-BSO in D10 and D10$^{\gamma GCS\text{-}HA}$-2.
Panel A: The inhibitory effect of L-BSO on parasite growth was determined in the presence and absence of 5 mM NAC for wild-type D10 and D10$^{\gamma GCS\text{-}HA}$-2. IC_{50} values were similar under both conditions with D10$^{\gamma GCS\text{-}HA}$-2 being 2.5 times less susceptible to the drug. The IC_{50} for L-BSO alone was 165±21 µM for D10$^{\gamma GCS\text{-}HA}$-2 (●) and 64±5 µM for D10 (■). IC_{50} values in presence of 5 mM NAC were 72±7 µM and 178±39 µM for D10 (▼) and D10$^{\gamma GCS\text{-}HA}$ (▲), respectively.

3.8 Co-transfection of PfγGCS knockout and expression plasmids

After having shown that the *pfygcs* gene locus can be targeted and that expression of PfγGCS-HA from an episomal plasmid is possible, I attempted to knockout the gene in presence of an episomal copy of *pfygcs*. If the *pfygcs* gene is indeed essential, it is anticipated that the presence of an episomal copy should result in sufficient generation of γGCS for parasite survival. The knockout construct pCC4-Δ*ygcs* and the expression plasmid pCHD-Hsp86-γGCS-HA were co-

transfected at the same time into wild-type D10 parasites to generate the line D10$^{pCC4\text{-}\Delta ygcs/\gamma GCS\text{-}HA}$. The transfected parasites were selected with Bla and WR99210 and were first observed 6 weeks after transfection. For drug selection, only Bla was omitted form the cultures while the WR99210 pressure was maintained to continuously select for the expression plasmid. Parasites were taken through 3 selection cycles and gDNA was isolated after each cycle and analysed by Southern blot.

Figure 3-11 displays a schematic diagram of the expected banding pattern for a Southern blot after diagnostic *Nde*I digest of the gDNA. Red arrows indicate the fragments which can be detected with gene specific probes homologous to the two inserts of pCC4-Δ*ygcs*. Blue arrows indicate those fragments which can be detected with probes for the selectable marker genes *bsd* and *hdhfr*. Digest with *Nde*I results in a 3.88 kb fragment for the endogenous locus of *pfygcs* in D10, which can only be detected with the gene specific probes (Figure 3-11A, I). For the pCC4-Δ*ygcs* plasmid (Figure 3-11A, II) two fragments at 7.27 kb and at 0.65 kb are expected with the gene specific probes. Only the larger fragment is detectable with the *bsd* specific probe. A 9.89 kb fragment is expected for the pCHD-Hsp86-γGCS-HA plasmid for both gene- and *hdhfr*-specific probes (Figure 3-11A, III). In the event of a gene replacement by pCC4-Δ*ygcs* (Figure 3-11A, IV), two fragments at 2.18 kb and 1.01 kb are expected for the recombined locus with the gene specific probes while a *bsd*-specific probe can only detect the 2.18 kb band.

The Southern blot for D10$^{pCC4\text{-}\Delta ygcs/\gamma GCS\text{-}HA}$ using *pfygcs* specific probes is displayed in Figure 3-11B. In lane 1 gDNA of untransfected D10 wild-type parasites was loaded. Lane 2 contains gDNA of D10$^{pCC4\text{-}\Delta ygcs/\gamma GCS\text{-}HA}$ isolated in drug selection cycle 0 when parasites were first obtained following transfection and lane 3 contains gDNA isolated in drug selection cycle 3. The 3.88 kb band corresponding to the endogenous *pfygcs* locus is present in the wild-type parasites and in selection cycles 0 and 3 of the D10$^{pCC4\text{-}\Delta ygcs/\gamma GCS\text{-}HA}$ line (Figure 3-11B, lanes 1-3). In addition, two bands at 7.27 kb and 0.65 kb corresponding to the pCC4-Δ*ygcs* plasmid can be detected in D10$^{pCC4\text{-}\Delta ygcs/\gamma GCS\text{-}HA}$ in cycle 0 and cycle 3 in lanes 2 and 3, respectively. Surprisingly, the diagnostic 9.89 kb band for the expression construct is not present in either cycle. Instead, an additional band not corresponding in size to either the expression plasmid or integration of pCC4-

Δ*ygcs* is visible just below the band for the endogenous gene in the D10$^{pCC4-\Delta ygcs/\gamma GCS-HA}$ line (Figure 3-11B, lanes 2 and 3). This additional band also does not correspond in size to a recombination event between the expression plasmid and the endogenous locus as described in 3.7.1.

To closer investigate this pattern the membrane was stripped and re-probed with *bsd*- and *hdhfr*-specific probes (Figure 3-11C). As expected, no bands are recognized in lane 1, which contains gDNA of D10 wild-type parasites. In lanes 2 and 3 (gDNA of D10$^{pCC4-\Delta ygcs/\gamma GCS-HA}$ in selection cycle 0 and 3, respectively) two bands are visible. The top band at 7.2 kb corresponds to the pCC4-Δ*ygcs* knockout construct. The bottom band appears to be the same additional band that was seen when the blot was probed with the gene specific probes in Figure 3-11B. The 9.89 kb band diagnostic for the expression plasmid is not recognized, indicating loss or possibly recombination of the expression construct. This co-transfection did not lead to a knockout of the *pfygcs* target gene, probably because the expression plasmid was lost or altered through recombination and thus was no longer able to provide expression of functional PfγGCS protein to substitute for a *pfygcs* knockout.

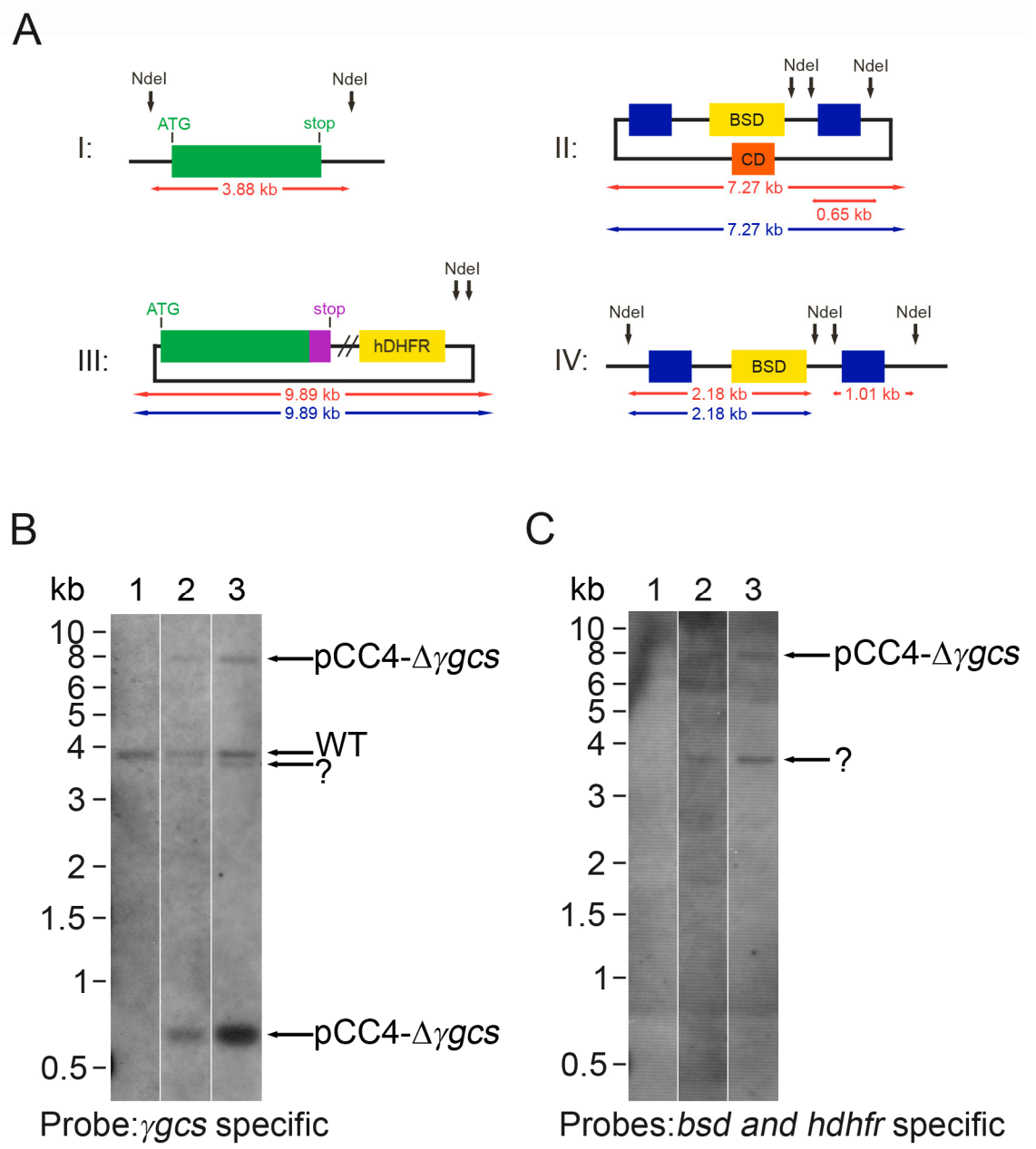

Figure 3-11: Knockout of *pfγgcs* by gene replacement in presence of an episomal copy.
Panel A: Schematic diagram (not to scale) of the D10 *pfγgcs* locus (I), the pCC4-Δ*γgcs* knockout plasmid (II), the pCHD-Hsp86-γGCS-HA expression plasmid (III) and the *pfγgcs* locus following recombination with the pCC4-Δ*γgcs* plasmid by double crossover (IV). The pCC4-Δ*γgcs* plasmid (II) containes two 485 bp and 522 bp inserts (blue boxes) homologous to regions of the 5'-and 3'-end of the *pfγgcs* coding region (green box). This plasmid contains a BSD selectable marker cassette (yellow box) for positive selection of transfected parasites and a CD cassette (orange box) for negative selection against parasites maintaining the plasmid as episome. The expression plasmid pCHD-Hsp86-γGCS-HA contains the full length *pfγgcs* coding region of the 3D7 strain (III, green box) cloned in frame with an HA-tag (purple box). The expression construct contains an hDHFR selectable marker cassette (III, yellow box) for positive selection of transfected parasites. Following recombination with pCC4-Δ*γgcs*, the endogenous *pfγgcs* is replaced by the BSD selectable marker (IV). Diagnostic digests were performed with *Nde*I. Restriction sites are indicated by black arrows. Southern blot was performed with *pfγgcs* specific probes or probes specific for the selectable markers *bsd* and *hdhfr*. Fragments detected with gene-specific probes are indicated by red arrows. Fragments detected with the probes for selectable markers are indicated by blue arrows. **Panel B:** Southern blot using a *pfγgcs*-specific probe on untransfected D10 wild-type parasites (lane 1) and the D10$^{\text{pCC4-}\Delta\gamma gcs/\gamma\text{GCS-HA}}$ transfected parasite line in selection cycle 0 and cycle 3 (lanes 2 and 3, respectively). The 3.88 kb band corresponding to the endogenous *pfγgcs* gene (WT) is visible in both wild-type and transfected parasites (lane 1-3). In the transfected line the two bands corresponding to pCC4-Δ*γgcs* are visible at 7.27 kb and 0.65 kb in drug selection cycle 0 and cycle 3 (lanes 2 and 3). An additional band is visible below the band corresponding to

the endogenous gene which does not correspond to any band expected for either pCHD-Hsp86-γGCS-HA or integration of pCC4-Δ*γgcs*. **Panel C** shows the same blot after re-probing with probes for the selectable markers *bsd* and *hdhfr*. No bands can be detected on the D10 wild-type gDNA. In lane 2 and 3 of the transfected parasites in cycle 0 and cycle 3, respectively, two bands are visible. The larger one corresponds to the 7.27 kb fragment of the pCC4-Δ*γgcs* plasmid containing the BSD cassette. The smaller band at approximately 3.6 kb does not correspond to any expected band (see diagram in Panel A).

To further investigate the possibility of recombination of the expression construct, isolated gDNA of D10$^{pCC4\text{-}\Delta\gamma gcs/\gamma GCS\text{-}HA}$ was used for bacterial transformation in order to recover any plasmids present in the parasites. This plasmid rescue was performed with gDNA of parasites in selection cycle 0 and cycle 1. However, only for the gDNA prepared in selection cycle 0 bacteria colonies were obtained. Nine of the colonies were picked for isolation of plasmid DNA and the obtained plasmids were analysed by restriction digest with *Pvu*II. Using this enzyme, two fragments of 8.26 kb and 2.36 kb size are expected for the expression construct pCHD-Hsp86-γGCS-HA. Two smaller fragments of 3.60 kb and 4.76 kb are expected for the knockout construct pCC4-Δ*γgcs*.

The restriction analysis showed that two different types of plasmids were obtained (Figure 3-12). One plasmid appeared to be present in higher copy number in the bacteria and gave a pattern of two bands at approximately 1.8 kb and 2.2 kb (Figure 3-12, lanes 1, 2, 4, 8 and 9). The other type of plasmid gave a pattern of five bands and appeared to be present at a low copy number. The fragments of the second plasmid had sizes of approximately 1.8 kb, 2.2 kb, 3.5 kb, 4 kb and 5 kb (Figure 3-12, lanes 3, 5, 6 and 7). Neither of the two patterns observed for the isolated plasmids correspond to those expected for the plasmids pCHD-Hsp86-γGCS-HA and pCC4-Δ*γgcs*. These results again indicate that the two plasmids have undergone recombination. Surprisingly, not even pCC4-*Δγgcs* which was detected on the Southern blot could be isolated. It is possible that the number of colonies screened was not large enough in order to find a clone containing this plasmid.

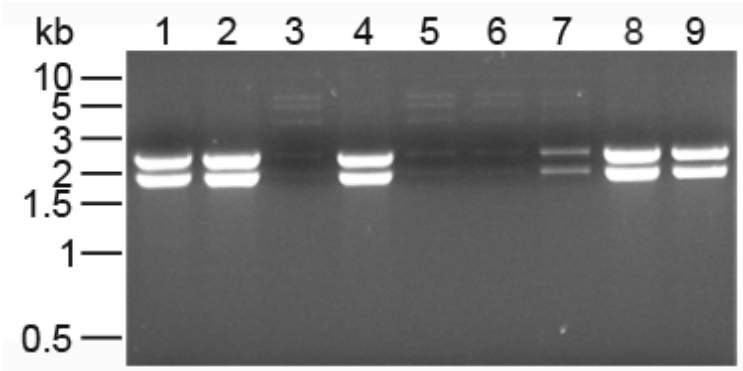

Figure 3-12: Plasmids isolated from D10$^{pCC4\text{-}\Delta ygcs/\gamma GCS\text{-}HA}$ gDNA.
D10$^{pCC4\text{-}\Delta ygcs/\gamma GCS\text{-}HA}$ gDNA was used for bacterial transformation to recover plasmids present in the parasites. Nine colonies were selected for plasmid isolation and the plasmids were subsequently digested with *Pvu*II (lanes 1-9). The expected sizes were 8.26 kb and 2.36 kb for pCHD-Hsp86-γGCS-HA and 3.60 kb and 4.76 kb for pCC4-Δ*ygcs*. None of the isolated plasmids corresponded to the expected patterns.

3.9 Summary

- The length of *pfygcs* differs between different strains of *P. falciparum* due to the variable number of a repetitive motif of unknown purpose. The 3D7 strain possesses only one copy of the motif. D10 possesses 9 repeats of the motif.

- Localization studies with episomally expressed PfγGCS-GFP indicate that PfγGCS is cytosolic.

- A knockout of *pfygcs* could not be achieved by either gene disruption with the construct pHH1-Δ*ygcs* or by gene replacement with the construct pCC4-Δ*ygcs*. However, the gene locus was targeted with the knock-in control construct pHH1-*ygcs*con and it was also possible to tag the endogenous locus with an HA-tag. Together these results indicate that *pfygcs* is essential for the survival of erythrocytic stages of *P. falciparum in vitro*.

- Parasites transfected with an expression construct for PfγGCS-HA express the fusion protein. Recombination between the expression construct and the gene locus is possible and leads to a pseudo-diploid locus with two copies of the gene. Expression of PfγGCS-HA decreases the susceptibility of *P. falciparum* to the γGCS inhibitor L-BSO, but addition of NAC does not change the susceptibility of the parasites to L-BSO.

- The knockout of *pfygcs* by gene replacement with pCC4-Δ*ygcs* in presence of an episomal copy of the gene was not possible due to recombination of the expression construct pCHD-Hsp86-γGCS-HA. Transfected parasites did not contain the original constructs and no knockout was observed.

4 Glutathione Synthetase

4.1 Introduction

The second step of the biosynthesis of GSH, the addition of glycine to the dipeptide L-γ-glutamyl-L-cysteine (γGC), is catalysed by glutathione synthetase (GS) (Reaction 3).

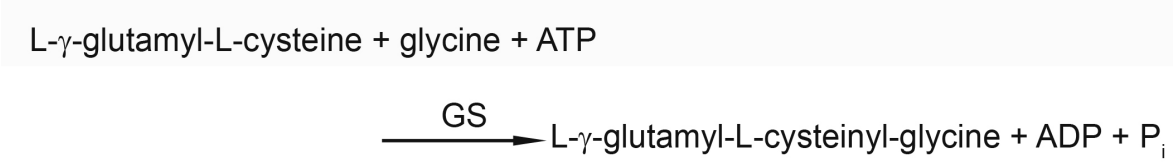

Reaction 3: The second step of GSH biosynthesis.
The ATP-dependent ligation of glycine to γGC is catalysed by GS.

In this chapter the subcellular localization of PfGS is investigated by expression of recombinant PfGS-GFP in erythrocytic stages of *P. falciparum*. The role and importance of PfGS for the survival of *P. falciparum* is analysed by reverse genetic approaches. Two different methods were used to attempt the knockout of *pfgs*, a gene disruption and a gene replacement strategy and it was further analysed whether the gene locus can be targeted by knock-in constructs. A third approach to assess the essentiality of PfGS was to express an inactive mutant of PfGS C-terminally tagged to the destabilization domain FKBP12 (Armstrong and Goldberg, 2007; Banaszynski et al., 2006). In the absence of the stabilising agent Shld1 the tagged protein is subject of immediate degradation and should thus not lead to the formation of inactive GS dimers and thus not affect viability of the parasites. In presence of Shld1 the PfGS mutant protein should be stabilized and dilute out the endogenously expressed active from of PfGS. Lastly, PfGS-HA was expressed in *P. falciparum*.

4.2 Localization of PfGS

The subcellular localization of PfGS was investigated expressing C-terminally GFP tagged PfGS from an episomal expression plasmid. Using MultiSite Gateway® technology the full-length *pfgs* ORF was cloned in frame with the sequence of the GFP-tag (van Dooren et al., 2005). The expression was under control of the Hsp86 promotor and the expression plasmid pCHD-Hsp86-GS-GFP (see Table 2-1)

was transfected on two independent occasions into D10 wild-type parasites, generating the parasite lines $D10^{GS\text{-}GFP}$-1 and $D10^{GS\text{-}GFP}$-2. Live parasites were observed in the transfected cultures after 3 weeks. Both parasite lines showed GFP-fluorescence in the cytosol. Images presented here were taken of parasite line $D10^{GS\text{-}GFP}$-1 (Figure 4-1A). To ensure that the observed fluorescence was due to the full length PfGS-GFP fusion protein and not to a degradation product, protein was extracted from the parasites and analysed by Western blotting with an anti-GFP antibody (Figure 4-1B). A single band of the expected molecular size of the full-length PfGS-GFP fusion protein at 104.7 kDa was detected, demonstrating that the GFP-fluorescence observed in the transfected parasites is indeed the result of the expression of the full-length PfGS-GFP from the pCHD-Hsp86-GS-GFP plasmid. These data show that PfGS is located in the parasite cytosol.

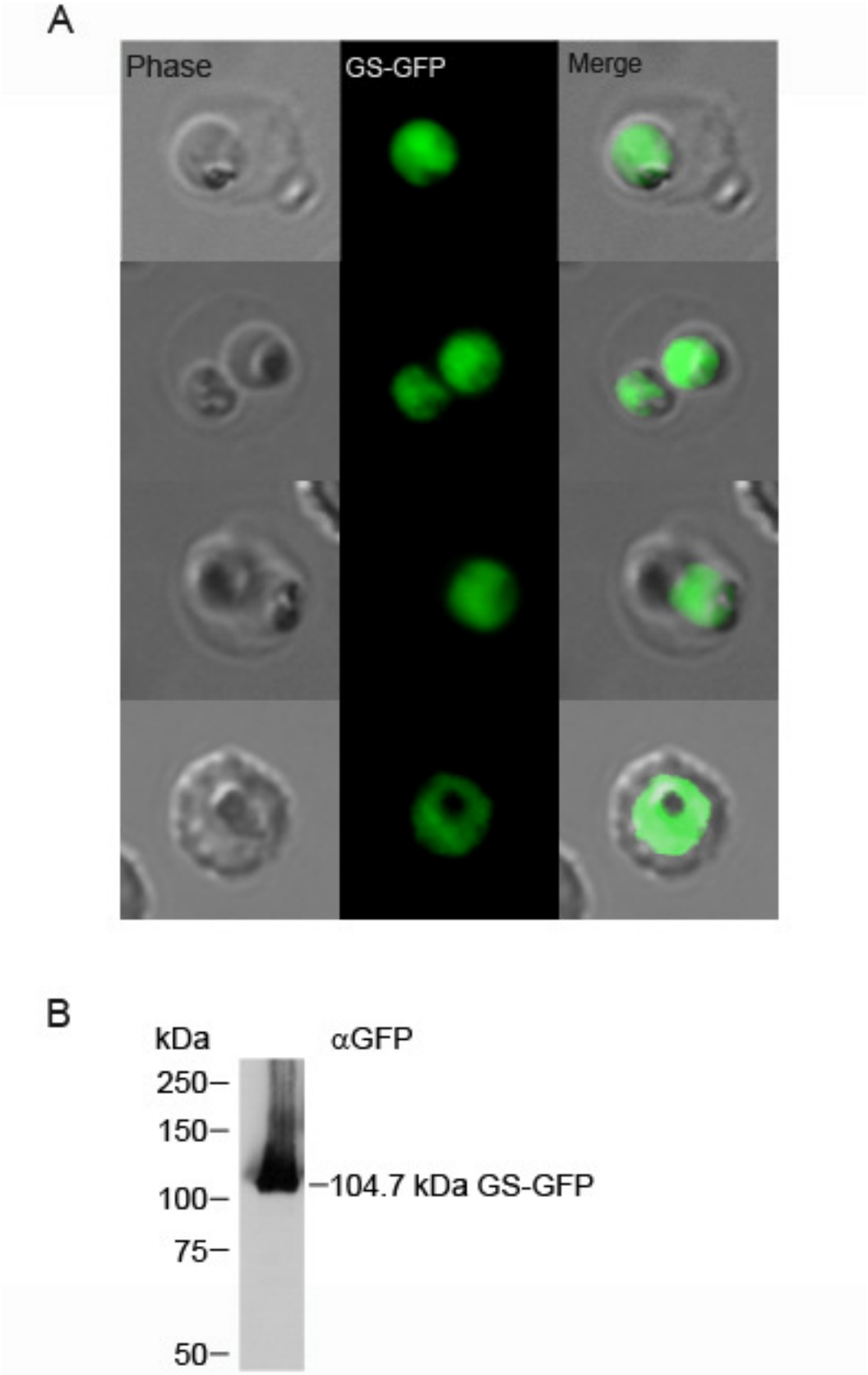

Figure 4-1: Subcellular localization of PfGS-GFP.
Panel A: The subcellular localization of PfGS in erythrocytic stages was determined by expressing a PfGS-GFP fusion protein in the parasites. The full length *pfgs* ORF was cloned in frame with the sequence for a C-terminal GFP-tag and D10 parasites were transfected twice with an episomal expression construct for PfGS-GFP under control of the Hsp86 promotor. The fusion protein was localized in the parasite cytosol. Images were taken of the transfected line $D10^{GS\text{-}GFP}$-1. **Panel B:** Western Blot analysis of protein extract of $D10^{GS\text{-}GFP}$-1 parasites with an anti-GFP antibody showed the full length PfGS-GFP fusion protein.

4.3 Knockout studies

4.3.1 Knockout by gene disruption

To assess whether PfGS is essential for the survival of intra-erythrocytic stages of *P. falciparum*, knockout studies by gene disruption were performed using the plasmid pHH1 (Reed et al., 2000). A 1000 bp DNA fragment homologous to a part of the target gene was cloned into the plasmid. The fragment lacked the 5'- and 3'-end of *pfgs* and contained an artificial stop codon. The resulting plasmid was named pHH1-*Δgs* (Table 2-1) and was transfected into wild-type 3D7 parasites on two independent occasions. Transfected parasites were selected with the drug WR99210 because the pHH1 plasmid contains an hDHFR selectable marker cassette. It was expected that the plasmid leads to a knockout by integration of the vector into the target gene locus following a single cross-over event if *pfgs* is not essential. The target gene locus is disrupted into a pseudo-diploid locus with two truncated copies of the gene. One copy lacks the 3'-end and contains a premature stop codon while the second copy is truncated at the 5'-end and lacks the start codon.

Transfected parasite lines were named $3D7^{pHH1\text{-}\Delta gs}$-1 and $3D7^{pHH1\text{-}\Delta gs}$-2 and parasites were observed in Giemsa stained thin smears four to five weeks after transfection. To select for parasites with a disrupted gene locus, cultures were subjected to drug selection cycles as outlined in section 3.4. Parasites transfected with the pHH1-Δ*gs* construct were taken through four drug selection cycles and gDNA was isolated after each complete cycle and analysed by Southern blot after a diagnostic restriction digest with *Eco*RV and *Xho*I (Figure 4-2).

Figure 4-2A shows a diagram of the expected restriction pattern for the Southern blot. Using a *pfgs* specific probe generated from the insert of pHH1-Δ*gs*, an 8.47 kb band should be visible indicative of the endogenous *pfgs* locus. A 1.26 kb fragment is expected for the plasmid with this probe and in the case of a recombination event with the *pfgs* gene locus two bands at 1.93 kb and 7.80 kb are expected (Figure 4-2A). Black arrows indicate the restriction sites of *Eco*RV and *Xho*I. The sizes of the expected fragments are indicated by red arrows.

The Southern blot in Figure 4-2B shows gDNA isolated from 3D7$^{pHH1\text{-}\Delta gs}$-1 and 3D7$^{pHH1\text{-}\Delta gs}$-2 in selection cycle 0 (lanes 2 and 4, respectively) and cycle 4 (lanes 3 and 5, respectively) in comparison to gDNA extracted from 3D7 wild-type parasites (lane 1). No recombination of the plasmid was observed; in either of the transfected parasite lines only bands corresponding to the plasmid and the endogenous *pfgs* locus were detected (1.26 kb and 8.47 kb, respectively; Figure 4-2B, lanes 2-5). For the untransfected wild-type parasites only the 8.47 kb band corresponding to the intact endogenous *pfgs* locus is visible. This suggests that either the gene is essential or that the gene locus cannot be targeted.

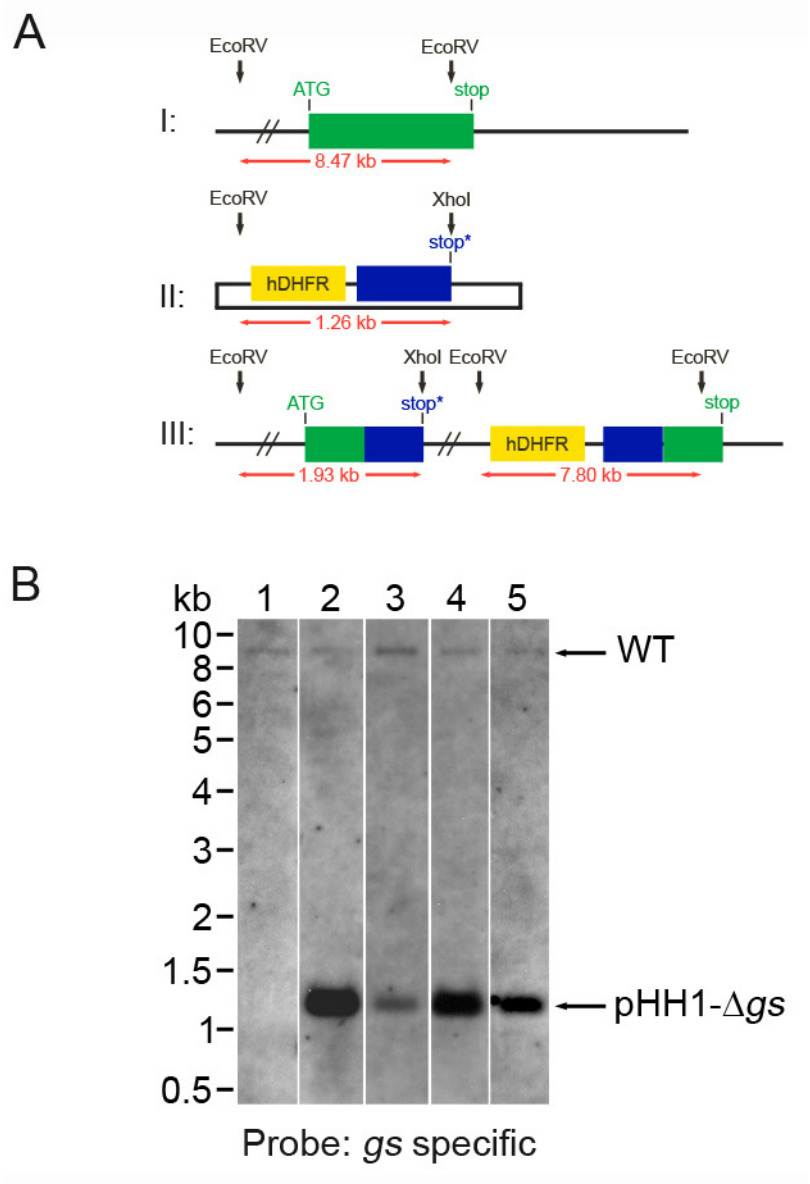

Figure 4-2: Knockout studies of *P. falciparum gs* by gene disruption.
For knockout studies by single cross-over the plasmid pHH1 was used. **Panel A** displays a schematic diagram (not to scale) of the wild-type endogenous gene locus (I), the transfected pHH1-Δ*gs* construct (II) and the gene locus following recombination (III). The wild-type locus (I) was targeted with a pHH1-Δ*gs* construct (II) containing a 1 kb insert (II, blue box) homologous to a part of the *pfgs* ORF (I, green box). The insert lacks the start ATG codon and part of the 5'-end and contains an artificial stop codon (stop*) whilst lacking the 3'-end. An hDHFR selectable marker cassette (yellow box) allows for selection of transfected parasites. Knockout of the *gs* gene is achieved through disruption of the gene locus following a single cross-over event between the plasmid and the wild-type locus. This leads to the formation of a pseudo-diploid locus (III) with two truncated copies of the gene, one truncated at the C-terminus by the artificial stop codon (III, stop*, green-blue box) and one truncated at the N-terminus lacking a start codon (III, blue-green box). Parasite lines were analysed by Southern blot following restriction digest of gDNA with *Eco*RV and *Xho*I. Red arrows indicate the expected fragment sizes detected with a gene specific probe. **Panel B** shows a Southern blot of two independently transfected parasite lines after diagnostic digest with *Nde*I and *Xho*I. The expected pattern is indicated by red arrows in Panel A. Lane 1 contains gDNA of untransfected 3D7 wild-type parasites. Lanes 2 and 3 contain gDNA of selection cycle 0 and cycle 4 of $3D7^{pHH1\text{-}\Delta gs}$-1, respectively. Lanes 4 and 5 contain gDNA of selection cycle 0 and cycle 4 of $3D7^{pHH1\text{-}\Delta gs}$-2, respectively. In all five lanes the diagnostic wild-type band is present at 8.47 kb (WT). In lanes 2-5 the band corresponding to the plasmid is detected at 1.26 kb. No integration specific bands at 1.93 kb and 7.80 kb can be observed in lanes 2-5.

4.3.2 Knockout by gene replacement

In a second approach to test whether *pfgs* is essential, knockout studies by gene replacement were performed using the plasmid pCC4 (Maier et al., 2006). Two 0.48 kb inserts homologous to regions of the 5'- and 3'-ends of the *pfgs* gene were cloned into the plasmid, thus generating the construct pCC4-Δ*gs* (see Table 2-1). Recombination via double cross-over between the pCC4 construct and the gene locus results in replacement of the target gene with the *blasticidin-S-deaminase* (*bsd*) selectable marker. In addition to the *bsd* selectable marker for selection of transfected parasites, the plasmid also contains a *cytosine deaminase* (*cd*) gene for negative selection against parasites maintaining the plasmid episomally and against parasites that integrated the plasmid by single crossover. This death gene is lost when the vector recombines with the target gene by double crossover. Transfections were performed independently in 3D7 and D10 wild-type parasites. Transfected parasites were selected with Blasticidin-S-HCl (Bla) and to account for the possibility that parasites could survive the loss of PfGS by scavenging GSH, culture medium was supplemented with 2 mM GSH.

Transfected parasites $3D7^{pCC4\text{-}\Delta gs}$ and $D10^{pCC4\text{-}\Delta gs}$ were taken through drug selection cycles by removing Bla pressure for three weeks before adding the drug again as described previously. After each complete Bla selection cycle the cultures were divided into two independent cultures. One flask was cultured normally and taken through further drug selection cycles while the other was treated with Ancotil®. In case of a double crossover recombination between pCC4-Δ*gs* and the *pfgs* gene the *cd* gene is lost and thus parasites become Ancotil® resistant. Ancotil® was added at a concentration equivalent to 1 µM 5-fluorocytosine. Parasites in cultures treated with Ancotil® began to die within 2-4 days, suggesting that Bla resistant parasites still contained the plasmid and the *cd* gene. No viable parasites were observed after one week, indicating the continued presence of the *cd* gene in the episomal plasmid. The Ancotil® drug pressure was maintained for several weeks. For $3D7^{pCC4\text{-}\Delta gs}$ no Ancotil®-resistant parasites were obtained following Ancotil® treatment while for the $D10^{pCC4\text{-}\Delta gs}$ parasite line Ancotil®-resistant parasites were isolated after selection cycle 4. Ancotil®-resistant parasites were first detected in Giemsa stained thin smears after 4 weeks of culturing in the presence of Ancotil®.

To analyse the genotype of transfected parasites, gDNA was prepared of 3D7$^{pCC4\text{-}\Delta gs}$ and D10$^{pCC4\text{-}\Delta gs}$ in Bla selection cycle 0 and after each subsequent cycle and analysed by Southern blotting (Figure 4-3, Panel B and C). The gDNA was digested in a diagnostic restriction digest with *Ear*I. Figure 4-3A displays a schematic diagram depicting the expected pattern for the endogenous *pfgs* locus (AI), the pCC4-Δ*gs* plasmid (AII) and the *pfgs* locus following a double crossover recombination event between the wild-type gene and the knockout construct (AIII). Gene specific probes homologous to the two inserts of pCC4-Δ*gs* were used to analyse the parasite lines. The sizes of the expected fragments were 0.94 kb and 4.82 kb for the *pfgs* wild-type locus, 5.90 kb for the plasmid and 6.83 kb for a gene replacement.

In Figure 4-3B and C Southern blots of D10$^{pCC\text{-}\Delta gs}$ and 3D7$^{pCC4\text{-}\Delta gs}$ are displayed. Both transfected parasite lines contained the plasmid in selection cycle 0 (Figure 4-3B lane 2 and Figure 4-3C lane 2) and maintained the plasmid until cycle 3 (lane 3B and lane 3C) as indicated by the presence of a 5.90 kb band. No band diagnostic for gene replacement at 6.83 kb was visible in either of the lines. The D10$^{pCC4\text{-}GS}$ parasites resistant to Ancotil® still contain the endogenous gene indicated by two bands at 0.94 kb and 4.82 kb and there is no indication of recombination of pCC4-Δ*gs* with the endogenous gene locus (Figure 4-3C lane 4). However, it appears that the plasmid was lost from this parasite line as no 5.90 kb band is visible on the Southern blot, suggesting that the parasites have maintained Bla resistance while losing the *cd* death gene. This possibility was not further analysed. Potentially the plasmid may have recombined, allowing the parasites to keep the part containing the *bsd* gene while losing the *cd* gene and the inserts homologous to the *gs* gene, which should have been detectable on the Southern blot. Performing Southern blot analysis with probes specific for the *bsd* and *cd* genes could elucidate for instance the fate of the plasmid. These results again indicate that the *pfgs* gene is essential for the survival of intra-erythrocytic stages of *P. falciparum*.

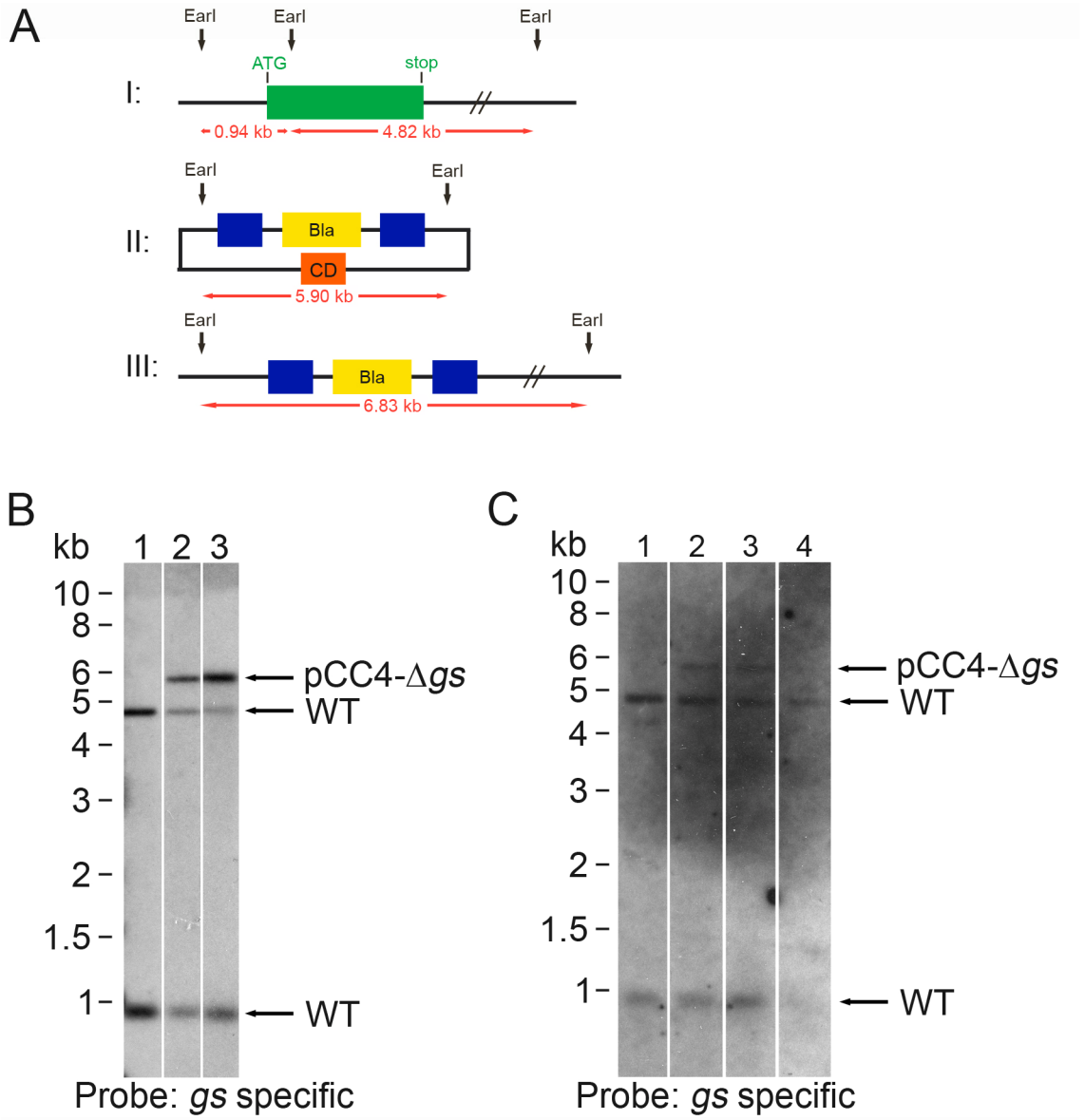

Figure 4-3: Knockout studies by double cross-over of *P. falciparum gs*
For knockout by gene replacement the plasmid pCC4 was used**. Panel A** displays a schematic diagram (not to scale) of the *pfgs* wild-type locus (I), the pCC4-Δ*gs* construct (II) and the gene locus following recombination by double crossover (III). The plasmid contains two 0.48 kb inserts (II, blue boxes) homologous to the 5'- and the 3'-ends of the *pfgs* coding region (I, green box). Following double cross over recombination, the gene is replaced by the *blasticidin-S-deaminase* selectable marker cassette (II, III, yellow box). To analyse transfected parasite lines by Southern blotting, gDNA was digested with the restriction enzyme *Ear*I. Red arrows indicate the sizes of the fragments for wild-type gene, plasmid and recombined locus that can be detected with a gene-specific probe. **Panel B** shows a Southern blot of the transfected 3D7$^{pCC4\text{-}\Delta gs}$ parasite line in comparison to the 3D7 wild-type after diagnostic digest of gDNA with *Ear*I. The expected pattern is described in Panel A. Lane 1 contains 3D7 wild-type gDNA. Two bands according to the wild-type (WT) gene locus at 0.94 kb and 4.82 kb can be observed. Lane 2 contains gDNA of 3D7$^{pCC4\text{-}\Delta gs}$ in cycle 0. In addition to the wild-type gene (WT), a 5.90 kb band corresponding to the plasmid is visible. Lane 3 shows the same parasite line after selection cycle 3. Again only the bands corresponding to the endogenous gene and the plasmid are present. **Panel C** shows a Southern blot of the D10$^{pCC4\text{-}\Delta gs}$ parasite line in comparison to the untransfected D10 wild-type after diagnostic digest of gDNA with *Ear*I. The expected pattern is described by the diagram in Panel A. Lane 1 contains D10 wild-type gDNA. Only two bands at 0.94 kb and 4.82 kb corresponding to the wild-type gene locus are detected. Lane 2 and 3 contain gDNA of D10$^{pCC4\text{-}\Delta gs}$ in drug selection cycle 0 and cycle 3, respectively. In both the wild-type gene specific bands (WT) are visible as well as the 5.90 kb band corresponding to the plasmid. Lane 4 contains gDNA of the Ancotil® resistant parasites that were obtained after cycle 3. The wild-type gene is still present in this line. The plasmid band has disappeared.

4.3.3 Knockout control studies

To rule out the possibility that the *pfgs* gene locus cannot be targeted parasites were transfected with the construct pHH1-*gs*con (Reed et al., 2000). Similar to the knockout construct, the pHH1-*gs*con control construct targets the *pfgs* gene locus in a single cross-over event. The 1.08 kb insert homologous to the target gene in this construct is truncated at the 5'-end but contains the full length 3'-end including the endogenous stop codon of the *pfgs* coding region (see Table 2-1). Integration of the construct into the wild-type locus creates a pseudo-diploid locus with a full-length and a truncated copy of the gene (Figure 4-4A). Thus parasites still have a functional copy of the gene despite disruption of the *pfgs* gene locus. 3D7 wild-type parasites were transfected with the pHH1-Δ*gs* control plasmid and selected with WR99210. Parasites resistant to WR99210 were obtained 4 weeks after transfection.

Transfected parasites 3D7$^{pHH1\text{-}gscon}$ were taken through two drug selection cycles as described previously and for each cycle gDNA was prepared and analysed by Southern blotting after digestion with *Eco*RI and *Xho*I. The expected fragments detectable with a *pfgs* gene specific probe corresponding to the insert of pHH1-*gs*con are 6.40 kb for the endogenous wild-type locus (Figure 4-4A, I) and 3.30 kb for the plasmid (Figure 4-4A, II). Two fragments of 1.80 kb and 7.90 kb size are expected for an integration event (Figure 4-4A, III).

After two drug selection cycles, the gene locus had been targeted and parasites were cloned by limiting dilution. Figure 4-4B shows a Southern blot of the untransfected 3D7 wild-type (lane 1) and the transfected parasite line in cycle 0, prior to integration (lane 2), and a clone isolated after cycle 2 (lane 3). A band corresponding to endogenous *pfgs* at 6.40 kb is visible in wild-type 3D7 (Figure 4-4B, lane 1) and in 3D7$^{pHH1\text{-}gscon}$ in cycle 0 (lane 2). In the transfected parasites (lane 2) a band corresponding to the plasmid at 3.30 kb can be seen in addition to the endogenous wild-type band. Lane 3 shows an exemplary clone with two bands at 1.80 kb and 7.90 kb visible diagnostic for homologous recombination of the *pfgs* gene locus with the plasmid. The band corresponding to the wild-type gene locus is absent (Figure 4-4B). This demonstrates that the *pfgs* gene locus can be targeted. The cloned parasite line still contains the episomal plasmid as indicated by the presence of a 3.30 kb band. Since the selectable marker has

integrated into the gene locus the plasmid is no longer essential for the survival of the parasites. However, sometimes plasmids are maintained even after integration, possibly because this means higher expression level for the hDHFR selectable marker and an advantage for parasite survival.

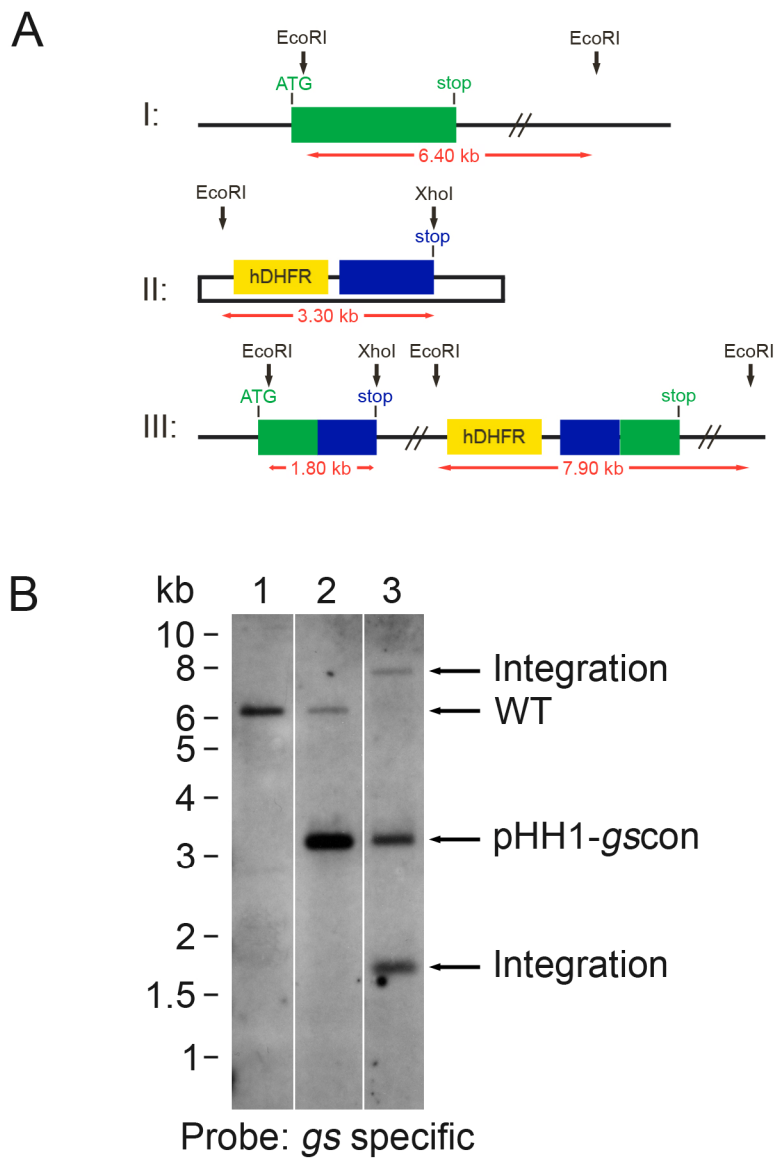

Figure 4-4: Knock-in control studies of *P. falciparum gs*
Panel A displays a schematic diagram (not to scale) of the *pfgs* wild-type locus (I), the pHH1-*gs*con construct (II) and the *pfgs* locus after recombination by single cross-over (III). The pHH1 construct contains a 1077 bp insert (II, blue box) homologous to the 3'-end of the coding region of the *pfgs* target gene (I, green box) and a hDHFR selectable marker (yellow box). The insert of the knock-in construct is truncated at the 5'-end, but it contains the full 3'-end of *pfgs*. Following recombination between plasmid and wild-type locus, the target gene is disrupted (III) and two copies of *pfgs* result, one full length copy (green-blue box) and one copy truncated at the 5'-end (blue-green box). gDNA of transfected parasites was digested with restriction enzymes *Eco*RI and *Xho*I for analysis by Southern blotting. Black arrows indicate restriction sites. The expected fragments detectable with a gene specific probe are indicated by red arrows. **Panel B** shows a Southern blot of *Eco*RI and *Xho*I digested gDNA of untransfected 3D7 wild-type parasites (lane 1), transfected parasites in cycle 0 (lane 2) and an exemplary clone following integration in selection cycle 2 (lane 3). The expected sizes of the restriction fragments are 6.40 kb for the endogenous *pfgs* locus, 3.30 kb for the plasmid and 1.80 kb and 7.90 kb for an integration event. The 6.40 kb band for the wild-type gene locus (WT) is visible in the 3D7 wild-type (lane 1) and in cycle 0 of the transfected line $3D7^{pHH1\text{-}gscon}$ (lane 2). The latter also shows a 3.30 kb band corresponding to the plasmid. The clone in lane 3 shows two integration specific bands at 1.80 kb and 7.90 kb in addition to the plasmid at 3.30kb. The 6.40 kb fragment corresponding to the wild-type gene is absent in this clone.

4.4 Expression of $GS^{E206K/N208A}$-FKBP12

The previous experiments have established that the *pfgs* gene locus can be targeted by a knock-in construct. However, neither a single crossover construct nor a double crossover construct in the presence of negative selection leads to a gene disruption or replacement, respectively. These results suggest an important if not essential function for PfGS. To further elucidate this possibility, the expression of a dominant-negative PfGS mutant protein in the erythrocytic stages of the parasites was considered a possibility to down-regulate internal PfGS activity. This approach was taken because PfGS is active as a dimer. The presence of a PfGS dead mutant next to the active form should result in the formation of inactive-active hybrid dimers as well as to active-active and inactive-inactive dimers and thus dilute the endogenous PfGS. This should decrease the overall PfGS activity in the parasite and potentially lead to a decrease in the intracellular GSH level in transfected parasite lines. To control the level of mutant PfGS present in the parasites, the gene was cloned in frame with the sequence for a C-terminal destabilization domain. The destabilization domain is a mutant form of the human FKBP12 protein (hereafter referred to as FKBP12) which leads to rapid proteasomal degradation of the fusion protein (Armstrong and Goldberg, 2007; Banaszynski et al., 2006). Shld1 is a ligand for FKBP12 and binds with high affinity to the destabilization domain thereby stabilizing the tagged protein. Thus cellular levels of any FKBP12 fusion protein can be regulated by adjusting the concentration of available ligand.

4.4.1 Sequence considerations

Alignment of PfGS with the HsGS reveals an overall sequence identity of 18.2 %. However, several domains appear to be highly conserved (Meierjohann et al., 2002a). Recent studies on mutant forms of the human enzyme identified the role and importance of four amino acid residues within the ATP-binding domain of the human enzyme for enzyme activity (Dinescu et al., 2004). In particular the negatively charged Glu-144 residue was shown to have a major role in catalysis and is presumably involved in the stabilization of the γ-glutamylcysteinyl-phosphate intermediate. Mutation of this amino acid to Lys completely abolished the activity of HsGS. Other residues shown to be of importance for activity of the human enzyme were Asn-146, Lys-305 and Lys-364. All four residues are

conserved in the PfGS (Figure 4-5). To generate an inactive form of PfGS, Glu-206 and Asn-208 corresponding to Glu-144 and Asn-146 in the human enzyme were both mutated to Lys and Ala, respectively, thus generating $PfGS^{E206K/N208A}$. Mutagenesis was performed using the pJC40-PfGS expression construct available in our laboratory (Meierjohann et al., 2002a) as template, generating the construct $pJC40\text{-}GS^{E206K/N208A}$. The $pJC40\text{-}GS^{E206K/N208A}$ construct was then used as template for cloning of $PfGS^{E206K/N208A}$ into the pCHD-3/4 vector using the MultiSite Gateway® system for expression of $PfGS^{E206K/N208A}$-FKBP12 in *P. falciparum*. The expression was controlled by the Hsp86 promotor to allow high levels of expression throughout the parasite intra-erythrocytic cycle. The expression construct was named pCHD-Hsp86-$GS^{E206K/N208A}$-FKBP12 (see Table 2-1).

```
Pf3D7GS         MERKVDEFYKVIEKEVLNYFTCPNGKNEYLSYERIKSLIKDMIAFLNTESYYIFTNSYKN
HsGS            --------------------MATNWGSLLQDKQQLEELARQAVDRALAEGVLLRTSQEPT
                                     ..*  .   . ::::.* :: :    :*.  : *..  .

Pf3D7GS         EYNIDFLYNPKLFSFTLLPHRLDKKLLELCKYSTLLYSELFDNMVCDLSYLLSIFENIKE
HsGS            SSEV-VSYAP----FTLFPSLVPSALLEQAYAVQMDFNLLVDAVSQNAAFLEQTLSSTIK
                . :: . * *    ***:*  : . *** .    : :. *.* :  : ::* . :..  :

Pf3D7GS         HDFFVKKMLEVCKKVYGDNSDNSDNSDNSNNSNNSNNSNNFRNIKDDIRCVIGRSDYMTN
HsGS            QDDFTARLFDIHKQVLKE------------------------GIAQTVFLGLNRSDYMFQ
                :* *. ::::: *:*  :                        .* : :   :.***** :

Pf3D7GS         RNNDIIDDKEKIDDENINDKDIKQIEYNTISVAFGNLSSILFNGHKYILKQIYKEYFPYI
HsGS            RSAD-------------GSPALKQIEINTISASFGGLASRTPAVHRHVLSVLSK------
                *. *             ..  :**** ****.:**.*:*     *:::*. : *

Pf3D7GS         GNEEEQKEVNDILDKKFDNNFVQGIITCFKKCHDIYISEYKPLLGSHKVIMMSILHEDDF
HsGS            -----TKEAGKIL----SNNPSKGLALGIAKAWELY--------GSPNALVLLIAQEKER
                      **...**    .**  :*:   : *. ::*        ** :.::: * :*.:

Pf3D7GS         NSFDKYKTTNELNKININQKALTINEIKLLFESKKLFLNYKDETLIDSLKRIKNKEYNPY
HsGS            NIFDQRAIENELLARNIHVIRRTFEDI-----SEKGSLDQDRRLFVDGQ-----------
                * **:    ***   **:    *:::*     *:*  *: . . ::*.

Pf3D7GS         NEIFKPGKLLIDLNDLEDILNVDCININDILKNINKYERNIFEISVLYFRALYTPNHFNE
HsGS            ------------------------------------------EIAVVYFRDGYMPRQYSL
                                                          **:*:***  * *.::.

Pf3D7GS         NIWKIREMFEFSDAIKIPSLPYQLVGSKKIQMLLLDNDILKKYISLNLNKEKKSDEQITK
HsGS            QNWEARLLLERSHAAKCPDIATQLAGTKKVQQELSRPGMLEMLLP-------GQPEAVAR
                : *: * ::* *.* * *.:. **.*:**:*  *   .:*:  :.        . * :::

Pf3D7GS         DMTLLKKTFALQVDPSQNINAHIIQDAINNENNYLLKPQREGGKNNLHGNQVKQKLKLFY
HsGS            LRATFAGLYSLDVGEEGD---QAIAEALAAPSRFVLKPQREGGGNNLYGEEMVQALKQLK
                  : :   ::*:*. . :   : * :*:   ..::******** ***:*::: * ** :

Pf3D7GS         DHNKKQTLSHYVLMQRLFPSTFTAIHCRTQEMKNEICTTNISNEQQKKKPSHLIQFSPEK
HsGS            DSEERAS---YILMEKIEPEPF------------ENCLL------RPGSPARVVQ-----
                * ::: :   *:**::: *..*            * *        :  .*::::*

Pf3D7GS         SISEFSLFHNFIFYKNKNILNEQKGYLVRTKNYTEKEGGAICGISSLDSFFLTEH
HsGS            CISELGIFGVYVRQEKTLVMNKHVGHLLRTKAIEHADGGVAAGVAVLDNPYPV--
                .***:.:*  ::  ::. ::*:: *:*:***   . :**. .*:: **. : .
```

Figure 4-5: Alignment of the PfGS amino acid sequence with the human GS amino acid sequence.
PfGS was aligned with HsGS using the programme T-Coffee showing identical residues (*), conserved residues (:) and homologous residues (.). For maximal alignment several gaps were introduced (-). The sites Glu-206, Asn-208, Lys-448 and Lys-517 in PfGS that are homologous to Glu-144, Asn-146, Lys-305 and Lys-364 in HsGS are highlighted in yellow.

4.4.2 Recombinant expression of GS^{wt} and $GS^{E206K/N208A}$ in *E.coli*

In order to assess whether the mutations that were introduced into PfGS affect the activity, both wild-type and mutant forms of the enzyme were recombinantly expressed in *E. coli*, purified and activity assays performed. To confirm the optimal expression conditions described by Meierjohann *et al.* (Meierjohann et al., 2002a) for $PfGS^{wt}$ and to establish them for $PfGS^{E206K/N208A}$ in *E. coli* BLR (DE3), small scale test expressions at different temperatures were performed using the pJC40 constructs. The temperatures tested were 18°C, 25°C, 30°C and 37°C. Samples of bacteria cultured after induction with 1 mM IPTG were prepared using the BugBuster extraction protocol and insoluble and

soluble fractions were analysed by western blotting using an anti-His-tag antibody. Figure 4-6A shows a western blot for the $PfGS^{wt}$ recombinant protein after expression over night. A band of the expected size (77.5 kDa) corresponding to the recombinant protein can be seen in the soluble fractions at 18°C, 25°C and 30°C (Figure 4-6A, lanes 5,6 and 7, respectively). No $PfGS^{wt}$ was detected in the soluble fractions after expression at 37°C (Figure 4-6A, lane 8). The largest amount of soluble protein was found to be expressed at 25°C over night. Bands of the expected size for PfGS are also visible in the insoluble fraction (Figure 4-6A, lanes 1-4). The $PfGS^{wt}$ recombinant protein was expressed overnight at 25°C for purification. Figure 4-6B shows a western blot analysis of the $PfGS^{E206K/N208A}$ test expression. Protein was expressed for either four hours (Figure 4-6B, lanes 1-4) or over night (Figure 4-6B, lanes 5-8). Only the soluble fractions were loaded for this blot. Again, the temperatures tested were 18°C (lanes 1 and 5), 25°C (lanes 2 and 6), 30°C (lanes 3 and 7) and 37°C (lanes 4 and 8). Small amounts of the recombinant protein were detected after expression for 4 h at 18°C and 37°C (Figure 4-6B, lanes 1 and 4, respectively). Overnight incubation leads to expression of $PfGS^{E206K/N208A}$ recombinant protein at all four temperatures (Figure 4-6B, lanes 5-8). However, some smaller fragments detected suggest degradation or premature termination of protein translation, especially at 18°C (lane 5). The lowest number of smaller fragments can be detected after expression at 30°C (Figure 4-6B, lane 7). Thus the best expression condition for $PfGS^{E206K/N208A}$ appears to be incubation at 30°C overnight.

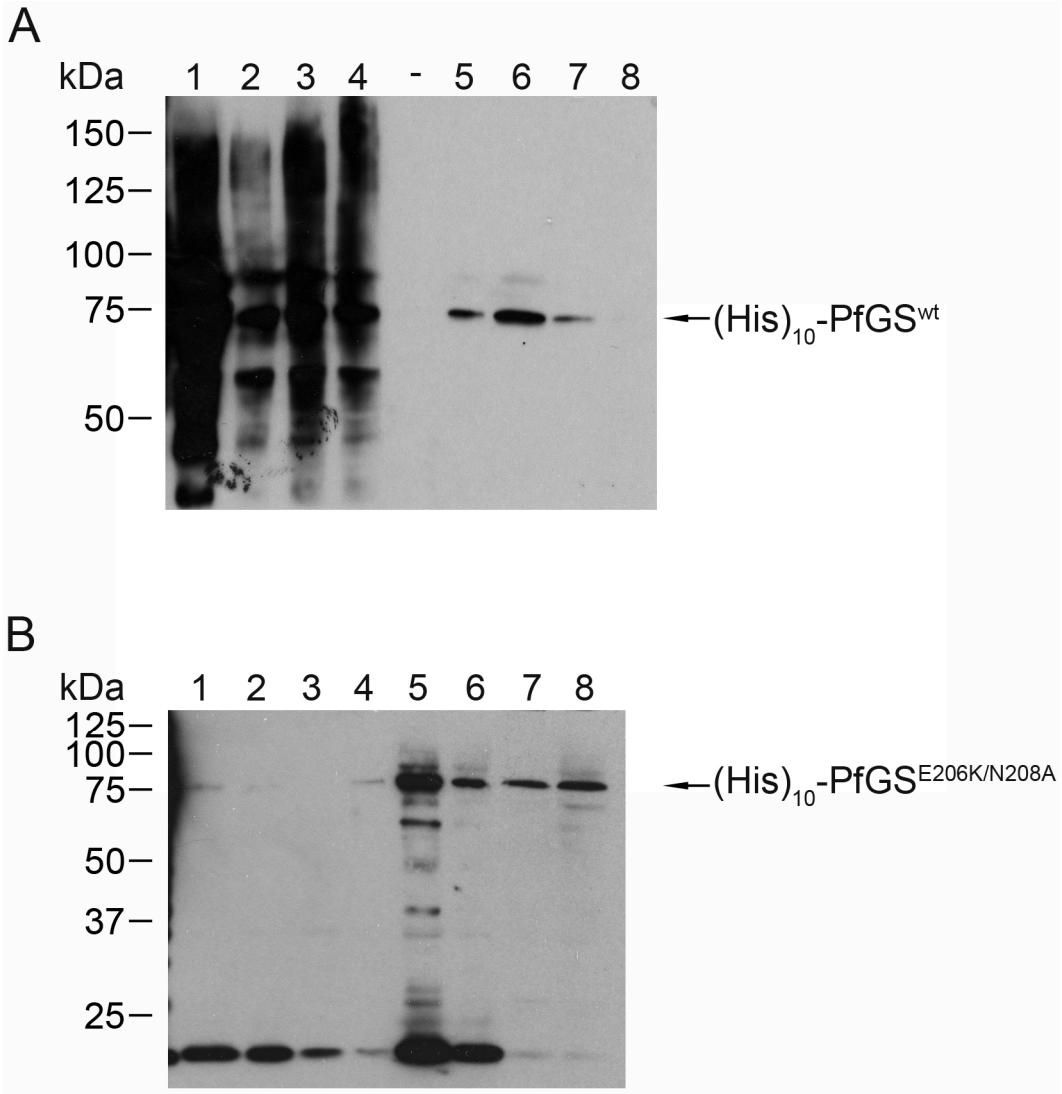

Figure 4-6: Western blot analysis of PfGS test expression.
Panel A: PfGS^{wt} protein was expressed overnight after induction with 1 mM IPTG at 18°C (lanes 1 and 5), 25°C (lanes 2 and 6), 30°C (lanes 3 and 7) and 37°C (lanes 4 and 8) and samples were extracted using the BugBuster method. Lanes 1-4 contain the insoluble fractions and lanes 5-8 soluble fractions. The expected size for PfGS^{wt} is 77.5 kDa. Equal amounts of protein were loaded for insoluble and soluble fractions. **Panel B**: Mutant PfGS^{E206KN208A} was expressed after induction with 1 mM IPTG for four hours (lanes 1-4) and over night (lanes 5-8) at 18°C (lanes 1 and 4), 25°C (lanes 2 and 5), 30°C (lanes 3 and 7) and 37°C (lanes 4 and 8). Equal amounts of the soluble fractions were loaded for this blot.

PfGS^{wt} and PfGS$^{E206K/N208A}$ were purified using the Ni^{2+}-NTA affinity batch method. Both forms of the protein could be enriched, but the preparation was not very clean and numerous additional bands were observed on a SDS-PAGE (Figure 4-7A). A double band was prominent at the expected size of the PfGS protein (77.5 kDa) and the larger band was confirmed to be either $(His)_{10}$-GS^{wt} or $(His)_{10}$-GS$^{E206K/N208A}$ protein by western blotting using an anti-His-tag antibody (Figure 4-7B). Some of the additional bands visible on the SDS-PAGE gel were also detected on the western blot, suggesting they are breakdown products of the recombinant proteins.

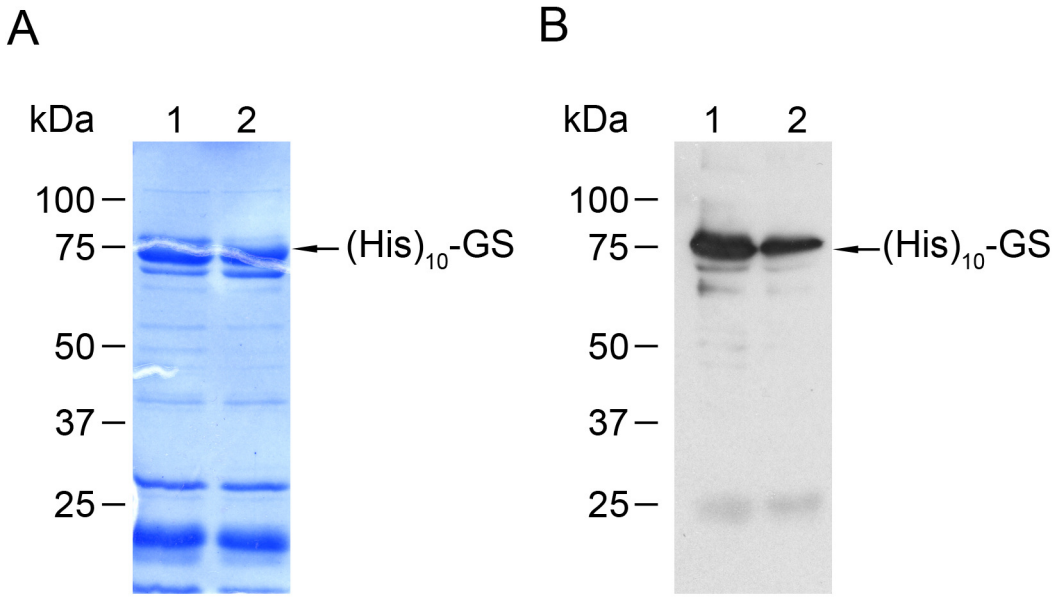

Figure 4-7: Expression and purification of $(His)_{10}$-tagged GS.
Panel A: Coomassie stained gel of purified $PfGS^{wt}$ (lane 1) and $PfGS^{E206K/N208A}$ (lane 2). **Panel B**: Western Blot of the purified protein $PfGS^{wt}$ (lane 1) and $PfGS^{E206K/N208A}$ (lane 2) using anti His-tag antibody.

The activity of the recombinant enzymes was determined as previously described (Huang et al., 1995; Meierjohann et al., 2002a). Briefly, ADP produced by PfGS or $PfGS^{E206K/N208A}$ is used by pyruvate kinase to produce pyruvate and ATP from phosphoenolpyruvate. Lactate dehydrogenase in the assay uses NADH present in the reaction mix to convert pyruvate to lactate. The activity is measured by following the change of absorbance at 340 nm when NADH is oxidized to NAD^+. As a substrate, γ-glutamyl-α-aminobutyrate (γ-GluAbu) was used rather than γ-GC in order to avoid thiol oxidation (Huang et al., 1995; Meierjohann et al., 2002a).

In preliminary tests enzymatic activity was detectable for the wild-type form of PfGS but not for the $PfGS^{E206K/N208A}$ mutant (Figure 4-8). The measured activity of $PfGS^{wt}$ was proportional to the amount of protein used. No activity was detected if the substrate γ-GluAbu was omitted from the reaction mix, indicating that the $PfGS^{wt}$ and not one of the contaminating proteins were responsible for the detected activity. The activity measured for $PfGS^{wt}$ was 0.42 µmol / min / mg.

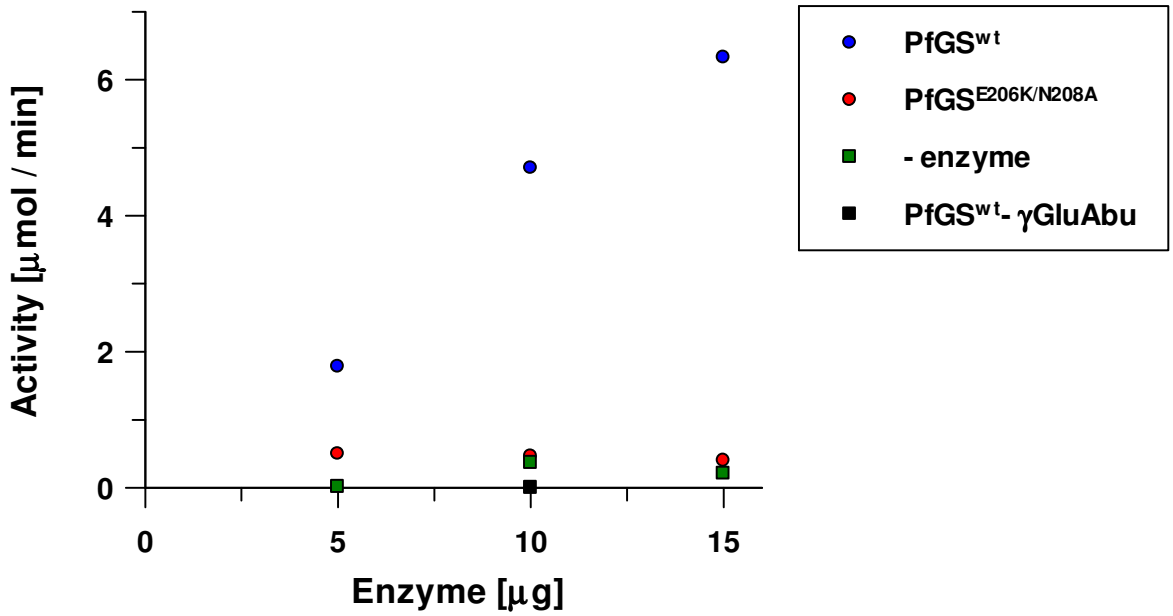

Figure 4-8: Activity of recombinant PfGS.
The enzyme activity was determined spectrophotometrically by coupling the release of ADP by PfGS to oxidation of NADH to NAD^+ through pyruvate kinase and lactate dehydrogenase. $PfGS^{wt}$ was active and the detected activity was proportional to the amount of enzyme. The activity of $PfGS^{wt}$ was dependant on the presence of the substrate γ-GluAbu. The mutant protein $PfGS^{E206K/N208A}$ was not active. This assay was only performed once.

The specific activity was approximately ten times lower than previously reported for the homogenous protein (5.24 ±0.7 µmol / min /mg) (Meierjohann et al., 2002a). This is likely due to the fact that the purified protein preparation still contains multiple contaminants that affect the overall specific activity determined. However, the purification was not further optimized for this study due to time limitations. Future work will be to purify the proteins further and to repeat the activity assays. Since no activity was detected for $PfGS^{E208K/N208A}$ it can be presumed that the Glu-206 and Asn-208 residues are important for not only HsGS but also for PfGS enzyme activity.

4.4.3 Phenotypic analyses of *P. falciparum* expressing $PfGS^{E206K/N208A}$-FKBP12

P. falciparum D10 wild-type parasites were independently transfected twice with the pCHD-Hsp86-$GS^{E206K/N208A}$-FKBP12 expression construct (see Table 2-1) creating the parasite lines $D10^{GS\text{-}E206K/N208A\text{-}FKB12}$-1 and $D10^{GS\text{-}E206K/N208A\text{-}FKBP12}$-2. It was first established that both lines express the $PfGS^{E206K/N208A}$-FKBP12 fusion protein and whether the protein can be stabilized by addition of Shld1. Parasites were cultured in presence of 0.25 µM Shld1 for 8 hours and 24 hours prior to protein extraction and western blot analyses using an anti-FKBP12 antibody

(Figure 4-9). As a control, protein was extracted from parasites grown in the absence of Shld1 and from non-transfected D10 wild-type parasites. For each sample, 20 µg of total protein were loaded according to Bradford assay. The presence of protein in each lane was confirmed by staining of the membrane with Ponceau-S.

No PfGS$^{E206K/N208A}$-FKBP12 protein was detected in non-transfected D10 wild-type parasites (Figure 4-9, lane 1). Neither was the tagged protein detected in D10$^{GS-E206K/N208A-FKBP12}$-1 and D10$^{GS-E206K/N208A-FKBP12}$-2 in the absence of the stabilising compound Shld1 (Figure 4-9, lanes 2 and 5, respectively), indicating complete degradation of the recombinant fusion protein due to the destabilization domain. Addition of Shld1 to the cultures only had an effect in the line D10$^{GS-E206K/N208A-FKBP12}$-1. The PfGS$^{E206K/N208A}$-FKBP12 protein was detected after 8h and 24 h (Figure 4-9, lanes 3 and 4, respectively). No protein was detectable in D10$^{GS-E206K/N208A-FKBP12}$-2 after addition of 0.25 µM Shld1 to the culture medium for 8 or 24 hours (lanes 6 and 7). This suggests that only D10$^{GS-E206K/N208A-FKBP12}$-1 expresses the tagged mutant protein and it is stabilized by Shld1. The second parasite line D10$^{GS-E206K/N208A-FKBP12}$-2 seems to not express the fusion protein and therefore it cannot be stabilized. All further analyses were performed using only D10$^{GS-E206K/N208A-FKBP12}$-1.

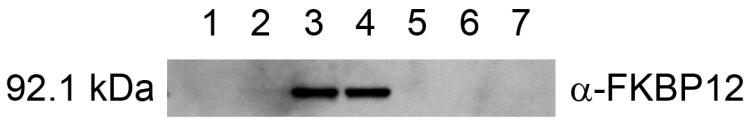

Figure 4-9: Stabilization of PfGS$^{E206K/N208A}$-FKBP12 in D10$^{GS-E206K/N208A-FKBP12}$-1 and D10$^{GS-E206K/N208A-FKBP12}$-2 in presence of 0.25 µM Shld1.
Western analysis was performed using an anti-FKBP12 antibody. No recombinant protein was present in the untransfected D10 wild-type negative control (lane 1). Equally, no protein was detected in the PfGS$^{E206K/N208A}$-FKBP12 expressing parasite lines D10$^{GS-E206K/N208A-FKBP12}$-1 and D10$^{GS-E206K/N208A-FKBP12}$-2 in the absence of Shld1 (lanes 2 and 5, respectively). In the presence of 0.25 µM Shld1 GS-FKBP12 is expressed and stabilized in D10$^{GS-E206K/N208A-FKBP12}$-1 after 8 (lane 3) and 24 hours (lane 4). No stabilized protein can be detected in D10$^{GS-E206K/N208A-FKBP12}$-2 protein extract under these conditions after 8 (lane 6) and 24 hours (lane 7).

To investigate if increasing the Shld1 concentration in the culture medium increases the amount of PfGS$^{E206K/N208A}$-FKBP12 in D10$^{GS-E206K/N208A-FKBP12}$-1, mixed stage parasites were cultured in the presence of 0.25 µM, 0.5 µM and 1 µM Shld1 for 8 hours prior to protein extraction and Western analyses (Figure 4-10A, lanes 2, 3 and 4, respectively). To investigate if the presence of Shld1 had any obvious effect on the parasite appearance, parasites were visually inspected (Figure

4-10B). Western blots were performed using the FKBP12 antibody and an antibody against the α-subunit of *P. falciparum* casein kinase 2 (PfCK2α) as a loading control. As a negative control, protein extract of parasites grown in the absence of Shld1 was loaded (Figure 4-10A, lane 1). Upon addition of Shld1 the PfGS$^{E206K/N208A}$-FKBP12 protein is present at all drug concentrations tested. Surprisingly, differing from the result of the western blot shown in Figure 4-9, this time a double band was observed with the anti-FKBP12 antibody. Potentially this indicates the presence of a smaller degradation product. The levels of PfGS$^{E206K/N208A}$-FKBP12 do not increase when the Shld1 concentration is doubled from 0.25 µM to 0.5 µM (lanes 2 and 3). This suggests that the amount of stabilized PfGS$^{E206K/N208A}$-FKBP12 is already at a maximum at a concentration of 0.25 µM Shld1 and cannot be increased any further. Probably the overall expression level of the tagged protein is limiting its stabilization and the PfGS$^{E206K/N208A}$-FKBP12 protein present is already saturated with Shld1 at the lower concentration. Interestingly, increasing the Shld1 concentration even more to 1 µM has a reverse effect, lowering the amount of GS$^{E206K/N208A}$-FKBP12 present in the parasites. No obvious effect of the drug on the morphology of the parasites was observed in Giemsa stained thins smears during the course of this experiment. All stages of parasite development were present in the mixed cultures and looked healthy at the three Shld1 concentrations tested. No dead parasites were observed.

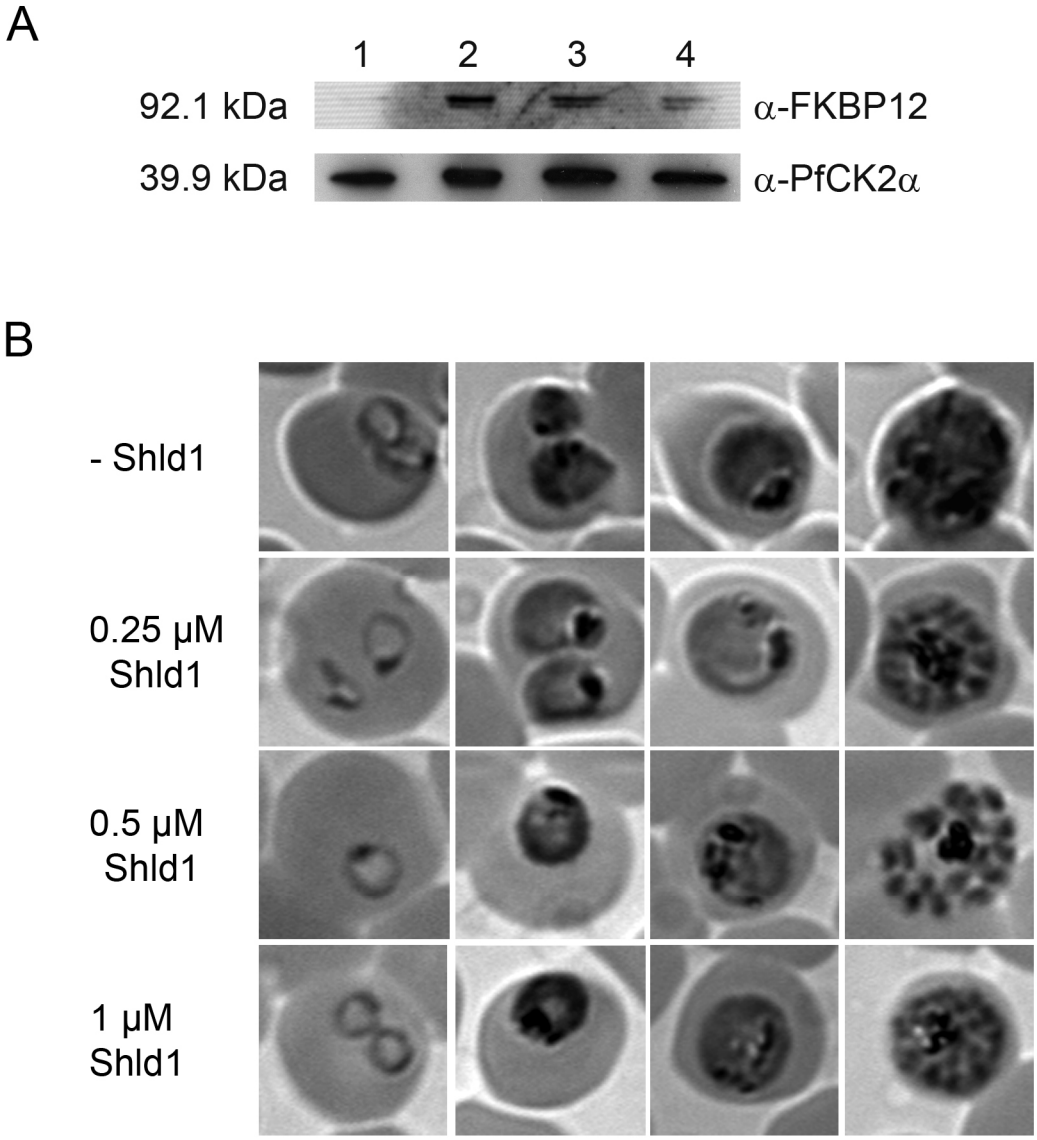

Figure 4-10: Effect of varying Shld1 concentrations on stabiliztion of PfGS$^{E206K/N208A}$-FKBP12. Panel A: Western blot of D10$^{GS-E206K/N208A-FKBP12}$-1 protein extracted after parasites were cultured for 8 hours without Shld1 (lane 1), in presence of 0.25 µM Shld1 (lane 2), 0.5 µM Shld1 (lane 3) and 1 µM Shld1 (lane 4). An antibody against FKBP12 was used to detect PfGS$^{E206K/N208A}$-FKBP12. An antibody against the Casein Kinase 2 α-subunit (PfCK2α) was used as loading control. **Panel B:** Thin smears of the cultures prior to harvesting showed healthy looking parasites in different stages for all tested concentrations of Shld1.

To assess whether the presence of Shld1 and hence the stabilization and presence of PfGS$^{E206K/N208A}$-FKBP12 affects growth and survival of D10$^{GS-E206K/N208A-FKBP12}$-1, a drug assay was performed to determine the IC_{50} concentration of Shld1 for wild-type D10 parasites and for D10$^{GS-E206K/N208A-FKBP12}$-1 (Figure 4-11). Growth of both parasite lines, D10 and D10$^{GS-E206K/N208A-FKBP12}$-1, was unaffected at concentrations of Shld1 up to 0.2 µM. At higher concentrations the growth rate was affected in both parasite lines. The IC_{50} concentrations were determined to be 1.6 µM and 2.5 µM for D10 and D10$^{GS-E206K/N208A-FKBP12}$-1, respectively. Because

the IC_{50} test was only performed twice in duplicate for D10 and D10$^{GS\text{-}E206K/N208A\text{-}FKBP12}$-1 a full statistic analysis was not possible. The inhibition of the D10 wild-type parasites by Shld1 indicates unspecific toxicity of the compound. Because of this unspecific toxicity, the IC_{50} assay was repeated once in duplicate with 3D7 wild-type parasites. Again toxicity of Shld1 was found at concentrations higher than 0.2 µM (Figure 4-11).

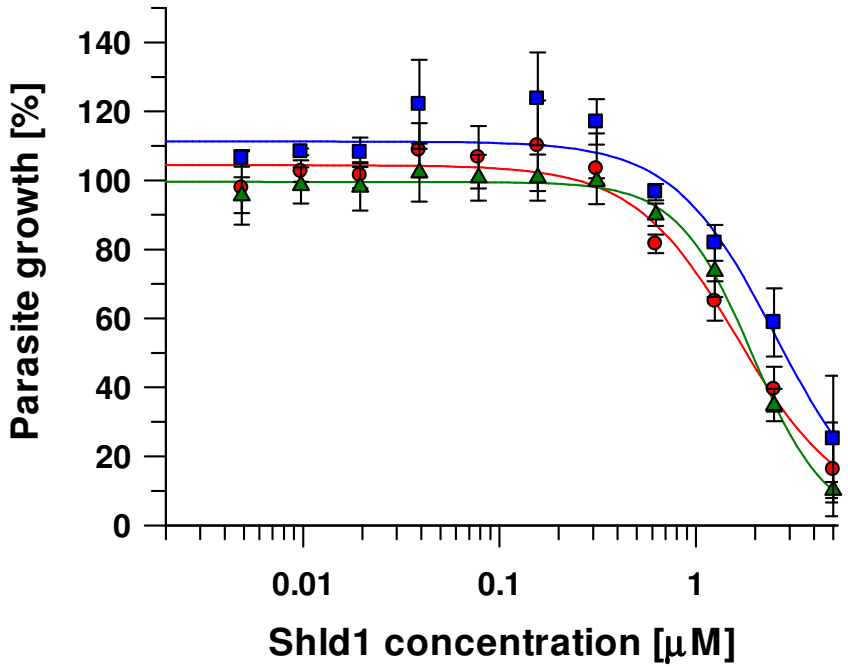

Figure 4-11: Effect of Shld1 on the proliferation of D10 and 3D7 wild-type parasites and D10$^{GS\text{-}E206K/N208A\text{-}FKBP12}$-1.
IC_{50} concentrations were determined twice in duplicate for D10 (●) and D10$^{GS\text{-}E206K/N208A\text{-}FKBP12}$-1 (■) and once in duplicate for 3D7 parasites (▲). The IC_{50} concentrations for Shld1 were 1.6 µM for D10, 2.5 µM for D10$^{GS\text{-}E206K/N208A\text{-}FKBP12}$-1 and 1.9 µM for 3D7. Results are presented as mean ± S.D.

It was further investigated if an extended exposure to Shld1 during which the parasites undergo their intra-erythrocytic developmental cycle repeatedly affects parasite growth. Over a seven day period tightly synchronized D10$^{GS\text{-}E206K/N208A\text{-}FKBP12}$-1 parasites were cultured in the absence and in the presence of 0.25 µM Shld1 (Figure 4-12). This concentration was chosen because it was the highest non-toxic concentration (Figure 4-11) which leads to stabilization of the fusion protein according to western analyses (Figure 4-10A). It was presumed that maximal stabilization of PfGS$^{E206K/N208A}$-FKBP12 was achieved whilst minimising unspecific toxicity of Shld1. Parasites were diluted to an initial parasitemia of 0.5 % and their growth was monitored by counting Giemsa stained thin smears. Every second day cultures were diluted 1:5. No difference was found between the different treatments. D10$^{GS\text{-}E206K/N208A\text{-}FKBP12}$-1 grew at the same rate in the presence and absence of 0.25 µM Shld1. The overall growth rate

was however rather low, regardless of the presence of Shld1, with the parasites struggling to reach a parasitemia higher than 2 % and the experiment was terminated after seven days. This shows that the stabilization and presence of the mutant PfGS$^{E206K/N208A}$ protein in the parasites did not affect their growth. However, it suggests that the presence of the plasmid itself negatively affects parasite growth regardless of stabilization of PfGS$^{E206K/N208A}$-FKBP12.

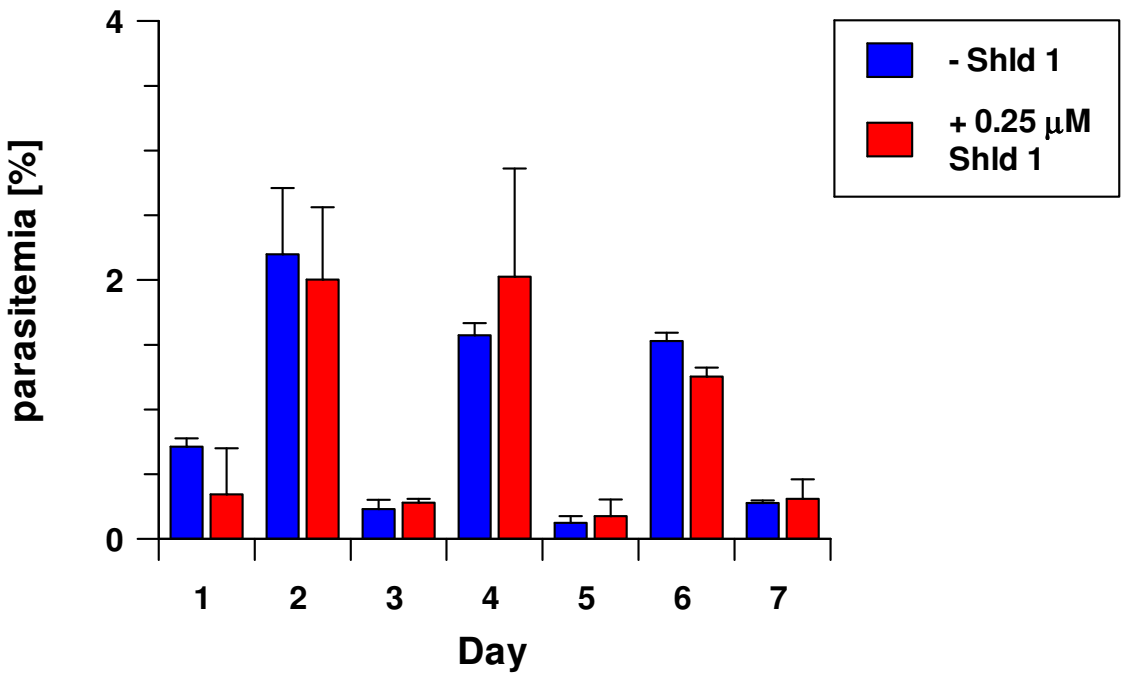

Figure 4-12: Growth rate of D10$^{GS-E206K/N208A-FKBP12}$-1 in presence and absence of Shld1.
The growth of D10$^{GS-E206K/N208A-FKBP12}$-1 in the absence (-Shld1, blue bars) and in the presence of 0.25 µM Shld1 (red bars) was monitored over a seven day period. Tightly synchronized ring stage parasites were diluted to 0.5 % parasitemia on day 0 and their growth was monitored from the following day by counting Giemsa stained blood smears. Every second day cultures were diluted 1:5. Results of one experiment performed in duplicate are presented as mean ± S.D.

Overall the phenotypic analyses of parasites expressing PfGS$^{E206K/N208A}$-FKBP12 revealed no phenotype that can be related to the presence of the inactive fusion protein. The level of the stabilized recombinant protein was low in D10$^{GS-E206K/N208A-FKBP12}$-1 and undetectable in D10$^{GS-E206K/N208A-FKBP12}$-2, which may mean that there is not enough of PfGS$^{E206K/N208A}$-FKBP12 present to dilute the active form of PfGS. The unspecific toxicity that was observed for Shld1 makes further studies with this system difficult, as a phenotype that might be observed in the presence of this compound is potentially related to its toxicity and not the stabilization of PfGS$^{E206K/N208A}$-FKBP12 in the parasites.

4.4.4 Genotypic analyses of transfected parasite lines

Genotypic analyses of D10$^{GS\text{-}E206K/N208A\text{-}FKBP12}$-1 and D10$^{GS\text{-}E206K/N208A\text{-}FKBP12}$-2 were performed in order to determine if recombination of the expression plasmid is the reason for poor expression of the PfGS$^{E206K/N208A}$-FKBP12 protein in *P. falciparum*. Even though the plasmid pCHD-HSP86-GS$^{E206K/N208A}$-FKBP12 is not designed for recombination with the *pfgs* wild-type gene, recombination between the two is possible due to the homologous *pfgs* sequence. Recombination between the expression construct and the endogenous gene locus can explain the low expression of the recombinant PfGS$^{E206K/N208A}$-FKBP12 protein in *P. falciparum*. To determine the genotype of the transfected parasite lines, gDNA was isolated and analysed by Southern blotting after a diagnostic restriction digestion with *Pac*I and *Bam*HI (Figure 4-13).

The expected Southern blot pattern when using a *pfgs* specific probe is depicted in Figure 4-13A. The expected size of the fragment corresponding to the wild-type *pfgs* locus is 4.84 kb (Figure 4-13A, I). For the expression plasmid a band of 9.67 kb is expected (Figure 4-13A, II). Should recombination occur, two bands of 6.77 kb and 7.76 kb are expected (Figure 4-13A, III). Such a recombination event leads to a pseudo-diploid locus with two copies of the gene, one under control of the endogenous promotor and possessing the FKBP12-tag and the other under control of the Hsp86 promotor. It not possible to predict which copy would contain the mutation. If a single cross-over occurred towards the 5'-end of *pfgs*, the first copy of the gene under control of the endogenous promotor and possessing the FKBP12-tag would also contain the mutation. However, if a single cross-over occurred between sequences downstream of the mutated site, the second copy under control of the Hsp86-promotor would contain the mutation. In order to determine the position of the mutation after a homologous recombination event, the recombined locus needs to be sequenced.

Southern blot analysis revealed that both transfected parasite lines D10$^{GS\text{-}E206K/N208A\text{-}FKBP12}$-1 and D10$^{GS\text{-}E206K/N208A\text{-}FKBP12}$-2 contained the plasmid, as indicated by a diagnostic band at 9.67 kb (Figure 4-13B, lanes 2 and 3, respectively). There appears to be less plasmid present in D10$^{GS\text{-}E206K/N208A\text{-}FKBP12}$-2, which potentially is the reason why no recombinant protein can be detected in this parasite line.

However, both parasite lines also showed an additional band not corresponding to the expected pattern. The additional bands differed in size between the two parasite lines, being approximately at 7.0 kb for D10$^{GS\text{-}E206K/N208A\text{-}FKBP12}$-1 (Figure 4-13B, lane 2) and 7.5 kb for D10$^{GS\text{-}E206K/N208A\text{-}FKBP12}$-2 (Figure 4-13B, lane 3). Single cross over recombination between the wild-type *pfgs* locus and the transfected plasmid should result in the appearance of two diagnostic bands at 6.77 kb and 7.76 kb in a Southern blot. The additional band seen in D10$^{GS\text{-}E206K/N208A\text{-}FKBP12}$-1 (Figure 4-13B, lane 2) may correspond to the smaller one of the two, while the additional band in D10$^{GS\text{-}E206K/N208A\text{-}FKBP12}$-2 (Figure 4-13B, lane 3) potentially corresponds to the 7.76 kb band. However, if the plasmid recombined with the endogenous *pfgs* locus both bands should be detectable. It is possible that integration into a random gene locus of the genome has occurred leading to the single additional band in each line. The wild-type diagnostic band can be detected in both parasite lines, though it appears less pronounced in D10$^{GS\text{-}E206K/N208A\text{-}FKBP12}$-1, further indicating a recombination event in which the wild-type gene is lost or altered. As the parasite lines represent a non-clonal population it cannot be concluded with certainty that the additional bands detected are corresponding to recombination of the plasmid with the endogenous gene locus. In the case of an integration event into the *pfgs* locus it would be possible to isolate clones without the wild-type gene that only possess a recombined gene. The cloning of the D10$^{GS\text{-}E206K/N208A\text{-}FKBP12}$-1 and D10$^{GS\text{-}E206K/N208A\text{-}FKBP12}$-2 lines in order to further analyse their genotype will be part of future work. The results of the genotypic analyses do possibly provide an explanation for the observed low levels of expression for the recombinant PfGS$^{E206K/N208A}$-FKBP12 protein as expression levels of PfGS$^{E206K/N208A}$-FKBP12 may be affected through a recombination of the expression plasmids.

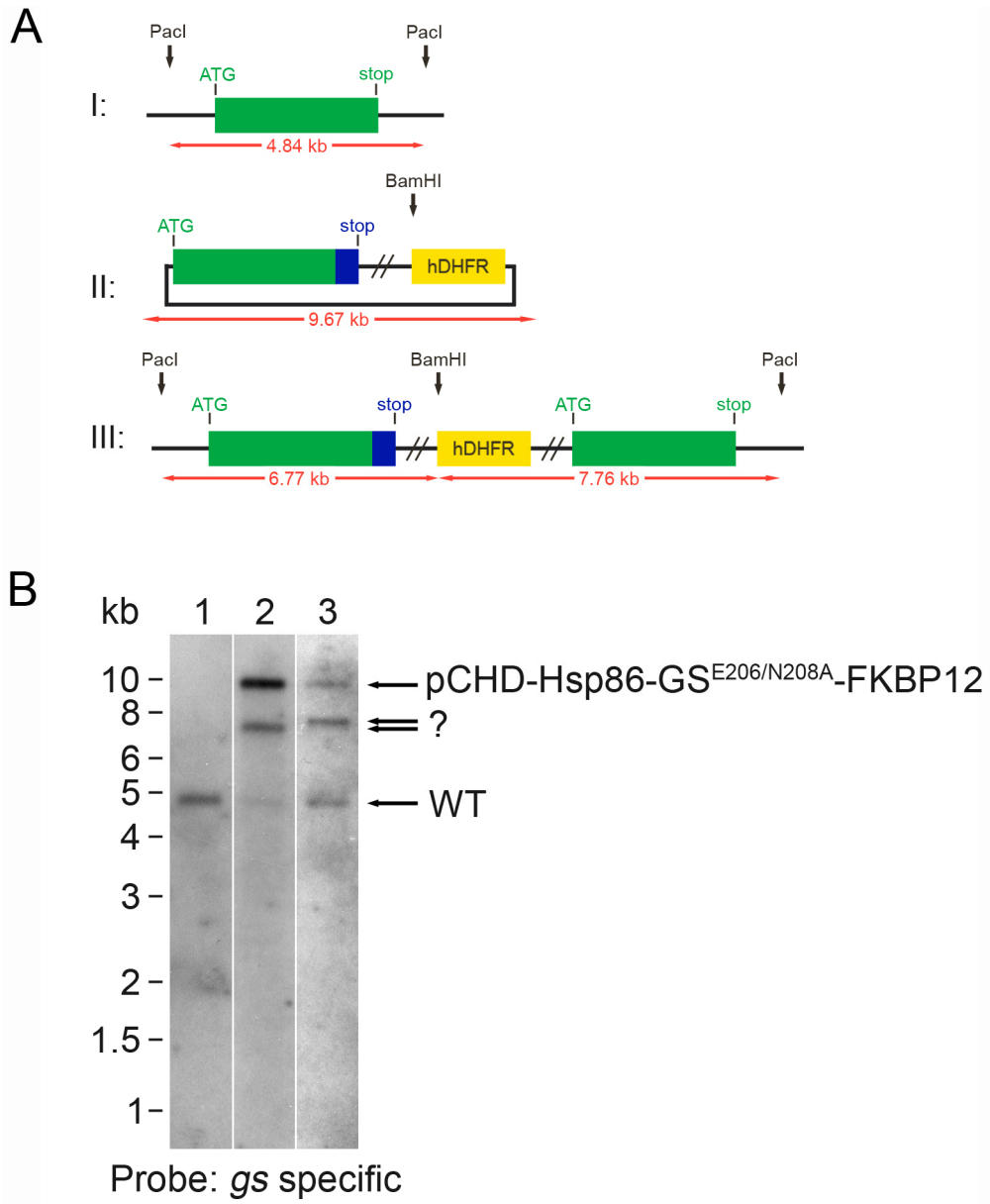

Figure 4-13: Genotypic analyses of PfGS$^{E206K/N208A}$-FKBP12 expressing parasite lines D10$^{GS-E206K/N208A-FKBP12}$-1 and D10$^{GS-E206K/N208A-FKBP12}$-2.

Panel A displays a schematic diagram (not to scale) of the *pfgs* wild-type gene locus (I), the expression construct pCHD-Hsp86-GS$^{E206K/N208A}$-FKBP12 (II) and the recombined locus (III) should single cross-over recombination between the plasmid and the endogenous gene occur. The expression construct contains the full length *pfgs* ORF (green box) in frame with a C-terminal FKBP12 tag (blue box) and a hDHFR cassette as selectable marker (yellow box). Should recombination by single cross over between the wild-type locus and the expression construct occur (III), it would lead to a pseudo- diploid locus containing two copies of the *pfgs* gene, one encoding for a GS-FKBP tagged fusion protein under control of the endogenous promoter and one for the untagged protein under control of the Hsp86 promoter. It cannot be predicted which copy will contain the mutations. Southern analysis was performed using the restriction enzymes *Pac*I and *Bam*HI. Restriction sites are indicated by black arrows. The expected sizes of the resulting fragments are indicated by red arrows. **Panel B** shows the Southern analyses after diagnostic digest with *Pac*I and *Bam*HI of the parasite lines D10$^{GS-E206K/N208A-FKBP12}$-1 (lane 2) and D10$^{GS-E206K/N208A-FKBP12}$-2 (lane 3) in comparison to non- transfected D10 wild-type parasites (lane 1). The expected pattern is depicted in Panel A. In all three lanes the endogenous *pfgs* specific band is present at 4.84 kb (WT). The two transfected lines contain the expression construct visible as a diagnostic band at 9.67 kb (lanes 2 and 3). For the D10$^{GS-E206K/N208A-FKBP12}$-1 line (lane 2) an additional band at approximately 7 kb is visible and for the D10$^{GS-E206K/N208A-FKBP12}$-2 line (lane 3) an additional band at approximately 7.5 kb was detected. The additional bands possibly correspond to either the smaller or larger of the expected integration bands. However, in both parasite lines the second expected integration band is missing.

4.5 Expression of PfGS^{wt}-HA in *P. falciparum*

4.5.1 Genotypic analyses

In order to continuously express recombinant C-terminally HA-tagged wild-type PfGS in erythrocytic stages of *P. falciparum*, the expression construct pCHD-Hsp86-GS-HA was cloned using MultiSite® Gateway technology (van Dooren et al., 2005). The Hsp86 promotor in the plasmid allows for high level expression of PfGS-HA in the parasites throughout the intra-erythrocytic stages. The full length ORF of *pfgs* was cloned in frame with the sequence for the C-terminal HA-tag. Wild-type D10 parasites were transfected once with pCHD-Hsp86-GS-HA and transfected parasites were selected with WR99210. Resistant parasites were observed in the culture 5 weeks after transfection and the parasite line was named D10^{GS-HA}. To analyse the genotype of the transfected parasites, gDNA was extracted and analysed by Southern blotting after diagnostic digest with *Pac*I and *Bam*HI.

The diagram in Figure 4-14A describes the expected banding pattern following *Pac*I and *Bam*HI digest if a *pfgs* gene specific probe is used. A single fragment of 4.84 kb is expected for the endogenous *pfgs* locus. Likewise, a single band is expected for the plasmid at 9.40 kb. The plasmid is not intended for integration studies, but single crossover recombination between the homologous *pfgs* sequence of plasmid and endogenous locus is possible. In the case of such a recombination event, two fragments of 6.50 kb and 7.76 kb are expected for the recombined locus. To analyse the transfected parasites, the same probe that was also used for analysis of the knock-in control parasite line described in section 4.3.3 was used.

Figure 4-14B displays a Southern blot of D10^{GS-HA} (lane 2) in comparison to wild-type D10 parasites (lane 1). The 4.84 kb band corresponding to the endogenous *pfgs* gene locus is visible in both lanes. In the transfected parasites (Figure 4-14B, lane 2) a second 9.40 kb fragment corresponding to the expression construct pCHD-Hsp86-GS-HA can be detected. In addition to the wild-type locus and the plasmid the presence of a third band at approximately 7.0 kb was observed in the D10^{GS-HA} line (Figure 4-14B, lane 2). This additional band does not correspond to the expected pattern for a recombination event between the

plasmid and the endogenous gene locus. For this case, two bands at 6.50 kb and 7.76 kb are expected. Potentially some unspecific recombination of the plasmid has occurred, leading to the detection of this single band. This will have to be analysed in greater detail in the future.

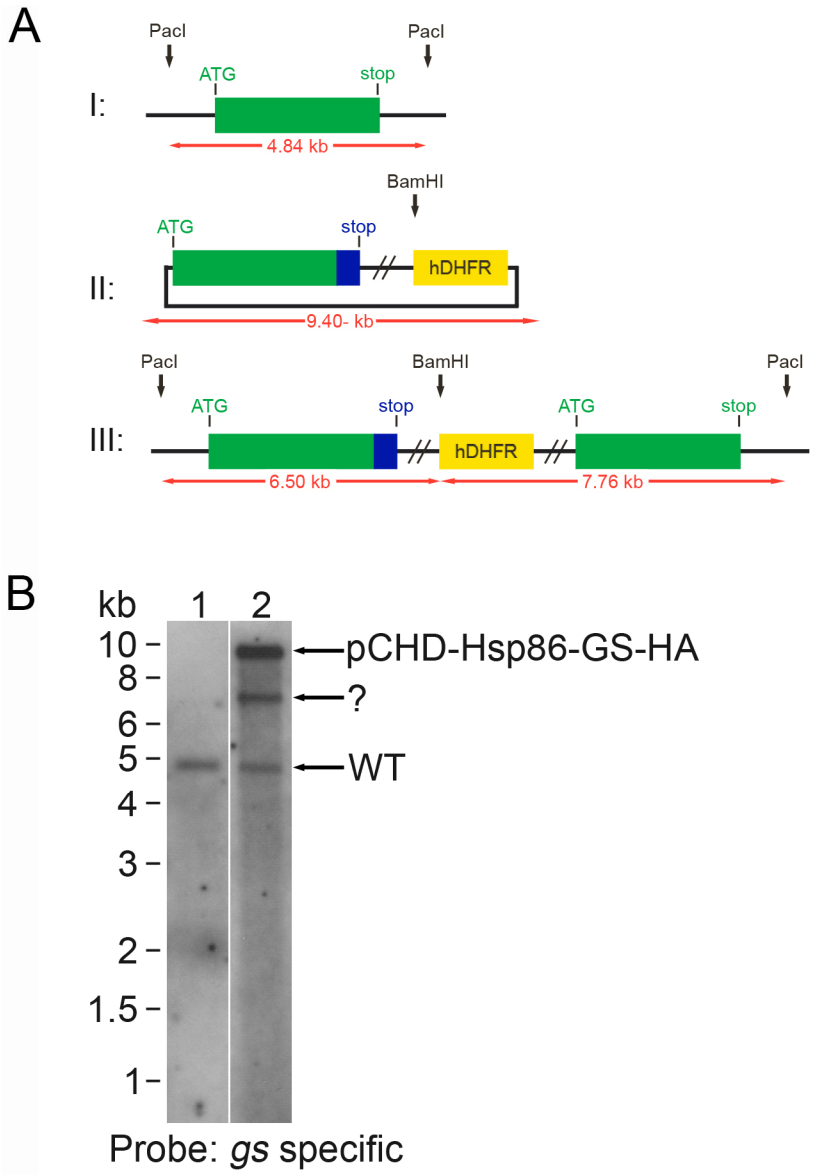

Figure 4-14: Genotypic analysis of D10$^{GS\text{-}HA}$.
Panel A: Schematic diagram (not to scale) of the *pfgs* wild-type locus (I), the expression plasmid pCHD-Hsp86-GS-HA (II) and the gene locus in case of a single crossover recombination event between the plasmid and the endogenous gene (III). Following diagnostic digest with *Pac*I and *Bam*HI, a 4.84 kb fragment is expected for the endogenous *pfgs* locus and a 9.40 kb fragment for the plasmid. A single crossover event between plasmid and wild-type gene leads to two fragments of 6.50 kb and 7.76 kb. Black arrows indicate restriction sites for BamHI and PacI. Red arrows indicate the sizes of the expected fragments which can be detected with a *pfgs*-gene specific probe. **Panel B:** Southern blot analyses of wild-type D10 (lane 1) and D10$^{GS\text{-}HA}$ (lane 2) gDNA after diagnostic digest with *Pac*I and *Bam*HI. The red arrows in Panel A indicate the expected fragments. A 4.84 kb band visible in both lanes corresponds to the endogenous *pfgs* locus (WT). In lane 2 a 9.40 kb band indicates the presence of the expression plasmid pCHD-Hsp86-GS-HA. An additional band is present in this lane at approximately 7 kb that may correspond to one of the two expected bands diagnostic for integration of the plasmid into the gene locus. However, the second expected band is not visible.

4.5.2 Phenotypic analyses

The phenotypic analyses of D10^{GS-HA} were performed by M. L. Laine under my supervision. In order to determine whether the PfGS-HA fusion protein is expressed and present in D10^{GS-HA}, protein was extracted from the parasites and 5 µg were analysed by western blotting with an anti-HA antibody (Figure 4-15). A signal detected in the extract at the predicted size of PfGS-HA at 82.9 kDa shows the recombinant protein is expressed in the parasites. Three smaller bands indicate some degradation of the recombinant protein.

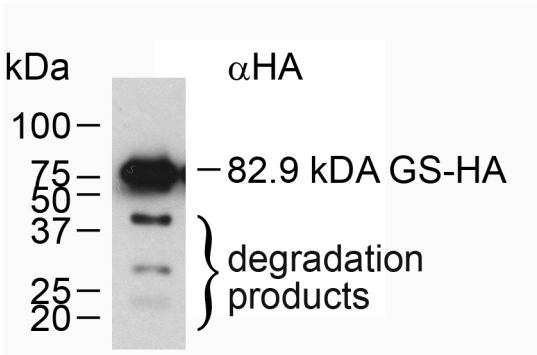

Figure 4-15: Western analysis of D10^{GS-HA}.
Protein extract of D10^{GS-HA} was analysed with an anti-HA antibody. 5 µg of extracted protein were loaded on a 10% SDS-PAGE gel. This Western blot was performed by M. L. Laine.

After it was shown that D10^{GS-HA} parasites are expressing the recombinant protein, it was analysed whether the presence of PfGS-HA influences the susceptibility of the parasites to the GSH depleting inhibitor of γGCS, L-BSO. The IC_{50} value for the drug was determined in the absence and in the presence of 5 mM NAC, because it is possible that the availability of cysteine is limiting the GSH biosynthesis rate. Therefore, parasites over-expressing PfGS-HA may not have altered GSH levels due to a lack of available γGC substrate. NAC increases γGC and thus GSH biosynthesis by providing cysteine.

In Figure 4-16A, the effect of L-BSO on the survival of D10 and D10^{GS-HA} is displayed. In the absence of NAC, D10^{GS-HA} is more susceptible to L-BSO than wild-type D10 parasites. The IC_{50} value for the PfGS-HA expressing parasite line was determined at 48.1 ±2.2 µM, whereas the wild-type parasites had an IC_{50} of 63.3 ±5.3 µM. Addition of 5 mM NAC only shows a marginal effect on wild-type D10 parasites and the IC_{50} value at 72.1 ±7.2 was similar to the IC_{50} determined in the absence of NAC. In the D10^{GS-HA} line the addition of 5 mM NAC increased the L-BSO IC_{50} by approximately 57 % to 75.6 ±6.8 µM, which is similar to the IC_{50}

of the wild-type. These experiments were only performed once in duplicate. Therefore it cannot be concluded if the observed differences are significant.

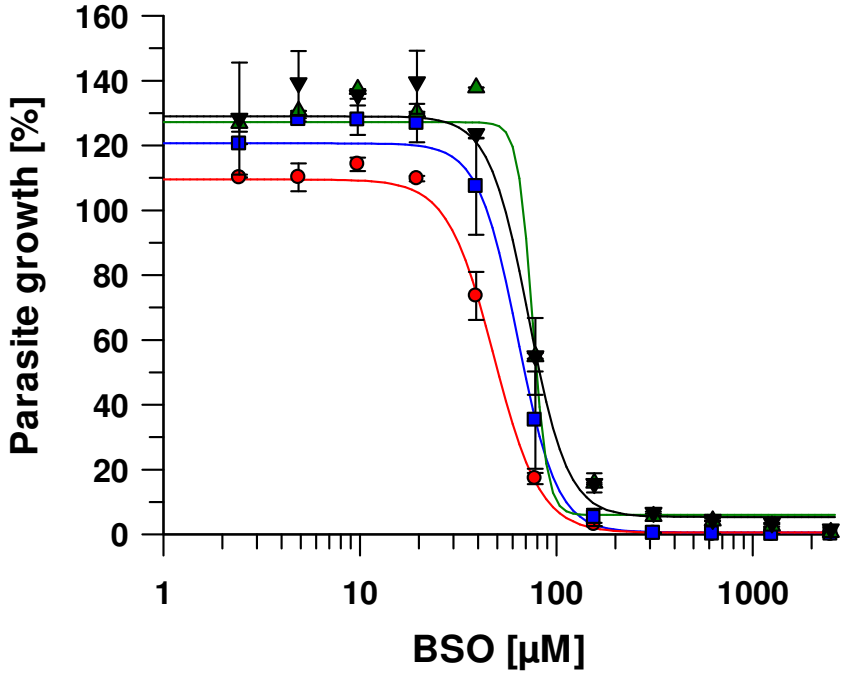

Figure 4-16: Determination of IC_{50} values for L-BSO for D10 and $D10^{GS\text{-}HA}$.
The effect of L-BSO on parasite survival was measured in the presence and absence of 5 mM NAC. In the absence of NAC, the L-BSO IC_{50} for D10 (■) was slightly higher at 63.6±5.3 µM than for $D10^{GS\text{-}HA}$ (●) at 48.1 ±2.2 µM. In presence of 5 mM NAC, the IC_{50} values were similar at 75.6 ±6.8 µM and 72.1±7.2 µM for $D10^{GS\text{-}HA}$ (▲) and D10 (▼), respectively.

4.6 Summary

- Localization studies with episomally expressed PfGS-GFP showed the fusion protein is present in the parasite cytosol of erythrocytic stages of *P. falciparum*.

- A knock out of the *pfgs* gene was not achieved by gene disruption using the plasmid pHH1-Δ*gs*. Targeting the gene locus with a pHH1 control construct was possible, indicating that the *pfgs* gene may be essential for erythrocytic stages *in vitro*.

- Knock-out by gene replacement using the plasmid pCC4-Δ*gs* while supplementing cells with extracellular GSH was also not possible. Negative selection with Ancotil® against parasites maintaining the episomal construct lead to death of the parasites except for one occasion were parasites had lost the plasmid and acquired Bla and Ancotil®

resistance without replacement of the target gene. This further indicates that the gene is essential.

- Alignment of PfGS and human GS revealed four conserved sites that are involved in ATP binding in the human enzyme. A PfGS mutant $PfGS^{E206K/N208A}$ was generated mutating two conserved sites to abolish the activity of the enzyme. Preliminary data show that recombinant $PfGS^{E206K/N208A}$ protein has no detectable activity while recombinantly expressed GS^{wt} is active, indicating that the two residues are of importance for enzyme activity in PfGS.

- In *P. falciparum* episomal expression of inactive $PfGS^{E206K/N208A}$ from the expression construct pCHD-Hsp86-$GS^{E206K/N208A}$-FKBP12 is possible. Expression of the mutant $PfGS^{E296K/N208A}$-FKBP12 fusion protein in *P. falciparum* was confirmed in one transfected parasite line. The fusion protein is fully degraded and undetectable in absence of the stabilizing agent Shld1 and can be detected upon addition of Shld1. Increasing Shld1 concentrations do however not increase the amount of $PfGS^{E296K/N208A}$-FKBP12 in the parasites and unspecific toxicity of the compound was observed at concentrations higher than 0.25 µM. Shld1 equally affects proliferation in the wild-type strains D10 and 3D7 at higher concentrations. No effect on parasite survival and growth rate could be observed upon stabilization of $PfGS^{E296K/N208A}$-FKBP12 with 0.25 µM Shld1. Genotypic analyses showed potential recombination of the construct, possibly explaining the low expression level observed.

- Parasites transfected with an expression construct for C-terminally HA-tagged active wild-type PfGS express the recombinant protein at high levels. The presence of the fusion protein seems to lead to a slight increase in the susceptibility of the parasites to L-BSO compared to wild-type D10 parasites. Addition of 5 mM NAC does not affect the L-BSO IC_{50} in wild-type parasites, but increases the IC_{50} in the PfGS-HA expressing parasites to wild-type level.

5 Glutathione and chloroquine resistance

5.1 Introduction

In this chapter, the potential role of GSH in chloroquine (CQ) resistance is analysed. CQ prevents the detoxification of heme, which is released during the breakdown of host cell hemoglobin in the parasites' digestive vacuoles (DV), leading to an increase of toxic free heme, which is eventually lethal for the parasites (Banyal and Fitch, 1982; Chou et al., 1980; Fitch, 1989; Fitch et al., 1982). In CQ resistant *P. falciparum* parasites, reduced accumulation of CQ within the DV has been linked to mutations in the parasites *chloroquine resistance transporter* (*pfcrt*) gene. Other factors are also likely to contribute to CQ resistance such as other transporters like the P-glycoprotein homologue 1 (Pgh1, encoded by *pfmdr1*) and the multidrug resistance protein-1 (PfMRP1) (Foote et al., 1989; Mu et al., 2003; Reed et al., 2000).

Another mechanism that has been put forward, was that GSH contributes to CQ resistance by competing with the drug for free heme and by destroying heme non-enzymatically (Ginsburg et al., 1998; Ginsburg and Golenser, 2003). Indeed, elevated GSH levels were found in the CQ resistant strain Dd2 in comparison to the sensitive strain 3D7 (Meierjohann et al., 2002b). However, these parasite lines differed widely in their genetic background. Dd2 is not only resistant to CQ, but indeed multi-drug resistant (Gonzales et al., 2008) and it remains unclear, whether the elevated GSH levels are not related to a compensating mechanism that emerged in response to the various mutations in several genes such as *pfcrt* and *pfmdr1* that occurred in order to establish multi-drug resistance. Another difficulty with the hypothesis that GSH can contribute to CQ resistance is that heme is generated in the DV and GSH biosynthesis takes place in the cytosol as shown in chapters 3 and 4 of this study. Ginsburg and colleagues suggested that free heme can escape from the DV and therefore suggests that cytosolic GSH can contribute to protection of the parasites. However, a later study found that more than 90 % of heme remains in the food vacuole (Egan et al., 2002; Ginsburg et al., 1998). These controversial findings make it difficult to fully understand how cytosolic GSH would be able to contribute to CQ resistance.

In this study I investigated the GSH metabolism and the influence of modifications to the GSH metabolism on CQ resistance in three isogenic parasite lines, which only differ in their *pfcrt* allele (Sidhu et al., 2002). These parasite lines were a kind gift of D. Fidock, Albert Einstein College, New York, USA. They were generated by Sidhu *et al*. through allelic exchange of the endogenous *pfcrt* carried by the wild-type line GC03 with alleles of the CQ resistant strains Dd2 and 7G8, thus generating the CQ resistant lines $C3^{Dd2}$ and $C6^{7G8}$ (Sidhu et al., 2002). GC03 is the progeny of a genetic cross between the CQ resistant Dd2 and CQ sensitive HB3 line and carries the sensitive *pfcrt* allele of HB3 (Wellems et al., 1990). As a control for any influence of the insertion of the transfected construct the $C2^{GC03}$ parasite line was generated, which possesses the original sensitive *pfcrt* allele of GC03. Table 5-1 displays the respective haplotypes of PfCRT in these lines. Because these parasite lines share the same genetic background, it is possible to investigate the influence of GSH on CQ resistance without having the complications that arise when comparing field isolates of different genetic backgrounds.

Clone	Name of *pfcrt* allele	CQ sensitivity	Functional PfCRT haplotype								
			Amino acid position								
			72	74	75	76	220	271	326	356	371
GC03	HB3	sensitive	C	M	N	K	A	Q	N	I	R
$C2^{GC03}$	HB3	sensitive	C	M	N	K	A	Q	N	I	R
$C3^{Dd2}$	Dd2	resistant	C	I	E	T	S	E	S	T	I
$C6^{7G8}$	7G8	resistant	S	M	N	T	S	Q	D	L	R

Table 5-1: PfCRT haplotype of recombinant parasite lines used in this study.
The Dd2 haplotype represents commonly found haplotypes of Africa and Asia, while the 7G8 haplotype represents those commonly found in South America. The recombinant parasite lines were a kind gift of D. Fidock. Table adapted from Sidhu *et al.* (Sidhu et al., 2002).

5.2 Influence of extracellular glutathione on chloroquine susceptibility

In order to investigate a potential influence of extracellular GSH on the susceptibility of *P. falciparum* to CQ, IC_{50} values were determined for each parasite line in the absence and presence of 1 mM extracellular GSH (Figure 5-1). The average IC_{50} concentrations determined in normal IC_{50} medium without additional GSH (Figure 5-1, - symbol) were 17.2 ±1.9 nM and 11.3 ±1.9 nM for the sensitive parasite lines GC03 and $C2^{GC03}$, respectively. The resistant lines $C3^{Dd2}$ and $C6^{7G8}$ were 20- and 8.5-fold less sensitive to the drug than GC03 and $C2^{GC03}$ with IC_{50} values of 272.3 ±41.0 nM and 118.4 ±15.1 nM, respectively.

Upon addition of 1 mM GSH to the medium, the IC_{50} for CQ did not change significantly in any of the four parasite lines (Figure 5-1, + symbol). The average IC_{50} values determined for GC03 and $C2^{GC03}$ were 15.0±2.6 nM and 15.4±2.0, respectively. In the CQ resistant parasite lines $C3^{Dd2}$ and $C6^{7G8}$ the average IC_{50} values in the presence of 1 mM extracellular GSH increased marginally and were determined to be 302.3 ±12.0 nM and 146.8 ±10.3 nM, respectively.

For statistical analysis of the effect of extracellular GSH on the CQ IC_{50} of each individual parasite line, unpaired two-tailed student t-tests were performed, comparing the IC_{50} values measured in the absence of GSH to the IC_{50} in the presence of 1 mM GSH. The P values for all four parasite lines were >0.2, showing that there is not significant effect of 1 mM extracellular GSH on the susceptibility of the parasites to CQ in any of the lines investigated.

The results are summarised in Table 5-2. These IC_{50} data indicate that if there is a correlation between increased GSH levels and a decreased susceptibility to CQ, this cannot be influenced by increasing the extracellular GSH concentration in the medium. The reason for this lack of an effect potentially is related to insufficient uptake of GSH.

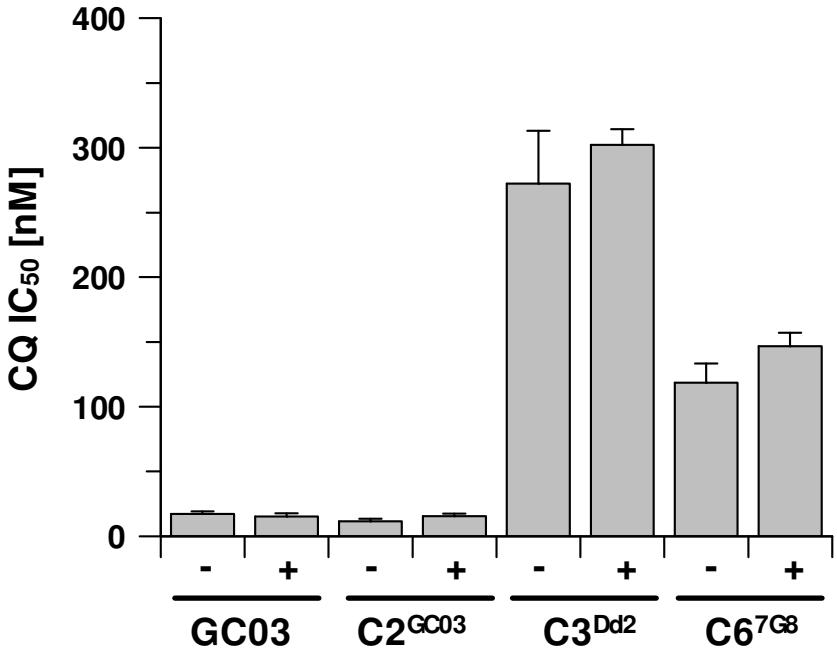

Figure 5-1: Influence of extracellular GSH on CQ IC_{50} of CQ sensitive and resistant parasite lines.
CQ IC_{50} values were determined for four isogenic parasite lines in normal IC_{50} medium (-) and in medium supplemented with 1 mM GSH (+). The parasite lines $C3^{Dd2}$ and $C6^{7G8}$ possessing mutant *pfcrt* alleles are highly resistant to CQ regardless of the presence of extracellular GSH. No significant change was observed after addition of 1 mM GSH for both sensitive and resistant lines. The IC_{50} values were determined in triplicate on 2-6 independent occasions. Results are presented as mean ± standard error of the mean (S.E.M).

Parasite line	CQ IC_{50} [nM]	CQ IC_{50} with 1 mM GSH [nM]	t test comparison of CQ and CQ+GSH IC_{50}
GC03	17.2 ± 1.9 (n=2)	15.0 ± 2.6 (n=3)	P=0.59
$C2^{GC03}$	11.3 ± 1.9 (n=6)	15.4 ± 2.0 (n=3)	P=0.22
$C3^{Dd2}$	272.3 ± 41.0 (n=6)	302.3 ± 12.0 (n=3)	P=0.64
$C6^{7G8}$	118.4 ± 15.1 (n=6)	146.8 ± 10.3 (n=3)	P=0.26

Table 5-2: Average CQ IC_{50} in absence and in presence of 1 mM extracellular GSH.
IC_{50} values were determined in triplicate on several independent occasions. The number of repeats (n) for each parasite line is given in brackets. The IC_{50} values are presented as mean ± S.E.M. For each individual parasite line, the CQ IC_{50} values in the absence and presence of GSH were compared in an unpaired two-tailed student t test.

It is possible that increasing the extracellular GSH concentration beyond 1 mM affects the parasites' susceptibility to CQ. It was however noted that increasing extracellular GSH concentrations further had an adverse effect on parasite growth. The adverse effect of GSH was related to decreased buffer capacity of the medium and rapid acidification of the medium which is not supportive of parasite growth.

5.3 Glutathione levels and susceptibility to glutathione depleting agents

Using a spectrophotometric assay, the total GSH levels in the three isogenic parasite lines $C2^{GC03}$, $C3^{Dd2}$ and $C6^{7G8}$ and the wild-type parasite line GC03 were determined. Initially GSH levels were measured after enriching the cultures to ~90-95 % parasitemia with Miltenyi Biotec MACS® columns. However, it was noticed that this method altered GSH levels negatively. Because blood cell suspension and buffers enter the columns by gravity flow when using this method, it is very difficult to standardize the experimental setup. It was noticeable that longer binding of the parasites to the columns led to a decrease in the measured GSH levels (Figure 5-2). Therefore the method of sample preparation was changed and tightly synchronized parasite cultures containing young trophozoite stages (approximately 28-32 hours after invasion) were used instead without purification of infected red blood cells prior to saponin lysis. It was presumed that the modified method minimized the stress the parasites were subjected to. In Figure 5-2 data obtained by the two different methods of sample preparation are compared. GSH levels determined in the parasite lines $C2^{GC03}$ and $C6^{7G8}$ without initial enriching of infected red blood cells are 2.5- to 3.5-fold higher than the levels determined after MACS purification. Therefore, GSH levels were measured for all four parasite lines without initial purification of infected RBC.

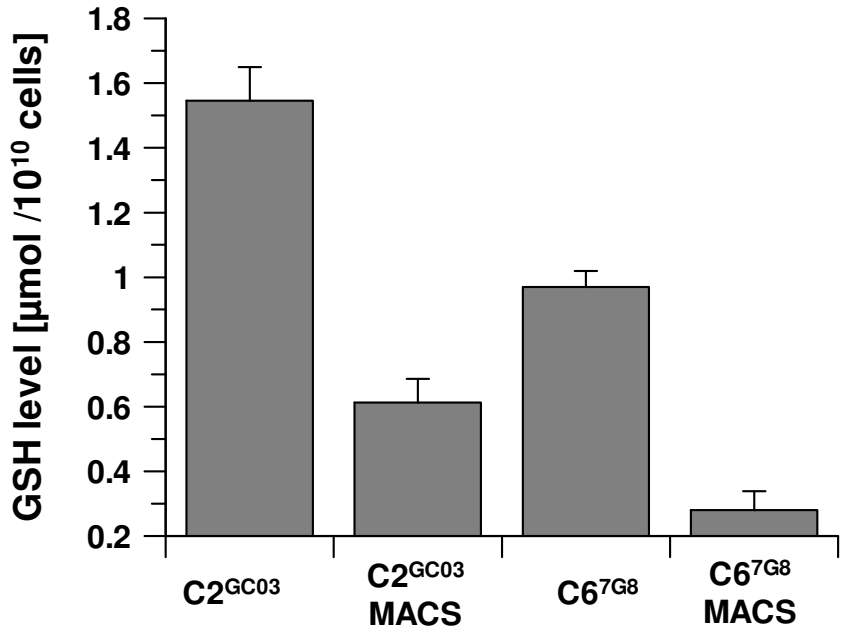

Figure 5-2: Influence of sample preparation on parasite GSH levels.
Two different methods were used to generate samples or the spectrophotometric determination of total GSH in isolated parasites. In one method, tightly synchronized, trophozoite infected red blood cells were used directly for saponin lysis ($C2^{GC03}$ and $C6^{7G8}$). In the second method, trophozoite infected RBCs were enriched with MACS columns prior to saponin lysis ($C2^{GC03}$ MACS and $C6^{7G8}$ MACS). Results are presented as mean ±S.E.M. of 3-5 independent determinations.

GSH levels determined for the three isogenic parasite lines $C2^{GC03}$, $C3^{Dd2}$ and $C6^{7G8}$ and for the wild-type GC03 line differed between the lines (Figure 5-3). The differences between $C2^{GC03}$ and $C6^{7G8}$ were detected regardless which method was used (Figure 5-2). Comparing all four isogenic parasite lines, GSH levels were determined to be 0.71 ±0.20 µmol/ 10^{10} cells and 0.93 ±0.05 µmol/ 10^{10} cells for the CQ resistant lines $C3^{Dd2}$ and $C6^{7G8}$, respectively, and 1.55 ±0.10 µmol/ 10^{10} cells and 1.27 ±0.07 µmol/ 10^{10} cells for the CQ sensitive lines $C2^{GC03}$ and GC03, respectively (Figure 5-3).

One way ANOVA showed that these differences are significant ($F_{3,8}$= 8.50, P< 0.01). Post hoc Newman-Keuls analysis shows that there is no significant difference between the two sensitive lines GC03 and $C2^{GC03}$. Equally, there was no significant difference between $C3^{Dd2}$ and $C6^{7G8}$. However, both resistant lines are significantly different to $C2^{GC03}$ (P <0.01 and <0.05) and $C3^{Dd2}$ contained significantly less GSH than GC03 (P <0.05).

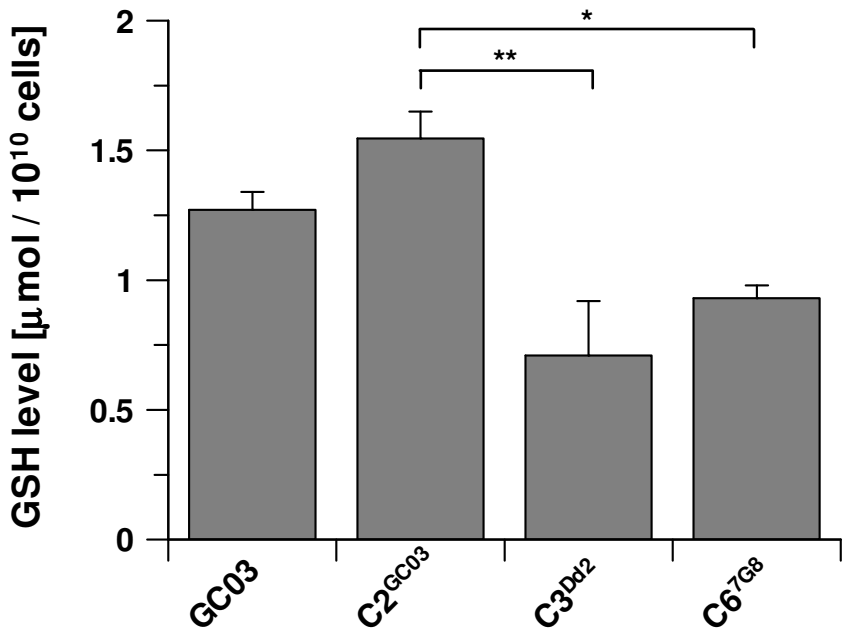

Figure 5-3: GSH levels in isogenic *P. falciparum* lines.
Total GSH levels were determined using tightly synchronized trophozoite stages after saponin lysis to remove RBC contaminations. The GSH levels of the CQ resistant strains $C3^{Dd2}$ (0.71±0.2 µmol/ 10^{10} cells) and $C6^{7G8}$ (0.93±0.05 µmol/ 10^{10} cells) are significantly lower than those determined for the CQ sensitive line $C2^{GC03}$ (1.55±0.10 µmol/ 10^{10} cells) (*: P<0.05; **: P<0.01). The GSH level determined for GC03 was 1.27±0.07 µmol/ 10^{10} cells. Results are presented as average of three independent measurements ± S.E.M.

To elucidate whether the four parasite lines are differently affected by the specific γGCS inhibitor L-buthionine sulfoximine (L-BSO), the IC_{50} concentrations for this compound were determined. In order to further analyse whether *P. falciparum* can utilize extracellular GSH added to the culture medium, the IC_{50} concentrations for L-BSO in the presence and the absence of 1 mM GSH in the medium were determined (Figure 5-4).

In the absence of additional extracellular GSH, the L-BSO IC_{50} values for the CQ resistant strains are lower than those for the sensitive lines (59.1 ±4.1 µM and 66.6 ±7.4 µM for GC03 and $C2^{GC03}$ and 33.0 ±3.5 µM and 36.5 ±7.7 µM for $C3^{Dd2}$ and $C6^{7G8}$, respectively), (see Figure 5-4). This result corresponds to the observed lower GSH levels in the resistant lines and is consistent with differences in the GSH levels between the four isogenic parasite lines.

A one way ANOVA test shows that these differences are significant ($F_{3,11}$= 6.76, P <0.01) and a Newman-Keuls post hoc analysis showed that $C3^{Dd2}$ and $C6^{7G8}$ were significantly different to both $C2^{GC03}$ and GC03 (P <0.05). No significant differences were found between GC03 and $C2^{GC03}$ or between $C3^{Dd2}$ and $C6^{7G8}$.

Upon addition of 1 mM GSH to the medium, the effect of L-BSO is alleviated in all four parasite lines. In the CQ sensitive lines GC03 and $C2^{GC03}$ the addition of 1 mM GSH led to an increase of the IC_{50} value for L-BSO by 20-50 % to 89.1 ±9.9 µM and 80.1 ±12.6 µM, respectively. In the CQ resistant cell lines the IC_{50} values increased by 70- 120 % to 73.2 ±0.8 µM and 64.3 ±8.7 µM for $C3^{Dd2}$ and $C6^{7G8}$, respectively. Thus, the L-BSO IC_{50} values for all four parasite lines analysed were in a similar range upon addition of 1 mM GSH. The IC_{50} values for BSO are summarized in Table 5-3.

One way ANOVA analysis followed by Newman-Keuls post-test showed that no significant differences exist between the four parasite lines for their susceptibility to BSO if 1 mM GSH is added to the medium. However, the only significant increase for the L-BSO IC_{50} in the presence of 1 mM GSH was found for the parasite line $C3^{Dd2}$ ($P < 0.05$).

This suggests that extracellular GSH is taken up into infected red blood cells albeit not with high enough efficiency to fully compensate for the effects of L-BSO. Whether this effect is attributable to uptake of GSH into the host erythrocyte or the parasite is not clear from these experiments.

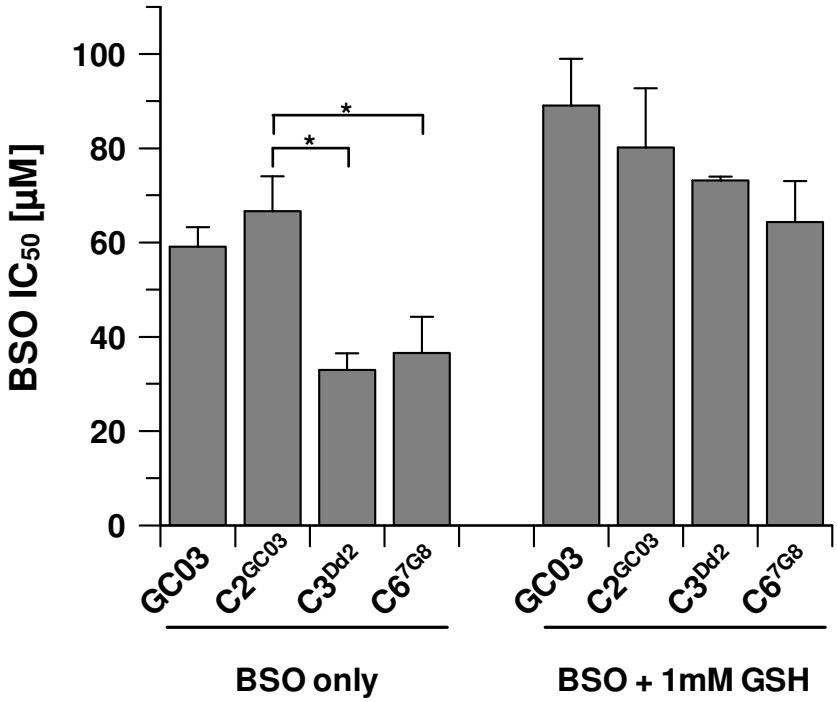

Figure 5-4: L-BSO IC_{50} of isogenic CQ resistant and CQ sensitive parasite lines.
IC_{50} values for L-BSO were determined in triplicate on at least three independent occasions in absence and in the presence of 1 mM GSH. Without addition of GSH, the CQ resistant parasite lines $C3^{Dd2}$ and $C6^{7G8}$ are significantly more susceptible to L-BSO than the CQ sensitive lines GC03 and $C2^{GC03}$ (*: $P<0.05$). In the presence of 1 mM GSH, the effect of L-BSO is alleviated in all

four lines and there is no significant difference between the parasite lines. Results are presented as mean ±S.E.M. The respective IC_{50} values are summarized in Table 5-3.

The effect of another GSH depleting agent, 1-chloro-2,4-dinitrobenzene (CDNB), was tested on the four parasite lines in absence and presence of 1 mM GSH (Figure 5-5). CDNB is a substrate for the enzyme glutathione-S-transferase (GST) and a less specific way to deplete GSH. The IC_{50} values for CDNB in the absence of GSH are in the low µM range between 9.5 µM and 13 µM for all four parasite lines (see Table 5-3) and one way ANOVA analysis showed that differences between the lines under these conditions are not significant ($F_{3,10}$= 0.22, P=0.88).

With addition of 1 mM GSH to the culture medium, the IC_{50} values increased 5 to 10 fold, suggesting again that GSH enters infected red blood cells. The effect of 1 mM GSH was most pronounced in the $C2^{GC03}$ parasite line.

One way ANOVA analysis indicated significant differences with $F_{7,11}$= 9.51 and P<0.001. Newman-Keuls post hoc analyses showed that the increase of the CDNB IC_{50} in presence of 1 mM GSH is significant in all four parasite lines (P<0.05 for GC03, $C3^{Dd2}$ and $C6^{7G8}$ and <0.01 for $C2^{GC03}$). Comparison between the parasite lines indicate that in presence of 1 mM GSH the IC_{50} values of the lines $C2^{GC03}$ and $C3^{Dd2}$ are significantly different (P <0.01). However, no significant differences exist between $C2^{GC03}$ and the other two parasite lines GC03 and $C6^{7G8}$ and there are equally no significant differences between $C3^{Dd2}$ and GC03 and $C6^{7G8}$.

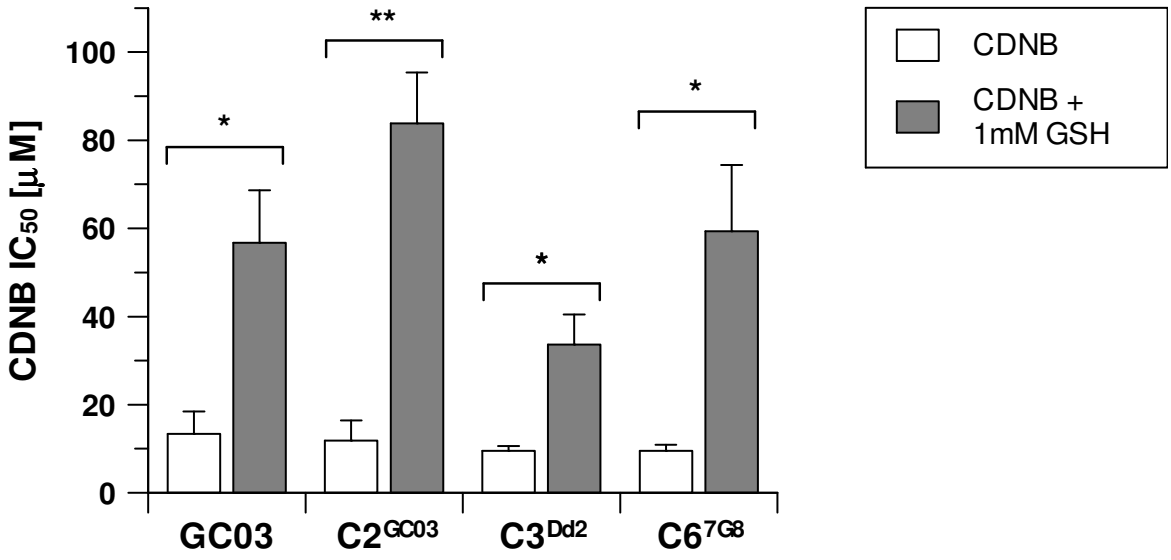

Figure 5-5: CDNB IC_{50} in the absence and presence of 1 mM GSH.
CNDB IC_{50} values were determined in triplicate on at least three independent occasions. There was no significant difference between the four parasite lines in the absence of GSH. IC_{50}s were significantly higher in the presence of 1 mM GSH (*: $P<0.05$; **: $P<0.01$). Results are presented as mean ±S.E.M.

The influence of higher extracellular GSH concentrations was tested once with 10 mM GSH, but this concentration was found to be detrimental to parasite survival in absence of any drug. It was noted that the pH of the medium was greatly acidified by addition of GSH and had to be very carefully re-adjusted to pH 7.4. Most likely GSH affects the buffer capacity of the medium and thus leads to a rapid acidification if used in the cultures. This is potentially the reason for the observed negative growth effect of GSH at higher concentrations. In order to support the addition of high GSH concentrations, the medium composition needs to be changed and optimized, which was beyond the scope of this study.

Parasite line	BSO IC_{50}	BSO IC_{50} with 1mM GSH	CDNB IC_{50}	CDNB IC_{50} with 1mM GSH
GC03	59.1±4.1 (n=4)	89.1±9.9 (n=3)	13.4±5.1 (n=4)	56.7±11.9 * (n=4)
$C2^{GC03}$	66.6±7.4 (n=4)	80.1±12.6 (n=3)	11.8±4.6 (n=4)	83.8±11.5 ** (n=4)
$C3^{Dd2}$	33.0±3.5 (n=3)	73.2±0.8 * (n=3)	9.5±1.1 (n=3)	33.6±6.8 * (n=4)
$C6^{7G8}$	36.5±7.7 (n=4)	64.3±8.7 (n=3)	9.5±1.4 (n=3)	59.3±15.1 * (n=4)

Table 5-3: IC_{50} of GSH depleting agents.
IC_{50} values for L-BSO and CDNB were determined in triplicates on at least three independent occasions. The number of repeats (n) is given in brackets. Asterisks indicate significant increases of IC_{50} values in the presence of 1 mM GSH (*: P<0.05; **: P<0.01). Results are presented as mean ±S.E.M.

5.4 Susceptibility to oxidative stressors

In order to determine if the decreased GSH levels affected the susceptibility of the parasite lines to oxidative stress, the IC_{50} values for two inducers of intracellular oxidative stress, phenazine methyl sulphate (N-methylphenanzonium methyl sulphate) and juglone (5-hydroxy-1,4-naphthoquinone), were determined for GC03, $C2^{GC03}$, $C3^{Dd2}$ and $C6^{7G8}$. The IC_{50} values for both compounds are listed in Table 5-4.

For phenazine methyl sulphate the determined IC_{50}s for GC03 and $C2^{GC03}$ were 0.76 ±0.11 µM and 0.90 ±0.13 µM, respectively (Figure 5-6A). The IC_{50} for $C3^{Dd2}$ was slightly higher at 1.13 ±0.19 µM and the IC_{50} for $C6^{7G8}$ was the lowest at 0.4 ±0.01 µM. The differences were however not significant according to one-way ANOVA analysis ($F_{3,8}$= 3.90, P =0.055).

Equally, no significant difference was found between the IC_{50}s for GC03, $C2^{GC03}$, $C3^{Dd2}$ and $C6^{7G8}$ for juglone (Figure 5-6B). The CQ sensitive lines GC03 and $C2^{GC03}$ had IC_{50} values of 17.1±3.3 µM and 15.7±5.0 µM, respectively. The IC_{50} for $C3^{Dd2}$ was 18.0±2.1 µM. Again, $C6^{7G8}$ was most susceptible to the stressor with an IC_{50} at 10.8±2.1 µM, albeit this is not significantly lower. The results of one way ANOVA analysis were $F_{3,8}$= 1.02, P= 0.44.

These results show that despite containing different GSH levels, the four parasite lines analysed do not differ significantly in their susceptibility to compounds inducing oxidative stress.

Parasite line	Phenazine methyl sulphate [µM]	Juglone IC_{50} [µM]
GC03	0.76±0.11	17.1±3.
$C2^{GC03}$	0.90±0.13	15.7±5.0
$C3^{Dd2}$	1.13±0.19	18.0±2.1
$C6^{7G8}$	0.47±0.10	10.8±2.1

Table 5-4: IC_{50} values for oxidative stress inducing compounds.
The IC_{50} concentrations for phenazine methyl sulphate and juglone were determined in triplicates on three independent occasions. Results are presented as mean ± S.E.M.

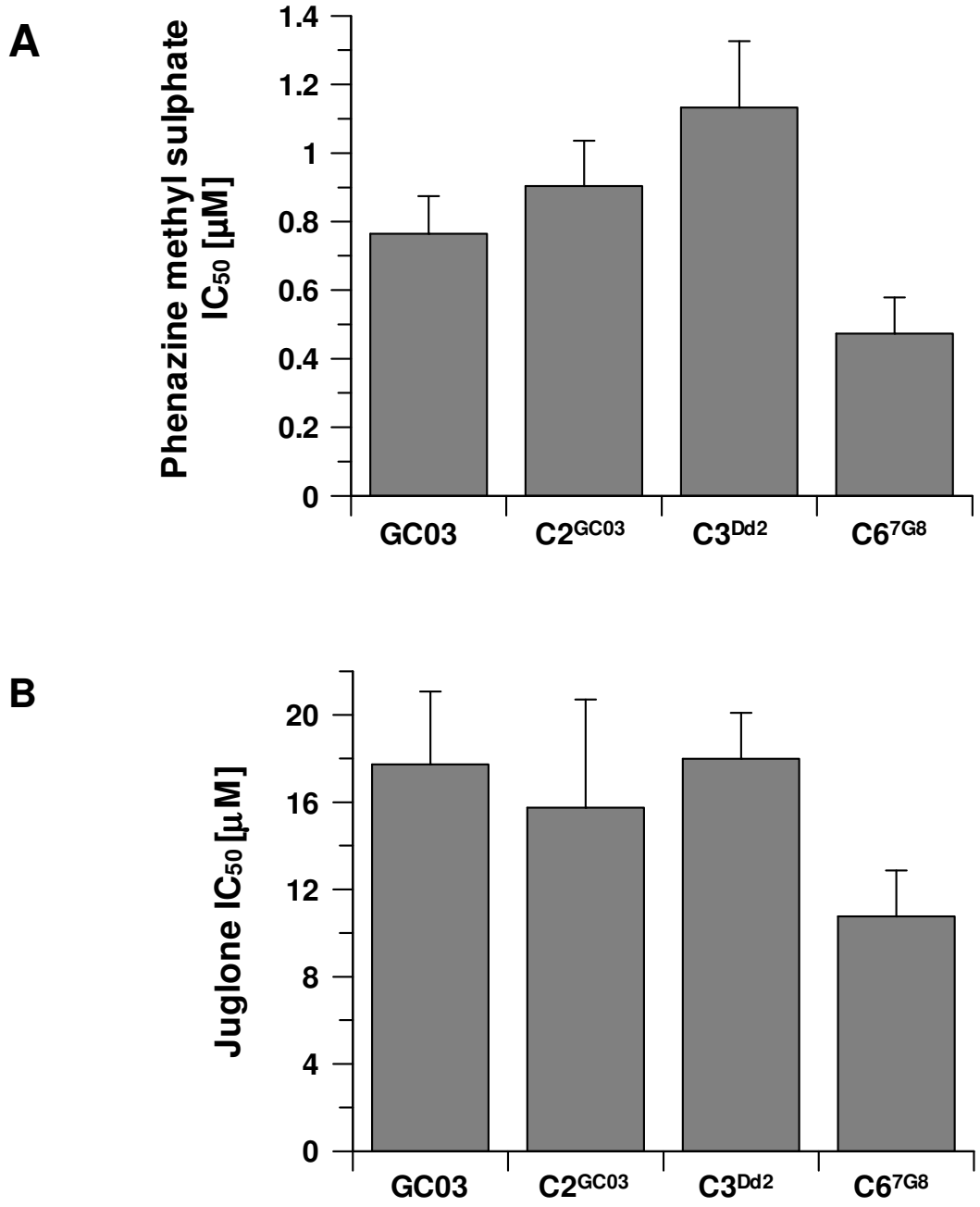

Figure 5-6: IC_{50} values of oxidative stress inducing compounds.
IC_{50} values for phenazine methyl sulphate and juglone were determined in triplicate on three independent occasions. No significant differences were found between the CQ sensitive parasite lines GC03 and $C2^{GC03}$ and the resistant lines $C3^{Dd2}$ and $C6^{7G8}$ for either drug. Results are presented as mean of three independent determinations ±S.E.M.

5.5 Expression of glutathione producing and consuming enzymes

A possible explanation for the observed differences in GSH levels and susceptibility to L-BSO are differences in the expression levels of the proteins producing or consuming GSH. Therefore the expression levels of the biosynthesis enzymes PfγGCS and PfGS, the GSH reducing enzyme glutathione reductase (PfGR) and the GSH consuming enzyme PfGST were determined. In addition, expression levels of PfCRT were analysed because earlier studies had reported reduced expression of PfCRT in the genetically modified lines (Sidhu et al., 2002).

Because there is currently no antibody available for PfγGCS and PfGS, the expression of these two enzymes could only be determined on mRNA level by quantitative real time PCR. We have not been able to express and purify recombinant PfγGCS in previous attempts in our laboratory and previous attempts to raise an antibody against recombinant expressed PfGS did not yield a specific antibody.

Only slight variations were observed in the mRNA levels for *pfygcs* and *pfgs* between the parasite lines and the differences were not significant (One way ANOVA, $P > 0.05$). This indicates no changes in transcription of the expression of the two genes responsible for GSH biosynthesis. Thus, changes in GSH biosynthesis do not appear to be responsible for the differential GSH levels.

The transcription levels of *pfcrt* were equally analysed by quantitative real-time PCR and appeared to be similar between the four parasite lines.

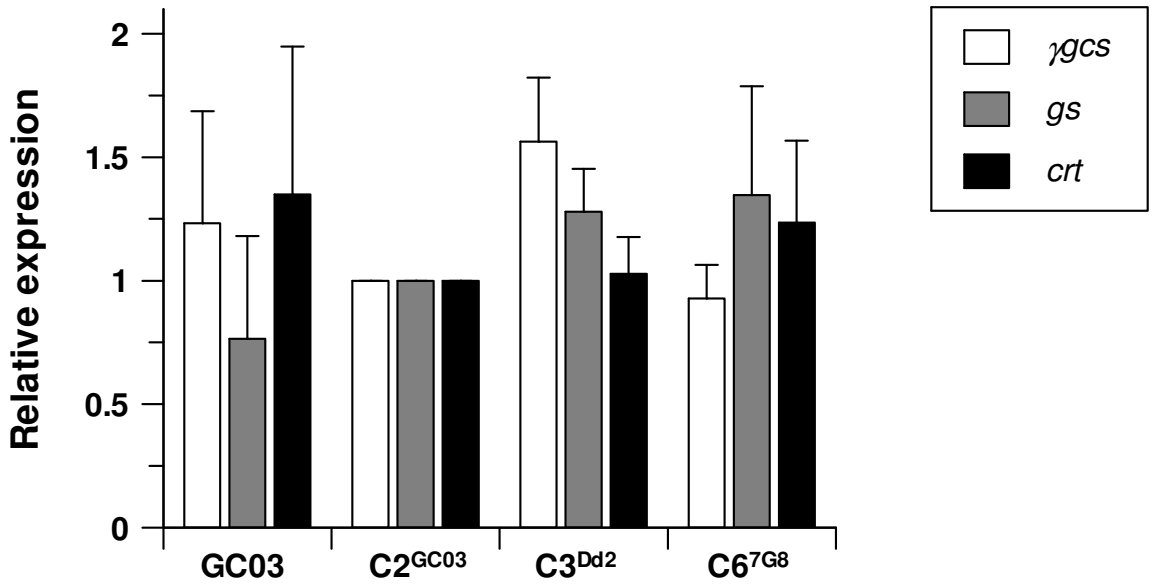

Figure 5-7: Relative expression of *γgcs*, *gs* and *crt*.
The relative expression of *γgcs, gs* and *crt* was determined by quantitative real time PCR relative to $C2^{GC03}$. As a housekeeping gene control, seryl-tRNA-synthetase was used. The results are shown as mean ± S.E.M. of five independent determinations.

The abundances of the GSH reducing enzyme PfGR and of PfGST, the major GSH consuming enzyme, were determined by western blotting using specific antibodies against both enzymes (Figure 5-8). The expression of PfCRT was also determined on protein level. For all three western analyses, equal amounts of protein extracts of tightly synchronized trophozoites were loaded. An antibody against the α-subunit of the *P. falciparum* casein kinase 2 (PfCK2α) was used as loading control. Both PfGR and PfGST appeared to be present in equal amounts in the four investigated parasite lines and did not appear to be either up- or down-regulated. These results indicate that PfGR or PfGST are not the likely cause for the differential GSH levels and their expression does not appear to be changed in response to the observed differences in GSH levels either. However, the western analyses do not allow any conclusions about their activities which may be influenced by the available amount of substrates.

The amounts of PfCRT present are similar in the four parasite lines, in line with the results obtained by the real-time PCR analysis.

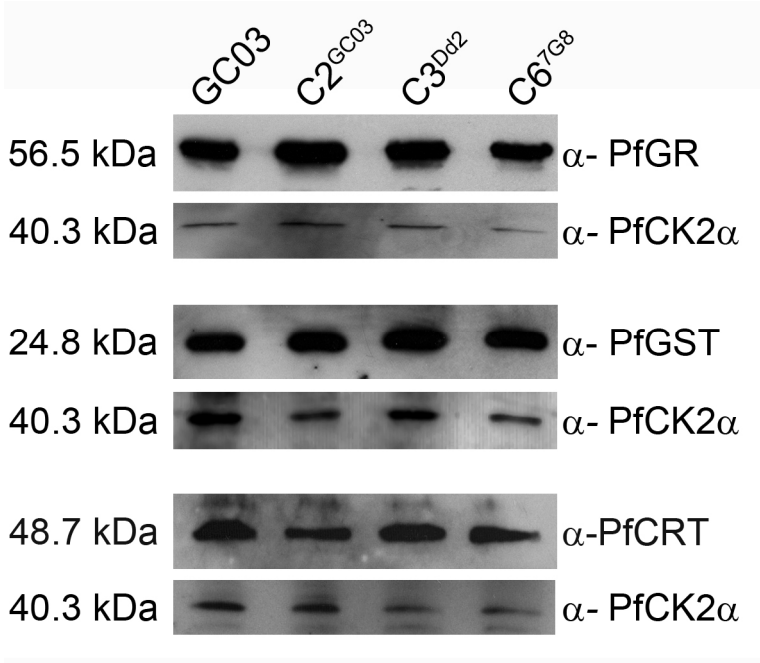

Figure 5-8: Western analysis of the expression levels of PfGR, PfGST and PfCRT.
Western blots were performed on lysates of the two CQ sensitive and two CQ resistant lines. 5 µg of protein were loaded per lane and the blots were probed with anti-PfGR, anti-PfGST or anti-PfCRT antibodies to assess the level of expression of each protein. The blots were then stripped and re-probed with an anti-PfCK2α antibody to control for equal loading.

5.6 Glutathione uptake

None of the previous results give an explanation for the observed differences in GSH levels in the analysed parasite lines. Alterations in the uptake of substrates required for GSH biosynthesis or even in uptake of GSH itself are another potential explanation why GSH levels differ and are lower in parasite lines possessing a mutant form of PfCRT.

To account for differences in GSH uptake, the uptake of GSH into infected RBC was investigated. The uptake of radio-labelled GSH in infected RBC was measured using MACS purified infected red blood cells. Uptake was measured over the course of 20 min and samples were taken at 5 min intervals. Uptake was rather slow and no significant differences were observed between uninfected RBC and trophozoite infected RBC during the first ten minutes. After 15 min, more radioactive GSH was measured in infected RBC than in uninfected RBC. A baseline level of radioactivity was measured for the RBC control, which did not increase over time. Because this baseline activity can already be detected at t=0 at the beginning of the experiment, this is likely to be background due to unspecific binding of the labelled GSH to the cells which was not completely removed by the oil. Uptake was not followed for longer than 20

min because the quality of purified infected RBC rapidly declines after 30 min due to the high parasitemia of >90 %. Parasitized RBC could not be maintained under these conditions for long and lysis of the parasitized cells was indicated by the presence of free hemoglobin in the uptake solution.

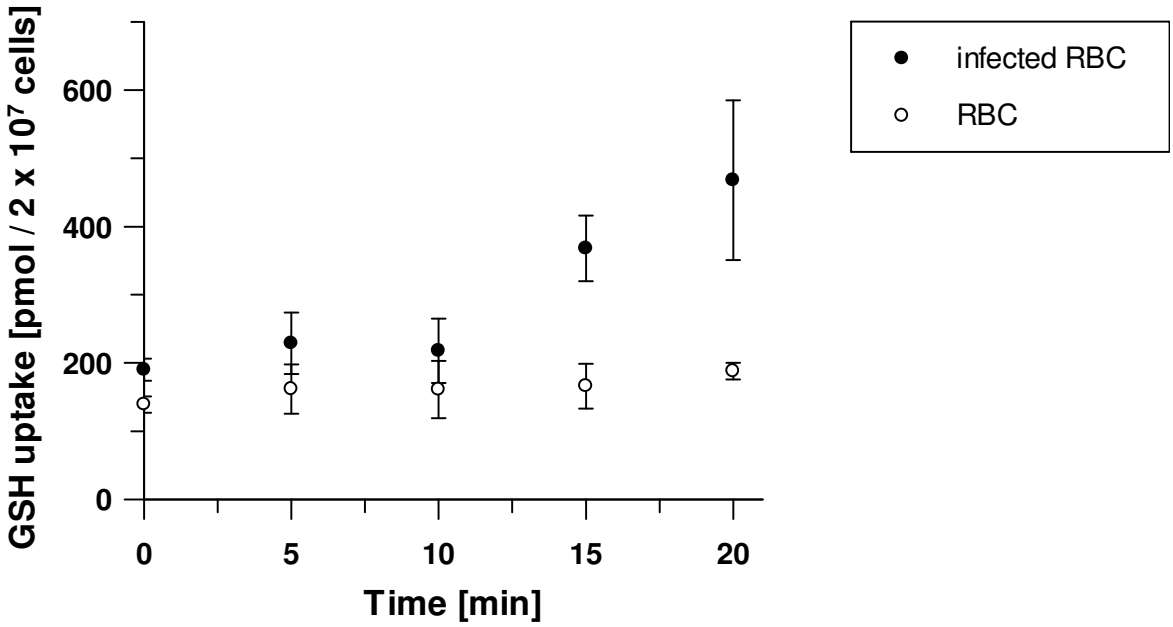

Figure 5-9: Uptake of GSH into trophozoite infected red blood cells.
MACS column enriched $C2^{GC03}$ parasites (90-95 % parasitemia) and uninfected RBC were incubated in EBSS solution containing 3 mM GSH and 1 µCi/ml [^{3}H]-GSH. Aliquots were taken in five minute intervals to determine the cell-associated radioactivity. Results are mean of 3 independent experiments ±S.D.

In order to determine whether GSH uptake is dependent on the extracellular GSH concentration, uptake of [^{3}H]-GSH was measured in the presence of different concentrations of cold GSH in the uptake solution (Figure 5-10). The concentrations tested were 1 mM, 2 mM and 3 mM GSH. Indeed, GSH uptake was proportional to the concentration of total GSH in the uptake solution.

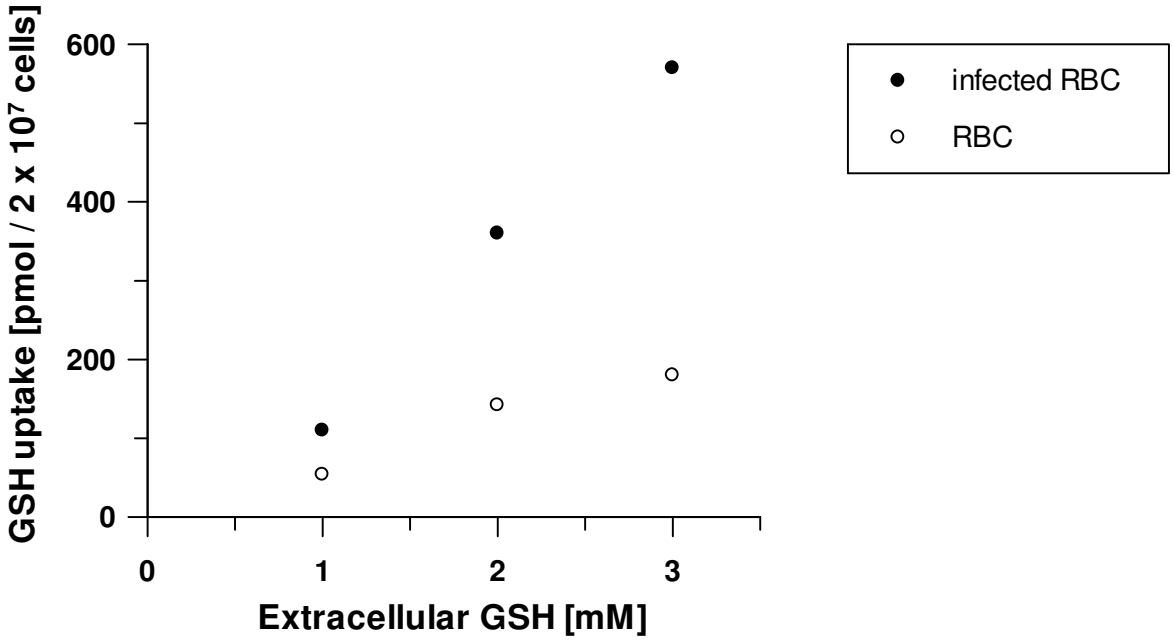

Figure 5-10: GSH uptake in increasing extracellular GSH
GSH uptake into MACS purified $C2^{GC03}$ trophozoite infected RBC in EBSS solution containing 1 mM, 2 mM or 3 mM GSH with 1 µCi/ml [^{3}H]-GSH. Cell-associated radioactivity was measured after uptake for 20 min. This experiment was only performed once.

No difference could be observed in GSH uptake between the CQ sensitive line $C2^{GC03}$ and the CQ resistant line $C6^{7G8}$. Over a 20 min period both parasite lines took up similar amounts of GSH if being incubated in 3 mM GSH and 1 µCi/ml [^{3}H]-GSH. At the start of the experiment (t=0) the amount of radioactivity measured for the infected RBC was similar to the uninfected RBC. After 20 min only a very slight increase was found for the uninfected RBC, but in infected RBC the detected radioactivity showed an increase from 194 ±10 pmol/ $2x10^7$ cells to 339 ±34 pmol/ $2x10^7$ cells for $C2^{GC03}$ and from 165 ±46 pmol/ $2x10^7$ cells to 367 ±19 pmol/ $2x10^7$ cells in $C6^{7G8}$ infected RBC, respectively. There was no apparent difference between the sensitive and the resistant line, indicating the mutations in $PfCRT^{7G8}$ do not alter GSH uptake into infected RBC.

One way ANOVA showed differences were significant ($P<0.0001$, $F_{5,6}=26.63$), and Newman-Keuls *post hoc* analyses showed that after 20 min radio-labelled GSH was significantly increased in the infected RBC ($P<0.001$), but not in uninfected RBC. No significant differences were found between $C2^{GC03}$ and $C6^{7G8}$ infected RBC ($P>0.05$).

Future work will need to establish the compartmentalization of GSH taken up in the host-parasite unit. The current data do not indicate whether GSH reaches the parasite compartment or if it is only taken up into the host cell.

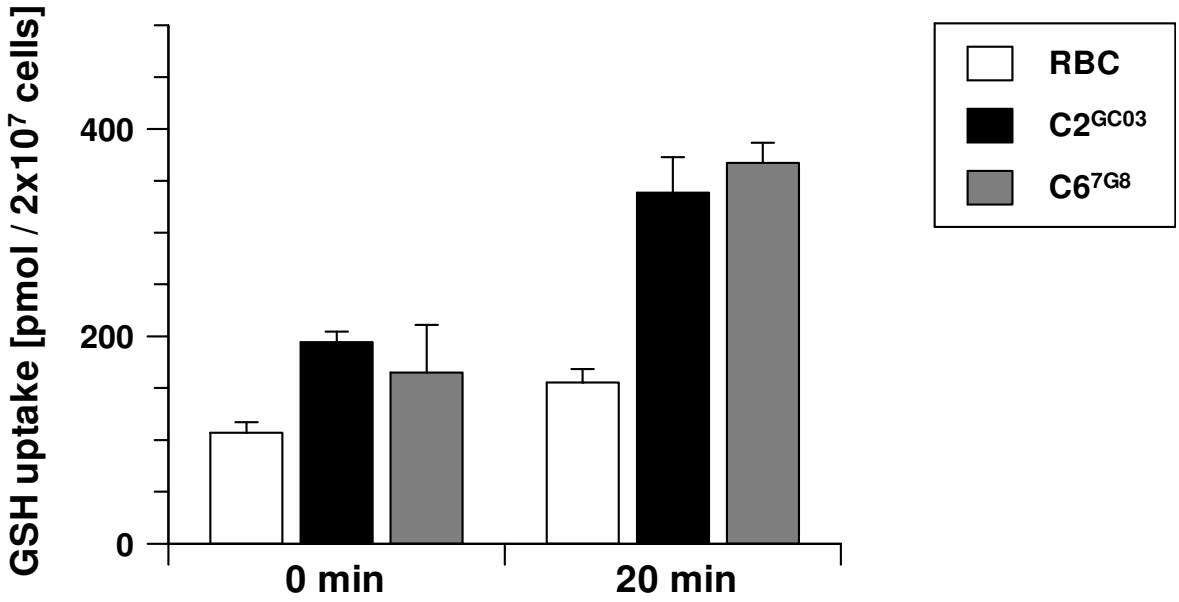

Figure 5-11: Uptake of GSH in $C2^{GC03}$ and $C6^{7G8}$.
GSH uptake into MACS purified trophozoite infected RBC of CQ sensitive $C2^{GC03}$ and CQ resistant $C6^{7G8}$ parasites was measured before and after 20 min incubation in EBSS solution containing 3 mM GSH and 1 µCi/ml [^{3}H]-GSH. At the start of the incubation (t=0) GSH measured for uninfected RBC was 106 ±10 pmol/ $2x10^7$ cells and 194 ±10 pmol/ $2x10^7$ cells and 165 ±46 pmol/ $2x10^7$ cells for $C2^{GC03}$ and $C6^{7G8}$, respectively. After 20 min, GSH measured was 155 ±13 pmol/ $2x10^7$ cells for RBC and 339 ±34 pmol/ $2x10^7$ cells and 367 ±19 pmol/ $2x10^7$ cells for $C2^{GC03}$ and $C6^{7G8}$, respectively. Data is presented as mean of 3 independent experiments ±S.E.M.

5.7 Data obtained by collaborators

The following results were not generated by me but by our collaborators at the Liverpool School of Tropical Medicine. I am listing them here in order to complete the data set on our analyses of the relation between of mutations of *pfcrt*, CQ resistance and GSH metabolism.

5.7.1 Effect of N-acetylcysteine on chloroquine susceptibility

Earlier studies found that the addition of N-acetylcysteine (NAC) to the culture medium decreased the sensitivity of parasites to CQ (Ginsburg et al., 1998). These findings were confirmed in this study. Addition of 5 mM NAC in the CQ resistant line $C3^{Dd2}$, significantly increased the CQ IC_{50} by 2-3 folds from 56.0 ±2.4 nM to 153.0 ±7.3 nM. Interestingly, on the CQ sensitive line $C2^{GC03}$ the addition of 5 mM NAC had a much smaller effect and the CQ IC_{50} changed only marginally from 6.6 ±0.9 nM to 8.5 ±0.9 nM.

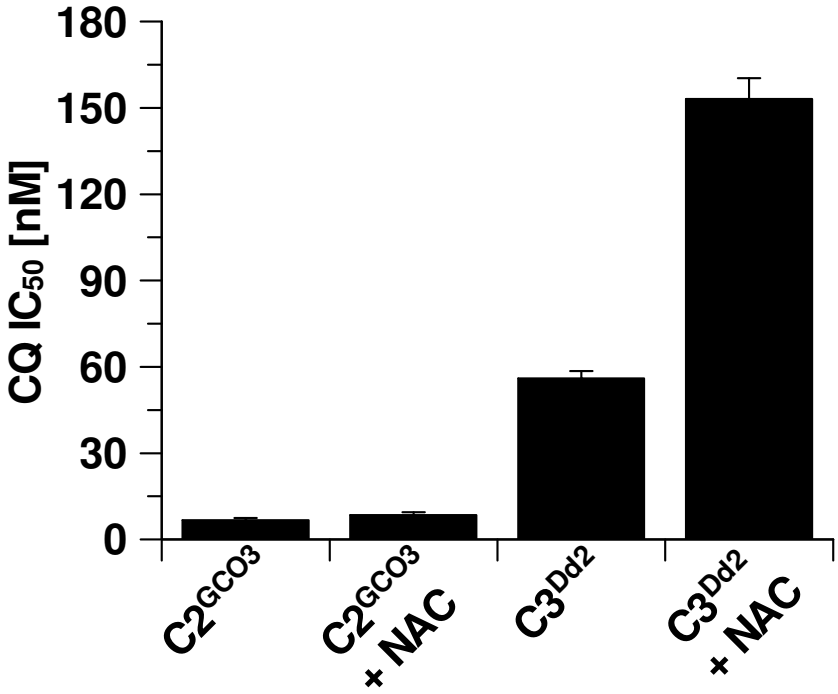

Figure 5-12: Effect of NAC on CQ IC_{50}.
The presence of 5 mM NAC increases the CQ IC_{50} in the resistant parasite line $C3^{Dd2}$ from 56.0 ±2.4 nM to 153.0 ±7.3 nM, but has only a marginal effect on the CQ IC_{50} for sensitive line $C2^{GC03}$, where 5 mM NAC led to an increase of the IC_{50} from 6.6 ±0.9 nM to 8.5 ±0.9 nM. These IC_{50} values were determined at the Liverpool Tropical School of Medicine.

5.7.2 Chloroquine accumulation and chloroquine binding

Previous studies showed that GSH depletion made parasites more susceptible to CQ while increasing GSH levels made them less susceptible (Ginsburg et al., 1998). These observations were linked to heme degradation by GSH; decreased GSH levels were suggested to increase free heme and thus elevate CQ binding and the susceptibility of the parasites to the drug.

This was tested by measuring the accumulation of [^{3}H]-CQ while depleting GSH in the parasites with increasing concentrations of CDNB in the CQ sensitive line $C2^{GC03}$ and the resistant line $C3^{Dd2}$ (Figure 5-13A). CQ accumulation was hardly affected in the sensitive line, while CDNB markedly stimulated CQ accumulation in the resistant parasites. The increase of the CQ cellular accumulation ratio (CAR) in $C3^{Dd2}$ was most pronounced at a CDNB concentration of 10 µM and was comparable to the effect of 10 µM verapamil, a known CQ resistance reversing agent.

A similar experiment testing a single CDNB concentration was performed with two other parasite lines N3D7 and R2B8 (Figure 5-13B). Both parasite lines are derived from the CQ resistant parent line Dd2. In N3D7 the K76T mutation of

resistant PfCRT was converted back to T76K, making this line again sensitive to CQ (Lakshmanan et al., 2005). The line R2B8 carries the original Dd2 allele of *pfcrt* and is resistant to the drug. 10 µM CDNB has a similar effect on the resistant line as it has on $C3^{Dd2}$; R2B8 parasites accumulate more CQ in the presence of 10 µM CDNB than in the absence of the drug. This effect is again comparable to the reversal of CQ resistance by verapamil (Figure 5-13B, black bars). In contrast, the presence of 10 µM CDNB does not affect the CQ CAR in the sensitive line N3D7 (Figure 5-13B, white bars). This indicates that the effect of CDNB on CQ accumulation is directly linked to the K76T mutation in PfCRT.

The data so far indicate that GSH potentially has access to heme in the DV and is therefore able to destroy it. This would reduce the amount of free heme in the DV of resistant parasites. Because the concentration of free heme cannot easily be measured directly it was estimated by analysis of CQ equilibrium binding experiments on intact infected erythrocytes (Figure 5-13C) (Bray et al., 1998; Chou et al., 1980{Bray, 1999 #279)}. In the Scatchard plot (Figure 5-13C), the apparent affinity of binding is calculated from the reciprocal of the slope and the X-axis intercept gives the approximated equilibrium binding capacity.

Least squares analysis of the CQ binding isotherms estimates the CQ equilibrium binding capacities of $C2^{GC03}$ at 35 ±1.1 µmol / l and of $C3^{Dd2}$ and $C6^{7G8}$ at 30 ±0.8 µmol / l and 29 ± 1.7 µmol / l, respectively. The CQ resistant lines have an approximately 15 % reduced binding capacity for CQ in comparison to the sensitive line. These changes are consistent with a modest reduction in the concentration of free heme in the resistant lines analysed.

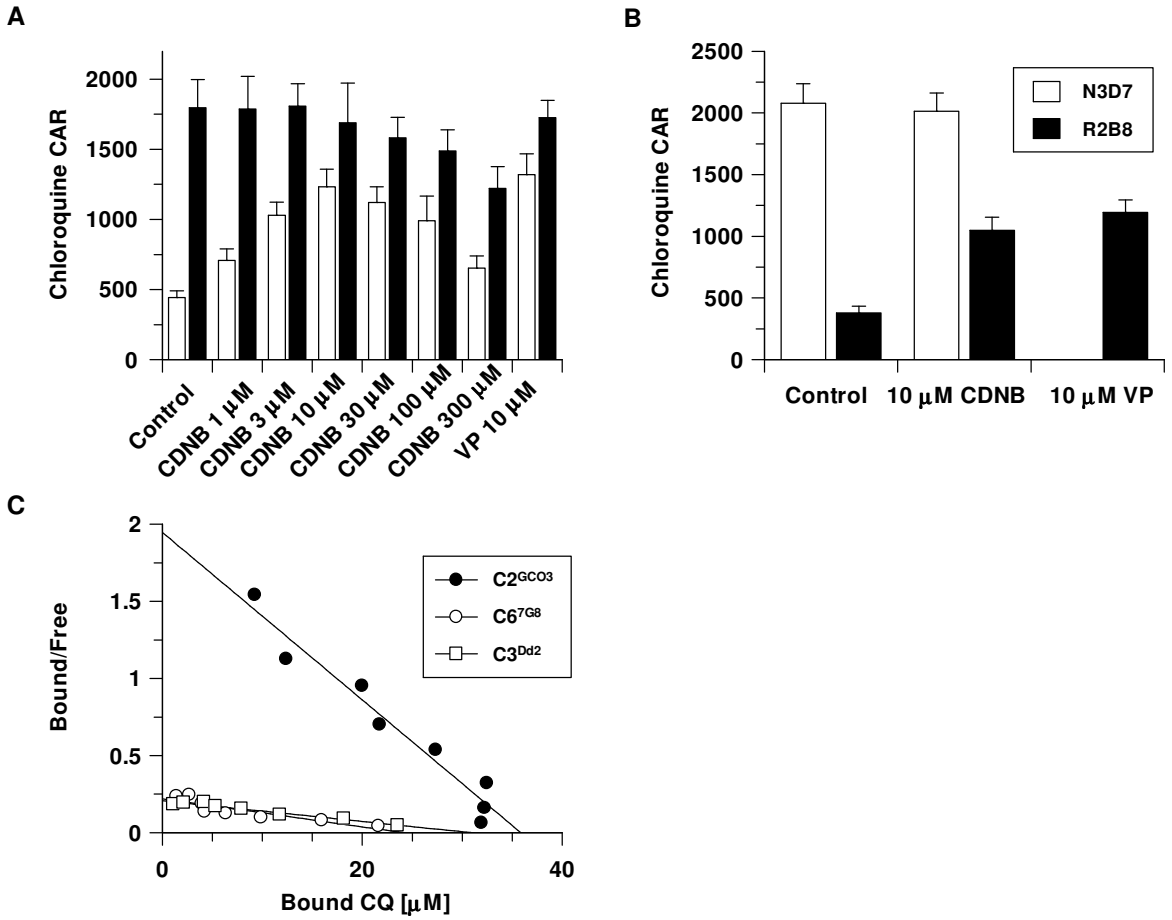

Figure 5-13: CQ accumulation and CQ equilibrium binding studies.
Panel A displays the differential effect of CDNB on the cellular accumulation ratio (CAR) for [^{3}H]-CQ in trophozoites of the CQ sensitive $C2^{GC03}$ line (black bars) and the CQ resistant $C3^{Dd2}$ line (white bars). Increasing CDNB concentrations markedly affect the resistant line, but hardly affect the sensitive line. CQ uptake in the presence or absence of various CDNB concentrations was measured by collaborators of the Liverpool School of Tropical medicine as previously described (Lakshmanan et al., 2005{Bray, 1998 #276)}. Over a 20 min period, steady state CQ uptake was measured at a concentration of 5 nM [^{3}H]-CQ. **Panel B** displays CQ uptake in the isogenic lines N3D7 and R2B8. Both parasite lines are derived from the Dd2 parental line. In N3D7 the K76T mutation in PfCRT has been converted back to T76K, thus making this line CQ sensitive. R2B8 carries the original K76T mutation and is CQ resistant. Again, steady state CQ uptake was measured at the Liverpool School of Tropical medicine at a concentration of 5 nM [^{3}H]-CQ over a 20 min period as previously described (Bray et al., 1998; Lakshmanan et al., 2005). **Panel C** shows the Scatchard plot analysis of CQ equilibrium binding studies on $C2^{GC03}$, $C3^{Dd2}$ and $C6^{7G8}$. These studies were performed at a concentration of 2 nM [^{3}H]-CQ and a range of concentrations of unlabelled CQ and the results were corrected for nonspecific uptake as described in Bray *et al* (Bray et al., 1998). The number of CQ binding sites for each parasite line was interpolated from the graph.

5.7.3 Expression of PfCRT in *Xenopus laevis* oocytes

To test the possibility that PfCRT is directly responsible for the translocation of GSH across the membrane of the digestive vacuole, the *X. laevis* heterologous expression system was used to express wild-type and mutant forms of PfCRT and to test the uptake of GSH by this system (Figure 5-14). The PfCRT alleles expressed were the wild-type HB3 allele, which is also found in GC03 and $C2^{GC03}$, the CQ resistant Dd2 allele that is present in $C3^{Dd2}$ and a K76T mutant form of

the HB3 wild-type, which is not naturally found in parasite isolates. As a positive control the *A. thaliana* Chloroquine-like-transporter-1 (AtCLT1) protein was used, which was recently shown to transport GSH and γGC (Maughan *et al.*, submitted).

To demonstrate the correct localization of PfCRT on the oocyte plasma membrane, indirect immunofluorescence was performed (Figure 5-14A). The results show that all three forms of PfCRT are expressed and present in the plasma membrane. In the water-injected control group of oocytes hardly any fluorescence is detected.

The uptake studies show that there is a basal level of GSH uptake in the water injected negative control oocytes, which is presumably due to a low activity of endogenous transporters in the oocytes' plasma membrane. The uptake in the oocytes expressing the HB3 allele of PfCRT is not significantly different from the negative control (Mann-Whitney U-test), suggesting that HB3 PfCRT does not transport GSH (Figure 5-14B). However, the oocytes expressing either of the mutant forms of PfCRT, the Dd2 allele and the K76T mutant, show significantly increased GSH uptake ($P<0.01$), similar to the uptake observed in oocytes expressing AtCLT1. These results confirm a role of mutant PfCRT in the transport of GSH.

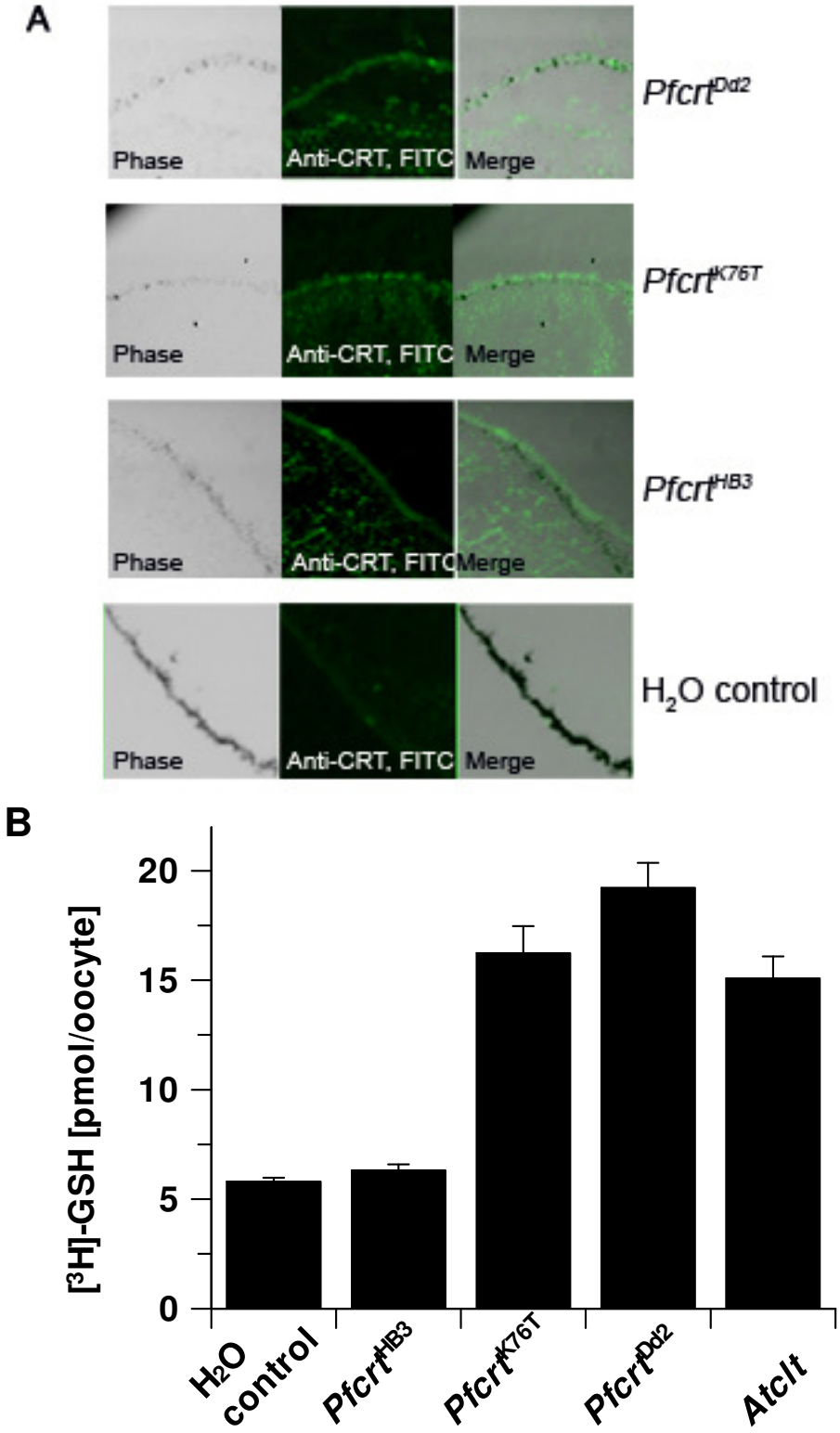

Figure 5-14: Expression of PfCRT in *X. laevis* oocytes.
Panel A: Indirect immunofluorescence studies on oocytes expressing different alleles of *pfcrt* and on water injected control oocytes using anti-PfCRT antibodies. Images are presented for oocytes expressing the HB3, Dd2 and K76T variants of PfCRT and for the negative control water injected oocytes. **Panel B:** Uptake of [^{3}H]-GSH by Xenopus oocytes expressing wild-type or mutant PfCRT or AtCLT1. Oocytes were incubated with 52 nM GSH for 30 min. Data is presented as mean ±S.E.M. of five independent experiments. For each experiment at least seven oocytes were used which were obtained each time from a different batch of oocytes from a different frog. Oocytes expressing mutant forms of PfCRT, PfCRT^{K76T} or PfCRT^{Dd2} and oocytes expressing the positive control AtCLT-1 were significantly different from the negative control oocytes injected with water. The differences were significant for each group of experiments as well as for the pooled data. Oocytes expressing the HB3 variant of PfCRT are not significantly different from water injected oocytes. Data is presented as mean ±S.E.M. Statistical significance was assessed by Mann-Whitney U test.

Mature female *X. laevis* were purchased from Xenopus Express (Vernassal, Haute-Loire, France) and oocytes were obtained after immersing frogs in euthanasic concentration of MS-222 (ethyl 3-aminobenzoate methanesulfonate, Sigma, 0.5 % w/v) in 5 mM Tris base, pH 7.4. After removal, ovary lobes were divided into smaller sacs and individual oocytes were manually isolated. After 2 washes oocytes were kept at 18°C for 2 hours in complete modified Barth's solution (MBS) (88 mM NaCl, 1 mM KCl, 15 mM HEPES pH 7.6, 0.82 mM $MgSO_4$, 0.3 mM $Ca(NO_3)_2$, 1 mM $CaCl_2$, 1 ml/l of 10000 U penicillin/ 10000 U streptomycin solution, Sigma). Stage IV-V oocytes were selected for injection of 50 nl DEPC-treated water or capped complementary RNA (cRNA) solutions at 1 µg/µl with a semi-automatic injector (Drummond, Nanoject, Broomall, PA, USA). *Pfcrt* gene cDNA was synthesized from total mRNA using Thermoscript (Invitrogen) and amplified by PCR with *Taq High Fidelity polymerase* (Invitrogen) following manufacturer's instructions. *Pfcrt* genes of the HB3 and Dd2 strains and a mutant form of HB3 carrying the K76T mutation were cloned into the plasmid pSP64T using the *Xho*I-*Nco*I sites. AtCLT1 was cloned into the plasmid pT7TS (pGEM4Z modified vector, Promega Madison, WI, USA) using *Bgl*II-*Spe*I sites. In vitro transcription of cRNA was performed using *Eco*RI-linearized pSP64T plasmids or *Sal*I-linearized pT7TS plasmids with the SP6 or T7 message machine kits (Ambion, Austin, TX, USA), respectively. Following injection of oocytes with cRNA or water, enzymatic dissociation and defolliculation was completed after four days by 30 min *collagenase* treatment (1mg/ml, Sigma) in MBS without calcium. Uptake assays were performed at 2 µCi/ml of [^{3}H]-GSH (38.6 Ci/mmol, American Radiolabelled Chemicals, St Louis, MO, USA) corresponding to 52 nM GSH. Seven to ten oocytes were incubated in 1 ml Ringer solution with 5 % DTT at room temperature. Oocytes were washed 12 times on ice before being individually collected and immersed in 1 ml scintillation fluid. Oocytes were incubated overnight and radioactive decay was counted in a Wallac 1450 Microbeta scintillation counter. For indirect immunofluorescence, oocytes were immersed in 1 ml OCT medium (RA Lamb Ltd., Eastbourne, UK) before freeze down in 2-methylbutane in liquid N_2 and immersion in liquid N_2 for 30 sec. 10 µm sections were prepared on coated glass slides and fixed in cold acetone for 10 min. The slides were blocked in 4 % BSA in PBS (w/v) for one hour before incubation with primary antibody in 4 % BSA in PBS (w/v) for one hour at room temperature. Slides were washed three times with PBS and the secondary antibody was applied in 4 % BSA in PBS (w/v) for one hour. Sides were washed again three times with PBS and glass cover slips were mounted with a drop of Hard Vector Shield (Burlingame, CA). Slides were dried for 30 min before examination under a confocal microscope.

5.8 Summary

- Analysis of three isogenic lines and their parental parasite line only differing in their *pfcrt* allele shows that IC_{50} values for CQ are not changed by the presence of 1 mM extracellular GSH. However, data of collaborators show an effect of N-acetylcysteine on the CQ IC_{50} predominantly in a CQ resistant parasite line, but not in a sensitive line.

- Determination of GSH levels in the four parasite lines showed a reduction of total GSH in the CQ resistant parasite lines compared to the sensitive lines. These parasite lines are also more susceptible to the γGCS inhibitor L-BSO, while no differences in their susceptibility to the GST substrate CDNB was observed.

- Extracellular GSH alleviates the effect of L-BSO and CDNB, indicating that extracellular GSH can be utilized in the infected red blood cell. This effect is more pronounced for CDNB.

- Changes in expression levels of enzymes responsible for GSH biosynthesis, GSH reduction or GSH consumption were not found between the four parasite lines and are unlikely to be the reason for the observed differences in GSH levels.

- Uptake of GSH was observed in infected red blood cells and the uptake ratio was not different between a CQ sensitive and a CQ resistant parasite line.

- Cellular accumulation ratios of CQ determined in the presence of CDNB by collaborators at the Liverpool School of Tropical Medicine show a similar effect of CDNB on the CQ uptake in CQ resistant parasites as the resistance reverting agent verapamil. No effect of CDNB on the accumulation of CQ in sensitive parasites was observed.

- CQ resistant parasites analysed by our collaborators in this study showed a reduced binding capacity for CQ, indicating reduced levels of free heme in resistant lines in comparison to the sensitive line $C2^{GC03}$.

- Data of collaborators at the Liverpool School of Tropical Medicine also show that *X. laevis* oocytes expressing mutant but not wild-type PfCRT take up radio-labelled GSH. This means that mutant, but not wild-type PfCRT transports GSH.

6 Discussion

The tripeptide GSH serves a variety of important functions in many prokaryotic and eukaryotic organisms. Previously it has been suggested to be of particular importance for the malaria parasite *P. falciparum*, which lives in an environment of increased oxidative stress. Studies with L-BSO, an inhibitor of the first step of GSH biosynthesis, have shown the importance of the tripeptide for the survival of the parasites (Lüersen et al., 2000; Meierjohann et al., 2002b). However, it is still unclear to what extent the parasites depend on GSH *de novo* biosynthesis, since L-BSO equally affects the parasite's host cell. To answer some of the remaining questions about GSH biosynthesis and its significance for survival of intra-erythrocytic stages of *P. falciparum* I determined the cellular localization of the GSH biosynthesis pathway and investigated whether this pathway is essential for the blood stage development of the parasite.

Furthermore, I investigated the hypothesis that GSH is involved in resistance against the antimalarial drug CQ. Because of its ability to destroy FPIX, the intracellular target of CQ, a role for the tripeptide in the resistant phenotype of *Plasmodium* has previously been implicated. Altering intracellular GSH levels with various compounds such as L-BSO and NAC can modulate sensitivity of *Plasmodium* to CQ. Increasing GSH levels caused an increase in CQ resistance while depleting or decreasing GSH levels had the opposite effect. It was suggested that the higher GSH levels resulted in an increase of FPIX degradation, after FPIX escaped from the DV into the parasite cytosol. In fact the resistant *P. falciparum* field isolate Dd2 has been shown to contain higher GSH levels than the CQ sensitive isolate 3D7, giving some credence to this hypothesis (Atamna and Ginsburg, 1995; Deharo et al., 2003; Ginsburg et al., 1998; Ginsburg and Golenser, 2003; Meierjohann et al., 2002b). However, the escape of FPIX to the cytosol is controversially discussed (Atamna and Ginsburg, 1995; Egan et al., 2002; Ginsburg et al., 1998; Ginsburg and Golenser, 2003) and thus the mechanism by which GSH potentially contributes to CQ resistance needs to be further clarified.

6.1 Localization of the glutathione biosynthesis pathway

The GSH biosynthesis pathway, consisting of γGCS and GS is localized in the cytosol in mammals and other non-plant eukaryotes analysed so far. In plants GSH biosynthesis is found in the plastids and the cytosol, with γGCS localized in the plastids and GS predominantly localized in the cytosol and to a smaller extent in the plastids (Hell and Bergmann, 1988; Hell and Bergmann, 1990; Lash, 2006; Meister, 1988; Pasternak et al., 2008; Radyuk et al., 2009). PfγGCS and PfGS are homologues to the enzymes of non-plant eukaryotes and therefore it has been postulated that they are both cytosolic. Indeed, I found the recombinant fusion proteins PfγGCS-GFP and PfGS-GFP were localized in the parasite cytosol, consistent with their predicted localization (Becker et al., 2003b; Müller, 2004).

This indicates that GSH is synthesized in the cytosol in *P. falciparum* and has to be imported into several organelles such as the endoplasmatic reticulum (ER), the mitochondrion and possibly the apicoplast as has been previously reported for yeast and mammalian cells (Banhegyi et al., 1999; Chakravarthi and Bulleid, 2004; Hwang et al., 1992; Lash, 2006; Meister, 1988; Molteni et al., 2004). Most studies on intra-organelle GSH transport have been performed on mitochondria. Because GSH is negatively charged at the physiological pH of the cytosol, it cannot enter the equally negative lumen of mitochondria by passive diffusion and thus organic anion transporters were suggested to be responsible for the import of GSH into the organelle (Chen and Lash, 1998). In yeast mitochondria the GSH uptake rate is not altered by removal of the outer membrane, suggesting that either transport through the inner membrane is rate limiting or that the responsible transporter is a “connected” transporter through both membranes (Cummings et al., 2000). In mammalian mitochondria cis-inhibition and trans-stimulation of GSH transport by malate and succinate has been observed, suggesting a role for the dicarboxylate carrier and the 2-oxoglutarate carrier as transporters of GSH across the mitochondrial membrane (Chen and Lash, 1998). In *Plasmodium* species homologues of a putative oxoglutarate/ malate transporter protein exist (PF08_0031 in *P. falciparum*, http://plasmodb.org/plasmo/), but it is not known, whether the transporter is functional and localizes to the parasite’s mitochondrion. Future studies are needed to determine if malate and succinate influence GSH transport into the

mitochondrion of malaria parasites. GSH uptake into mitochondria is very efficient in plants and mammals. Mutants of *A. thaliana* containing approximately 80 % less of the tripeptide than wild-type plants display severely depleted GSH levels in the cytosol, while the levels in the mitochondria are almost normal (Zechmann et al., 2008). This also emphasizes the special need for the mitochondrion to maintain its reducing environment. GSH levels in the nucleus also remained high despite depletion of total GSH levels, indicating that the nuclear GSH pool is discretely regulated from the cytosol and that mechanisms controlling nuclear GSH levels exist (Zechmann et al., 2008). Similar results for organelle-specific GSH pools were obtained with mouse fibroblasts, where mitochondria and nuclear GSH pools are more resistant to depletion with L-BSO (Green et al., 2006). So far only total GSH levels have been determined in *Plasmodium* parasites, no studies have been performed on mitochondrial and nuclear GSH pools.

A recent study showed that in the fruit fly *Drosophila melanogaster* the catalytic, but not the regulatory subunit of γGCS undergoes nuclear shuttling and can move from the predominant site of GSH biosynthesis in the cytosol into the nucleus in order to increase GSH concentration in the nucleus (Radyuk et al., 2009). This nuclear shuttling appears to be regulated in response to oxidative stress and is mainly observed in dividing cells of the fly. Although a classical bipartite nuclear localization signal has been found in the γGCS of *S. cervisiae* by *in silico* analyses, such a motif is absent from mammalian homologues (Radyuk et al., 2009) and studies on mice fibroblasts did not detect γGCS in nuclear extracts (Markovic et al., 2007) . We did not investigate the possibility of nuclear shuttling of γGCS in *P. falciparum*, but no nuclear localization signal is predicted in PfγGCS.

6.2 Uptake of extracellular glutathione

In mammalian cells uptake of extracellular GSH depends on the action of γ-glutamyl transpeptidase. The transpeptidase is able to cleave the γ-glutamyl linkage between glutamate and cysteine and transfers the glutamyl residue onto other amino acids. The highest affinity acceptor is the cysteine dimer cystine, thus γ-glutamylcystine is predominantly generated and taken up. Inside the cells, reduction of γ-glutmaylcystine leads to the formation of γGC, which then

feeds into GSH biosynthesis (Dalton et al., 2004). RBCs lack γ-glutamyl transpeptidase, thus uninfected RBC do not take up the tripeptide.

Previous studies, as well as the present study, have however shown uptake of radio-labelled GSH by *P. falciparum* infected red blood cells (Atamna and Ginsburg, 1997; Raj et al., 2008). During the course of the present study, GSH uptake was investigated primarily to measure potential differences between CQ resistant and sensitive parasite lines rather than to characterize GSH transport. GSH uptake by infected RBC was similar between RBCs infected with CQ resistant $C6^{7G8}$ and sensitive $C2^{GC03}$ parasites.

Over a 20 min period, the amounts of GSH taken up in the presence of 3 mM extracellular GSH were in a similar range to those reported by Atamna and Ginsburg in the presence of 5 mM GSH (Atamna and Ginsburg, 1997). Converting the GSH uptake in both studies to nmol/ 10^{10} cells, Atamna and Ginsburg measured approximately 150 nmol/ 10^{10} cells, compared to 250 nmol/ 10^{10} cells found in the present study. In a recently published study, Raj *et al.* reported a much lower uptake ranging between 0.01 and 0.02 nmol/ 10^{10} cells, which is likely due to the low, 1-6 nM, extracellular GSH concentration used in their experiments and is corresponding to the dependence of the GSH uptake on the extracellular GSH concentration. The findings of Raj *et al.* are however in contrast to the findings by Atamna and Ginsburg, who reported that GSH uptake is only observed in the presence of high extracellular GSH concentrations (Atamna and Ginsburg, 1997; Raj et al., 2008).

The rate of GSH uptake I observed was slow at the beginning of a 20 min period, whereas previous reports showed a much faster initial uptake. This is likely related to technical reasons. I kept parasites on ice prior to uptake and presumably it took some time to adjust the incubation mix to 37°C. For future experiments a longer equilibration step should be included prior to addition of GSH to allow more time for parasites to recover to physiological temperature. Because lysis of infected RBC was observed after 30 min of incubation, I did not follow the GSH uptake beyond that. Raj *et al.* reported a peak of GSH uptake at 20 min, while in the study by Atamna and Ginsburg, GSH uptake reached a constant level after approximately 60 min (Atamna and Ginsburg, 1997; Raj et al., 2008).

The study by Atamna and Ginsburg showed that GSH is taken up by *P. falciparum* infected red blood cells, but uptake does not occur when free parasites are examined. This suggests that a permeability pathway exists in infected RBCs, but parasites do not possess a transporter for GSH in their plasma membrane (Atamna and Ginsburg, 1993). A possible alternative pathway for GSH uptake is the endocytosis of host cell cytosol containing GSH (Platel et al., 1999) and the subsequent uptake into the parasite's cytosol through transporters in the parasite's DV membrane. However, because extracellular GSH has been shown to increase the GSH level within the host cell compartment but not in the parasite itself, it has been previously concluded that the tripeptide does not enter the parasites (Atamna and Ginsburg, 1997).

However, GSH biosynthesis may be regulated by feedback inhibition of γGCS in *P. falciparum* as it is in other organisms (Huang et al., 1988; Lueder and Phillips, 1996). Thus, an increased uptake of the tripeptide possibly leads to down-regulation of biosynthesis and the overall GSH level remains unchanged. Raj *et al.* presume that GSH is entering the parasite compartment, because the knock-out of the parasite's multi-drug resistance protein PfMRP increases the accumulation of radio-labelled GSH in infected RBC to almost twice the level observed in the parental line (Raj et al., 2008). They hypothesized that PfMRP plays a role in the efflux of GSH and that the loss of the protein in the parasite's plasma membrane leads to a decrease in GSH efflux and thus causes an increase in GSH accumulation (Raj et al., 2008). This indicates a high and rapid turnover of GSH in the parasite. A rapid turnover of GSH has also been suggested for infected RBC by Atamna and Ginsburg, who hypothesized that the rapid oxidization and excretion in the form of GSSG is the reason why GSH uptake was not observed at low concentrations of the tripeptide (Atamna and Ginsburg, 1997). Lüersen *et al.* also reported rapid GSSG efflux from infected RBC (Lüersen et al., 2000). The efflux of GSSG offers another possible explanation why total GSH levels do not increase despite uptake of the tripeptide by the parasites. However, the observation that extracellular GSH cannot rescue *P. falciparum* parasites in the case of a *ygcs* or *gs* knockout indicates that the tripeptide is either not or only at insufficient levels taken up.

It remains an open question whether GSH taken up into infected RBC is also taken up into the parasite. Future studies are needed to further investigate the

subcellular localization of radio-labelled GSH following uptake into infected RBC. Rather than measuring GSH levels in the different compartments, the distribution of the radioactive label can be analysed in order to trace the fate of GSH in the infected RBC.

6.3 Knockout of Glutathione biosynthesis

Homologues of *ygcs* have previously been shown to be essential in various eukaryotic organisms, but not in prokaryotes such as *E. coli*. Several studies on *ygcs* employing a variety of methods showed that the gene is essential in *S. cerevisiae, C. albicans, T. brucei* and *D. discoideum* (Baek et al., 2004; Grant et al., 1996; Huynh et al., 2003; Kim et al., 2005; Lee et al., 2001). In all these cases, the loss of a functional γGCS enzyme could be compensated when cells were supplemented with GSH, GSSG or γGC and in some cases with other thiols such as DTT and NAC.

The fact that the gene is not essential for the survival of blood stages of *P. berghei* and only essential in the mosquito stages is unusual for a eukaryotic organism (Vega-Rodriguez et al., 2009). However, GSH was still detected at approximately 5-14 % of the wild-type GSH levels in the blood stages of the *pbygcs* knockout lines, showing that despite the loss of a functional biosynthesis pathway, the product is still present in the parasite cells (Vega-Rodriguez et al., 2009).

The possibility of an alternative pathway of γGC biosynthesis, independent of γGCS has previously been described in yeast. A deletion mutant of *S. cerevisiae* lacking γGCS has been shown to survive under both aerobic and anaerobic conditions because trace amounts of GSH are synthesized due to additional mutations in the *pro2* gene of the proline biosynthesis pathway (Lee et al., 2001; Spector et al., 2001). *Pro2* encodes for glutamylphosphate reductase, which converts γ-glutamylphosphate, provided by glutamate-5-kinase in the previous step, to L-glutamate-γ-semialdehyde. Mutation of the glutamylphosphate reductase allows the condensation of γ-glutamylphosphate with cysteine and thus synthesis of γGC in this step, but it is not understood if the mutant glutamylphosphate reductase alone is involved or if additional enzymes play a role (Spector et al., 2001). Homologues of glutamate-5-kinase and

glutamylphosphate reductase are absent from the *P. falciparum* genome (Gardner et al., 2002) and have not been identified in other *Plasmodium* species either (http://plasmodb.org/plasmo/), thus suggesting that a similar mechanism is not possible in malaria parasites. Residual GSH in *pbygcs* knockout parasites is likely derived from the host cell and was attributed to endocytic uptake of GSH from the host cell cytosol into the food vacuole (Vega-Rodriguez et al., 2009).

Neither the *pfygcs* nor the *pfgs* gene could be disrupted or replaced in two different strains of *P. falciparum* by the strategies employed in this study. This is surprising, given that the knockout of the *ygcs* gene in *P. berghei* was possible (Vega-Rodriguez et al., 2009).

However, there are several significant differences between *P. falciparum* and *P. berghei* parasites. There have been previous reports where orthologous genes were found to be essential in one parasite species, but not the other. For example the mitogen-activated protein kinase 2 (map2) has an essential function in erythrocytic stages of *P. falciparum* and a knockout is impossible to generate in these parasites, while the protein is only required for formation of male gametocytes in *P. berghei* and a knockout in the blood stages can be achieved (Dorin-Semblat et al., 2007; Rangarajan et al., 2005; Tewari et al., 2005).

The gene loci of both genes were targeted in *P. falciparum*, showing they are not refractory to recombination and that the changes to the gene loci through the integration of the transfection plasmids are not deleterious. This implies that null mutants for either gene are not viable and thus both genes are essential in *P. falciparum*. The loss of GSH biosynthesis in the human parasite cannot be compensated for by either uptake of the tripeptide or by redundancy between the GSH system and other antioxidant systems such as the thioredoxin system.

In case of the pHH1-Δ*ygcs* construct, non-homologous integration into a non-related gene locus was observed. We have previously observed random integrations of other pHH1-based knockout constructs targeting different unrelated genes in our laboratory. Random integrations were predominantly observed with knockout constructs targeting essential genes, where parasites were not viable, if integration into the correct gene locus occurred, and less frequently for knock-in control constructs which leave target genes functional.

Thus random integration of this plasmid appears to occur fairly regularly, albeit at a lower rate than integration into the destination locus and seems to be selected for when integration into the target locus is lethal or leads to a growth defect (Günther et al., 2009).

The use of the pCC4-based constructs should avoid this problem due to the presence of the negative selectable marker *cd*. The presence of this gene allows selection against random integration as well as against episomal plasmids (Maier et al., 2006). However, in the present study parasites frequently became resistant to Ancotil®, despite the continued presence of the plasmids and thus the *cd* death gene in most transfected lines, as shown by Southern analyses. Of all three parasite lines transfected with the plasmid pCC4-Δ*ygcs* and one parasite line transfected with pCC4-Δ*gs*, Ancotil® resistant parasites were isolated. Resistance consistently occurred after transfectants had been taken through at least three drug selection cycles with Bla, while the cultures were sensitive to Ancotil® immediately after transfection and in the earlier Bla cycles. This shows that the parasites had not been resistant to Ancotil® when they were originally transfected and changes conferring resistance to Ancotil® were established in these lines.

Ancotil® resistance has previously been reported on various occasions for anti-fungal therapy. In clinical use, the active component of Ancotil®, 5-FC, is not used as monotherapy because resistance rapidly develops. Fungal resistance to 5-FC is established in two ways. Deficiency in the uptake or metabolism of 5-FC, due to changes in the fungal pyrimidine salvage pathway, causes a decrease in the toxic metabolite 5-FU, and thus a decrease in inhibition of fungal DNA and RNA synthesis (Chapeland-Leclerc et al., 2005; Papon et al., 2007). Changes in the pyrimidine biosynthetic pathway causes increased prevalence of pyrimidines which compete with 5-FU for binding to its targets. (Sanglard, 2002; Vermes et al., 2000).

Ancotil® resistant parasites were isolated frequently and emerged after a comparably short time period of three to four weeks of continuous Ancotil® pressure, indicating that it is unlikely that several changes in multiple genes were established in order to generate resistance. *P. falciparum* relies solely on pyrimidine biosynthesis (Reyes et al., 1982), thus changes to the parasite salvage

pathway are not possible. It is unknown how 5-FC is taken up by the parasite, but mutations in a transporter responsible for the uptake of the drug or a substantial down-regulation of its expression are potential mechanisms how resistance may have been established in the transfected parasite lines. Equally, expression of the *cd* gene from the pCC4 plasmids may be down-regulated through changes and mutations in the promoter region of the *cd* gene and pyrimidine biosynthesis is potentially up-regulated in the Ancotil® resistant parasites. Indeed, the plasmid or the part of the plasmid containing the *cd* gene was absent in two of the resistant lines, pointing to changes in the transfected plasmid rather than any parasite genes being responsible for the development of resistance. In the other lines generated for this study the respective part of the plasmid containing the *cd* gene was present according to Southern blot analyses, but it is possible that no active CD enzyme was expressed. These possibilities can be analysed in the future by assessing the presence of CD protein in the parasites and investigating the expression levels of genes involved in pyrimidine biosynthesis.

The knockout of *pfygcs* in presence of an episomal copy of the gene could not be achieved due to recombination of the plasmids. This is a technical problem which will need to be solved in the future. One possibility to minimize recombination of the expression plasmid with the endogenous gene locus or the knockout plasmid is to express a homologous γGCS protein of another *Plasmodium* species such as *P. berghei*.

The knockout of thioredoxin reductase in presence of an additional copy of the gene has previously been achieved after both plasmids were simultaneously transfected (Krnajski et al., 2002). However, in the thioredoxin reductase study recombination between the two plasmids also occurred prior to integration. Potentially transfection of a knockout plasmid into a parasite line already expressing the recombinant enzyme from an episomal plasmid is more efficient and can be attempted in the future with the PfγGCS-HA expressing line $D10^{\gamma GCS-HA}$-2 generated for this study. This line has been shown to contain only the episomal expression plasmid and the endogenous gene, while expressing recombinant protein. No such line has yet been generated for PfGS-HA, as the line presented in this study showed signs of recombination of the plasmid with the parasite genome.

6.3.1 Possible differences between *P. berghei* and *P. falciparum* glutathione metabolisms

There are two possibilities why the *ygcs* gene is not essential for the intra-erythrocytic stages of *P. berghei*, but is indispensable for the survival of *P. falciparum* in this stage: (1) *P. berghei* is able to scavenge GSH from its host at higher levels than *P. falciparum* (2) *P. berghei* requires less GSH for its survival than *P. falciparum* and the amounts taken up from the host cell are sufficient for the survival of the rodent parasite.

Vega-Rodriguez *et al*. reported GSH levels of only 5-14 % of the wild-type level in *pbygcs* knockout lines despite absent GSH biosynthesis and only observed a slight growth defect in the RBC stages (Vega-Rodriguez et al., 2009). It has previously been reported for *P. falciparum* that after short term GSH depletion, with 0.5 -2 mM CDNB for 15 min, to 12 % of the normal wild-type levels, parasites showed no apparent growth defect *in vitro* (Ayi et al., 1998). It is not known if *P. falciparum* parasites are also able to survive with these depleted GSH levels for a longer period of time and as shown in the present study long term exposure to CDNB is lethal for the parasites at much lower concentrations, albeit it is not known to what extent the prolonged CDNB exposure decreases the parasite's GSH levels before its death. Thus it cannot be concluded if *P. falciparum* requires higher GSH levels than *P. berghei* for intra-erythrocyte survival.

As discussed above, it is generally thought that *Plasmodium* parasites do not take up GSH from their host cell. However, this was only tested in *P. falciparum* and not in *P. berghei* parasites (Atamna and Ginsburg, 1997). The presence of GSH in the *pbygcs* knockout line indicates that *P. berghei* parasites are indeed capable of its uptake and this will have to be investigated in the future to uncover how precisely GSH enters these parasites. Possibly GSH present in the host cell is taken up into vesicles and eventually reaches the DV along with other contents of the host cell such as hemoglobin (Platel et al., 1999; Vega-Rodriguez et al., 2009). Without a transport mechanism allowing GSH to leave the DV, it would presumably be degraded by peptidases present in this organelle and the resulting amino acids taken up into the parasite cytosol or excreted as waste products. It has not been determined if *P. berghei* can recover GSH from its DV

and it is possible that *P. berghei* possesses a transporter for GSH in the DV that is absent in *P. falciparum*.

In collaboration with Dr Bray and colleagues at the Liverpool School of Tropical Medicine it was shown in the present study that point mutations in PfCRT, a potential transporter or channel in the DV membrane, allow the translocation of GSH across the DV membrane in *P. falciparum*. For reasons discussed below we believe this flux may be concentration dependent and in parasites with a functional GSH biosynthesis pathway directed into the DV due to the higher GSH concentration in the parasite cytosol. The loss of GSH biosynthesis might reverse the flow and may allow GSH to enter the parasites. This offers the possibility for a knockout of *pfygcs* or *pfgs* in CQ resistant lines of *P. falciparum* possessing a mutant *pfcrt* allele. The capability for the transport of GSH by the CRT homologue may already be present in *P. berghei* and further mutational changes may not be required in order to allow the parasites to take up GSH. These possibilities will be studied in detail in the future to fully understand the role of CRT in GSH homeostasis.

The problem of insufficient GSH uptake by *P. falciparum* can potentially be avoided by using GSH-esters to supplement transfected cultures, as these esters can easily cross cell membranes (Lüersen et al., 2000; Meister, 1988). However, the release of GSH from methyl- or ethyl-esters leads to the release of toxic methanol and ethanol and thus provides a different problem for parasites.

There are further differences between the human and the rodent parasite, which may determine whether PfγGCS is an essential enzyme or not. *P. berghei* preferentially infects reticulocytes which contain almost two times higher GSH levels than the mature erythrocytes infected by *P. falciparum* (Cromer et al., 2006; Janse et al., 1989; McNally et al., 1992; Sailaja et al., 2003). Therefore the rodent parasite is provided by its reticulocyte host cell with a larger GSH pool to allow for compensation of the loss of biosynthesis. Another difference between reticulocytes and mature erythrocytes is that the latter have lost the activity of multiple enzymes and no longer possess a nucleus and the machinery for the translation of proteins (Geminard et al., 2002; Thorburn and Beutler, 1991). Therefore mature RBC are unable to respond to decreasing GSH levels in the same way as reticulocytes, which are still able of increasing the expression

of γGCS and GS and potentially compensate a loss of GSH to the parasite by up-regulation of their own GSH biosynthesis.

Even if GSH only reaches the DV of *P. berghei* and does not reach the cytosol, the DV is one of the major sites for the generation of oxidative stress because of the degradation of hemoglobin. Therefore any GSH taken up can maintain the redox balance within this organelle and detoxify reactive oxygen species generated in this environment. Within the cytosol other components of the parasite antioxidant and redox system may take over other functions of GSH. Differences in the antioxidant system between *P. berghei* and *P. falciparum* may be responsible for greater redundancy in the rodent parasite's antioxidant system and thus allow compensation for the loss of GSH biosynthesis in this organism and not in the human parasite.

Redundancy between the thioredoxin and the GSH system is the reason why null mutants of the γGCS encoding gene *gshA* of *E. coli* are viable albeit showing reduced growth (Gardner and Fridovich, 1993). In contrast, double mutants for thioredoxin reductase and γGCS or thioredoxin reductase and GR are barely viable under aerobic conditions (Prinz et al., 1997). Similar results are seen for an *E. coli* triple mutant for both thioredoxins (*trxA* and *trxC*) and glutaredoxin 1 (*grxA*), which is only viable when cultured anaerobically (Stewart et al., 1998). The thioredoxin reductase of *P. falciparum* has previously been shown to be essential for the erythrocytic stages of the parasite, indicating that the GSH and thioredoxin system are not redundant in this species and cannot easily replace each other (Krnajski et al., 2002). However, the thioredoxin reductase of *P. berghei* appears to be non-essential (K. Becker, personal communication), again emphasizing the distinct metabolic requirements of the two parasites.

6.3.2 γ-Glutamylcysteine as glutathione substitute

The observation that the second gene of the GSH biosynthesis pathway encoding for PfGS is equally essential in *P. falciparum* shows that the GSH precursor γGC is not sufficient for the survival of the parasites and cannot compensate for the loss of GSH in this organism.

Previous findings that *S. cerevisiae* can survive in the presence of only γGC indicate that some functions of GSH can be adopted by γGC (Grant et al., 1997).

The dipeptide has some similar properties to GSH and possesses the thiol group important for many of the functions of GSH. However, γGC is more prone to oxidation and therefore needs to be efficiently reduced by the organisms GSSG reductase. The marine bacterium *Halobacterium halobium* depends entirely on γGC as its primary low molecular weight thiol and does not synthesize GSH (Sundquist and Fahey, 1989). *H. halobium* is specialized for the use of γGC and enzymes, which are normally GSH-dependent, are γGC-dependent in this organism. It possesses a γGC reductase and efficiently maintains a high reduced γGC to oxidized γGC ratio (Sundquist and Fahey, 1989), which is likely to be one of the problems encountered by organisms specialized for the use of GSH if the *gs* gene is lost. As well as in *P. falciparum*, the loss of active GS is lethal for the plant *A. thaliana* and the yeast *S. pombe*. *A. thaliana gs* insertion mutants show a seedling lethal phenotype and *S. pombe gs* knockout cells are GSH auxotroph (Chaudhuri et al., 1997; Pasternak et al., 2008). Interestingly, the *S. cervisiae* mutant described by Grant *et al.* showed poor growth on minimal medium despite γGC hyper-accumulation. The growth defect could be alleviated by supplementing the cells with even more γGC, indicating that despite the already five times higher levels of γGC, the dipeptide is not used as efficiently as GSH and is needed at far higher concentrations to support wild-type growth rates (Grant et al., 1997). Seedling lethality of homozygous *A. thaliana gs* insertion mutants occurs in a stage, where residual GSH, provided in the seed by the paternal heterozygous plant, can still be detected at significant levels (Pasternak et al., 2008). This led the authors to the hypothesis that hyper-accumulation of γGC itself may be deleterious to cells.

Probably *P. falciparum* cannot utilize γGC with the same efficiency as GSH and although the non-enzymatic functions of GSH can be taken over by γGC, the dipeptide is likely to be a poor substrate for GSH-dependent enzymes. Inefficient reduction of oxidized γGC by PfGR probably cause changes to the cytosolic redox potential and leads to a decreased buffer capacity. The mechanism of maintaining a high GSH:GSSG ratio through export of GSSG is likely to be inefficient for the excretion of oxidized γGC (Lüersen et al., 2000). Decreased import of γGC into organelles where GSH is normally required may have an immense impact on the function of these organelles. γGC is also more prone to auto-oxidation under conditions found in the parasite cytosol, while the high salt concentrations in *H. halobium* can protect γGC (Sundquist and Fahey, 1989).

To further analyse the importance of PfGS, I attempted the regulated dominant-negative expression of a mutant PfGS protein to down-regulate endogenous PfGS activity in the parasites. Because PfGS functions as a dimer (Meierjohann et al., 2002a), the presence of an inactive dead mutant should cause the formation of inactive-active heterodimers as well as active-active and inactive-inactive homodimers. Overall this should decrease the PfGS activity in the parasites and reduce GSH levels. Sequence alignment of the PfGS and HsGS amino acid sequences revealed the presence of four conserved residues that are of great importance for the activity of the human enzyme (Dinescu et al., 2004). PfGS residues Glu-206 and Asn-208 correspond to HsGS Glu-144 and Asn-146 and are in a region highly conserved between the two species. The mutation to Lys and Ala, respectively, abolished the activity of PfGS, as has previously been reported for the human enzyme (Dinescu et al., 2004). The results for the activity of recombinant $PfGS^{E206K/N208A}$ are preliminary at this stage and have to be confirmed after optimization of the purification protocol for the recombinant proteins. However, despite similar contamination with other proteins, recombinant wild-type PfGS is active, thus suggesting that the activity of the mutant is greatly reduced in order to be undetected. In the human enzyme Glu-144 participates in the formation and stabilization of the γ-glutamylcysteinyl-phosphate intermediate while coordinating the Mg^{2+} ions involved in the catalysis. Asn-146 is also involved in the coordination of a Mg^{2+} ion and possibly takes part in catalysis (Dinescu et al., 2004). Probably both residues serve similar functions in PfGS.

Two independent parasite lines transfected with the expression construct for $PfGS^{E206K/N208A}$-FKBP12 were generated. In one parasite line no FKBP12-tagged $GS^{E206K/N208A}$ was stabilized by Shld1, despite the presence of the expression plasmid. However, in the second line the recombinant protein was stabilized with Shld1, while being undetectable in the absence of the compound, indicating its destabilization by the FKBP12-tag and complete degradation. This is in contrast to previous reports that C-terminally tagged fusion proteins are less efficiently degraded than N-terminal fusion proteins and are still present in the cells in the absence of Shld1 (Armstrong and Goldberg, 2007; Banaszynski et al., 2006; Maynard-Smith et al., 2007).

The stabilization of PfGS$^{E206K/N208A}$ did however not result in a growth phenotype. There are three possible explanations for this observation: (a) reducing PfGS activity and the reduction in GSH levels does not have an adverse effect on the parasites; (b) PfGS activity is not decreased by the presence of the stabilized recombinant protein; (c) PfGS activity is decreased, but GSH levels are not reduced below a level that causes an adverse effect in the parasites.

Because the knockout studies suggest that PfGS is an essential enzyme, the first possibility is unlikely. Potentially the activity of PfGS is not decreased to an extent that significantly affects GSH levels and the parasite's growth. The reason for this could be either that the level of stabilized PfGS$^{E206K/N208A}$-FKBP12 is not high enough to sufficiently dilute the active enzyme or that the recombinant protein is not able to form heterodimers with the active form. In the human enzyme the corresponding mutations do not affect the folding of HsGS; single mutants of the human enzyme for either residue are inactive, but show no affected tertiary structure (Dinescu et al., 2004), suggesting that PfGS is folded correctly despite the mutations. Therefore the introduced mutations should not prevent the formation of heterodimers with wild-type PfGS. Expression studies of recombinant wild-type PfGS in *E. coli* show that N-terminally His-tagged recombinant PfGS forms dimers (Meierjohann et al., 2002a), but the presence of the C-terminal FKBP12-tag can potentially influence dimer formation. Future studies can determine the GSH levels of the parasites in the presence of stabilized PfGS$^{E206K/N208A}$-FKBP12 and the GS activity in the parasites treated with Shld1.

Low expression levels of C-terminally FKB12-tagged proteins are a common problem when this system is used in *T. gondii* (D. Soldati, personal communication). Indeed, the relative expression of wild-type PfGS tagged with either C-terminal GFP- or HA-tags using the same pCHD-plasmid and Hsp86-promotor, appears to be higher than the levels of stabilized PfGS$^{E206K/N208A}$-FKBP12 as determined by western blotting. This is potentially due to the specificity of the different antibodies against the tags. However, increasing concentrations of Shld1 from 0.25 µM to 0.5 µM and 1 µM did not increase the amount of stabilized protein in this study, suggesting a saturation of the recombinant protein in the parasites already at the lower concentration of the compound. This also indicates low expression levels of PfGS$^{E206K/N208A}$-FKBP12,

since other authors reported a constant increase of stabilized protein if the Shld1 concentration was raised (Armstrong and Goldberg, 2007; Banaszynski et al., 2006). Potentially low expression levels of the recombinant protein are linked to recombination of the plasmid. However, in the line that appears to contain more of the original transfected plasmid, no expression was detected at all, suggesting that a recombination event alone is not responsible for low expression.

Another problem encountered during the dominant-negative expression of PfGS$^{E206K/N208A}$-FKBP12 is the toxicity of the Shld1 ligand in wild-type parasite lines. The growth effect of the compound was obvious after 48 hours at concentrations higher than 0.2 µM and toxicity of Shld1 has also been reported independently in a recent study (Russo et al., 2009). It is not clear what the cause of Shld1 toxicity is. In a study on mammalian cells, Shld1 changed the expression levels of several genes, but because at various concentrations different genes were found to be affected, the authors assumed that off-target effects of Shld1 were too random to cause any general harmful effect in mammalian cells (Maynard-Smith et al., 2007). *P. falciparum* may however be more susceptible to Shld1 than mammalian species.

Unspecific toxicity makes the use of high Shld1 concentrations problematic and should be taken into account for future studies. Therefore the FKBP12 system may not be a good tool for over-expression studies which require high concentrations of Shld1 in order to achieve high levels of stabilized recombinant proteins in the parasites. In a recent study a FKBP12-based method was used for the regulated knockdown of an endogenous protein (Russo et al., 2009). In case of a regulated knockdown, the endogenous gene is tagged with the sequence for the destabilization domain and the encoded protein is continuously stabilized by constant presence of Shld1 in the cultures. Because the levels of a stabilized protein required for parasite survival are lower than the levels required for a mutant form to efficiently dilute the active protein, the stabilization of an endogenous active enzyme requires less Shld1 than the over-expression of a dead mutant. For future studies constructs can be designed to tag the endogenous gene with the degradation domain sequence following single cross-over recombination, thus ensuring that the protein will be degraded once Shld1 is withdrawn from the cultures.

6.3.3 An essential function for glutathione

The observation that both *pfgycs* and *pfgs* are essential for erythrocytic stages of *P. falciparum* raises the question which essential function GSH serves in the parasites.

The GSH deficient strains of *S. cerevisiae* can survive with as little as 0.5-1 % of the normal wild-type levels of GSH, either because it is supplemented in the medium or because trace amounts of GSH are synthesized due to additional mutations in the *pro2* gene of the proline biosynthesis pathway (Lee et al., 2001; Spector et al., 2001). Interestingly, low GSH levels are still required for the survival of *S. cerevisiae* under anaerobic conditions, indicating that the lethal phenotype is not related to oxidative stress (Grant et al., 1996; Lee et al., 2001; Spector et al., 2001). The *P. berghei ygcs* null mutants are also surviving in RBC stages despite severely reduced GSH levels and showed only a slight growth defect (Vega-Rodriguez et al., 2009).

Several authors have suggested the role of GSH for the maintenance of mitochondrial function (Martensson et al., 1989; Martensson and Meister, 1989; Vega-Rodriguez et al., 2009). This is also likely to be the case in *P. falciparum*, where the active electron transport chain is required for maintenance of the electrochemical gradient across the inner mitochondrial membrane and as an electron acceptor for dihydrofolate dehydrogenase, an essential component of the pyrimidine biosynthesis pathway (Painter et al., 2007). A functional electron transport chain potentially leads to the generation of ROS, which have to be detoxified to avoid damage to the organelle. Several systems were suggested to be involved in the removal of ROS in the mitochondrion (Müller, 2004) and the maintenance of the mitochondrial redox state is likely to be crucial for the integrity of the organelle.

Treatment of mice and rats with L-BSO needs to cause a marked decrease of GSH in the organelle, before mitochondrial damage occurs. Mitochondrial swelling as well as rupture of cristae and disintegration of mitochondrial membranes is observed in several tissues such as skeletal muscle, lungs, epithelia of jejunum and colon following GSH depletion through L-BSO treatment (Martensson et al.,

1989; Martensson et al., 1990a; Martensson et al., 1991; Martensson et al., 1990b; Martensson and Meister, 1989).

S. cerevisiae strains with a deleted *gsh1* gene encoding γGCS are often respiratory deficient (petite) strains lacking functional mitochondria and are unable to grow on non-fermentable carbons sources, thus indicating the importance of GSH for mitochondrial function in yeast (Grant et al., 1996). A *S. cerevisiae* grande strain with a *ygcs* null mutation was generated, which possesses functional mitochondria but displays a nine times increased tendency to form petite daughter cells and demonstrates again the importance of GSH for the maintenance of functional mitochondria (Lee et al., 2001).

Other cellular changes due to the lack of GSH were reported to occur in *S. cerevisiae* and mammals before any damage in mitochondria is detected. Removal of GSH from the culture medium of a GSH auxotroph Δ*gsh1* strain of *S. cerevisiae* allows these cells to continue growing for approximately 10 cell cycles before GSH levels become limiting and growth arrest is observed (Sipos et al., 2002). After depleting GSH for 8 cell divisions, the mitochondria of these cells are still intact and Fe-S cluster maturation within them is normal and several mitochondrial enzymes display unchanged activity. However, maturation of cytosolic Fe-S proteins is already severely impaired under these conditions, even when cells are cultured under anaerobic conditions (Sipos et al., 2002). The high efficiency of GSH import into the mitochondria, which has been reported in other organisms, may also protect these organelles in *S. cerevisiae* longer from the effects of GSH depletion (Green et al., 2006; Zechmann et al., 2008). In mammalian cells, depletion of GSH leads to increased formation of aberrant proteins in the endoplasmatic reticulum (ER) (Chakravarthi and Bulleid, 2004; Molteni et al., 2004). Unlike in the cytososl, the GSH:GSSG ratio in the ER is between 1:1 and 3:1 and thus allows efficient formation of disulphide bonds (Chakravarthi et al., 2006). GSH acts as the main antagonist of the human Ero1 protein, an oxidase for human protein disulphide isomerase. While Ero1 increases the formation of disulphide bonds in the ER lumen, GSH decreases their formation and can either directly reduce non-native bonds or maintain protein disulphide isomerases in a reduced state so they can in turn reduce and isomerize non-native disulphide bonds in other proteins (Chakravarthi and Bulleid, 2004; Chakravarthi et al., 2006; Molteni et al., 2004). Loss of GSH

decreases the cell's ability to isomerize disulphide bonds and leads to accumulation of aberrant non-native forms of proteins.

GSH is also vital for the function of glutaredoxins. *S. cerevisiae* contains five glutaredoxins (grx1 to 5) and while single null mutants for each glutaredoxin are viable, double mutants for grx2 and grx5 or triple mutants of grx3, grx4 and grx5 are non viable (Rodriguez-Manzaneque et al., 1999). GSH is the hydrogen donor for the reduction of glutaredoxins, which in turn supply reducing equivalents for other enzymes. One important protein that is maintained in a reduced state by glutaredoxins is ribonucleotide reductase, an enzyme involved in deoxyribonucleotide formation for DNA biosynthesis (Holmgren, 1976; Luthman et al., 1979; Prinz et al., 1997).

It may not be one but several cellular processes that depend on the presence of GSH for their function in *P. falciparum* and thus multiple effects may cause lethality if GSH is not present.

6.3.4 Over-expression studies

The generation of three parasite lines expressing recombinant PfγGCS-HA and one line expressing PfGS-HA was in the first instance aimed at elucidating whether (a) episomal expression of both enzymes was possible and (b) whether recombination of the expression plasmids with the endogenous genes is possible and if the respective gene loci can be tagged with the HA-tag sequence.

The genotype of the lines was analysed by Southern blotting and it has also been established by western blotting that both enzymes can be expressed from episomal copies. However, for co-transfection studies the genotypes of any lines have to be established before transfections with knockout constructs, because of the possibility of recombination of the expression constructs with the endogenous gene locus. The recombination between pCHD-derived plasmids and endogenous genes offers the possibility to use this plasmid in the future not only for episomal expression of recombinant proteins, but also to C-terminally tag endogenous genes. The tagging of endogenous genes can also be achieved using sequences homologous to only the 3'-end of the target gene rather than the full ORF, thus ensuring that only one functional copy of the target gene is present in the recombined locus. The generation of parasite lines encoding for endogenous

HA-tagged *pfygcs* and *pfgs* under control of their endogenous promoter without the presence of an additional copy of the genes will be of interest for future studies to analyse the expression pattern of these proteins.

Preliminary data indicate that PfγGCS-HA over-expression decreases sensitivity to L-BSO, while PfGS-HA appears to cause a slight increase in sensitivity to the drug. While no statistical analysis of the significance of these data is possible yet, the decreased sensitivity of the PfγGCS over-expressing line strongly suggests that the parasite enzyme is targeted by the drug and that the anti-malarial effect of L-BSO is not primarily caused by the premature death of the host cell. If the latter was the case, one would expect that changing expression levels in the parasites does not influence the susceptibility to the drug. It also indicates correct folding of the recombinant PfγGCS protein, as the substrate analogue L-BSO binds to the active site in order to inhibit the enzyme and thus would not likely be sequestered by misfolded enzyme.

The observation that PfGS over-expression may increase L-BSO sensitivity in the parasite is rather peculiar and may be caused by an adverse effect of the enzyme in the absence of the substrate γGC. However, this experiment has only been performed once and thus needs to be confirmed in the future. Because of the unexpected banding pattern detected in the genotype analysis of this line, a negative effect of a random recombination event of the plasmid in these parasites is also possible. To further analyse this, a second transfected parasite line should be generated to confirm the results.

Future steps will involve analyses of the GSH levels in these lines, as an over-expression of the biosynthesis enzymes may not generate high GSH levels if the availability of substrates is limited. These lines can provide a tool to determine if γGCS is rate limiting in *P. falciparum*. In yeast, over-expression of the rate limiting γGCS leads to an increase in GSH levels, while the over-expression of GS cannot change GSH levels due to an unchanged supply of γGC (Grant et al., 1997). They can also offer further insight in the role of GSH on redox metabolism and on the redox state of mitochondria and ER. With regard to the hypothesis that elevated GSH levels are related to CQ resistance, the analysis of the susceptibility of these lines to CQ will be highly interesting.

6.4 Glutathione and chloroquine resistance

6.4.1 Glutathione transport by mutant PfCRT

Resistance to CQ is primarily conferred by mutated forms of PfCRT, a DV transmembrane protein that functions either as a channel or a transporter to reduce CQ accumulation in the DV. Other factors also contribute to CQ resistance; parasite strains possessing the same PfCRT allele can widely differ in their susceptibility to CQ. One factor previously suggested to be involved in CQ resistance was GSH.

While in *P. berghei* CQ resistance was found to be correlated with increased GSH levels and increased activity of GST, no such correlation was found in *P. chabaudi*, another murine species (Dubois et al., 1995; Ferreira et al., 2004). In *P. falciparum* CQ resistance appears not to be linked to the activity of GST either, since no CQ conjugates or metabolites can be observed in resistant parasites (Berger et al., 1995). There was no up-regulation of GST expression detected in the CQ resistant parasites in this study.

It has been shown *in vitro* that the tripeptide destroys heme, the target of CQ. Thus it was proposed that GSH modulates CQ sensitivity through removal of the target rather than by direct interaction with CQ (Atamna and Ginsburg, 1995). The heme degradation by GSH can be competitively inhibited by CQ and amodiaquine, suggesting that elevated GSH levels may result in increased CQ resistance (Ginsburg et al., 1998; Ginsburg and Golenser, 2003). Indeed, artificial increase or decrease of GSH levels leads to increased or decreased sensitivity to CQ *in vitro* and *in vivo* (Deharo et al., 2003; Dubois et al., 1995; Ginsburg et al., 1998; Ginsburg and Golenser, 2003; Platel et al., 1999). Higher GSH levels have been reported for the CQ resistant parasite strain Dd2 in comparison to the sensitive strain 3D7 (Meierjohann et al., 2002b).

However, while earlier studies hypothesized that up to 70 % of heme released during hemoglobin degradation reach the cytosol (Ginsburg et al., 1998), later studies showed that the heme released is largely contained within this organelle and less than 5 % reach the cytosol (Egan et al., 2002). The hypothesis that elevated GSH levels contribute to CQ resistance is not consistent with the

intracellular organization of the parasite if GSH is synthesized in the cytosol, as shown in the present study and heme is released and contained within the DV (Egan et al., 2002). Moreover, in CQ resistant parasites CQ is expelled from the food vacuole by mutant PfCRT and it remains unclear how both CQ and GSH should compete for binding to heme retained in the DV (Sanchez et al., 2007b; Valderramos and Fidock, 2006).

To address these problems, we investigated the GSH metabolism and its influence on CQ resistance in four isogenic parasite lines, genetically only differing in their *pfcrt* alleles. The lines analysed were the CQ sensitive lines GC03 and $C2^{GC03}$ and the resistant lines $C3^{Dd2}$ and $C6^{7G8}$. In previous studies on *P. falciparum*, strains widely differing in their genetic background were used and thus it is difficult to conclude if differences in GSH metabolism are a cause or a consequence of CQ resistance. We proposed that with the lines used in this study, we would be able to manipulate GSH levels and be able to directly analyse the effects of GSH metabolism on CQ susceptibility in CQ sensitive and resistant parasites. In collaboration with colleagues at the Liverpool School of Tropical Medicine we found an unsuspected role for PfCRT in changing the distribution of GSH within the parasite cell.

I confirmed the susceptibility to CQ of the four lines and found that all lines show the expected CQ sensitive or resistant phenotype (Sidhu et al., 2002). Extracellular GSH has only a marginal effect on the CQ IC_{50} in these lines. Despite uptake of GSH into infected RBC, the increase of GSH in the RBC cytosol has little effect on the CQ IC_{50}. Several lines of evidence suggest that GSH in the host cell cytosol is delivered to the DV within endocytotic vesicles and thus an increase of RBC GSH can potentially benefit parasites under CQ pressure. This was in particular suggested as a mechanism of decreased susceptibility for CQ resistant *P. berghei* parasites infecting reticulocytes (Platel et al., 1999; Vega-Rodriguez et al., 2009). However, GSH uptake into the DV by this mechanism may be too little and the rate of endocytosis too slow to allow additional GSH in the medium to compete against CQ, which can enter the DV much faster by diffusion. It is possible that higher concentrations of extracellular GSH than the 1 mM concentration tested in this study have a more pronounced effect.

Surprisingly, the allelic exchange of *pfcrt* led to significantly reduced GSH levels in the two CQ resistant lines analysed. In some previous studies GSH levels of *P. falciparum* were reported to be between 0.07 and 0.14 µmol/ 10^{10} cells in sensitive and resistant parasites (Lüersen et al., 2000; Meierjohann et al., 2002b), while other authors reported higher GSH levels of 0.79 µmol / 10^{10} cells (Atamna and Ginsburg, 1997). The GSH levels I determined in the present study were between 0.75 and 1.5 µmol/ 10^{10} cells and thus similar to those reported by Atamna and Ginsburg. Both Lüersen and Meierjohann determined GSH levels after parasitized RBC had been purified from non-infected RBC with Percoll and gelafundin gradients. During this study, I found that purification with MACS columns greatly decreases the GSH levels in the parasites and it is likely that other purification methods have similar effects on the GSH levels, which can explain the differences between the various studies. The GSH levels I determined without initial enriching of infected RBC were also in the range of GSH levels previously reported for *P. berghei* parasites, where infected RBC equally had not been purified prior to lysis and determination of GSH content (Dubois et al., 1995; Platel et al., 1999). The *P. berghei* GSH levels ranged from 0.2 µmol/ 10^{10} cells for CQ sensitive strains to 2.7 µmol/ 10^{10} cells for CQ resistant stains. Interestingly, the differences I detected between CQ sensitive $C2^{GC03}$ parasites and CQ resistant $C6^{7G8}$ parasites remained, regardless of the isolation method employed, with the resistant line displaying lower GSH levels. The lower GSH levels in $C3^{Dd2}$ and $C6^{7G8}$ are not consistent with the previous hypothesis that CQ resistant parasites display elevated GSH levels (reviewed in(Ginsburg and Golenser, 2003)).

Despite the different GSH levels, the susceptibility to oxidative stress remained largely unchanged in the parasites. Both juglone and phenazine methyl sulphate are considered as inducers of intracellular oxidative stress due to their ability to cross cell membranes. While juglone is a redox-active naphthoquinone, phenazine methyl sulphate generates superoxide anions (Kampkotter et al., 2003; Nishikimi et al., 1972). This suggests that even though reduced in CQ resistant lines, GSH levels are still sufficient for the maintenance of an efficient antioxidant system. Using a less specific way to deplete GSH with CDNB, a GST substrate, I found no significant differences between the isogenic parasite lines, although the resistant lines appeared slightly more susceptible to the drug. A technical problem with CDNB and both juglone and phenazine methyl sulphate is

their low solubility in aqueous solutions such as RPMI medium. This results in a high variability between the data in independent assays and therefore it has to be considered that small differences between the parasite lines may not have been detected.

The lower GSH levels in CQ resistant parasites were however accompanied by significantly increased sensitivity to the inhibition of GSH biosynthesis by L-BSO. This is not due to a difference in mRNA expression of the two genes involved in GSH biosynthesis and presumably also not the amount of the proteins in the cells. GSH uptake into infected RBC was investigated in one sensitive and one resistant line and no significant difference was detected. This suggests that the lower GSH levels may be caused by an increased loss of GSH from the resistant parasites. A decrease in GR can potentially cause an increased efflux of GSSG from the cells in order to maintain a high GSH:GSSG ratio and thus lead to an enhanced loss of GSH (Lüersen et al., 2000). This efflux should be investigated in future studies. However, we did not find a difference in GR expression between the lines analysed, suggesting that this might not be the reason for increased loss of GSH or GSSG. Equal levels of GST also suggest that there is no difference in GSH-conjugation between the PfCRT allelic-exchanged lines. We did not investigate the activity of these enzymes in the parasites and it is possible that lower GSH levels could negatively affect the activity of GST (Tripathi et al., 2007).

When PfCRT was expressed in oocytes of *X. laevis* our collaborators found conclusive evidence that the mutant, but not the wild-type form of PfCRT, is capable of transporting GSH across membranes. A role of PfCRT as transporter for small peptides has previously been suggested from bioinformatic studies (Martin and Kirk, 2004), but no natural substrate has yet been identified. Unfortunately our study does not change this, as we only observed uptake of GSH by mutant, but not wild-type PfCRT.

6.4.2 Effects of glutathione re-distribution

How can the transport of GSH by mutant PfCRT explain the lower GSH levels and greater sensitivity to L-BSO in resistant parasites? The transport of erythrocyte derived GSH from the DV into the cytosol should increase the GSH levels in these

parasites rather than decrease them. The data presented in this study suggest that GSH is likely to be transported into the opposite direction, from the cytosol into the DV. Inside this organelle the multitude of peptidases may eventually destroy GSH by proteolysis and thus decrease the overall GSH level in the parasite. Destruction of GSH by carboxypeptidases and dipeptidases has been suggested for plant vacuoles, which do not contain any detectable levels of GSH (Foyer et al., 2001; Wolf et al., 1996; Zechmann et al., 2008). Degradation of erythrocyte derived GSH may be an important source for the amino acids cysteine and glutamate, which are both limited in hemoglobin (Francis et al., 1997).

The efflux of GSH into the DV of resistant parasite lines only offers an explanation as to why NAC increases the CQ IC_{50} of resistant $C3^{Dd2}$ while only marginally affecting sensitive $C2^{GC03}$ parasites. If GSH cannot enter the DV and thus has no access to heme, an increase in its biosynthesis can only have a slight effect on the parasites' general fitness by protecting it from some of the CQ induced damage. However, if GSH biosynthesis is increased and the tripeptide is subsequently transported into the DV, increased heme degradation by GSH results in a reduced concentration of the heme target and increased CQ resistance. GSH was shown to destroy heme at neutral pH as well as at the acidic pH found inside the DV, albeit less efficiently (Atamna and Ginsburg, 1995).

A reduced concentration of free heme due to degradation by GSH is consistent with the reduced accumulation ratio of CQ observed in this study and with reduced CQ binding in the CQ resistant progeny of a genetic cross reported previously (Sanchez et al., 1997). It is also consistent with the reported lower hemozoin concentration of the $C3^{Dd2}$ line compared to $C2^{GC03}$ (Gligorijevic et al., 2006b). In addition to the destruction of free heme, GSH inside the DV is able to compete with CQ for the binding to the remaining heme (Ginsburg et al., 1998).

It is currently a subject of debate whether PfCRT acts as a channel, permitting passive diffusion, or an active transporter for CQ (recently reviewed in (Sanchez et al., 2007b). Our results do not offer any further insight which model is appropriate, as the transport or flux of GSH across the DV membrane can be accommodated into both models. It is likely that the GSH concentration inside the DV is substantially lower than the millimolar concentration found in the

cytosol and the resulting gradient potentially drives the influx of GSH. Furthermore, in the near neutral pH of the parasite cytosol GSH is deprotonated and thus negatively charged. The positive charge in the DV may also drive the flux of GSH. In the wild-type form of PfCRT, the positive charge at the lysine at position 76 possibly retains negatively charged GSH and thus does not allow flux of the tripeptide into the food vacuole. If PfCRT is a carrier and not a channel, GSH translocation is potentially coupled to CQ transport and the inward movement could trans-accelerate the CQ efflux. These hypotheses will be investigated in detail in the future.

We found an intriguing effect of CDNB on CQ accumulation in this study. While killing parasites at low µM concentrations and reversing CQ resistance (Ginsburg et al., 1998), it also caused an increase in CQ accumulation in resistant parasites similar to the effect of verapamil. The depletion of GSH by CDNB minimizes or stops the influx of GSH into the DV and thus CQ no longer has to compete with the tripeptide for the binding to heme and accumulation increases. Regarding the carrier model of PfCRT, the depletion the tripeptide potentially depletes a trans-acceleration of CQ efflux by GSH. It is further possible, that the GS-CDNB adduct is another substrate for mutated PfCRT, but unlike GSH alone, the lipophilic adduct could inhibit a channel or transporter in a similar way as postulated for verapamil (Bray et al., 2005; Cooper et al., 2002; Lakshmanan et al., 2005; Sidhu et al., 2002).

If mutations of PfCRT are responsible for the translocation of GSH into the DV where it is subsequently degraded, it raises the question why the previously analysed CQ resistant line Dd2 has a higher GSH level than the sensitive line 3D7 (Meierjohann et al., 2002b). These two lines are however not isogenic and the Dd2 line has been shown to contain a higher activity of PfγGCS than 3D7, which is likely to compensate for any loss of GSH into the DV. Such adaptations are likely to be important for the parasites as the reduced cytoplasmic GSH levels may well have a fitness cost for these lines. The four isogenic parasite lines analysed in this study did not display any differences in their expression levels for PfγGCS and PfGS, suggesting they may not have adapted in a similar way as the field isolates to the re-distribution of GSH. These laboratory generated lines will not have encountered the same selective pressures that can cause changes in field isolates. Since the GC03 parental line of our genetically modified

parasites is the progeny of a genetic cross between the strains HB3 and Dd2, it is also possible that the isogenic lines have inherited the adaptations in the Dd2 GSH metabolism responsible for high levels of GSH biosynthesis. This suggests that potentially the two CQ sensitive lines GC03 and $C2^{GC03}$ have a comparably high GSH level and the resistant lines $C3^{Dd2}$ and $C6^{7G8}$ have a more normal level. This could be further investigated by determination of GSH levels in a variety of parasite strains of the Dd2 x HB3 progeny in order to determine an "average" GSH level for CQ sensitive *P. falciparum*. Comparisons to other studies are difficult, because as I have shown here the method of sample preparation can deplete cells of GSH.

The re-emergence of CQ sensitive parasites after withdrawal of CQ use in areas where resistance has been widespread, indicates that changes to PfCRT have a negative effect on parasite fitness. One of these negative side effects caused by PfCRT mutations is the decrease in the cytosolic GSH concentration, where GSH has to be constantly re-synthesized to maintain a variety of cellular functions.

Recently it has been demonstrated that the DV in CQ resistant parasites is larger than in sensitive parasites (Gligorijevic et al., 2006a). The GSH influx and thus increasing GSH concentration inside the DV is a potential reason for increased osmotic pressure and swelling of the DV. Furthermore, influx of GSH may further acidify the DV and thus offers one possible explanation for the lower DV pH of resistant parasites found in some studies (Bennett et al., 2004; Gligorijevic et al., 2006a).

6.5 Conclusions and future perspectives

The low molecular weight thiol GSH serves very important functions in the malaria parasite *P. falciparum* and several studies have indicated that the tripeptide is an essential metabolite for the parasites (Atamna and Ginsburg, 1997; Lüersen et al., 2000). However, several organisms can scavenge GSH, provided they are supplied with high enough concentrations of the tripeptide and thus are not dependent on its *de novo* synthesis (Baek et al., 2004; Grant et al., 1996; Huynh et al., 2003; Kim et al., 2005; Lee et al., 2001). This appears to be the case in the rodent parasite, *P. berghei* (Vega-Rodriguez et al., 2009). However, the results of this study indicate a different situation in the human

parasite *P. falciparum*, where a knockout of the GSH biosynthesis pathway cannot be achieved. The reasons for this are likely to be that *P. falciparum* cannot scavenge GSH to the same extent as *P. berghei*, as well as a greater redundancy in the antioxidant system of the murine parasite than in that of the human pathogen. Future studies will need to investigate the possibility of GSH uptake by the parasites in more detail.

Overall these results show a great importance for an effective antioxidant system in malaria parasites. That GSH levels in the host cell and in the blood plasma may determine the importance of the GSH biosynthesis has some implications on the potential of γGCS and GS as drug targets for malaria parasites in general, especially for those species that invade reticulocytes such as *P. vivax*. The importance of GSH for malaria parasites remains unquestioned, but the importance of its *de novo* biosynthesis appears to vary between the different species of *Plasmodium*. Redundancy between single components of the antioxidant system means that more than one component will have to be targeted at any one time to inhibit or kill the parasites. However, drugs lowering GSH levels in parasites may be interesting for combination therapies.

The results of this study also show some of the problems when working with a model organism. Despite the obvious advantages of working with an *in vivo* rather than an *in vitro* system and being able to study all the life cycle stages of *Plasmodium* in the rodent parasite, *P. berghei* does not always resemble the situation in *P. falciparum*.

We found an unsuspected additional role for mutant PfCRT in CQ resistance through the redistribution of GSH. This redistribution can amplify CQ resistance and provides further insight into how the variety of resistant phenotypes of *P. falciparum* is established, which cannot be explained by the efflux of CQ alone. It also offers an answer to the question how cytosolic GSH can gain access to and destroy FPIX in the parasites DV. This can be further analysed in the future with parasite lines over-expressing PfγGCS and PfGS in CQ sensitive and CQ resistant backgrounds. From the results obtained in this study, one would expect that the over-expression will significantly alter the CQ IC_{50} in those lines possessing mutant forms of PfCRT, but not in those with a wild-type form. CQ sensitive

lines over-expressing the enzymes have already been generated and the transfection of a CQ resistant strain is currently in progress.

The transport of GSH by the mutant forms of PfCRT clearly demonstrates the ability of PfCRT to transport small peptides, a function previously suggested by bioinformatic analyses (Martin and Kirk, 2004). Unfortunately the natural substrate of wild-type PfCRT sill remains elusive.

7 References

Akoachere, M., Iozef, R., Rahlfs, S., Deponte, M., Mannervik, B., Creighton, D. J., Schirmer, H., and Becker, K. (2005). Characterization of the glyoxalases of the malarial parasite *Plasmodium falciparum* and comparison with their human counterparts. Biol Chem *386*, 41-52.

Aly, A. S., and Matuschewski, K. (2005). A malarial cysteine protease is necessary for *Plasmodium* sporozoite egress from oocysts. J Exp Med *202*, 225-230.

Armstrong, C. M., and Goldberg, D. E. (2007). An FKBP destabilization domain modulates protein levels in *Plasmodium falciparum*. Nat Methods *4*, 1007-1009.

Aslan, M., and Freeman, B. A. (2007). Redox-dependent impairment of vascular function in sickle cell disease. Free Radic Biol Med *43*, 1469-1483.

Atamna, H., and Ginsburg, H. (1993). Origin of reactive oxygen species in erythrocytes infected with *Plasmodium falciparum*. Mol Biochem Parasitol *61*, 231-241.

Atamna, H., and Ginsburg, H. (1995). Heme degradation in the presence of glutathione. A proposed mechanism to account for the high levels of non-heme iron found in the membranes of hemoglobinopathic red blood cells. J Biol Chem *270*, 24876-24883.

Atamna, H., and Ginsburg, H. (1997). The malaria parasite supplies glutathione to its host cell--investigation of glutathione transport and metabolism in human erythrocytes infected with *Plasmodium falciparum*. Eur J Biochem *250*, 670-679.

Atamna, H., Pascarmona, G., and Ginsburg, H. (1994). Hexose-monophosphate shunt activity in intact *Plasmodium falciparum*-infected erythrocytes and in free parasites. Mol Biochem Parasitol *67*, 79-89.

Ayi, K., Cappadoro, M., Branca, M., Turrini, F., and Arese, P. (1998). *Plasmodium falciparum* glutathione metabolism and growth are independent of glutathione system of host erythrocyte. FEBS Lett *424*, 257-261.

Baek, Y. U., Kim, Y. R., Yim, H. S., and Kang, S. O. (2004). Disruption of gamma-glutamylcysteine synthetase results in absolute glutathione auxotrophy and apoptosis in *Candida albicans*. FEBS Lett *556*, 47-52.

Baldwin, J., Farajallah, A. M., Malmquist, N. A., Rathod, P. K., and Phillips, M. A. (2002). Malarial dihydroorotate dehydrogenase. Substrate and inhibitor specificity. J Biol Chem *277*, 41827-41834.

Balendiran, G. K., Dabur, R., and Fraser, D. (2004). The role of glutathione in cancer. Cell Biochem Funct *22*, 343-352.

Banaszynski, L. A., Chen, L. C., Maynard-Smith, L. A., Ooi, A. G., and Wandless, T. J. (2006). A rapid, reversible, and tunable method to regulate protein function in living cells using synthetic small molecules. Cell *126*, 995-1004.

Banerjee, R., Liu, J., Beatty, W., Pelosof, L., Klemba, M., and Goldberg, D. E. (2002). Four plasmepsins are active in the *Plasmodium falciparum* food vacuole, including a protease with an active-site histidine. Proc Natl Acad Sci U S A *99*, 990-995.

Banhegyi, G., Lusini, L., Puskas, F., Rossi, R., Fulceri, R., Braun, L., Mile, V., di Simplicio, P., Mandl, J., and Benedetti, A. (1999). Preferential transport of glutathione versus glutathione disulfide in rat liver microsomal vesicles. J Biol Chem *274*, 12213-12216.

Bannister, L. H., Hopkins, J. M., Fowler, R. E., Krishna, S., and Mitchell, G. H. (2000). A brief illustrated guide to the ultrastructure of *Plasmodium falciparum* asexual blood stages. Parasitol Today *16*, 427-433.

Banyal, H. S., and Fitch, C. D. (1982). Ferriprotoporphyrin IX binding substances and the mode of action of chloroquine against malaria. Life Sci *31*, 1141-1144.

Becker, K., Kanzok, S. M., Iozef, R., Fischer, M., Schirmer, R. H., and Rahlfs, S. (2003a). Plasmoredoxin, a novel redox-active protein unique for malarial parasites. Eur J Biochem *270*, 1057-1064.

Becker, K., Rahlfs, S., Nickel, C., and Schirmer, R. H. (2003b). Glutathione--functions and metabolism in the malarial parasite *Plasmodium falciparum*. Biol Chem *384*, 551-566.

Becker, K., Tilley, L., Vennerstrom, J. L., Roberts, D., Rogerson, S., and Ginsburg, H. (2004). Oxidative stress in malaria parasite-infected erythrocytes: host-parasite interactions. Int J Parasitol *34*, 163-189.

Bennett, T. N., Kosar, A. D., Ursos, L. M., Dzekunov, S., Singh Sidhu, A. B., Fidock, D. A., and Roepe, P. D. (2004). Drug resistance-associated pfCRT mutations confer decreased *Plasmodium falciparum* digestive vacuolar pH. Mol Biochem Parasitol *133*, 99-114.

Berger, B. J., Martiney, J., Slater, A. F., Fairlamb, A. H., and Cerami, A. (1995). Chloroquine resistance is not associated with drug metabolism in *Plasmodium falciparum*. J Parasitol *81*, 1004-1008.

Blackman, M. J. (2008). Malarial proteases and host cell egress: an 'emerging' cascade. Cell Microbiol *10*, 1925-1934.

Boucher, I. W., McMillan, P. J., Gabrielsen, M., Akerman, S. E., Brannigan, J. A., Schnick, C., Brzozowski, A. M., Wilkinson, A. J., and Muller, S. (2006). Structural and biochemical characterization of a mitochondrial peroxiredoxin from *Plasmodium falciparum*. Mol Microbiol *61*, 948-959.

Bozdech, Z., Llinas, M., Pulliam, B. L., Wong, E. D., Zhu, J., and DeRisi, J. L. (2003). The transcriptome of the intraerythrocytic developmental cycle of *Plasmodium falciparum*. PLoS Biol *1*, E5.

Bradford, M. M. (1976). A rapid and sensitive method for the quantitation of microgram quantities of protein utilizing the principle of protein-dye binding. Anal Biochem *72*, 248-254.

Braman, J., Papworth, C., and Greener, A. (1996). Site-directed mutagenesis using double-stranded plasmid DNA templates. Methods Mol Biol *57*, 31-44.

Bray, P. G., Janneh, O., Raynes, K. J., Mungthin, M., Ginsburg, H., and Ward, S. A. (1999). Cellular uptake of chloroquine is dependent on binding to ferriprotoporphyrin IX and is independent of NHE activity in *Plasmodium falciparum*. J Cell Biol *145*, 363-376.

Bray, P. G., Martin, R. E., Tilley, L., Ward, S. A., Kirk, K., and Fidock, D. A. (2005). Defining the role of PfCRT in *Plasmodium falciparum* chloroquine resistance. Mol Microbiol *56*, 323-333.

Bray, P. G., Mungthin, M., Hastings, I. M., Biagini, G. A., Saidu, D. K., Lakshmanan, V., Johnson, D. J., Hughes, R. H., Stocks, P. A., O'Neill P, M., *et al*. (2006). PfCRT and the trans-vacuolar proton electrochemical gradient: regulating the access of chloroquine to ferriprotoporphyrin IX. Mol Microbiol *62*, 238-251.

Bray, P. G., Mungthin, M., Ridley, R. G., and Ward, S. A. (1998). Access to hematin: the basis of chloroquine resistance. Mol Pharmacol *54*, 170-179.

Buchholz, K., Rahlfs, S., Schirmer, R. H., Becker, K., and Matuschewski, K. (2008). Depletion of *Plasmodium berghei* plasmoredoxin reveals a non-essential role for life cycle progression of the malaria parasite. PLoS ONE *3*, e2474.

Cappadoro, M., Giribaldi, G., O'Brien, E., Turrini, F., Mannu, F., Ulliers, D., Simula, G., Luzzatto, L., and Arese, P. (1998). Early phagocytosis of glucose-6-phosphate dehydrogenase (G6PD)-deficient erythrocytes parasitized by *Plasmodium falciparum* may explain malaria protection in G6PD deficiency. Blood *92*, 2527-2534.

Chakravarthi, S., and Bulleid, N. J. (2004). Glutathione is required to regulate the formation of native disulfide bonds within proteins entering the secretory pathway. J Biol Chem *279*, 39872-39879.

Chakravarthi, S., Jessop, C. E., and Bulleid, N. J. (2006). The role of glutathione in disulphide bond formation and endoplasmic-reticulum-generated oxidative stress. EMBO Rep *7*, 271-275.

Chang, L. S. (1996). The functional involvement of Lys-38 in the heavy subunit of rat kidney gamma-glutamylcysteine synthetase: chemical modification and mutagenesis studies. J Protein Chem *15*, 321-326.

Chapeland-Leclerc, F., Bouchoux, J., Goumar, A., Chastin, C., Villard, J., and Noel, T. (2005). Inactivation of the FCY2 gene encoding purine-cytosine permease promotes cross-resistance to flucytosine and fluconazole in *Candida lusitaniae*. Antimicrob Agents Chemother *49*, 3101-3108.

Chaudhuri, B., Ingavale, S., and Bachhawat, A. K. (1997). apd1+, a gene required for red pigment formation in ade6 mutants of *Schizosaccharomyces*

pombe, encodes an enzyme required for glutathione biosynthesis: a role for glutathione and a glutathione-conjugate pump. Genetics *145*, 75-83.

Chen, N., Kyle, D. E., Pasay, C., Fowler, E. V., Baker, J., Peters, J. M., and Cheng, Q. (2003). pfcrt Allelic types with two novel amino acid mutations in chloroquine-resistant *Plasmodium falciparum* isolates from the Philippines. Antimicrob Agents Chemother *47*, 3500-3505.

Chen, Z., and Lash, L. H. (1998). Evidence for mitochondrial uptake of glutathione by dicarboxylate and 2-oxoglutarate carriers. J Pharmacol Exp Ther *285*, 608-618.

Chou, A. C., Chevli, R., and Fitch, C. D. (1980). Ferriprotoporphyrin IX fulfills the criteria for identification as the chloroquine receptor of malaria parasites. Biochemistry *19*, 1543-1549.

Chou, A. C., and Fitch, C. D. (1993). Control of heme polymerase by chloroquine and other quinoline derivatives. Biochem Biophys Res Commun *195*, 422-427.

Cogswell, F. B. (1992). The hypnozoite and relapse in primate malaria. Clin Microbiol Rev *5*, 26-35.

Cooper, R. A., Ferdig, M. T., Su, X. Z., Ursos, L. M., Mu, J., Nomura, T., Fujioka, H., Fidock, D. A., Roepe, P. D., and Wellems, T. E. (2002). Alternative mutations at position 76 of the vacuolar transmembrane protein PfCRT are associated with chloroquine resistance and unique stereospecific quinine and quinidine responses in *Plasmodium falciparum*. Mol Pharmacol *61*, 35-42.

Cooper, R. A., Hartwig, C. L., and Ferdig, M. T. (2005). pfcrt is more than the *Plasmodium falciparum* chloroquine resistance gene: a functional and evolutionary perspective. Acta Trop *94*, 170-180.

Copley, S. D., and Dhillon, J. K. (2002). Lateral gene transfer and parallel evolution in the history of glutathione biosynthesis genes. Genome Biol *3*, research0025.

Cowman, A. F., Coppel, R. L., Saint, R. B., Favaloro, J., Crewther, P. E., Stahl, H. D., Bianco, A. E., Brown, G. V., Anders, R. F., and Kemp, D. J. (1984). The ring-infected erythrocyte surface antigen (RESA) polypeptide of *Plasmodium*

falciparum contains two separate blocks of tandem repeats encoding antigenic epitopes that are naturally immunogenic in man. Mol Biol Med *2*, 207-221.

Cowman, A. F., and Crabb, B. S. (2006). Invasion of red blood cells by malaria parasites. Cell *124*, 755-766.

Cowman, A. F., Galatis, D., and Thompson, J. K. (1994). Selection for mefloquine resistance in *Plasmodium falciparum* is linked to amplification of the pfmdr1 gene and cross-resistance to halofantrine and quinine. Proc Natl Acad Sci U S A *91*, 1143-1147.

Cowman, A. F., Karcz, S., Galatis, D., and Culvenor, J. G. (1991). A P-glycoprotein homologue of *Plasmodium falciparum* is localized on the digestive vacuole. J Cell Biol *113*, 1033-1042.

Crabb, B. S., Cooke, B. M., Reeder, J. C., Waller, R. F., Caruana, S. R., Davern, K. M., Wickham, M. E., Brown, G. V., Coppel, R. L., and Cowman, A. F. (1997). Targeted gene disruption shows that knobs enable malaria-infected red cells to cytoadhere under physiological shear stress. Cell *89*, 287-296.

Crabb, B. S., and Cowman, A. F. (1996). Characterization of promoters and stable transfection by homologous and nonhomologous recombination in *Plasmodium falciparum*. Proc Natl Acad Sci U S A *93*, 7289-7294.

Crabb, B. S., Rug, M., Gilberger, T. W., Thompson, J. K., Triglia, T., Maier, A. G., and Cowman, A. F. (2004). Transfection of the human malaria parasite *Plasmodium falciparum*. Methods Mol Biol *270*, 263-276.

Cromer, D., Evans, K. J., Schofield, L., and Davenport, M. P. (2006). Preferential invasion of reticulocytes during late-stage *Plasmodium berghei* infection accounts for reduced circulating reticulocyte levels. Int J Parasitol *36*, 1389-1397.

Cummings, B. S., Angeles, R., McCauley, R. B., and Lash, L. H. (2000). Role of voltage-dependent anion channels in glutathione transport into yeast mitochondria. Biochem Biophys Res Commun *276*, 940-944.

Dahl, E. L., and Rosenthal, P. J. (2005). Biosynthesis, localization, and processing of falcipain cysteine proteases of *Plasmodium falciparum*. Mol Biochem Parasitol *139*, 205-212.

Dahl, N., Pigg, M., Ristoff, E., Gali, R., Carlsson, B., Mannervik, B., Larsson, A., and Board, P. (1997). Missense mutations in the human glutathione synthetase gene result in severe metabolic acidosis, 5-oxoprolinuria, hemolytic anemia and neurological dysfunction. Hum Mol Genet *6*, 1147-1152.

Dalton, T. P., Chen, Y., Schneider, S. N., Nebert, D. W., and Shertzer, H. G. (2004). Genetically altered mice to evaluate glutathione homeostasis in health and disease. Free Radic Biol Med *37*, 1511-1526.

Deharo, E., Barkan, D., Krugliak, M., Golenser, J., and Ginsburg, H. (2003). Potentiation of the antimalarial action of chloroquine in rodent malaria by drugs known to reduce cellular glutathione levels. Biochem Pharmacol *66*, 809-817.

Desjardins, R. E., Canfield, C. J., Haynes, J. D., and Chulay, J. D. (1979). Quantitative assessment of antimalarial activity in vitro by a semiautomated microdilution technique. Antimicrob Agents Chemother *16*, 710-718.

Dinescu, A., Cundari, T. R., Bhansali, V. S., Luo, J. L., and Anderson, M. E. (2004). Function of conserved residues of human glutathione synthetase: implications for the ATP-grasp enzymes. J Biol Chem *279*, 22412-22421.

Dorin-Semblat, D., Quashie, N., Halbert, J., Sicard, A., Doerig, C., Peat, E., Ranford-Cartwright, L., and Doerig, C. (2007). Functional characterization of both MAP kinases of the human malaria parasite *Plasmodium falciparum* by reverse genetics. Mol Microbiol *65*, 1170-1180.

Dubois, V. L., Platel, D. F., Pauly, G., and Tribouley-Duret, J. (1995). *Plasmodium berghei*: implication of intracellular glutathione and its related enzyme in chloroquine resistance in vivo. Exp Parasitol *81*, 117-124.

Eaton, J. W., Eckman, J. R., Berger, E., and Jacob, H. S. (1976). Suppression of malaria infection by oxidant-sensitive host erythrocytes. Nature *264*, 758-760.

Eckstein-Ludwig, U., Webb, R. J., Van Goethem, I. D., East, J. M., Lee, A. G., Kimura, M., O'Neill, P. M., Bray, P. G., Ward, S. A., and Krishna, S. (2003). Artemisinins target the SERCA of *Plasmodium falciparum*. Nature *424*, 957-961.

Egan, T. J., Chen, J. Y., de Villiers, K. A., Mabotha, T. E., Naidoo, K. J., Ncokazi, K. K., Langford, S. J., McNaughton, D., Pandiancherri, S., and Wood, B.

R. (2006). Haemozoin (beta-haematin) biomineralization occurs by self-assembly near the lipid/water interface. FEBS Lett *580*, 5105-5110.

Egan, T. J., Combrinck, J. M., Egan, J., Hearne, G. R., Marques, H. M., Ntenteni, S., Sewell, B. T., Smith, P. J., Taylor, D., van Schalkwyk, D. A., and Walden, J. C. (2002). Fate of haem iron in the malaria parasite *Plasmodium falciparum*. Biochem J *365*, 343-347.

Eisen, D., Billman-Jacobe, H., Marshall, V. F., Fryauff, D., and Coppel, R. L. (1998). Temporal variation of the merozoite surface protein-2 gene of *Plasmodium falciparum*. Infect Immun *66*, 239-246.

Fahey, R. C., Brown, W. C., Adams, W. B., and Worsham, M. B. (1978). Occurrence of glutathione in bacteria. J Bacteriol *133*, 1126-1129.

Fairfield, A. S., Meshnick, S. R., and Eaton, J. W. (1983). Malaria parasites adopt host cell superoxide dismutase. Science *221*, 764-766.

Fairlamb, A. H., and Cerami, A. (1992). Metabolism and functions of trypanothione in the Kinetoplastida. Annu Rev Microbiol *46*, 695-729.

Farber, P. M., Arscott, L. D., Williams, C. H., Jr., Becker, K., and Schirmer, R. H. (1998). Recombinant *Plasmodium falciparum* glutathione reductase is inhibited by the antimalarial dye methylene blue. FEBS Lett *422*, 311-314.

Farber, P. M., Becker, K., Muller, S., Schirmer, R. H., and Franklin, R. M. (1996). Molecular cloning and characterization of a putative glutathione reductase gene, the PfGR2 gene, from *Plasmodium falciparum*. Eur J Biochem *239*, 655-661.

Feagin, J. E., Mericle, B. L., Werner, E., and Morris, M. (1997). Identification of additional rRNA fragments encoded by the *Plasmodium falciparum* 6 kb element. Nucleic Acids Res *25*, 438-446.

Feagin, J. E., Werner, E., Gardner, M. J., Williamson, D. H., and Wilson, R. J. (1992). Homologies between the contiguous and fragmented rRNAs of the two *Plasmodium falciparum* extrachromosomal DNAs are limited to core sequences. Nucleic Acids Res *20*, 879-887.

Ferreira, I. D., Nogueira, F., Borges, S. T., do Rosario, V. E., and Cravo, P. (2004). Is the expression of genes encoding enzymes of glutathione (GSH)

metabolism involved in chloroquine resistance in *Plasmodium chabaudi* parasites? Mol Biochem Parasitol *136*, 43-50.

Fibach, E., and Rachmilewitz, E. (2008). The role of oxidative stress in hemolytic anemia. Curr Mol Med *8*, 609-619.

Fidock, D. A., Nomura, T., Talley, A. K., Cooper, R. A., Dzekunov, S. M., Ferdig, M. T., Ursos, L. M., Sidhu, A. B., Naude, B., Deitsch, K. W., *et al*. (2000). Mutations in the *P. falciparum* digestive vacuole transmembrane protein PfCRT and evidence for their role in chloroquine resistance. Mol Cell *6*, 861-871.

Fitch, C. D. (1989). Ferriprotoporphyrin IX: role in chloroquine susceptibility and resistance in malaria. Prog Clin Biol Res *313*, 45-52.

Fitch, C. D. (2004). Ferriprotoporphyrin IX, phospholipids, and the antimalarial actions of quinoline drugs. Life Sci *74*, 1957-1972.

Fitch, C. D., Chevli, R., Banyal, H. S., Phillips, G., Pfaller, M. A., and Krogstad, D. J. (1982). Lysis of *Plasmodium falciparum* by ferriprotoporphyrin IX and a chloroquine-ferriprotoporphyrin IX complex. Antimicrob Agents Chemother *21*, 819-822.

Fojo, T., and Bates, S. (2003). Strategies for reversing drug resistance. Oncogene *22*, 7512-7523.

Foley, M., and Tilley, L. (1998). Quinoline antimalarials: mechanisms of action and resistance and prospects for new agents. Pharmacol Ther *79*, 55-87.

Foote, S. J., Thompson, J. K., Cowman, A. F., and Kemp, D. J. (1989). Amplification of the multidrug resistance gene in some chloroquine-resistant isolates of *P. falciparum*. Cell *57*, 921-930.

Foth, B. J., Stimmler, L. M., Handman, E., Crabb, B. S., Hodder, A. N., and McFadden, G. I. (2005). The malaria parasite *Plasmodium falciparum* has only one pyruvate dehydrogenase complex, which is located in the apicoplast. Mol Microbiol *55*, 39-53.

Foyer, C. H., Theodoulou, F. L., and Delrot, S. (2001). The functions of inter- and intracellular glutathione transport systems in plants. Trends Plant Sci *6*, 486-492.

Francis, S. E., Sullivan, D. J., Jr., and Goldberg, D. E. (1997). Hemoglobin metabolism in the malaria parasite *Plasmodium falciparum*. Annu Rev Microbiol *51*, 97-123.

Friedman, M. J. (1978). Erythrocytic mechanism of sickle cell resistance to malaria. Proc Natl Acad Sci U S A *75*, 1994-1997.

Fritsch, B., Dieckmann, A., Menz, B., Hempelmann, E., Fritsch, K. G., Fritsch, G., and Jung, A. (1987). Glutathione and peroxide metabolism in malaria-parasitized erythrocytes. Parasitol Res *73*, 515-517.

Gardner, M. J., Hall, N., Fung, E., White, O., Berriman, M., Hyman, R. W., Carlton, J. M., Pain, A., Nelson, K. E., Bowman, S., *et al*. (2002). Genome sequence of the human malaria parasite *Plasmodium falciparum*. Nature *419*, 498-511.

Gardner, P. R., and Fridovich, I. (1993). Effect of glutathione on aconitase in *Escherichia coli*. Arch Biochem Biophys *301*, 98-102.

Geminard, C., de Gassart, A., and Vidal, M. (2002). Reticulocyte maturation: mitoptosis and exosome release. Biocell *26*, 205-215.

Gilberger, T. W., Schirmer, R. H., Walter, R. D., and Muller, S. (2000). Deletion of the parasite-specific insertions and mutation of the catalytic triad in glutathione reductase from chloroquine-sensitive *Plasmodium falciparum* 3D7. Mol Biochem Parasitol *107*, 169-179.

Ginsburg, H., and Atamna, H. (1994). The redox status of malaria-infected erythrocytes: an overview with an emphasis on unresolved problems. Parasite *1*, 5-13.

Ginsburg, H., Famin, O., Zhang, J., and Krugliak, M. (1998). Inhibition of glutathione-dependent degradation of heme by chloroquine and amodiaquine as a possible basis for their antimalarial mode of action. Biochem Pharmacol *56*, 1305-1313.

Ginsburg, H., and Golenser, J. (2003). Glutathione is involved in the antimalarial action of chloroquine and its modulation affects drug sensitivity of human and murine species of *Plasmodium*. Redox Rep *8*, 276-279.

Giribaldi, G., Ulliers, D., Mannu, F., Arese, P., and Turrini, F. (2001). Growth of *Plasmodium falciparum* induces stage-dependent haemichrome formation, oxidative aggregation of band 3, membrane deposition of complement and antibodies, and phagocytosis of parasitized erythrocytes. Br J Haematol *113*, 492-499.

Gligorijevic, B., Bennett, T., McAllister, R., Urbach, J. S., and Roepe, P. D. (2006a). Spinning disk confocal microscopy of live, intraerythrocytic malarial parasites. 2. Altered vacuolar volume regulation in drug resistant malaria. Biochemistry *45*, 12411-12423.

Gligorijevic, B., McAllister, R., Urbach, J. S., and Roepe, P. D. (2006b). Spinning disk confocal microscopy of live, intraerythrocytic malarial parasites. 1. Quantification of hemozoin development for drug sensitive versus resistant malaria. Biochemistry *45*, 12400-12410.

Gonzales, J. M., Patel, J. J., Ponmee, N., Jiang, L., Tan, A., Maher, S. P., Wuchty, S., Rathod, P. K., and Ferdig, M. T. (2008). Regulatory hotspots in the malaria parasite genome dictate transcriptional variation. PLoS Biol *6*, e238.

Grant, C. M., MacIver, F. H., and Dawes, I. W. (1996). Glutathione is an essential metabolite required for resistance to oxidative stress in the yeast *Saccharomyces cerevisiae*. Curr Genet *29*, 511-515.

Grant, C. M., MacIver, F. H., and Dawes, I. W. (1997). Glutathione synthetase is dispensable for growth under both normal and oxidative stress conditions in the yeast *Saccharomyces cerevisiae* due to an accumulation of the dipeptide gamma-glutamylcysteine. Mol Biol Cell *8*, 1699-1707.

Gratepanche, S., Menage, S., Touati, D., Wintjens, R., Delplace, P., Fontecave, M., Masset, A., Camus, D., and Dive, D. (2002). Biochemical and electron paramagnetic resonance study of the iron superoxide dismutase from *Plasmodium falciparum*. Mol Biochem Parasitol *120*, 237-246.

Green, R. M., Graham, M., O'Donovan, M. R., Chipman, J. K., and Hodges, N. J. (2006). Subcellular compartmentalization of glutathione: correlations with parameters of oxidative stress related to genotoxicity. Mutagenesis *21*, 383-390.

Griffith, O. W. (1982). Mechanism of action, metabolism, and toxicity of buthionine sulfoximine and its higher homologs, potent inhibitors of glutathione synthesis. J Biol Chem *257*, 13704-13712.

Günther, S., Matuschewski, K., and Müller, S. (2009). Knockout studies reveal an important role of *Plasmodium* lipoic acid protein ligase A1 for asexual blood stage parasite survival. PLoS ONE *in press*.

Harwaldt, P., Rahlfs, S., and Becker, K. (2002). Glutathione S-transferase of the malarial parasite *Plasmodium falciparum*: characterization of a potential drug target. Biol Chem *383*, 821-830.

Hayward, R., Saliba, K. J., and Kirk, K. (2006). The pH of the digestive vacuole of *Plasmodium falciparum* is not associated with chloroquine resistance. J Cell Sci *119*, 1016-1025.

Hell, R., and Bergmann, L. (1988). Glutathione synthetase in tobacco suspension cultures: catalytic properties and localization. Physiologia Plantarum *72*, 70-76.

Hell, R., and Bergmann, L. (1990). λ-Glutamylcysteine synthetase in higher plants: catalytic properties and subcellular localization. Planta *180*, 603-612.

Ho, H. Y., Cheng, M. L., and Chiu, D. T. (2007). Glucose-6-phosphate dehydrogenase--from oxidative stress to cellular functions and degenerative diseases. Redox Rep *12*, 109-118.

Holmgren, A. (1976). Hydrogen donor system for *Escherichia coli* ribonucleoside-diphosphate reductase dependent upon glutathione. Proc Natl Acad Sci U S A *73*, 2275-2279.

Hopkins, J., Fowler, R., Krishna, S., Wilson, I., Mitchell, G., and Bannister, L. (1999). The plastid in *Plasmodium falciparum* asexual blood stages: a three-dimensional ultrastructural analysis. Protist *150*, 283-295.

Huang, C. S., He, W., Meister, A., and Anderson, M. E. (1995). Amino acid sequence of rat kidney glutathione synthetase. Proc Natl Acad Sci U S A *92*, 1232-1236.

Huang, C. S., Moore, W. R., and Meister, A. (1988). On the active site thiol of gamma-glutamylcysteine synthetase: relationships to catalysis, inhibition, and regulation. Proc Natl Acad Sci U S A *85*, 2464-2468.

Hunt, N., and Stocker, R. (1990). Oxidative stress and the redox status of malaria infected erythrocytes. Blood Cells *16*, 499-526.

Huynh, T. T., Huynh, V. T., Harmon, M. A., and Phillips, M. A. (2003). Gene knockdown of gamma-glutamylcysteine synthetase by RNAi in the parasitic protozoa *Trypanosoma brucei* demonstrates that it is an essential enzyme. J Biol Chem *278*, 39794-39800.

Hwang, C., Sinskey, A. J., and Lodish, H. F. (1992). Oxidized redox state of glutathione in the endoplasmic reticulum. Science *257*, 1496-1502.

Hyde, J. E. (2005). Exploring the folate pathway in *Plasmodium falciparum*. Acta Trop *94*, 191-206.

Imlay, J. A. (2003). Pathways of oxidative damage. Annu Rev Microbiol *57*, 395-418.

Imlay, J. A., Chin, S. M., and Linn, S. (1988). Toxic DNA damage by hydrogen peroxide through the Fenton reaction in vivo and in vitro. Science *240*, 640-642.

Jani, D., Nagarkatti, R., Beatty, W., Angel, R., Slebodnick, C., Andersen, J., Kumar, S., and Rathore, D. (2008). HDP-a novel heme detoxification protein from the malaria parasite. PLoS Pathog *4*, e1000053.

Janse, C. J., Boorsma, E. G., Ramesar, J., Grobbee, M. J., and Mons, B. (1989). Host cell specificity and schizogony of *Plasmodium berghei* under different in vitro conditions. Int J Parasitol *19*, 509-514.

Johnson, D. J., Fidock, D. A., Mungthin, M., Lakshmanan, V., Sidhu, A. B., Bray, P. G., and Ward, S. A. (2004). Evidence for a central role for PfCRT in conferring *Plasmodium falciparum* resistance to diverse antimalarial agents. Mol Cell *15*, 867-877.

Kampkotter, A., Volkmann, T. E., de Castro, S. H., Leiers, B., Klotz, L. O., Johnson, T. E., Link, C. D., and Henkle-Duhrsen, K. (2003). Functional analysis of the glutathione S-transferase 3 from Onchocerca volvulus (Ov-GST-3): a parasite

GST confers increased resistance to oxidative stress in Caenorhabditis elegans. J Mol Biol *325*, 25-37.

Kanzok, S. M., Schirmer, R. H., Turbachova, I., Iozef, R., and Becker, K. (2000). The thioredoxin system of the malaria parasite *Plasmodium falciparum*. Glutathione reduction revisited. J Biol Chem *275*, 40180-40186.

Kawazu, S., Tsuji, N., Hatabu, T., Kawai, S., Matsumoto, Y., and Kano, S. (2000). Molecular cloning and characterization of a peroxiredoxin from the human malaria parasite *Plasmodium falciparum*. Mol Biochem Parasitol *109*, 165-169.

Kawazu, S. I., Komaki-Yasuda, K., Oku, H., and Kano, S. (2007). Peroxiredoxins in malaria parasites: Parasitologic aspects. Parasitol Int.

Khattab, A., and Klinkert, M. Q. (2006). Maurer's clefts-restricted localization, orientation and export of a *Plasmodium falciparum* RIFIN. Traffic *7*, 1654-1665.

Kim, B. J., Choi, C. H., Lee, C. H., Jeong, S. Y., Kim, J. S., Kim, B. Y., Yim, H. S., and Kang, S. O. (2005). Glutathione is required for growth and prespore cell differentiation in *Dictyostelium*. Dev Biol *284*, 387-398.

Klokouzas, A., Tiffert, T., van Schalkwyk, D., Wu, C. P., van Veen, H. W., Barrand, M. A., and Hladky, S. B. (2004). *Plasmodium falciparum* expresses a multidrug resistance-associated protein. Biochem Biophys Res Commun *321*, 197-201.

Kobayashi, T., Sato, S., Takamiya, S., Komaki-Yasuda, K., Yano, K., Hirata, A., Onitsuka, I., Hata, M., Mi-ichi, F., Tanaka, T., *et al.* (2007). Mitochondria and apicoplast of *Plasmodium falciparum*: behaviour on subcellular fractionation and the implication. Mitochondrion *7*, 125-132.

Komaki-Yasuda, K., Kawazu, S., and Kano, S. (2003). Disruption of the *Plasmodium falciparum* 2-Cys peroxiredoxin gene renders parasites hypersensitive to reactive oxygen and nitrogen species. FEBS Lett *547*, 140-144.

Krauth-Siegel, R. L., Muller, J. G., Lottspeich, F., and Schirmer, R. H. (1996). Glutathione reductase and glutamate dehydrogenase of *Plasmodium falciparum*, the causative agent of tropical malaria. Eur J Biochem *235*, 345-350.

Krnajski, Z., Gilberger, T. W., Walter, R. D., Cowman, A. F., and Muller, S. (2002). Thioredoxin reductase is essential for the survival of *Plasmodium falciparum* erythrocytic stages. J Biol Chem *277*, 25970-25975.

Krnajski, Z., Gilberger, T. W., Walter, R. D., and Muller, S. (2001a). The malaria parasite *Plasmodium falciparum* possesses a functional thioredoxin system. Mol Biochem Parasitol *112*, 219-228.

Krnajski, Z., Walter, R. D., and Muller, S. (2001b). Isolation and functional analysis of two thioredoxin peroxidases (peroxiredoxins) from *Plasmodium falciparum*. Mol Biochem Parasitol *113*, 303-308.

Krungkrai, J., Cerami, A., and Henderson, G. B. (1990). Pyrimidine biosynthesis in parasitic protozoa: purification of a monofunctional dihydroorotase from *Plasmodium berghei* and *Crithidia fasciculata*. Biochemistry *29*, 6270-6275.

Krungkrai, J., Cerami, A., and Henderson, G. B. (1991). Purification and characterization of dihydroorotate dehydrogenase from the rodent malaria parasite *Plasmodium berghei*. Biochemistry *30*, 1934-1939.

Kuhn, Y., Rohrbach, P., and Lanzer, M. (2007). Quantitative pH measurements in *Plasmodium falciparum*-infected erythrocytes using pHluorin. Cell Microbiol *9*, 1004-1013.

Kwiatkowski, D. P. (2005). How malaria has affected the human genome and what human genetics can teach us about malaria. Am J Hum Genet *77*, 171-192.

Laemmli, U. K. (1970). Cleavage of structural proteins during the assembly of the head of bacteriophage T4. Nature *227*, 680-685.

Lakshmanan, V., Bray, P. G., Verdier-Pinard, D., Johnson, D. J., Horrocks, P., Muhle, R. A., Alakpa, G. E., Hughes, R. H., Ward, S. A., Krogstad, D. J., *et al*. (2005). A critical role for PfCRT K76T in *Plasmodium falciparum* verapamil-reversible chloroquine resistance. Embo J *24*, 2294-2305.

Lambros, C., and Vanderberg, J. P. (1979). Synchronization of *Plasmodium falciparum* erythrocytic stages in culture. J Parasitol *65*, 418-420.

Landy, A. (1989). Dynamic, structural, and regulatory aspects of lambda site-specific recombination. Annu Rev Biochem *58*, 913-949.

Lash, L. H. (2006). Mitochondrial glutathione transport: physiological, pathological and toxicological implications. Chem Biol Interact *163*, 54-67.

Le Bras, J., and Durand, R. (2003). The mechanisms of resistance to antimalarial drugs in *Plasmodium falciparum*. Fundam Clin Pharmacol *17*, 147-153.

Lee, J. C., Straffon, M. J., Jang, T. Y., Higgins, V. J., Grant, C. M., and Dawes, I. W. (2001). The essential and ancillary role of glutathione in *Saccharomyces cerevisiae* analysed using a grande gsh1 disruptant strain. FEMS Yeast Res *1*, 57-65.

Lee, K. O., Lee, J. R., Yoo, J. Y., Jang, H. H., Moon, J. C., Jung, B. G., Chi, Y. H., Park, S. K., Lee, S. S., Lim, C. O., *et al*. (2002). GSH-dependent peroxidase activity of the rice (*Oryza sativa*) glutaredoxin, a thioltransferase. Biochem Biophys Res Commun *296*, 1152-1156.

Li, W., Mo, W., Shen, D., Sun, L., Wang, J., Lu, S., Gitschier, J. M., and Zhou, B. (2005). Yeast model uncovers dual roles of mitochondria in action of artemisinin. PLoS Genet *1*, e36.

Liebau, E., Bergmann, B., Campbell, A. M., Teesdale-Spittle, P., Brophy, P. M., Luersen, K., and Walter, R. D. (2002). The glutathione S-transferase from *Plasmodium falciparum*. Mol Biochem Parasitol *124*, 85-90.

Lim, P., Chim, P., Sem, R., Nemh, S., Poravuth, Y., Lim, C., Seila, S., Tsuyuoka, R., Denis, M. B., Socheat, D., and Fandeur, T. (2005). In vitro monitoring of *Plasmodium falciparum* susceptibility to artesunate, mefloquine, quinine and chloroquine in Cambodia: 2001-2002. Acta Trop *93*, 31-40.

Lueder, D. V., and Phillips, M. A. (1996). Characterization of *Trypanosoma brucei* gamma-glutamylcysteine synthetase, an essential enzyme in the biosynthesis of trypanothione (diglutathionylspermidine). J Biol Chem *271*, 17485-17490.

Lüersen, K., Walter, R. D., and Müller, S. (1999). The putative gamma-glutamylcysteine synthetase from *Plasmodium falciparum* contains large insertions and a variable tandem repeat. Mol Biochem Parasitol *98*, 131-142.

Lüersen, K., Walter, R. D., and Müller, S. (2000). *Plasmodium falciparum*-infected red blood cells depend on a functional glutathione de novo synthesis attributable to an enhanced loss of glutathione. Biochem J *346 Pt 2*, 545-552.

Luthman, M., Eriksson, S., Holmgren, A., and Thelander, L. (1979). Glutathione-dependent hydrogen donor system for calf thymus ribonucleoside-diphosphate reductase. Proc Natl Acad Sci U S A *76*, 2158-2162.

Maier, A. G., Braks, J. A., Waters, A. P., and Cowman, A. F. (2006). Negative selection using yeast cytosine deaminase/uracil phosphoribosyl transferase in *Plasmodium falciparum* for targeted gene deletion by double crossover recombination. Mol Biochem Parasitol *150*, 118-121.

Markovic, J., Borras, C., Ortega, A., Sastre, J., Vina, J., and Pallardo, F. V. (2007). Glutathione is recruited into the nucleus in early phases of cell proliferation. J Biol Chem *282*, 20416-20424.

Martensson, J., Jain, A., Frayer, W., and Meister, A. (1989). Glutathione metabolism in the lung: inhibition of its synthesis leads to lamellar body and mitochondrial defects. Proc Natl Acad Sci U S A *86*, 5296-5300.

Martensson, J., Jain, A., and Meister, A. (1990a). Glutathione is required for intestinal function. Proc Natl Acad Sci U S A *87*, 1715-1719.

Martensson, J., Jain, A., Stole, E., Frayer, W., Auld, P. A., and Meister, A. (1991). Inhibition of glutathione synthesis in the newborn rat: a model for endogenously produced oxidative stress. Proc Natl Acad Sci U S A *88*, 9360-9364.

Martensson, J., Lai, J. C., and Meister, A. (1990b). High-affinity transport of glutathione is part of a multicomponent system essential for mitochondrial function. Proc Natl Acad Sci U S A *87*, 7185-7189.

Martensson, J., and Meister, A. (1989). Mitochondrial damage in muscle occurs after marked depletion of glutathione and is prevented by giving glutathione monoester. Proc Natl Acad Sci U S A *86*, 471-475.

Martin, R. E., and Kirk, K. (2004). The malaria parasite's chloroquine resistance transporter is a member of the drug/metabolite transporter superfamily. Mol Biol Evol *21*, 1938-1949.

Matuschewski, K. (2006). Getting infectious: formation and maturation of *Plasmodium* sporozoites in the *Anopheles* vector. Cell Microbiol *8*, 1547-1556.

Maynard-Smith, L. A., Chen, L. C., Banaszynski, L. A., Ooi, A. G., and Wandless, T. J. (2007). A directed approach for engineering conditional protein stability using biologically silent small molecules. J Biol Chem *282*, 24866-24872.

McNally, J., O'Donovan, S. M., and Dalton, J. P. (1992). *Plasmodium berghei* and *Plasmodium chabaudi chabaudi*: development of simple in vitro erythrocyte invasion assays. Parasitology *105 (Pt 3)*, 355-362.

Meierjohann, S., Walter, R. D., and Müller, S. (2002a). Glutathione synthetase from *Plasmodium falciparum*. Biochem J *363*, 833-838.

Meierjohann, S., Walter, R. D., and Müller, S. (2002b). Regulation of intracellular glutathione levels in erythrocytes infected with chloroquine-sensitive and chloroquine-resistant *Plasmodium falciparum*. Biochem J *368*, 761-768.

Meister, A. (1983). Selective modification of glutathione metabolism. Science *220*, 472-477.

Meister, A. (1988). Glutathione metabolism and its selective modification. J Biol Chem *263*, 17205-17208.

Meister, A., and Anderson, M. E. (1983). Glutathione. Annu Rev Biochem *52*, 711-760.

Meshnick, S. R. (1998). Artemisinin antimalarials: mechanisms of action and resistance. Med Trop (Mars) *58*, 13-17.

Miller, L. H., Baruch, D. I., Marsh, K., and Doumbo, O. K. (2002). The pathogenic basis of malaria. Nature *415*, 673-679.

Misra, H. P., and Fridovich, I. (1972). The generation of superoxide radical during the autoxidation of hemoglobin. J Biol Chem *247*, 6960-6962.

Molteni, S. N., Fassio, A., Ciriolo, M. R., Filomeni, G., Pasqualetto, E., Fagioli, C., and Sitia, R. (2004). Glutathione limits Ero1-dependent oxidation in the endoplasmic reticulum. J Biol Chem *279*, 32667-32673.

Mu, J., Ferdig, M. T., Feng, X., Joy, D. A., Duan, J., Furuya, T., Subramanian, G., Aravind, L., Cooper, R. A., Wootton, J. C., *et al*. (2003). Multiple transporters associated with malaria parasite responses to chloroquine and quinine. Mol Microbiol *49*, 977-989.

Müller, S. (2004). Redox and antioxidant systems of the malaria parasite *Plasmodium falciparum*. Mol Microbiol *53*, 1291-1305.

Müller, S., Gilberger, T. W., Farber, P. M., Becker, K., Schirmer, R. H., and Walter, R. D. (1996). Recombinant putative glutathione reductase of *Plasmodium falciparum* exhibits thioredoxin reductase activity. Mol Biochem Parasitol *80*, 215-219.

Murata, C. E., and Goldberg, D. E. (2003a). *Plasmodium falciparum* falcilysin: a metalloprotease with dual specificity. J Biol Chem *278*, 38022-38028.

Murata, C. E., and Goldberg, D. E. (2003b). *Plasmodium falciparum* falcilysin: an unprocessed food vacuole enzyme. Mol Biochem Parasitol *129*, 123-126.

Newton, G. L., and Fahey, R. C. (2002). Mycothiol biochemistry. Arch Microbiol *178*, 388-394.

Niang, M., Yan Yam, X., and Preiser, P. R. (2009). The *Plasmodium falciparum* STEVOR multigene family mediates antigenic variation of the infected erythrocyte. PLoS Pathog *5*, e1000307.

Nishikimi, M., Appaji, N., and Yagi, K. (1972). The occurrence of superoxide anion in the reaction of reduced phenazine methosulfate and molecular oxygen. Biochem Biophys Res Commun *46*, 849-854.

Orjih, A. U., Banyal, H. S., Chevli, R., and Fitch, C. D. (1981). Hemin lyses malaria parasites. Science *214*, 667-669.

Painter, H. J., Morrisey, J. M., Mather, M. W., and Vaidya, A. B. (2007). Specific role of mitochondrial electron transport in blood-stage *Plasmodium falciparum*. Nature *446*, 88-91.

Pandey, A. V., Tekwani, B. L., Singh, R. L., and Chauhan, V. S. (1999). Artemisinin, an endoperoxide antimalarial, disrupts the hemoglobin catabolism

and heme detoxification systems in malarial parasite. J Biol Chem *274*, 19383-19388.

Papon, N., Noel, T., Florent, M., Gibot-Leclerc, S., Jean, D., Chastin, C., Villard, J., and Chapeland-Leclerc, F. (2007). Molecular mechanism of flucytosine resistance in Candida lusitaniae: contribution of the FCY2, FCY1, and FUR1 genes to 5-fluorouracil and fluconazole cross-resistance. Antimicrob Agents Chemother *51*, 369-371.

Pasternak, M., Lim, B., Wirtz, M., Hell, R., Cobbett, C. S., and Meyer, A. J. (2008). Restricting glutathione biosynthesis to the cytosol is sufficient for normal plant development. Plant J *53*, 999-1012.

Pasternak, N. D., and Dzikowski, R. (2008). PfEMP1: An antigen that plays a key role in the pathogenicity and immune evasion of the malaria parasite *Plasmodium falciparum*. Int J Biochem Cell Biol.

Pasvol, G., Weatherall, D. J., and Wilson, R. J. (1978). Cellular mechanism for the protective effect of haemoglobin S against *P. falciparum* malaria. Nature *274*, 701-703.

Perez-Rosado, J., Gervais, G. W., Ferrer-Rodriguez, I., Peters, W., and Serrano, A. E. (2002). *Plasmodium berghei*: analysis of the gamma-glutamylcysteine synthetase gene in drug-resistant lines. Exp Parasitol *101*, 175-182.

Petter, M., Haeggstrom, M., Khattab, A., Fernandez, V., Klinkert, M. Q., and Wahlgren, M. (2007). Variant proteins of the *Plasmodium falciparum* RIFIN family show distinct subcellular localization and developmental expression patterns. Mol Biochem Parasitol *156*, 51-61.

Pisciotta, J. M., Coppens, I., Tripathi, A. K., Scholl, P. F., Shuman, J., Bajad, S., Shulaev, V., and Sullivan, D. J., Jr. (2007). The role of neutral lipid nanospheres in *Plasmodium falciparum* haem crystallization. Biochem J *402*, 197-204.

Platel, D. F., Mangou, F., and Tribouley-Duret, J. (1999). Role of glutathione in the detoxification of ferriprotoporphyrin IX in chloroquine resistant *Plasmodium berghei*. Mol Biochem Parasitol *98*, 215-223.

Price, R. N., Uhlemann, A. C., Brockman, A., McGready, R., Ashley, E., Phaipun, L., Patel, R., Laing, K., Looareesuwan, S., White, N. J., *et al*. (2004).

Mefloquine resistance in *Plasmodium falciparum* and increased pfmdr1 gene copy number. Lancet *364*, 438-447.

Prinz, W. A., Aslund, F., Holmgren, A., and Beckwith, J. (1997). The role of the thioredoxin and glutaredoxin pathways in reducing protein disulfide bonds in the *Escherichia coli* cytoplasm. J Biol Chem *272*, 15661-15667.

Prudencio, M., Rodriguez, A., and Mota, M. M. (2006). The silent path to thousands of merozoites: the *Plasmodium* liver stage. Nat Rev Microbiol *4*, 849-856.

Rachmilewitz, E. A., Weizer-Stern, O., Adamsky, K., Amariglio, N., Rechavi, G., Breda, L., Rivella, S., and Cabantchik, Z. I. (2005). Role of iron in inducing oxidative stress in thalassemia: Can it be prevented by inhibition of absorption and by antioxidants? Ann N Y Acad Sci *1054*, 118-123.

Radyuk, S. N., Rebrin, I., Luchak, J. M., Michalak, K., Klichko, V. I., Sohal, R. S., and Orr, W. C. (2009). The catalytic subunit of *Drosophila* glutamate-cysteine ligase is a nucleocytoplasmic shuttling protein. J Biol Chem *284*, 2266-2274.

Rahlfs, S., and Becker, K. (2001). Thioredoxin peroxidases of the malarial parasite *Plasmodium falciparum*. Eur J Biochem *268*, 1404-1409.

Rahlfs, S., Fischer, M., and Becker, K. (2001). *Plasmodium falciparum* possesses a classical glutaredoxin and a second, glutaredoxin-like protein with a PICOT homology domain. J Biol Chem *276*, 37133-37140.

Rahlfs, S., Nickel, C., Deponte, M., Schirmer, R. H., and Becker, K. (2003). *Plasmodium falciparum* thioredoxins and glutaredoxins as central players in redox metabolism. Redox Rep *8*, 246-250.

Rahlfs, S., Schirmer, R. H., and Becker, K. (2002). The thioredoxin system of *Plasmodium falciparum* and other parasites. Cell Mol Life Sci *59*, 1024-1041.

Raj, D. K., Mu, J., Jiang, H., Kabat, J., Singh, S., Sullivan, M., Fay, M. P., McCutchan, T. F., and Su, X. Z. (2008). Disruption of a *Plasmodium falciparum* multidrug resistance-associated protein (PFMRP) alters its fitness and transport of antimalarial drugs and glutathione. J Biol Chem.

Rangarajan, R., Bei, A. K., Jethwaney, D., Maldonado, P., Dorin, D., Sultan, A. A., and Doerig, C. (2005). A mitogen-activated protein kinase regulates male gametogenesis and transmission of the malaria parasite *Plasmodium berghei*. EMBO Rep *6*, 464-469.

Reed, M. B., Saliba, K. J., Caruana, S. R., Kirk, K., and Cowman, A. F. (2000). Pgh1 modulates sensitivity and resistance to multiple antimalarials in *Plasmodium falciparum*. Nature *403*, 906-909.

Reyes, P., Rathod, P. K., Sanchez, D. J., Mrema, J. E., Rieckmann, K. H., and Heidrich, H. G. (1982). Enzymes of purine and pyrimidine metabolism from the human malaria parasite, *Plasmodium falciparum*. Mol Biochem Parasitol *5*, 275-290.

Rodriguez-Manzaneque, M. T., Ros, J., Cabiscol, E., Sorribas, A., and Herrero, E. (1999). Grx5 glutaredoxin plays a central role in protection against protein oxidative damage in *Saccharomyces cerevisiae*. Mol Cell Biol *19*, 8180-8190.

Rug, M., Prescott, S. W., Fernandez, K. M., Cooke, B. M., and Cowman, A. F. (2006). The role of KAHRP domains in knob formation and cytoadherence of *P. falciparum*-infected human erythrocytes. Blood *108*, 370-378.

Russo, I., Oksman, A., Vaupel, B., and Goldberg, D. E. (2009). A calpain unique to alveolates is essential in *Plasmodium falciparum* and its knockdown reveals an involvement in pre-S-phase development. Proc Natl Acad Sci U S A *106*, 1554-1559.

Sailaja, Y. R., Baskar, R., and Saralakumari, D. (2003). The antioxidant status during maturation of reticulocytes to erythrocytes in type 2 diabetics. Free Radic Biol Med *35*, 133-139.

Salanti, A., Staalsoe, T., Lavstsen, T., Jensen, A. T., Sowa, M. P., Arnot, D. E., Hviid, L., and Theander, T. G. (2003). Selective upregulation of a single distinctly structured var gene in chondroitin sulphate A-adhering *Plasmodium falciparum* involved in pregnancy-associated malaria. Mol Microbiol *49*, 179-191.

Saliba, K. J., Folb, P. I., and Smith, P. J. (1998). Role for the *Plasmodium falciparum* digestive vacuole in chloroquine resistance. Biochem Pharmacol *56*, 313-320.

Sanchez, C. P., McLean, J. E., Rohrbach, P., Fidock, D. A., Stein, W. D., and Lanzer, M. (2005). Evidence for a pfcrt-associated chloroquine efflux system in the human malarial parasite *Plasmodium falciparum*. Biochemistry *44*, 9862-9870.

Sanchez, C. P., Rohrbach, P., McLean, J. E., Fidock, D. A., Stein, W. D., and Lanzer, M. (2007a). Differences in trans-stimulated chloroquine efflux kinetics are linked to PfCRT in *Plasmodium falciparum*. Mol Microbiol *64*, 407-420.

Sanchez, C. P., Stein, W., and Lanzer, M. (2003). Trans stimulation provides evidence for a drug efflux carrier as the mechanism of chloroquine resistance in *Plasmodium falciparum*. Biochemistry *42*, 9383-9394.

Sanchez, C. P., Stein, W. D., and Lanzer, M. (2007b). Is PfCRT a channel or a carrier? Two competing models explaining chloroquine resistance in *Plasmodium falciparum*. Trends Parasitol *23*, 332-339.

Sanchez, C. P., Wunsch, S., and Lanzer, M. (1997). Identification of a chloroquine importer in *Plasmodium falciparum*. Differences in import kinetics are genetically linked with the chloroquine-resistant phenotype. J Biol Chem *272*, 2652-2658.

Sanglard, D. (2002). Clinical relevance of mechanisms of antifungal drug resistance in yeasts. Enferm Infecc Microbiol Clin *20*, 462-469; quiz 470, 479.

Sarma, G. N., Nickel, C., Rahlfs, S., Fischer, M., Becker, K., and Karplus, P. A. (2005). Crystal structure of a novel *Plasmodium falciparum* 1-Cys peroxiredoxin. J Mol Biol *346*, 1021-1034.

Sherman, I. W. (2005). Molecular Approaches to Malaria (Washington, DC: ASM Press American Society for Microbiology).

Shi, Z. Z., Habib, G. M., Rhead, W. J., Gahl, W. A., He, X., Sazer, S., and Lieberman, M. W. (1996). Mutations in the glutathione synthetase gene cause 5-oxoprolinuria. Nat Genet *14*, 361-365.

Shi, Z. Z., Osei-Frimpong, J., Kala, G., Kala, S. V., Barrios, R. J., Habib, G. M., Lukin, D. J., Danney, C. M., Matzuk, M. M., and Lieberman, M. W. (2000). Glutathione synthesis is essential for mouse development but not for cell growth in culture. Proc Natl Acad Sci U S A *97*, 5101-5106.

Sidhu, A. B., Valderramos, S. G., and Fidock, D. A. (2005). pfmdr1 mutations contribute to quinine resistance and enhance mefloquine and artemisinin sensitivity in *Plasmodium falciparum*. Mol Microbiol *57*, 913-926.

Sidhu, A. B., Verdier-Pinard, D., and Fidock, D. A. (2002). Chloroquine resistance in *Plasmodium falciparum* malaria parasites conferred by pfcrt mutations. Science *298*, 210-213.

Sienkiewicz, N., Daher, W., Dive, D., Wrenger, C., Viscogliosi, E., Wintjens, R., Jouin, H., Capron, M., Muller, S., and Khalife, J. (2004). Identification of a mitochondrial superoxide dismutase with an unusual targeting sequence in *Plasmodium falciparum*. Mol Biochem Parasitol *137*, 121-132.

Sies, H. (1999). Glutathione and its role in cellular functions. Free Radic Biol Med *27*, 916-921.

Silvie, O., Mota, M. M., Matuschewski, K., and Prudencio, M. (2008). Interactions of the malaria parasite and its mammalian host. Curr Opin Microbiol *11*, 352-359.

Sinden, R. E., Canning, E. U., Bray, R. S., and Smalley, M. E. (1978). Gametocyte and gamete development in *Plasmodium falciparum*. Proc R Soc Lond B Biol Sci *201*, 375-399.

Sipos, K., Lange, H., Fekete, Z., Ullmann, P., Lill, R., and Kispal, G. (2002). Maturation of cytosolic iron-sulfur proteins requires glutathione. J Biol Chem *277*, 26944-26949.

Slater, A. F., and Cerami, A. (1992). Inhibition by chloroquine of a novel haem polymerase enzyme activity in malaria trophozoites. Nature *355*, 167-169.

Smith, J. D., Kyes, S., Craig, A. G., Fagan, T., Hudson-Taylor, D., Miller, L. H., Baruch, D. I., and Newbold, C. I. (1998). Analysis of adhesive domains from the A4VAR *Plasmodium falciparum* erythrocyte membrane protein-1 identifies a CD36 binding domain. Mol Biochem Parasitol *97*, 133-148.

Spector, D., Labarre, J., and Toledano, M. B. (2001). A genetic investigation of the essential role of glutathione: mutations in the proline biosynthesis pathway are the only suppressors of glutathione auxotrophy in yeast. J Biol Chem *276*, 7011-7016.

Srivastava, I. K., Morrisey, J. M., Darrouzet, E., Daldal, F., and Vaidya, A. B. (1999). Resistance mutations reveal the atovaquone-binding domain of cytochrome b in malaria parasites. Mol Microbiol *33*, 704-711.

Srivastava, I. K., Rottenberg, H., and Vaidya, A. B. (1997). Atovaquone, a broad spectrum antiparasitic drug, collapses mitochondrial membrane potential in a malarial parasite. J Biol Chem *272*, 3961-3966.

Srivastava, I. K., and Vaidya, A. B. (1999). A mechanism for the synergistic antimalarial action of atovaquone and proguanil. Antimicrob Agents Chemother *43*, 1334-1339.

Steenkamp, D. J. (2002). Thiol metabolism of the trypanosomatids as potential drug targets. IUBMB Life *53*, 243-248.

Stewart, E. J., Aslund, F., and Beckwith, J. (1998). Disulfide bond formation in the *Escherichia coli* cytoplasm: an in vivo role reversal for the thioredoxins. Embo J *17*, 5543-5550.

Storz, G., and Imlay, J. A. (1999). Oxidative stress. Curr Opin Microbiol *2*, 188-194.

Su, X., Kirkman, L. A., Fujioka, H., and Wellems, T. E. (1997). Complex polymorphisms in an approximately 330 kDa protein are linked to chloroquine-resistant *P. falciparum* in Southeast Asia and Africa. Cell *91*, 593-603.

Sundquist, A. R., and Fahey, R. C. (1989). The function of gamma-glutamylcysteine and bis-gamma-glutamylcystine reductase in *Halobacterium halobium*. J Biol Chem *264*, 719-725.

Sztajer, H., Gamain, B., Aumann, K. D., Slomianny, C., Becker, K., Brigelius-Flohe, R., and Flohe, L. (2001). The putative glutathione peroxidase gene of *Plasmodium falciparum* codes for a thioredoxin peroxidase. J Biol Chem *276*, 7397-7403.

Tewari, R., Dorin, D., Moon, R., Doerig, C., and Billker, O. (2005). An atypical mitogen-activated protein kinase controls cytokinesis and flagellar motility during male gamete formation in a malaria parasite. Mol Microbiol *58*, 1253-1263.

Thorburn, D. R., and Beutler, E. (1991). The loss of enzyme activity from erythroid cells during maturation. Adv Exp Med Biol *307*, 15-27.

Tietze, F. (1969). Enzymic method for quantitative determination of nanogram amounts of total and oxidized glutathione: applications to mammalian blood and other tissues. Anal Biochem *27*, 502-522.

Trager, W., and Jensen, J. B. (1976). Human malaria parasites in continuous culture. Science *193*, 673-675.

Tran, C. V., and Saier, M. H., Jr. (2004). The principal chloroquine resistance protein of *Plasmodium falciparum* is a member of the drug/metabolite transporter superfamily. Microbiology *150*, 1-3.

Tripathi, T., Rahlfs, S., Becker, K., and Bhakuni, V. (2007). Glutathione mediated regulation of oligomeric structure and functional activity of *Plasmodium falciparum* glutathione S-transferase. BMC Struct Biol *7*, 67.

Tu, Z., and Anders, M. W. (1998). Expression and characterization of human glutamate-cysteine ligase. Arch Biochem Biophys *354*, 247-254.

Uhlemann, A. C., Cameron, A., Eckstein-Ludwig, U., Fischbarg, J., Iserovich, P., Zuniga, F. A., East, M., Lee, A., Brady, L., Haynes, R. K., and Krishna, S. (2005). A single amino acid residue can determine the sensitivity of SERCAs to artemisinins. Nat Struct Mol Biol *12*, 628-629.

Ursing, J., Zakeri, S., Gil, J. P., and Bjorkman, A. (2006). Quinoline resistance associated polymorphisms in the pfcrt, pfmdr1 and pfmrp genes of *Plasmodium falciparum* in Iran. Acta Trop *97*, 352-356.

Valderramos, S. G., and Fidock, D. A. (2006). Transporters involved in resistance to antimalarial drugs. Trends Pharmacol Sci.

van Dooren, G. G., Marti, M., Tonkin, C. J., Stimmler, L. M., Cowman, A. F., and McFadden, G. I. (2005). Development of the endoplasmic reticulum, mitochondrion and apicoplast during the asexual life cycle of *Plasmodium falciparum*. Mol Microbiol *57*, 405-419.

van Dooren, G. G., Stimmler, L. M., and McFadden, G. I. (2006). Metabolic maps and functions of the *Plasmodium* mitochondrion. FEMS Microbiol Rev *30*, 596-630.

Vega-Rodriguez, J., Franke-Fayard, B., Dinglasan, R. R., Janse, C. J., Pastrana-Mena, R., Waters, A. P., Coppens, I., Rodriguez-Orengo, J. F., Jacobs-Lorena, M., and Serrano, A. E. (2009). The glutathione biosynthetic pathway of *Plasmodium* is essential for mosquito transmission. PLoS Pathog *5*, e1000302.

Vermes, A., Guchelaar, H. J., and Dankert, J. (2000). Flucytosine: a review of its pharmacology, clinical indications, pharmacokinetics, toxicity and drug interactions. J Antimicrob Chemother *46*, 171-179.

Vijaykadga, S., Rojanawatsirivej, C., Cholpol, S., Phoungmanee, D., Nakavej, A., and Wongsrichanalai, C. (2006). In vivo sensitivity monitoring of mefloquine monotherapy and artesunate-mefloquine combinations for the treatment of uncomplicated falciparum malaria in Thailand in 2003. Trop Med Int Health *11*, 211-219.

Waller, R. F., and McFadden, G. I. (2005). The apicoplast: a review of the derived plastid of apicomplexan parasites. Curr Issues Mol Biol *7*, 57-79.

Warhurst, D. C., Craig, J. C., and Adagu, I. S. (2002). Lysosomes and drug resistance in malaria. Lancet *360*, 1527-1529.

Wellems, T. E., Panton, L. J., Gluzman, I. Y., do Rosario, V. E., Gwadz, R. W., Walker-Jonah, A., and Krogstad, D. J. (1990). Chloroquine resistance not linked to mdr-like genes in a *Plasmodium falciparum* cross. Nature *345*, 253-255.

Wellems, T. E., Walker-Jonah, A., and Panton, L. J. (1991). Genetic mapping of the chloroquine-resistance locus on *Plasmodium falciparum* chromosome 7. Proc Natl Acad Sci U S A *88*, 3382-3386.

Williams, T. N. (2006). Red blood cell defects and malaria. Mol Biochem Parasitol *149*, 121-127.

Williams, T. N., Weatherall, D. J., and Newbold, C. I. (2002). The membrane characteristics of *Plasmodium falciparum*-infected and -uninfected heterozygous alpha(0)thalassaemic erythrocytes. Br J Haematol *118*, 663-670.

Wirth, D. F. (2002). Biological revelations. Nature *419*, 495-496.

Wolf, A. E., Dietz, K. J., and Schroder, P. (1996). Degradation of glutathione S-conjugates by a carboxypeptidase in the plant vacuole. FEBS Lett *384*, 31-34.

Yang, P., Ebbert, J. O., Sun, Z., and Weinshilboum, R. M. (2006). Role of the glutathione metabolic pathway in lung cancer treatment and prognosis: a review. J Clin Oncol *24*, 1761-1769.

Zechmann, B., Mauch, F., Sticher, L., and Muller, M. (2008). Subcellular immunocytochemical analysis detects the highest concentrations of glutathione in mitochondria and not in plastids. J Exp Bot *59*, 4017-4027.

Zhang, J., Krugliak, M., and Ginsburg, H. (1999). The fate of ferriprotorphyrin IX in malaria infected erythrocytes in conjunction with the mode of action of antimalarial drugs. Mol Biochem Parasitol *99*, 129-141.